

**STUDIES OF THE COORDINATION CHEMISTRY AND
CATALYTIC ACTIVITY OF RHODIUM AND RUTHENIUM N-
HETEROCYCLIC CARBENE COMPLEXES**

by

Jeremy M. Praetorius

A thesis submitted to the Department of Chemistry

In conformity with the requirements for

the degree of Doctor of Philosophy

Queen's University

Kingston, Ontario, Canada

(September, 2010)

Copyright ©Jeremy M. Praetorius, 2010

Abstract

The side-on dioxygen adducts of N-heterocyclic carbene (NHC) containing rhodium complexes, $[\text{ClRh}(\text{IPr})_2(\text{O}_2)]$ and $[\text{ClRh}(\text{IMes})_2(\text{O}_2)]$, previously synthesized in our laboratories possess a square planar geometry and O-O bond lengths of 1.323(3) and 1.341(4) Å, respectively. Both of these attributes are uncharacteristic of $\text{Rh}(\text{O}_2)$ complexes, which are typically octahedral and possess O-O bond lengths of approximately 1.45 Å. Full characterization by NMR, IR, Raman, DFT and XAS confirmed the short O-O bond lengths of these structures and revealed that they were rhodium(I) coordination complexes of singlet oxygen with no net oxidation/reduction process having taken place. The unique bonding mode appears to result from the interaction of a filled Rh d orbital with one of the two degenerate $\text{O}_2 \pi^*$ orbitals, which causes splitting of the $\text{O}_2 \pi^*$ orbitals, favoring spin pairing in the O_2 HOMO, and the inability of Rh to donate electron density to the empty π^* orbital. Initial investigations of these complexes as catalysts for the reduction and oxidation of C-O bonds, as well as singlet oxygen generation were also undertaken. $\text{Rh}(\text{IPr})_2$ coordination complexes of N_2 , H_2 and CO were also synthesized and characterized by X-ray crystallography, NMR and elemental analysis. Interestingly, the addition of hydrogen gas to rhodium *did* result in oxidation of the metal.

A Rh(NHC) complex featuring an anionic acetate ligand, $[(\text{AcO})\text{Rh}(\text{IPr})(\text{CO})_2]$, was synthesized and characterized by NMR, IR and X-ray crystallography. This complex proved to be an effective catalyst for the regioselective hydroformylation of aliphatic and aromatic alkenes, which occurred without isomerization of the alkene. Initial rates of hydroformylation with our catalyst were compared to the chloride analogue,

[ClRh(IPr)(CO)₂], and demonstrated the beneficial nature of replacing the halide with a carboxylate ligand, which is less inhibiting of the reaction.

The synthesis of a bifunctional hydrogenation catalyst featuring a protic-NHC was attempted by addition of benzimidazoles to [Cl₂Ru(diphosphine)]. Although these attempts were unsuccessful, a large number of complexes of the formula [Cl₂Ru(diphosphine)(κ-N3-benzimidazole)₂] were synthesized and proved to be effective catalysts for the chemoselective hydrogenation of ketones *versus* alkenes. Use of chiral diphosphines and 1-triphenylmethylbenzimidazole yielded catalysts capable of producing secondary alcohols with moderate enantioselectivity.

Acknowledgements

Though the words of this dissertation and the results they report are my own, there are a great number of people that helped to make this all possible. Completing a doctoral degree is a huge task and it would have been insurmountable without the support, encouragement and love of all those who have surrounded me over the last five years.

I would first like to thank all members of the Crudden laboratory past and present, for helping me choose this laboratory to pursue my graduate studies and making it a great place to work. For Daryl Allen, who mentored me during the first year of my studies and passed on the legacy of his research, I am greatly indebted. There was always time to discuss any and all things chemistry with Jon Webb, whose love and enthusiasm for chemistry was unmatched. Our partnership in the laboratory in the first couple years of our studies surely made me a better chemist, and I hope it was reciprocated. I am greatly indebted to Jenny Du and Mark Mohammed for all the great early morning runs and squash games. Without these to quench my nervous energy, I fear my ability to focus on my studies the rest of the day would have suffered greatly. Ben Glasspoole, Steve Dickson, Dave Edwards, Jason Hanthorn, and every other student, post-doc, professor, etcetera that ever shared a beer, a bite to eat or philosophy, you have all made the past five years that much better.

A great many thanks to Professor Cathleen Crudden, whose guidance, encouragement and belief in my abilities as a chemist and a writer over the last five years have afforded me the opportunities that lie ahead. Entering my graduate studies I was only sure that my education felt incomplete. I leave now with a strong passion for

chemistry, a desire to understand and the tools to make my contribution to the world. For this I am sincerely grateful to you Professor Crudden.

To my family, I would like to extend a very large, emphatic THANK YOU! You have always stood behind me, and this period of my life has been no exception. Mom, Dad, Dave, Lisa and Sara; Nanny; Oma and Opa: you've always encouraged me to pursue my dreams and for that I am forever indebted. Megan and Stephen Nicholson, your continuous support has been invaluable and I am grateful to be a part of your family. Ash, my wife and partner, there is of course, no possible way I could be who I am without you. It is because of you and our son Hudson that I have tried to be a little better every day and achieved what I have. You're the blest! I love you.

Statement of Originality

I hereby certify that all of the work described within this thesis is the original work of the author. Any published (or unpublished) ideas and/or techniques from the work of others are fully acknowledged in accordance with the standard referencing practices.

(Jeremy M. Praetorius)

(September, 2010)

Table of Contents

Abstract.....	ii
Acknowledgements	iv
Statement of Originality	vi
Table of Contents	vii
List of Schemes.....	x
List of Figures.....	xiii
List of Tables	xv
List of Abbreviations	xvii
Chapter 1: Introduction to N-Heterocyclic Carbenes. Synthesis, Transition Metal Coordination Chemistry and Catalytic Applications	1
1.1 Carbenes	1
1.2 Isolation of NHCs.....	4
1.3 Early Studies of M(NHC) Complexes	7
1.4 Synthetic Methods for the Preparation of M(NHC)s	10
1.5 Steric and Electronic Factors of NHC Ligands	16
1.6 Catalytic Applications of M(NHC) Complexes	20
1.6.1 Ru(NHC)-Catalyzed Olefin Metathesis.....	20
1.6.2 Pd(NHC)-Catalyzed Cross Coupling Reactions	23
1.6.3 Rh(NHC)-Catalyzed Reactions	27
1.7 Conclusions.....	32
1.8 Research Objectives	33

1.9 References.....	35
Chapter 2: Coordination Chemistry and Catalytic Activity of Rhodium bis-N-Heterocyclic Carbene Complexes.....	43
2.1 Introduction	43
2.1.1 Side-on Metal-Dioxygen Adducts	43
2.1.2 [CIRh(L)(L')(O ₂)] Complexes	46
2.2 Results and Discussion	49
2.2.1 Characterization of [CIRh(NHC) ₂ (O ₂)].....	49
2.2.2 Coordination of N ₂ , CO and H ₂ to [CIRh(IPr) ₂].....	57
2.2.3 Relative Stability of [CIRh(IPr) ₂ (XY)] Complexes	67
2.2.4 Oxidation/Reduction of C-O Bonds with [CIRh(IPr) ₂ (XY)]	69
2.2.5 Catalytic Generation of Singlet Oxygen.....	79
2.3 Conclusions.....	82
2.4 Experimental.....	84
2.5 References.....	90
Chapter 3: Synthesis of Rhodium-NHC Carboxylato Complexes For The Regioselective Hydroformylation of Terminal Alkenes	95
3.1 Introduction	95
3.1.1 Rhodium-Catalyzed Hydroformylation	95
3.1.2 Rh(NHC) Hydroformylation Catalysts	99
3.2 Results and Discussion	109
3.2.1 Synthesis and Characterization	109
3.2.2 Catalytic Activity.....	115
3.2.3 Initiation of [Rh(IPr)(CO) ₂ X]	120
3.3 Conclusions.....	126

3.4 Experimental.....	127
3.5 References.....	131
Chapter 4: Ruthenium-Catalyzed Enantioselective Hydrogenation of Ketones Without the Use of Protic Amino Ligands.....	134
4.1 Introduction	134
4.1.1 Noyori-Type Hydrogenations.....	134
4.1.2 Protic N-Heterocyclic Carbene Ligands	139
4.1.3 Synthesis of M(protic-NHC) Complexes	142
4.1.4 Reactivity of M(protic-NHC) Complexes.....	149
4.1.5 Mechanistic Aspects of the Formation of M(protic-NHC) Complexes	153
4.2 Results & Discussion	159
4.2.1 Attempted Synthesis of [Cl ₂ Ru(diphosphine)(protic-NHC) ₂] Complexes.....	159
4.2.2 Different Approach to Bifunctional Catalysis Without Amines	165
4.2.3 Catalytic Studies.....	166
4.3 Conclusions.....	179
4.4 Experimental.....	181
4.5 References.....	187
Chapter 5: Conclusions and Future Work.....	192
Appendix A: Crystallographic Data.....	196

List of Schemes

Scheme 1-1: Attempted synthesis of an NHC resulting in an enetetramine.....	5
Scheme 1-2: Fischer's synthesis of the first identified metal-carbene complex.....	8
Scheme 1-3: Preparation of Rh(NHC) complexes utilizing an isolated NHC.....	10
Scheme 1-4: Synthesis and utilization of a Ag(NHC) reagent.	12
Scheme 1-5: Oxidative addition of 2-iodo-imidazolium to form Pd(NHC) and Pt(NHC) complexes.	13
Scheme 1-6: Templated synthesis of M(NHC) from coordinated from 1-azido-2-isocyanobenzene.	16
Scheme 1-7: Relative donor strength of NHC ligands and the symmetric carbonyl frequency of their corresponding [IRh(NHC)(CO) ₂] complexes.....	18
Scheme 1-8: Mechanism of Ru-catalyzed olefin metathesis.	21
Scheme 1-9: Hydrogenation activity of rhodium catalysts with NHC ligands of increasing ring size.	30
Scheme 1-10: Enantioselective hydrosilylation of ketones with chiral Rh(NHC) complexes.	31
Scheme 2-1: Reaction of [ClRh(PPh ₃) ₂ (CO)] with ¹ O ₂ , and release of ³ O ₂	57
Scheme 2-2: Synthesis of bis-IPr rhodium complexes starting from complex 2-10.	62
Scheme 2-3: Relative reactivity of the [ClRh(IPr) ₂ (XY)] complexes.	68
Scheme 2-4: Proposed mechanism for the aerobic oxidation of alcohols by 2-14.	71
Scheme 2-5: Proposed catalytic cycle for Rh-catalyzed oxidation of alkenes to ketones.	72
Scheme 2-6: Crossover experiment between <i>sec</i> -phenethanol and 4-chloroacetophenone.	77
Scheme 2-7: Proposed transfer hydrogenation mechanism by 2-4 and 2-10.....	78
Scheme 2-8: Potential reactions of singlet oxygen with different alkene substrates.	79
Scheme 3-1: Possible products in the hydroformylation of terminal alkenes.	96
Scheme 3-2: Proposed dissociative mechanism for the rhodium-catalyzed hydroformylation of alkenes.	97
Scheme 3-3: Mechanism for isomerization to internal alkenes and resulting aldehydes during hydroformylation.	98

Scheme 3-4: Synthesis of IMes-containing analogues of Wilkinson's catalyst.	104
Scheme 3-5: Base-assisted mechanism for the generation of a rhodium hydride in the hydroformylation reaction.	108
Scheme 3-6: Synthesis of a Rh ^{III} (NHC) complex with a chelating acetate ligand.	115
Scheme 3-7: Possible mechanism for the activation of pre-catalyst 3-11.	124
Scheme 4-1: Ru(Binap) catalyzed hydrogenation of heteroatom functionalized ketones.	135
Scheme 4-2: Representative hydrogenation of a simple ketone using Noyori's bifunctional catalyst.	137
Scheme 4-3: Opposing mechanisms proposed by Noyori (path a) and Bergens (path b) for the enantiodetermining step in Noyori's bifunctional hydrogenation of ketones.	139
Scheme 4-4: <i>C,N</i> -1,2-tautomerization of imidazole and reaction of the conformers with an electrophile.	141
Scheme 4-5: Formation of an Mn(protic-NHC) via the base-promoted tautomerization of an imidazole ligand.	146
Scheme 4-6: Templated synthesis of a Ru(protic-NHC) via annulation of a coordinated 1,2-azidoisocyanide.	147
Scheme 4-7: Formation of Ru(protic-NHC) complex via tandem C-H, N-C activation.	148
Scheme 4-8: Rhodium-catalyzed intra- and intermolecular coupling of olefins to heterocycles.	149
Scheme 4-9: Proposed catalytic cycle for the rhodium-catalyzed annulation of alkene-substituted benzimidazoles.	150
Scheme 4-10: Competitive hydrogenation of a carbonyl containing alkene and a simple alkene with a Rh(protic-NHC) complex.	151
Scheme 4-11: Stoichiometric reactions demonstrating the bifunctional behaviour of 4-7.	152
Scheme 4-12: Proposed mechanism for the formation of Rh(protic-NHC) in catalytic heterocycle olefination.	154
Scheme 4-13: Formation of Ir(protic-NHC) complex and established equilibrium with the corresponding Ir-hydride tautomer.	155
Scheme 4-14: Calculated transition states for the tautomerization of 4-28, and their ΔG^\ddagger	156

Scheme 4-15: DFT calculated mechanism for the NH-tautomerization of 2-methylpyridine in the presence of $[\text{Cl}_2\text{Os}(\text{H})_2(\text{PMe}_3)_2]$	157
Scheme 4-16: Possible mechanisms for regeneration of MH_2 during hydrogenation in 2-propanol.	168
Scheme 4-17: Synthesis of BITr modified Ru(diphosphine) precatalysts.....	176
Scheme 4-18: Intermolecular competition experiment between acetophenone and α -methylstyrene.....	179

List of Figures

Figure 1-1: Frontier orbitals depicting the possible electronic configurations at the carbene carbon.	1
Figure 1-2: Perturbation orbital diagram showing influence of mesomeric effects on the electronic configuration of a carbene carbon.	3
Figure 1-3: Selected examples of isolated NHCs.	6
Figure 1-4: Reagents used to generate free NHCs via elimination of thermally labile groups.	15
Figure 1-5: Models for determining steric parameters of organometallic ligands: a) cone angle; b) percent volume buried ($\%V_{\text{bur}}$).	19
Figure 1-6: Ru(NHC) olefin metathesis catalysts.	22
Figure 1-7: Examples of Pd(NHC) ₁ pre-catalysts.	26
Figure 2-1: Raman spectra of complex 2-4 and its ¹⁸ O ₂ isotopomer.	52
Figure 2-2: Rh L-edge XAS spectra of 2-4 (black), RhCl ₃ -hydrate (blue) and Rh(IPr)(CO) ₂ (OAc) (red). Inset: first derivative plot of data for 2-4 and Rh(IPr)(CO) ₂ (OAc).	54
Figure 2-3: Energy level diagram of DFT-calculated MOs for 2-4t.	55
Figure 2-4: Crystallographically determined structure of 2-10.	59
Figure 2-5: Crystallographically determined structure of the major component in the synthesis of [ClRh(IPr) ₂ (H) ₂] (2-11).	63
Figure 2-6: Crystallographically determined structure of [ClRh(IPr) ₂ (CO)] (2-12).	64
Figure 2-7: Crystallographically determined structure of the paramagnetic impurity [Cl ₂ Rh(IPr) ₂] (2-13) in the synthesis of compound 2-11.	66
Figure 2-8: Effect of HOAc added on aerobic alcohol oxidation catalyzed by 2-4.	74
Figure 3-1: Examples of previously reported Rh(NHC) hydroformylation catalysts.	100
Figure 3-2: Crystallographically determined structure of 3-11.	111
Figure 3-3: Crystallographically determined structure of 3-12.	112
Figure 3-4: Hydroformylation of 1-decene with [XRhIPr(CO) ₂].	122
Figure 4-1: Possible conformations of 4-35 and related complexes.	162
Figure 4-2: Crystallographically determined structure of 4-36.	164

Figure 4-3: Relative acidities of imidazolium and benzimidazolium cations in DMSO and representative polarization of the C2-H bond by coordination of benzimidazole to a metal.....	166
Figure 4-4: Relevant areas of the ^{31}P spectra of compounds 4-38a and 4-38b.....	170
Figure 4-5: Crystallographically determined structure of 4-38a.....	171
Figure 4-6: Chiral atropisomeric diphosphine ligands used in this study.....	176

List of Tables

Table 1-1: Determination of Reaction Enthalpies and BDEs from formation of [Cp*Ru(L)Cl].	17
Table 1-2: Catalytic hydrogenation activity of catalysts 1-20 and 1-21.	27
Table 2-1: Previously reported transition metal η^2 -superoxo complexes.	44
Table 2-2: O-O bond lengths of isolated Rh-(O ₂) complexes in the Crudden laboratory.	47
Table 2-3: Typical examples of rhodium η^2 -peroxo complexes.	48
Table 2-4: Previously reported unusual Rh(O ₂) complexes.	56
Table 2-5: Crystallographic parameters for compounds 2-10, 2-11/2-13 and 2-12.	67
Table 2-6: Optimization of Alcohol Oxidation with Catalyst 2-4.	73
Table 2-7: Catalytic Generation of Singlet Oxygen by 2-4.	80
Table 3-1: Hydroformylation of styrenes with Rh phosphine and NHC catalysts.	105
Table 3-2: Hydroformylation of vinyl arenes with NHC catalyst 3-9.	106
Table 3-3: Hydroformylation of Styrene with Rhodium-Carbene Catalysts.	107
Table 3-4: Crystallographic Data for Compounds 3-11 and 3-12.	113
Table 3-5: Selected IR Stretches of Compounds 3-11 and 3-12.	115
Table 3-6: Optimization of the Hydroformylation of Styrene Using 3-11.	116
Table 3-7: Hydroformylation of Aromatic and Aliphatic Alkenes with 3-11.	118
Table 3-8: Hydroformylation of Aromatic and Aliphatic Alkenes by 3-12.	120
Table 4-1: Catalytic results in the hydrogenation of acetophenone with [Cl ₂ Ru((<i>rac</i>)-Binap)(BIME) ₂] (4-35).	167
Table 4-2: Crystallographic information for compounds 4-36 and 4-38a.	172
Table 4-3: Hydrogenation of acetophenone with [Cl ₂ Ru(diphosphine)] precatalysts bis-substituted with different benzimidazoles.	174
Table 4-4: Optimization of the solvent in hydrogenation of acetophenone by catalyst 4-37b.	175
Table 4-5: Turnover frequencies and enantioselectivities of 1-(triphenylmethyl)-benzimidazole-modified ruthenium-diphosphine precatalysts.	177

Table 4-6: Hydrogenation of various aromatic ketones with 4-38b.	178
---	-----

List of Abbreviations

Ac	acetyl
acac	acetylacetonate
atm	atmosphere(s)
Ar	aryl
B/L	branched-to-linear
BDE	bond dissociation energy
BIMe	1-methylbenzimidazole
Binap	2,2'-bis(diphenylphosphino)-1,1'-binaphthyl
bipy	2,2'-bipyridine
BITr	1-triphenylmethylbenzimidazole
bmim	1-butyl-3-methylimidazolium
bmim-y	1-butyl-3-methylimidazol-2-ylidene
BOC	<i>tert</i> -butoxycarbonyl
Bu	butyl
°C	Celcius
cm	centimeter
CM	cross metathesis
COD	1,5-cyclooctadiene
COE	cyclooctene
Cp	cyclopentadienyl
Cp*	1,2,3,4,5-pentamethylcyclopentadienyl
Cy	cyclohexyl

daipen	1,1-dianisyl-2-isopropyl-1,2-ethylenediamine
dba	dibenzylideneacetone
DPB	dibenzophosphole
DCE	1,2-dichloroethane
DCM	dichloromethane
Dipp	2,6-diisopropylphenyl
DFT	density functional theory
DMC	dimethylcarbonate
dpen	(<i>R,R</i>)-diphenylethylenediamine
<i>ee</i>	enantiomeric excess
EPR	electron paramagnetic resonance spectroscopy
Eq.	equation
equiv	equivalent(s)
Et	ethyl
eV	electron volt
GC	gas chromatography
h	hour(s)
HRMS	high-resolution mass spectrometry
Hz	hertz
IAd	1,3-diadamantylimidazol-2-ylidene
ICy	1,3-dicyclohexylimidazol-2-ylidene
ⁱ Pr ₂ Me ₂	1,3-diisopropyl-4,5-dimethylimidazol-2-ylidene
IMe	1,3-dimethylimidazol-2-ylidene

IMes	1,3-bis(2,4,6-trimethylphenyl)imidazol-2-ylidene
IPent	1,3-bis(2,6-neopentylphenyl)imidazol-2-ylidene
IPr	1,3-bis(2,6-diisopropylphenyl)imidazol-2-ylidene
IR	infrared spectroscopy
ItBu	1,3-bis(<i>tert</i> -butyl)imidazol-2-ylidene
<i>J</i>	coupling constant
K	kelvin
L	ligand
L/B	linear-to-branched
Me	methyl
MeCN	acetonitrile
MeOH	methanol
Mes	2,4,6-trimethylphenyl
^{Me} IiPr	1,3-diisopropyl-4,5-dimethylimidazol-2-ylidene
min	minute
MS	molecular sieves
ND	not determined
NHC	N-heterocyclic carbene
NMR	nuclear magnetic resonance
NR	no reaction
OLED	organic light-emitting diode
Ph	phenyl
ppm	parts per million

Pr	propyl
psi	pounds per square inch
pz ^{iPr} H	3,5-diisopropylpyrazole
RCM	ring-closing metathesis
ROMP	ring-opening metathesis polymerization
sens	sensitizer
SFC	super-critical fluid chromatography
SIMes	1,3-bis(2,4,6-trimethylphenyl)imidazolin-2-ylidene
SIPr	1,3-bis(2,6-diisopropylphenyl)imidazolin-2-ylidene
T	temperature
TFAA	trifluoroacetic acid
THF	tetrahydrofuran
TOF	turn over frequency
TOF-EI	time of flight – electrospray ionization
TolBinap	2,2'-bis(di-4-tolylphosphino)-1,1'-binaphthyl
TON	turn over number
Tp'	hydridotris(3-tert-butyl-5-methylpyrazolyl)borate
Tp''	hydridotris(3-tert-butyl-5-isopropylpyrazolyl)borate
Tp ^{iPr}	hydridotris(3,5-diisopropylpyrazolyl)borate
Tp ^{Me2}	hydridotris(3,5-dimethylpyrazolyl)borate
XAS	X-ray absorption spectroscopy
XylBinap	2,2'-bis(3,5-xylylphosphino)-1,1'-binaphthyl

Chapter 1: Introduction to N-Heterocyclic Carbenes. Synthesis, Transition Metal Coordination Chemistry and Catalytic Applications

1.1 Carbenes

Carbenes are molecules featuring a neutral divalent carbon atom with six valence shell electrons.^{1,2} The geometry of the carbene carbon is either linear or bent corresponding to sp or sp^2 hybridization, respectively. Linear sp -hybridized carbenes possess two non-bonding degenerate $2p$ orbitals at the carbon atom (p_x and p_y), while bending the molecule breaks the degeneracy of these orbitals as it adopts sp^2 -hybridization. This bending causes almost no change in the energy of the p_y orbital and stabilizes the p_x orbital by increasing its s -character; therefore in the bent carbenes these orbitals are generally referred to as the p_π and σ orbitals, respectively (Figure 1-1).

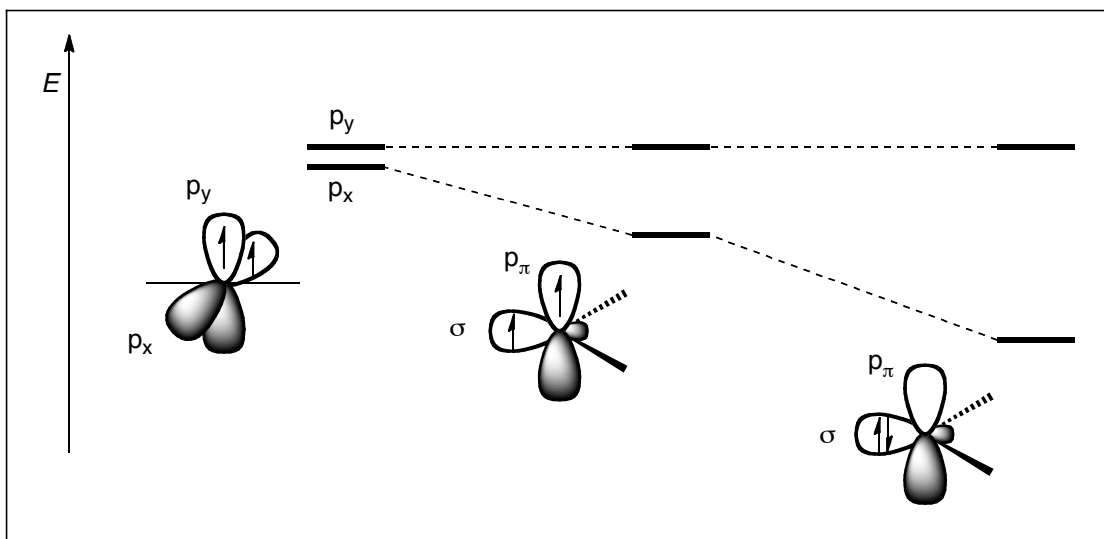


Figure 1-1: Frontier orbitals depicting the possible electronic configurations at the carbene carbon.

Depending on the relative energies of these two orbitals, different singlet or triplet ground state multiplicities can be expected, which fundamentally dictate the reactivity of the carbene.³ Calculations by Hoffmann predicted that an energy difference of 2.0 eV between the p_x and σ orbitals is required to favour a singlet ground state, while energy differences of less than 1.5 eV favour a triplet ground state.⁴ The electronic and steric properties of the substituents attached to the carbene carbon can therefore have a large effect on the molecule's ground state multiplicity. Electronic effects of the substituents at the carbene centre can be assessed in terms of inductive and mesomeric effects.

In terms of inductive effects, it is generally accepted that electronegative substituents stabilize the singlet ground state through σ -electron-withdrawing effects, which stabilize the σ orbital while leaving the p_x orbital relatively unchanged. Substituents with σ -electron donating effects instead destabilize the σ orbital, and thus favour the triplet state. In a specific example, Harrison et al. have computationally demonstrated that for the carbene $R_2C:$ upon changing R from electropositive lithium to hydrogen and eventually electronegative fluorine, the σ orbital is incrementally stabilized and the ground state moves from the triplet to the singlet state. It should be noted, however, that the larger decrease in energy of the σ orbital is seen upon moving from $H_2C:$ to $F_2C:$ and mesomeric effects undoubtedly have a significant role.

Substituents that partake in mesomeric interactions with the carbene centre can be divided into π -electron-donating groups (X, where X = -F, -Cl, -NR₂, OR, etc.) and π -electron-withdrawing groups (Z, where Z = -COR, -CN, -BR₂, etc.). Interaction of carbon's p_x lone pair with the lone pair of an electron-donating substituent increases its

energy relative to the carbon σ orbital, which remains relatively unperturbed. Thus, the p_x - σ gap is increased, and the singlet state is more strongly favoured (Figure 1-2a). Conversely, the presence of π -electron-withdrawing groups does not affect the p_x orbital and instead interacts with the σ orbital stabilizing it, again increasing the p_x - σ gap (Figure 1-2b). So, while inductive effects appear capable of favouring either the singlet *or* the triplet ground state, mesomeric effects – both positive and negative – work to stabilize the singlet ground state.

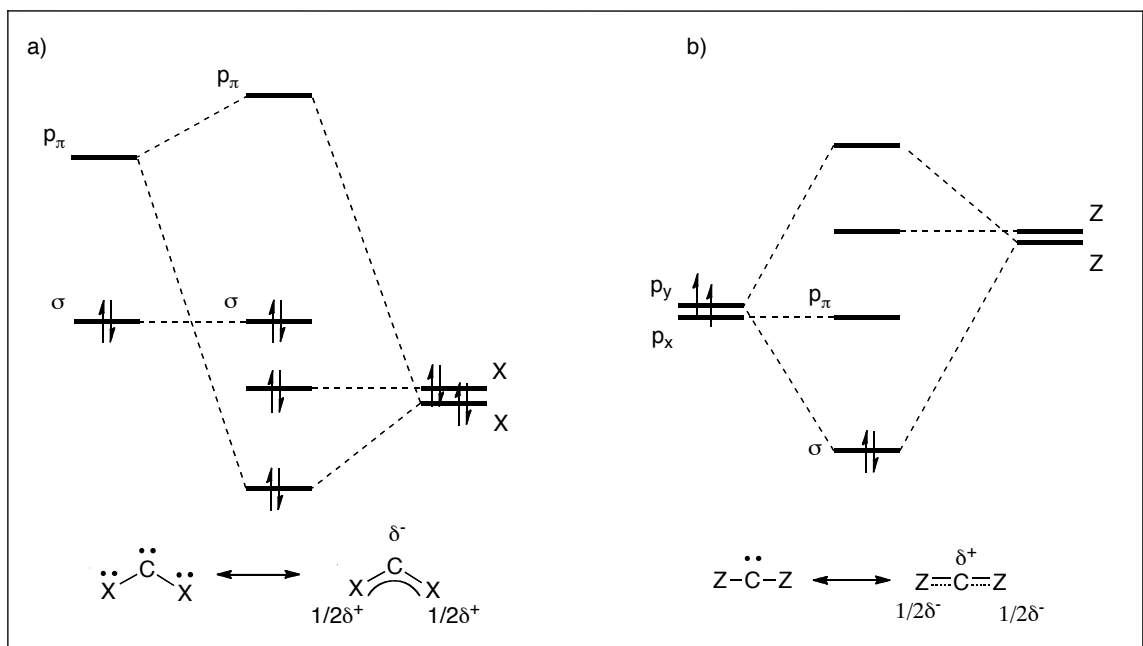


Figure 1-2: Perturbation orbital diagram showing influence of mesomeric effects on the electronic configuration of a carbene carbon.

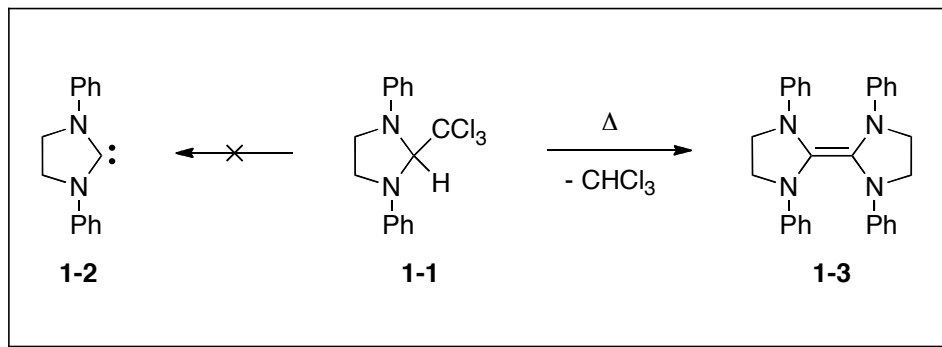
(X,X)-Substituted carbenes are predicted to be bent singlet carbenes, while (Z,Z)-carbenes are predicted to be linear or almost linear singlets.⁵ Both substitution patterns result in multiple bond character across the C-X or C-Z bonds, with donation of the X-substituent lone pairs resulting in a 4-electron 3-centre π system for (X,X)-carbenes, and the π -accepting interaction of Z-substituents resulting in a 2-electron 3-centre π system

for (Z,Z)-carbenes (Figure 1-2). Carbenes with both π -electron donors and acceptors ((X,Z)-carbenes) give singlet carbenes that are almost linear. Interaction of the X-substituent lone pair with the vacant p_y orbital, and interaction of the vacant orbital of the Z-substituent with the filled p_x orbital results in an allene-type electronic structure, as observed by Bertrand et al. in the isolation of stable phosphinosilyl- and phosphinophosphoniocarbenes.^{6,7}

The most representative (X,X)-carbenes are the transient dioxacarbenes⁸ and dihalocarbenes,⁹ and the stable diamino carbenes, of which cyclic diamino carbenes commonly known as N-heterocyclic carbenes (NHC), have become increasingly important ligands in organometallic chemistry and catalysis.¹⁰

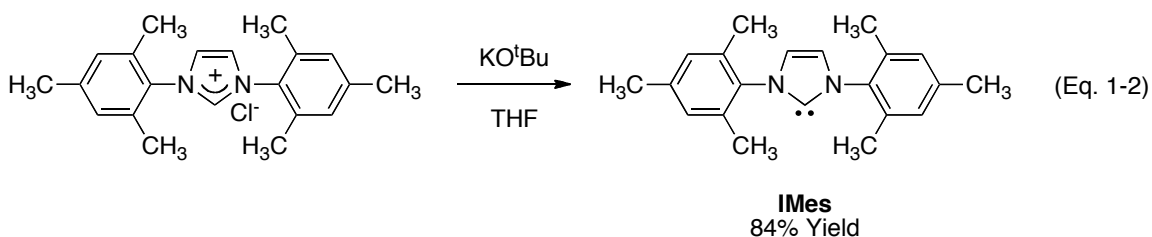
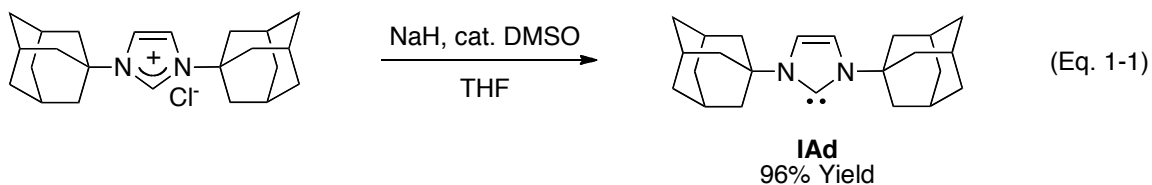
1.2 Isolation of NHCs

A laboratory curiosity for decades, and observed intermediates for long after that, the first stable carbenes were isolated by Bertrand⁶ and Arduengo^{11,12} in the late 1980's and early 1990's. In the 1960's, the laboratory of Wanzlick was interested in the isolation of NHCs, as they believed these would be stable compounds.¹³ The synthesis of 1,3-diphenylimidazolin-2-ylidene (**1-2**) was therefore attempted *via* thermal elimination of chloroform from 1,3-diphenyl-2-trichloromethylimidazolidine (**1-1**), however the corresponding enetetramine **1-3** was recovered instead (Scheme 1-1).¹⁴ Wanzlick's laboratory later proved the existence of the NHC **1-2** *via* deprotonation of the corresponding azolium salt with KO^tBu and trapping it, but was never able to isolate the free NHC.¹⁵

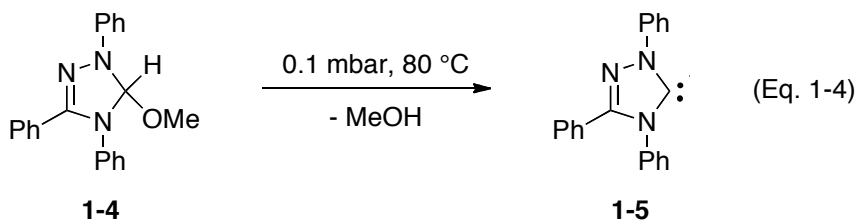
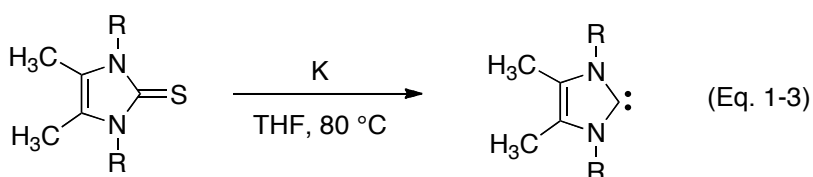


Scheme 1-1: Attempted synthesis of an NHC resulting in an enetetramine.¹⁴

Two decades later using this same principle, Arduengo and coworkers were able to isolate and characterize IAd¹¹ and IMes¹² via deprotonation with NaH/DMSO and KO^tBu, respectively (Eq. 1-1 and 1-2). The steric protection of the carbene carbon by the large N-mesityl and N-adamantyl groups of IMes and IAd, respectively, was thought to provide kinetic stability by preventing the dimerization observed by Wanzlick. Herrmann later demonstrated that imidazolium precursors could be deprotonated to generate NHCs much faster when liquid ammonia was employed as a co-solvent, allowing deprotonation at lower temperatures and thus, providing an exceptionally mild method for the preparation of thermally sensitive NHCs.^{16,17}



Other methods for the preparation of NHCs include the reduction of imidazole-2-thiones with potassium in boiling THF to yield *N*-alkyl substituted NHCs as reported by Kuhn (Eq. 1-3)¹⁸ and the isolation of 1,2,4-triazol-5-ylidene **1-5** via thermal elimination of MeOH from **1-4** in vacuo as reported by Enders (Eq. 1-4).¹⁹



Since the initial findings of Arduengo, Herrmann, Kuhn and Enders, numerous stable NHCs have been isolated, including recent examples in which the carbene carbon is stabilized by a single adjacent heteroatom. Selected examples are shown in Figure 1-3.

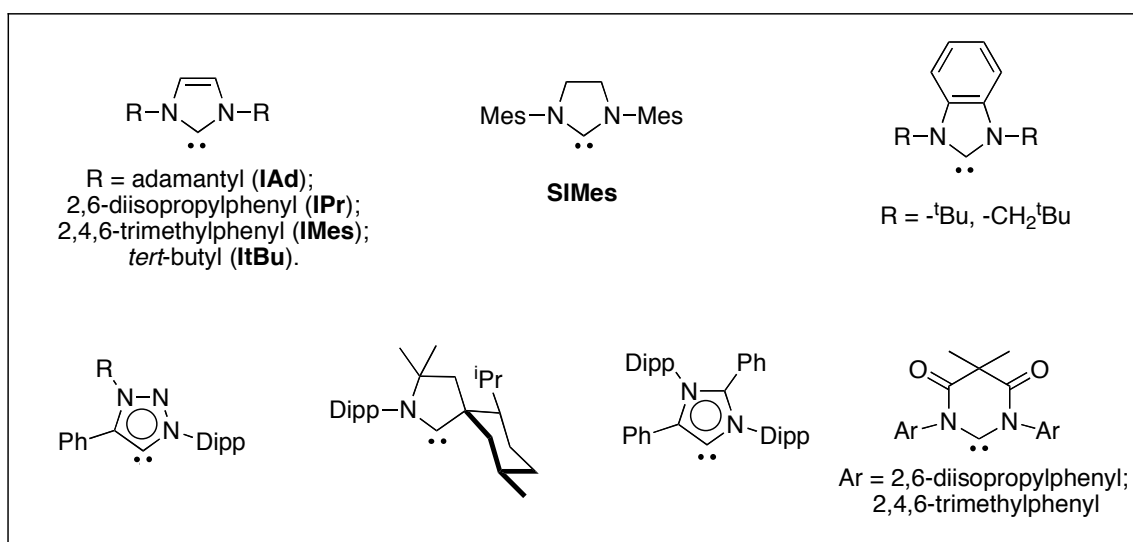
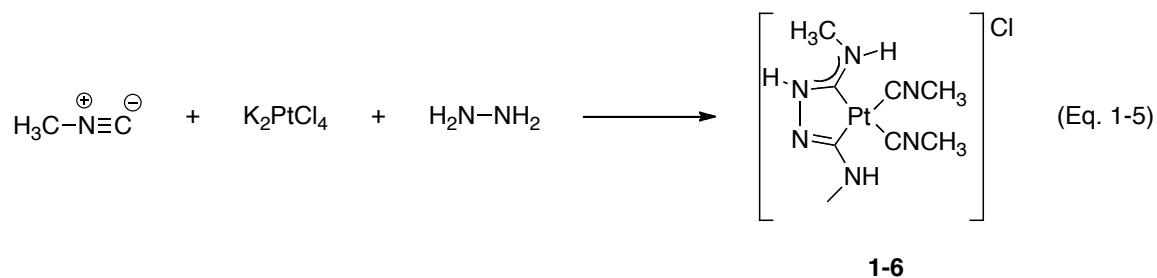


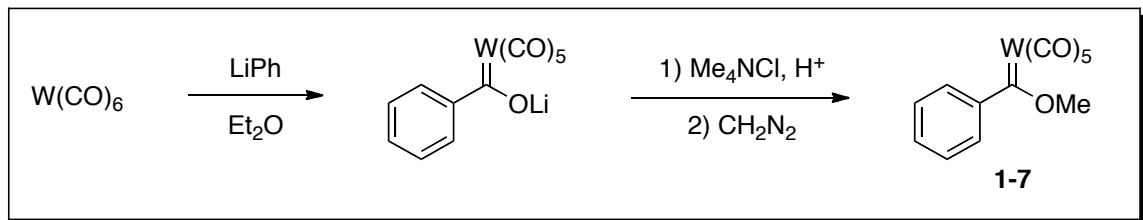
Figure 1-3: Selected examples of isolated NHCs.^{11,12,20,21}

1.3 Early Studies of M(NHC) Complexes

In 1915, Chugaev et al. reported the reaction of hydrazine with an isocyanide and K_2PtCl_4 to yield platinum complex **1-6** (Eq. 1-5).²² Unfortunately, at the time they were without the spectroscopic techniques to fully characterize the resulting complex. Future interest in this reaction, however, led to the synthesis of analogous complexes from hydrazine and isocyanides, and the definitive assignment of the complex as a metal-carbene was made nearly 60 years later.²³

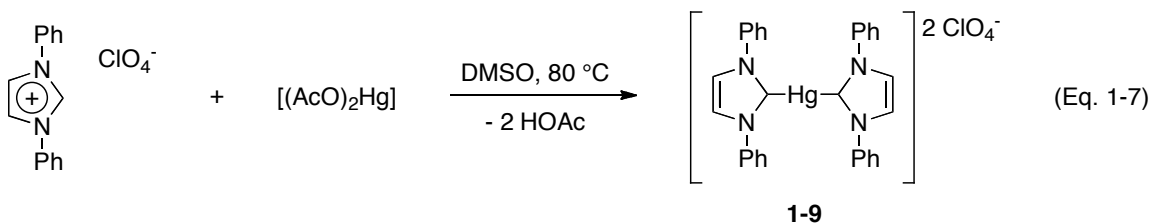
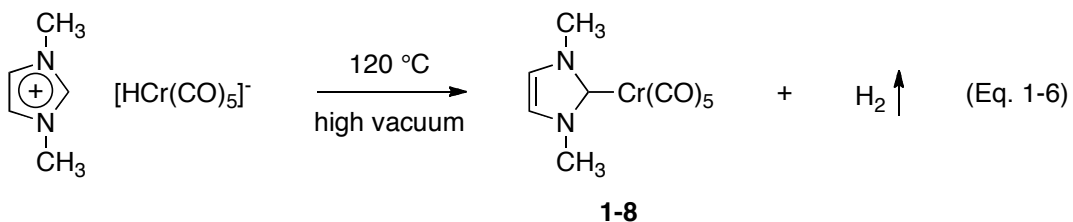


Before the true structure of **1-6** was revealed in 1973, Fischer et al. were the first to report a metal-carbene complex in 1964, when the methylated product from reaction of $\text{W}(\text{CO})_6$ with PhLi was assigned the structure **1-7** (Scheme 1-2).²⁴ The authors extended this methodology to the synthesis of a number of Cr^0 , Fe^0 and Mn^0 complexes with different alkoxy- and alkyl-groups,²⁵ now known as Fischer carbene complexes. Unlike $\text{M}(\text{NHC})$ complexes which possess a single bond from the carbene to the metal and are typically inert to nucleophilic and electrophilic attack, Fischer carbene complexes possess a true metal-carbon double-bond²⁶ and are reactive to electrophiles and nucleophiles at the metal-carbon bond and carbene centre, respectively.²⁶⁻²⁸



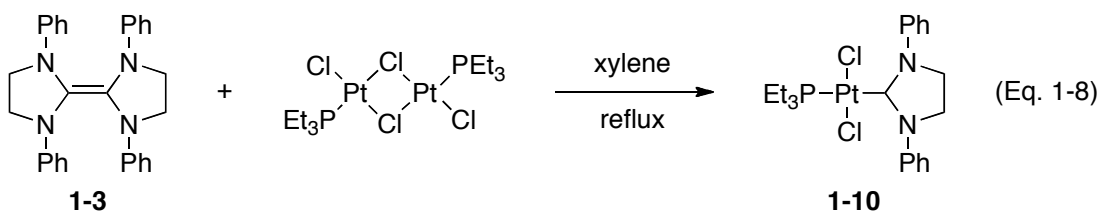
Scheme 1-2: Fischer's synthesis of the first identified metal-carbene complex.²⁴

A few years after Fischer's report of **1-7**, initial publications of M(NHC) complexes appeared independently from the laboratories of Öfele²⁹ and Wanzlick,³⁰ each describing a different *in situ* preparation from the corresponding imidazolium salts. In both instances, the acidity of the imidazolium salt was exploited by reaction with basic metal complexes to afford stable metal-carbene adducts: Öfele reported the synthesis of [Cr(IMe)(CO)₅] (**1-8**) from reaction of a 1,3-dimethylimidazolium salt with [CrH(CO)₅]⁻ (Eq. 1-6); Wanzlick reacted 1,3-diphenylimidazolium perchlorate with mercury(II) acetate to give **1-9** (Eq. 1-7).



From the initial discovery of M(NHC) complexes in the late 1960's until the isolation of free NHCs by Arduengo, the field appeared to receive attention from a single

laboratory. During this twenty-year gap, Lappert carried out considerable research on the synthesis of NHC-containing metal complexes utilizing electron-rich olefins, such as enetetramines, as NHC precursors. Initial communications by Lappert reported that stoichiometric reactions of the diene with platinum group metals^{31,32} gave carbene complexes analogous to those observed by Öfele and Wänzlick. For example, reaction of $[\text{Cl}_2\text{Pt}(\text{PEt}_3)]_2$ with enetetramine **1-3** yielded the platinum-NHC complex **1-10** (Eq. 1-6); the first example of a metal-NHC synthesized by this method.³¹



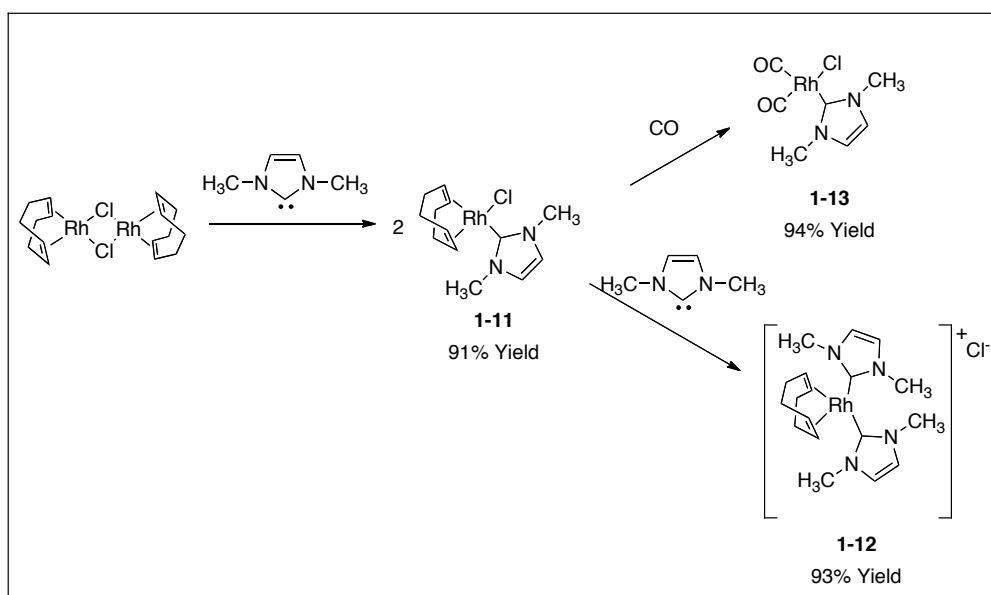
Lappert employed this method to synthesize a multitude of complexes of a variety of transition metals. Starting from various enetetramines, metal carbene complexes were formed by: a) splitting of halide-bridged transition metal dimers; b) displacement of a neutral ligand such as a phosphine, carbon monoxide, or alkene; or c) displacement of an anionic ligand such as a halide, or alkoxide to give cationic complexes. These methods allowed for the isolation and characterization of carbene complexes of a number of transition metals of differing oxidation states including Cr, Mo, W, Fe, Ru, Os, Ni, Rh, Ir, Ni, Pd, Pt and Au.^{27,33}

While the chemistry performed in this area by Lappert and coworkers was quite vast, the method itself was fraught with limitations, and may explain the lack of interest in the field of $\text{M}(\text{NHC})$ complexes during this time given the paucity of reliable syntheses. Difficulties included the requirement of relatively high temperatures to affect enetetramine splitting; the possibility of N,N' -coordination instead of carbene

formation,^{34,35} and the instability of the enetetramine itself, which is air and moisture sensitive and often requires *in situ* preparation followed by immediate reaction with the metal-containing species. In addition, enetetramines with bulky substituents are inaccessible.³⁵ Ironically, this difficulty in the preparation of bulkier enetetramines (R = ^tBu, ⁱPr, cyclohexyl, etc.)³⁵ is the same property that imparts much of the stabilization to isolable carbenes like IAd,¹¹ I^tBu,²¹ IMes¹² and IPr.³⁶

1.4 Synthetic Methods for the Preparation of M(NHC)s

Following the initial isolation of NHCs, Arduengo then published several reports describing the simple coordination of these new compounds to a series of transition metals (Ni,³⁷ Pt,³⁷ Cu,³⁸ Ag³⁸ and Zn³⁹), and main group elements.^{39,40} Herrmann was the first to demonstrate the considerable potential of these complexes in catalysis and in the mid- to late 1990's prepared numerous catalytically relevant transition metal complexes from isolated carbenes or *via in situ* deprotonation of imidazolium salts.⁴¹

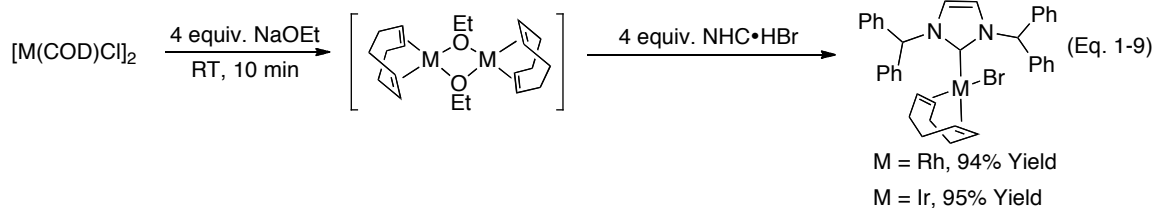


Scheme 1-3: Preparation of Rh(NHC) complexes utilizing an isolated NHC.⁴¹

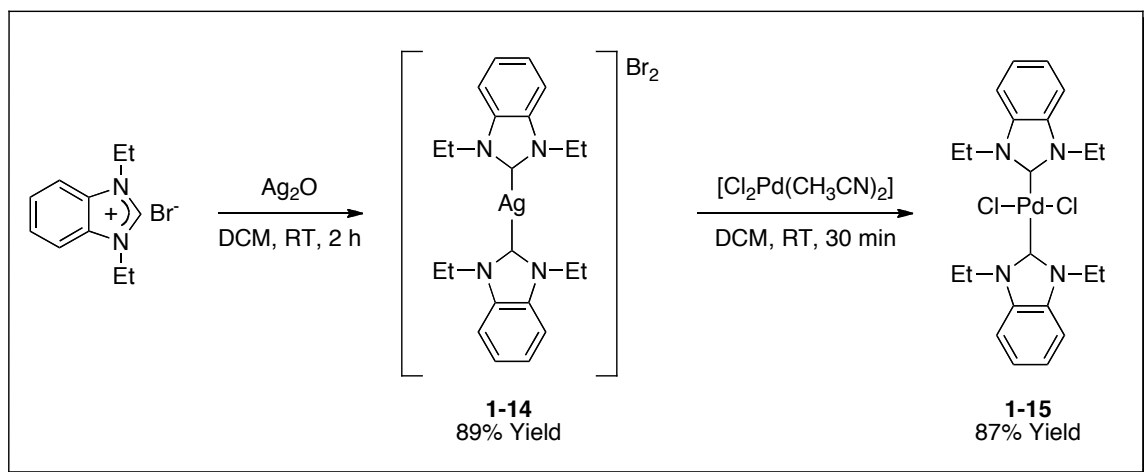
For example, the addition of IMe to $[\text{ClRh}(\text{COD})]_2$ splits the dimer to give complex **1-11**, which can react with a second equivalent of carbene to displace the chloro ligand giving cationic complex **1-12**. Alternatively, exposure to carbon monoxide displaces COD to give **1-13** (Scheme 1-3).¹⁶

The synthesis of an M(NHC) complex by employing the free NHC or the corresponding imidazolium salt and an equivalent amount of base is a reliable method with a considerable number of examples that have been extensively reviewed.^{2,42,43} However, the isolation of the desired NHC is not always trivial and the use of base may be incompatible with the desired target complex. Fortunately, a wide range of alternate methods have been developed given the wide applicability of M(NHC) complexes as catalysts for organic transformations.

For systems that are compatible with basic conditions, but the free NHC is simply unattainable, there are a number of examples that utilize basic metal precursors and imidazolium salts for the synthesis of M(NHC) complexes. For example, reaction of IMe•HI with $[\text{Pd}(\text{OAc})_2]$ or $[(\text{acac})\text{Rh}(\text{CO})_2]$ cleanly generates $[\text{I}_2\text{Pd}(\text{IMe})_2]$ and $[\text{IRh}(\text{IMe})(\text{CO})_2]$, respectively with expulsion of the protonated anionic ligands.^{16,44} An extension of this approach involves generating alkoxy-bridged metal dimers from their corresponding chloro-bridged dimers, followed by reaction with imidazolium salts (Eq. 1-9).⁴⁵ Cyclopentadienyl ligands (Cp) of metallocenes can also be sacrificed in the deprotonation of imidazolium salts generating $[(\text{Cp})\text{M}(\text{NHC})]$ complexes and 1,3-cyclopentadiene.⁴⁶



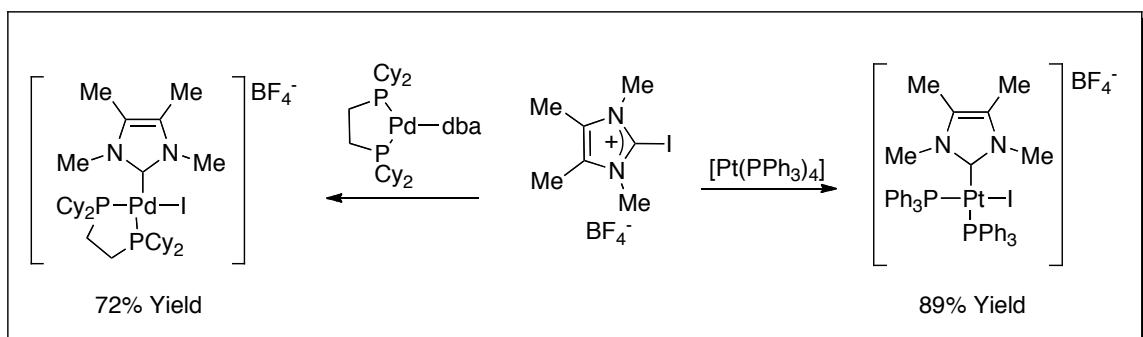
First discovered by Lin in 1998,⁴⁷ the use of Ag(NHC) complexes as transmetallating agents has become one of the most popular methods for the generation of M(NHC) complexes.^{42,48} These reagents are readily prepared by reaction of Ag₂O with the corresponding azolium ion, to give a Ag(NHC) complex, which can then be used to transfer the NHC to other metals. Both formation of the desired Ag(NHC) complex and the subsequent transmetallation can be performed in many solvents without rigorous exclusion of air or moisture, and have even been shown to occur in water.⁴⁹ For example, in the initial report by Lin, reaction of *N,N'*-diethylbenzimidazolium with Ag₂O in DCM gave Ag(NHC) complex **1-14** in 89% yield; this was then reacted with [Cl₂Pd(CH₃CN)₂] to give **1-15** (Scheme 1-4).⁴⁷



Scheme 1-4: Synthesis and utilization of a Ag(NHC) reagent.⁴⁷

The direct oxidative addition of the imidazolium C(2)–H bond to electron-rich late transition metals is another method for the preparation of M(NHC) complexes. The ability of mild bases to promote this reaction, considering the large difference in pK_a between the imidazolium ion and bases such as triethylamine or metal carbonates, suggests that deprotonation of the resulting M(NHC)-hydride is a driving force for this reaction.^{50,51} Early forays into this reaction were described by Cavell and Yates, who explored the addition of C(2)-X bonds of imidazolium salts to various platinum group metals using both experimental and computational methods.⁵²⁻⁵⁴ Oxidative additions of imidazolium ions to Pt^0 and Ni^0 were calculated to be more exothermic than reactions with Pd^0 . For palladium, the exothermicity of the reaction and its reaction barrier is predicted to increase in the order $X = \text{alkyl} < \text{hydrogen} < \text{halide}$.

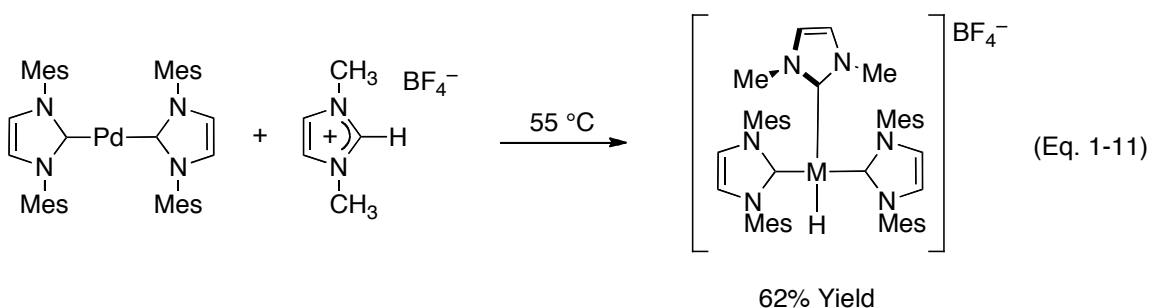
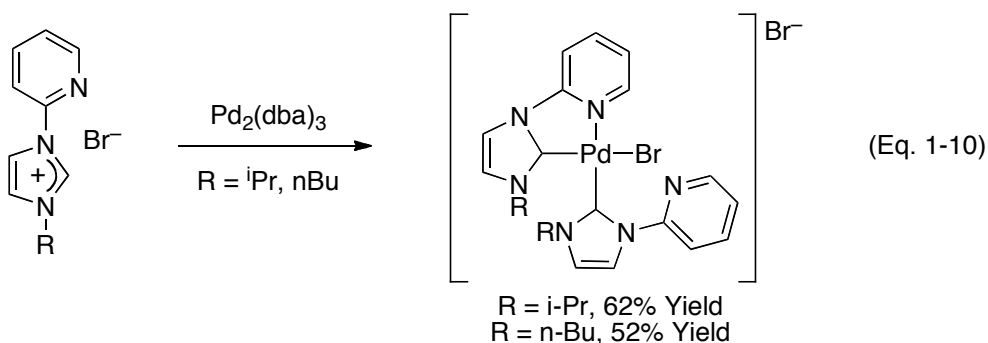
Experimental studies demonstrated that oxidative addition of C(2)–I imidazolium ions to both palladium and platinum was feasible (Scheme 1-5),⁵² however, while analogous C(2)-H imidazolium ions underwent oxidative addition with the same platinum complexes, this was not observed for palladium.⁵³



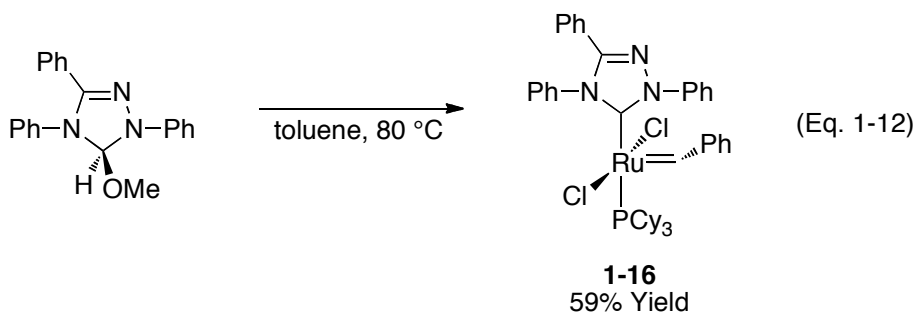
Scheme 1-5: Oxidative addition of 2-iodo-imidazolium to form Pd(NHC) and Pt(NHC) complexes.^{52,53}

Even so, palladium has been shown to oxidatively add the C(2)–H bond of imidazolium ions that possess additional chelating ligands (Eq. 1-10),⁵⁵ or in cases where

reductive elimination of the azolium ion from the resulting complex is disfavored (Eq. 1-11).⁵⁶ The oxidative addition of imidazolium ions to iridium, generating Ir^{III}(NHC)-hydrides has also been reported.^{50,57}



Another alternative to generating and handling the free carbene is to mask the C(2)-position of the imidazol-2-ylidene with various thermally labile groups, such that heating these adducts in the presence of transition metal precursors gives the desired M(NHC) complex (Figure 1-4). In an early example, Grubbs and co-workers found that heating the methanol adduct of Enders NHC **1-5** in a toluene solution of [(PCy₃)₂(Cl)₂Ru=CHPh] displaced one equivalent of tricyclohexylphosphine generating **1-16**, the Enders-NHC analogue of the famous Grubbs II catalyst (Eq. 1-12).⁵⁸



This methodology was extended to imidazoline carbenes with saturated backbones, which can be protected as methanol, *tert*-butanol or chloroform adducts.^{58,59} Even fluorinated aromatics such as H-C₆F₅ can react with carbenes and serve as protecting groups to be eliminated under relatively mild conditions.⁶⁰ Crabtree and co-workers have recently reported the use of imidazole-2-carboxylates⁶¹ as suitable precursors for the formation of a variety of transition metal NHC complexes.^{62,63} These air and moisture stable adducts are prepared from *N*-substituted imidazoles by reaction with dimethylcarbonate giving CO₂ adducts.⁶³

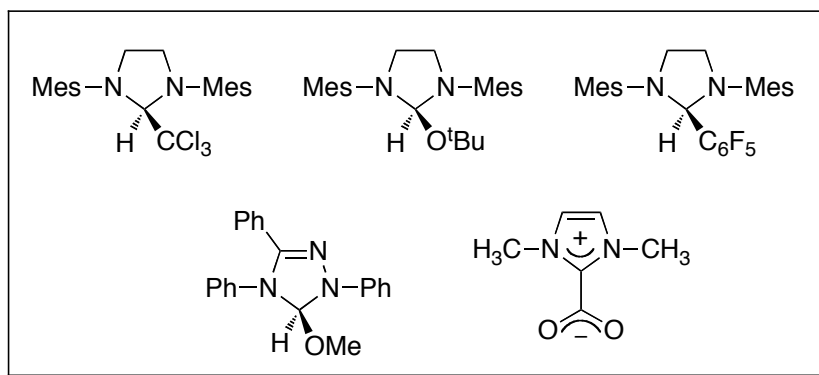
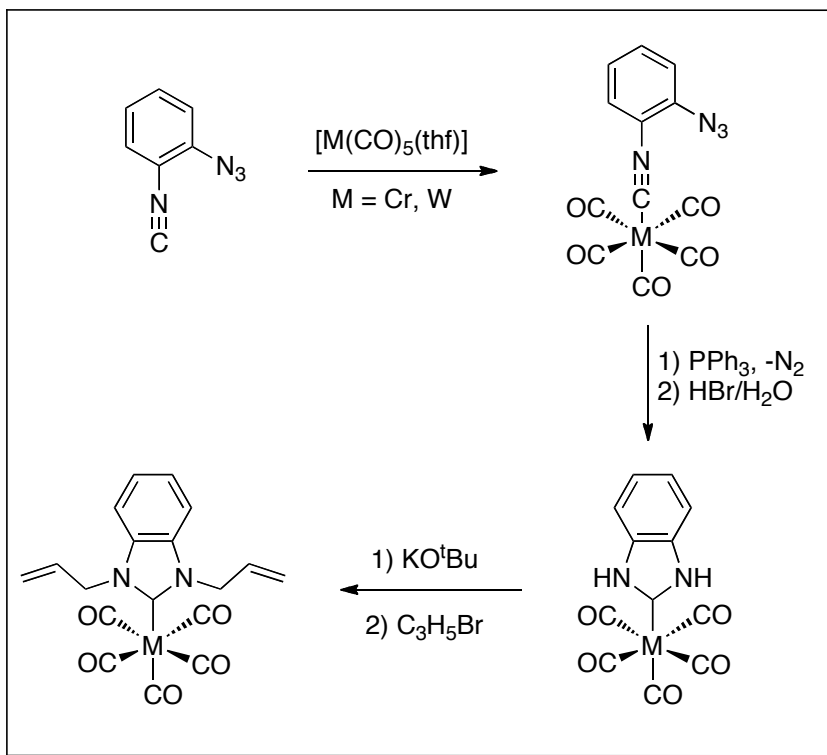


Figure 1-4: Reagents used to generate free NHCs via elimination of thermally labile groups.⁵⁸⁻⁶³

Another alternative is employ ligands that can be chemically transformed to an NHC while bound to a transition metal. Using 1-azido-2-isocyanobenzene⁶⁴ or 2-nitrophenyl isocyanide⁶⁵ as synthons for the unstable 2-amino isocyanide, diprotic

benzannulated NHC–metal complexes can be obtained, which can be alkylated to give *N,N'*-disubstituted benzimidazol-2-ylidenes (Scheme 1-6). Recently this methodology has been applied to the synthesis of Ru(NHC) complexes.⁶⁶



Scheme 1-6: Templated synthesis of M(NHC) from coordinated from 1-azido-2-isocyanobenzene.⁶⁴

1.5 Steric and Electronic Factors of NHC Ligands

A fundamental understanding of the electronic and steric parameters of a class of ligands is paramount to the development of organometallic synthesis and catalytic design. Both phosphines and NHCs are neutral σ -donating ligands, so it is not surprising that NHCs have seen the most interest as phosphine replacements in homogeneous catalytic reactions such as olefin metathesis and cross coupling reaction. Having assumed this role, NHC ligands have been probed in a variety of studies undertaken to make

systematic comparisons between their steric and electronic properties with those of phosphine ligands. Pioneering work by Tolman defined and quantified the electronic and steric parameters of phosphine ligands.⁶⁷ Thus, studies with NHC ligands have followed a similar vein, in search of similar, standardized parameters.

The strength of the M-C_{NHC} bond has been probed experimentally using [Cp*Ru(L)Cl] as a model system. Relative bond dissociation energies (BDE) were determined using anaerobic solution calorimetry⁶⁸ to measure the enthalpy from the reaction of [Cp*RuCl]₄ with four equivalents of a phosphine or NHC to afford [Cp*Ru(L)Cl]; the BDE was then obtained by dividing the enthalpy of reaction by the number of bonds formed (Table 1-1).⁶⁹⁻⁷¹ All the NHCs studied had higher BDEs than the strongly donating alkyl phosphines PⁱPr₃ and PCy₃, except IAd. This anomaly is likely due to the large *N*-adamantyl groups, which hinder efficient overlap of the carbene lone pair with metal orbitals. Thus, it appears that NHCs form stronger bonds to transition metals than even the most strongly donating alkyl phosphines.

Table 1-1: Determination of Reaction Enthalpies and BDEs from formation of [Cp*Ru(L)Cl].⁷¹

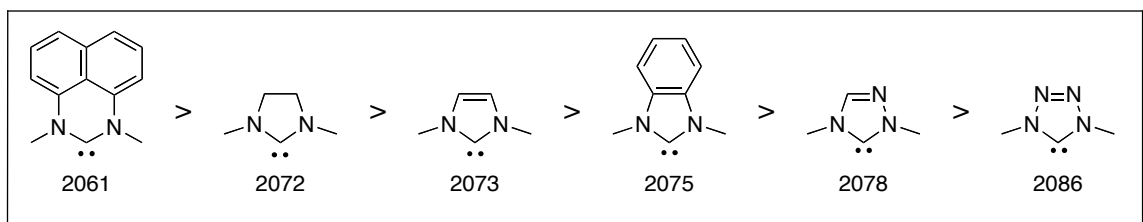
$$[\text{Cp}^*\text{RuCl}]_4 + 4 \text{ L} \xrightarrow[\text{THF}]{} 4 [\text{Cp}^*\text{Ru}(\text{L})\text{Cl}]$$

Entry	Ligand	ΔH_{rxn} (kcal/mol)	BDE (kcal/mol)
1	SIMes	-67.1	16.8
2	IMes	-62.6	15.6
3	SIPr	-48.5	12.1
4	IPr	-44.5	11.1
5	PCy ₃	-41.9	10.5
6	P ⁱ Pr ₃	-37.4	9.4

Numerous studies have been reported in which the $\nu(\text{CO})$ stretching frequencies of M(NHC)-carbonyl compounds have been compared. This was the approach used to

calculate the Tolman electronic parameter (TEP) in phosphines, defined as the symmetric carbonyl stretching frequency of a $[\text{Ni}(\text{CO})_3(\text{L})]$ complex.⁷² Thus, the carbonyl stretching frequency of $[\text{Ni}(\text{CO})_3(\text{NHC})]$ complexes has been determined both experimentally⁷³ and computationally⁷⁴ for a variety of NHCs. Interestingly, while all NHCs studied appear to be slightly stronger donors than the most electron-rich phosphines, the difference between different NHCs is slight and they appear to fall within a very narrow range.

Herrmann and co-workers have done a similar study with $[\text{IRh}(\text{CO})_2(\text{L})]$ systems in which all the NHCs employed were methylated at the nitrogen flanking the carbene carbon.⁷⁵ By fixing this variable, the difference observed in the symmetric $\nu(\text{CO})$ frequencies could be attributed solely to electronic factors of the NHC framework. Among the observed trends perimidin-2-ylidene was the most electron-donating carbene probed, little difference was observed between the strongly donating saturated and unsaturated imidazol-2-ylidenes, and the tetrazolinyliidene was the least donating (Scheme 1-7).



Scheme 1-7: Relative donor strength of NHC ligands and the symmetric carbonyl frequency of their corresponding $[\text{IRh}(\text{NHC})(\text{CO})_2]$ complexes.⁷⁵

The Tolman cone angle, used to define the steric requirements of monodentate phosphine ligands, is defined by placing the metal at the vertex and the atoms at the perimeter of the cone (Figure 1-5a).⁶⁷ This model is not sufficient to define the steric

environment of NHC ligands due to their unique and unsymmetrical structure, and other parameters have therefore been explored. Cavallo and Nolan have proposed a new model to define the steric requirements of NHC ligands known as the “percent buried volume” or $\%V_{\text{bur}}$. It is defined as the percent volume of a sphere – of defined radius with the metal at its centre – occupied by the ligand (Figure 1-5b).^{71,76} The values are obtained computationally with crystallographic data using software developed by Cavallo and coworkers which is now available on-line and is applicable to all classes of organometallic ligands.^{77,78}

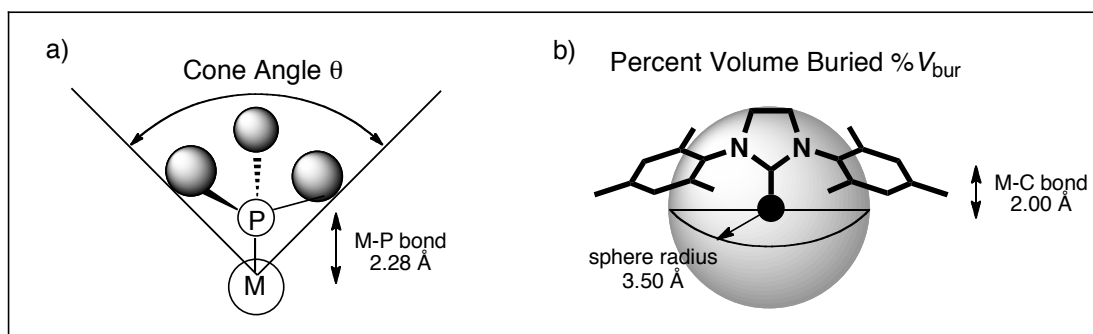


Figure 1-5: Models for determining steric parameters of organometallic ligands: a) cone angle; b) percent volume buried ($\%V_{\text{bur}}$).^{67,71,76}

Initial studies with the model demonstrated a strong correlation between the calculated $\%V_{\text{bur}}$ value and the BDE for $[\text{Cp}^*\text{Ru}(\text{NHC})\text{Cl}]$ complexes;⁷¹ correlation between $\%V_{\text{bur}}$ values and cone angles of phosphines has also been demonstrated.⁷⁶ When comparing NHCs it is interesting to note that while the *N*-alkyl substituted carbenes appear to have fixed $\%V_{\text{bur}}$ values, the values for *N*-aryl substituted carbenes are highly dependant on the metal fragment and demonstrate significant steric flexibility. While IAd and ItBu are more sterically demanding than IPr or SIPr in metal complexes of high coordination number, the trend is reversed for low coordination number metal complexes.

Given the nearly identical donor capabilities of these ligands, the tremendous success achieved with IPr and SIPr relative to other NHCs may be attributable to this steric flexibility.

1.6 Catalytic Applications of M(NHC) Complexes

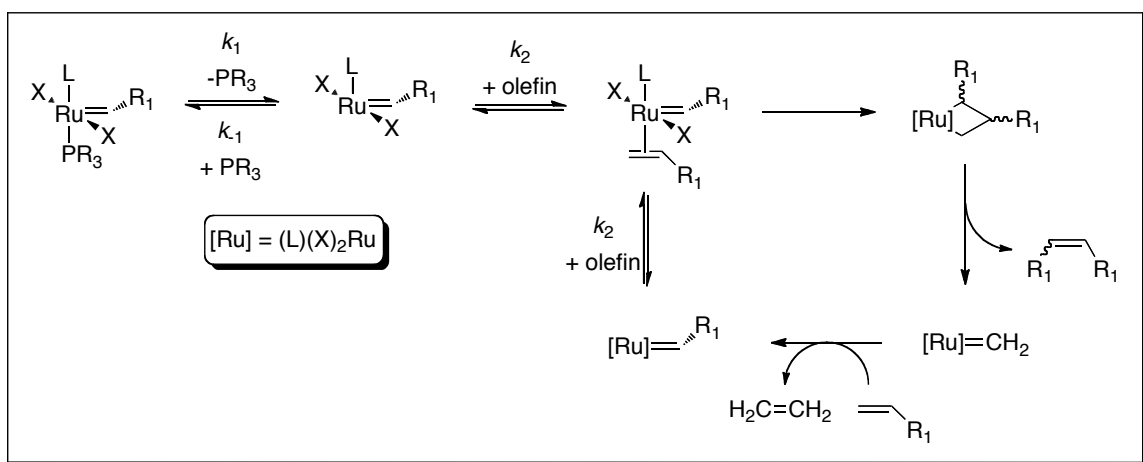
The frequent comparisons NHCs have drawn to phosphines, plus the added stability of the resulting M(NHC) complexes has led to their use as phosphine replacements in a wide range of transition-metal catalyzed reactions.^{10,79} The most notable examples of this are ruthenium-catalyzed olefin metathesis⁸⁰ and palladium-catalyzed cross-coupling reactions,⁸¹ two reactions which have seen a great expansion of scope and diversity as a result of employing NHCs in place of phosphines. Along with these two applications, Rh(NHC)-catalyzed reactions will also be discussed as they are of pertinent interest to our research laboratory.⁸²

1.6.1 Ru(NHC)-Catalyzed Olefin Metathesis

The area of catalysis in which the application of NHC ligands has had the largest impact is likely ruthenium-catalyzed olefin metathesis.⁸³ A powerful method for the formation of C-C bonds in both polymers and small molecules, the developments in this field were of such high achievement that Chauvin, Schrock and Grubbs received the Nobel Prize in 2005 for their contributions to this area.⁸⁴ Ruthenium complexes of the formula $[(L)_2(X)_2Ru=CHR]$, have been well-studied in many types of metathesis reactions, including ring-closing metathesis (RCM), cross-metathesis (CM) and ring-opening metathesis polymerization (ROMP).⁸⁵ The ruthenium complex

$[\text{Cl}_2(\text{PCy}_3)_2\text{Ru}=\text{CHPh}]$ - affectionately known as Grubbs I⁸⁶ - suffers from limited stability and low activity towards substituted double bonds.

Detailed mechanistic and theoretical studies led to the widely accepted “dissociative” mechanism for ruthenium-catalyzed olefin metathesis as shown in Scheme 1-8. Initial phosphine dissociation (k_1) was determined to be the rate determining step, and implied that the use of *stronger* donor ligands to facilitate this step would improve catalytic activity; a hypothesis that paved the way for the application of NHCs in this reaction.^{87,88}



Scheme 1-8: Mechanism of Ru-catalyzed olefin metathesis.^{87,88}

Herrmann was the first to venture into this forum, synthesizing a number of bis(NHC)-analogues of the Grubbs I catalyst, which, although stable, were not efficient catalysts.⁸⁹ This report was quickly followed by nearly simultaneous reports from the laboratories of Fürstner and Herrmann,⁹⁰ Grubbs⁹¹ and Nolan,^{69,92} who independently synthesized olefin metathesis catalysts of the formula $[(\text{NHC})(\text{PR}_3)\text{Cl}_2\text{Ru}=\text{CHPh}]$. The greatest success was found with SIMes,⁷¹ and $[(\text{PCy}_3)(\text{SIMes})\text{Cl}_2\text{Ru}=\text{CHPh}]$ is now known as the Grubbs II catalyst.

Mechanistic studies performed on these catalysts revealed, however, that the increase in catalytic activity was not due to a faster generation of the active species through dissociation of the phosphine, but their preferential binding of olefins *versus* phosphines (k_2/k_{-1}), which drives the reaction forward.⁸⁸ With this in mind considerable efforts were made towards the design of NHC-containing pre-catalysts that produce the same propagating species, but with faster initiation rates. Significant advances in this area include *o*-isopropoxybenzylidene Hoveyda catalyst **1-17**,⁹³ the pyridine containing Grubbs-Love catalyst **1-18**,⁹⁴ and the coordinatively unsaturated phosphonium alkylidene catalyst **1-19** by Piers (Figure 1-6).⁹⁵ These second generation NHC-containing catalysts extended the scope of these reactions permitting CM and RCM to afford tri-substituted olefins, as well as RCM and CM of electron-deficient olefins (Eq. 1-13 – 1-15), previously only accessible with molybdenum catalysts.

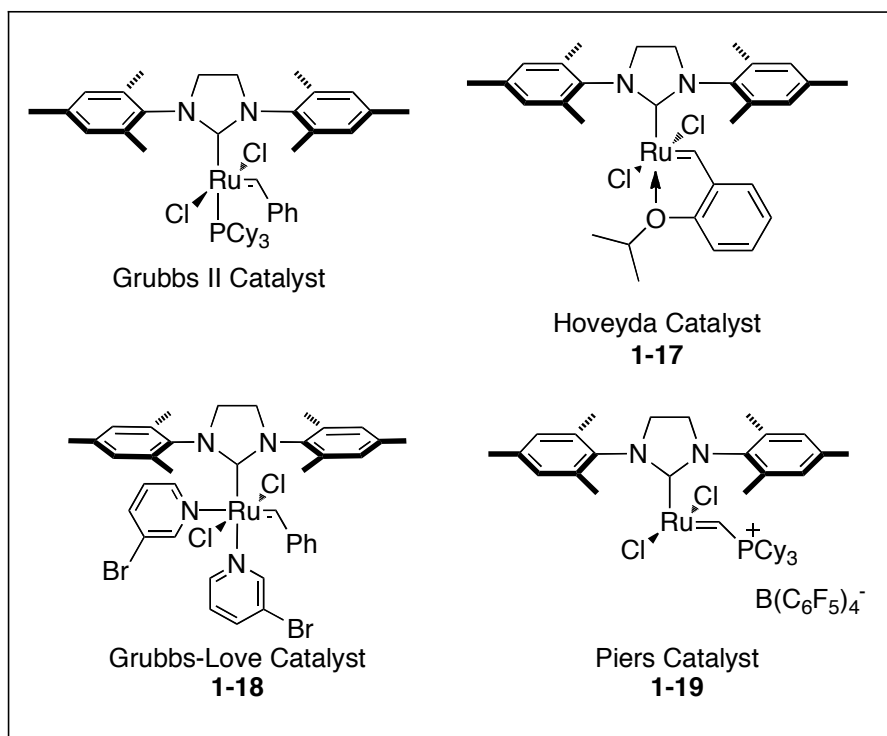
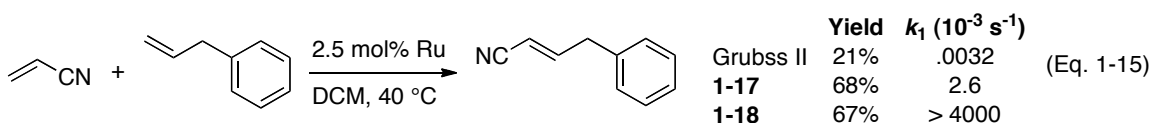
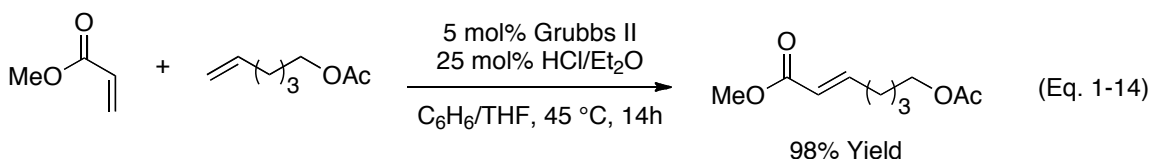
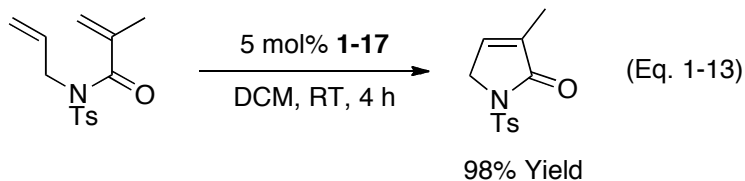


Figure 1-6: Ru(NHC) olefin metathesis catalysts.^{91,93-95}

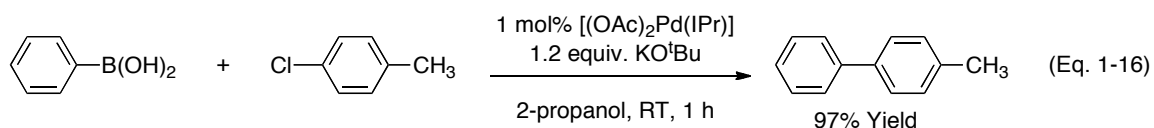


1.6.2 Pd(NHC)-Catalyzed Cross Coupling Reactions

In addition to metathesis chemistry, NHC-metal complexes have been successfully employed in a variety of palladium catalyzed cross-coupling reactions.⁸¹ In the past few decades, these types of transformations have blossomed into some of the most powerful methods for the formation of C-C, C-N and C-O bonds. The first step in the majority of these reactions is the oxidative addition of an organohalide or triflate to a Pd(0) species. While numerous catalytic systems exist for the activation of C(sp²)-I and C(sp²)-Br bonds, due to their increased stability, activation of C(sp²)-Cl bonds is a considerably greater challenge. The use of NHCs as ancillary ligands in these types of reactions has allowed the use of aryl chlorides as coupling partners under relatively mild conditions.

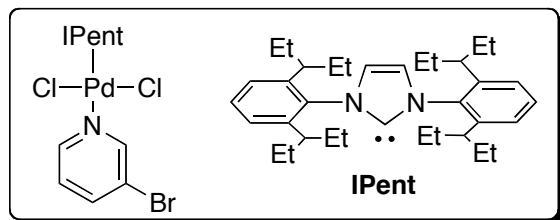
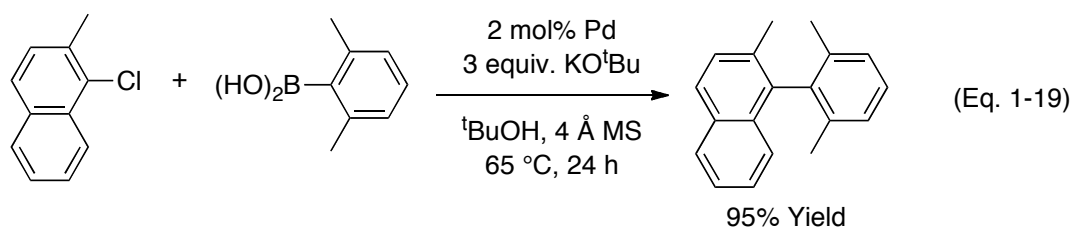
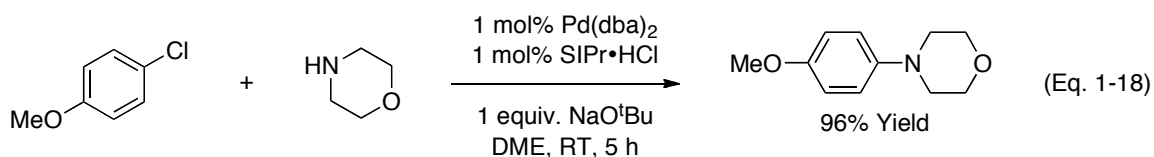
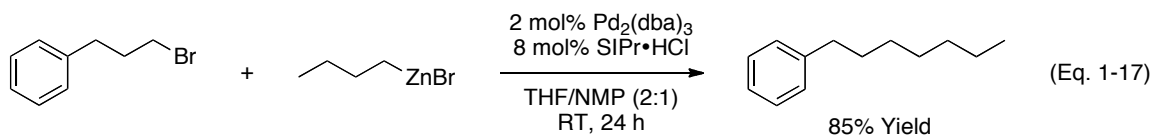
It is generally accepted that the oxidative addition of aryl halides in these reactions occurs from an unsaturated Pd⁰ complex having one or two neutral donor

ligands. For aryl chlorides, both experimental^{96,97} and theoretical⁹⁸ studies have indicated that a dissociative pathway is favoured, in which highly coordinatively unsaturated Pd(L)₁ complexes are the active species. Therefore, ligands employed for this transformation must be bulky to promote formation of the Pd(L)₁ species and strongly basic such that this low co-ordinate Pd species is capable of activating the aryl chloride. These characteristics are obviously perfectly met in the larger NHCs such as IMes, IPr and ItBu, which are highly basic and sterically encumbering and therefore not surprisingly are some of the most successful ligands for promoting the palladium catalyzed coupling of aryl chlorides.⁸¹ For example, [(OAc)₂Pd(IPr)] is capable of effecting the Suzuki-Miyaura coupling of aryl chlorides at room temperature in ⁱPrOH (Eq. 1-16).⁹⁹



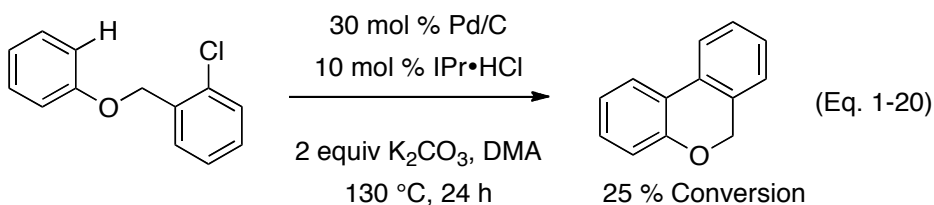
Pd(NHC) complexes have also proven to be efficient catalysts for a wide variety of cross coupling reactions including more challenging transformations such as room temperature alkyl/alkyl Negishi couplings (Eq. 1-17),¹⁰⁰ Buchwald-Hartwig amination of aryl chlorides (Eq. 1-18),¹⁰¹ and the Suzuki-Miyaura coupling of sterically encumbered aryl chlorides (Eq. 1-19).¹⁰² Notably, for all of these reactions IPr or SIPr showed superior results compared to all other ligands employed (including IMes and ItBu), and development of the new 2,6-neopentyl substituted ligand IPent, which is even more sterically demanding, has afforded further expansion of substrate scope in these reactions as demonstrated in Eq. 1-19.¹⁰² As mentioned earlier, this prolific reactivity compared to

other NHCs is likely a result of the steric flexibility of both the aryl rings and their *ortho*-substituents,⁷⁶ as well as the remarkable stability of the M-C_{NHC} bond and high reactivity of Pd(NHC)₁ species .



Consistent with the high catalytic activity of Pd(L)₁ type systems, a multitude of *in situ* generated catalytic systems have shown repeatedly that the optimal Pd/NHC ratio is 1:1.¹⁰⁰ While there are scattered reports in which the use of excess NHC precursor leads to more beneficial results, this has been attributed to the ability of this excess ligand to regenerate catalytically active Pd(NHC) species after loss of the NHC via decomposition reactions. For example, Fagnou et al. reported that the addition of excess IPr•HCl in systems employing precatalyst [(OAc)₂Pd(IPr)(H₂O)] leads to increases in

turnover numbers for intramolecular direct arylation of aryl chlorides.¹⁰³ Furthermore, even though Pd/C showed no activity itself, the addition of IPr•HCl under catalytic conditions resulted in the formation of an active catalyst (Eq. 1-20).



Consistent with these results, detailed mechanistic studies by Cloke et al. on the oxidative addition of chlorobenzene to Pd(NHC)₂ indicated a dissociative pathway in which Pd(NHC) is the active species.⁹⁷ Building on these observations, a great deal of work has been put into the synthesis of well-defined palladium precatalysts featuring a single NHC ligand (Figure 1-7).^{81,104}

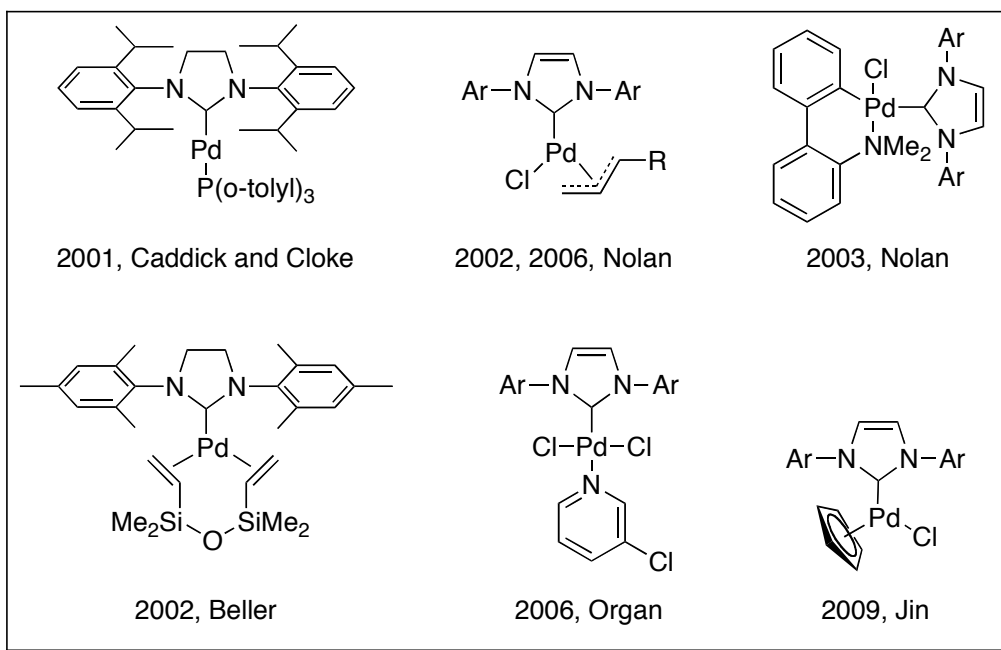
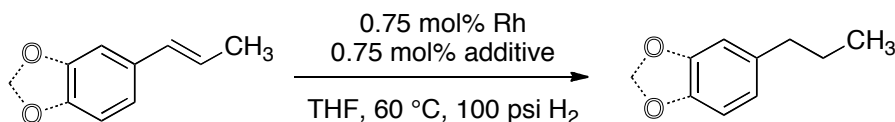


Figure 1-7: Examples of Pd(NHC)₁ pre-catalysts.^{81,104}

1.6.3 Rh(NHC)-Catalyzed Reactions

Rh(NHC) complexes have been employed in a variety of different reactions including the hydrosilylation of unsaturated organic functional groups and the arylation of carbonyl compounds; previous studies in the Crudden laboratory have explored the chemistry of Rh(NHC) complexes as catalysts for the hydrogenation and hydroformylation of alkenes.⁸² The latter of these reactions will be discussed in detail in Chapter 3. Wilkinson's catalyst, [ClRh(PPh₃)₃] (**1-20**),¹⁰⁵ has been an integral part of the development of homogeneous catalysis and is an excellent catalyst for the hydrogenation of alkenes.¹⁰⁶ Therefore, our group has synthesized a number of complexes of the formula *cis*-[ClRh(IMes)(PR₃)₂] (**1-21**), in which IMes replaced one of the phosphines of **1-20**, and tested them as catalysts for the hydrogenation of styrene derivatives (Table 1-2).¹⁰⁷⁻¹⁰⁹

Table 1-2: Catalytic hydrogenation activity of catalysts **1-20** and **1-21**.^{107,108}

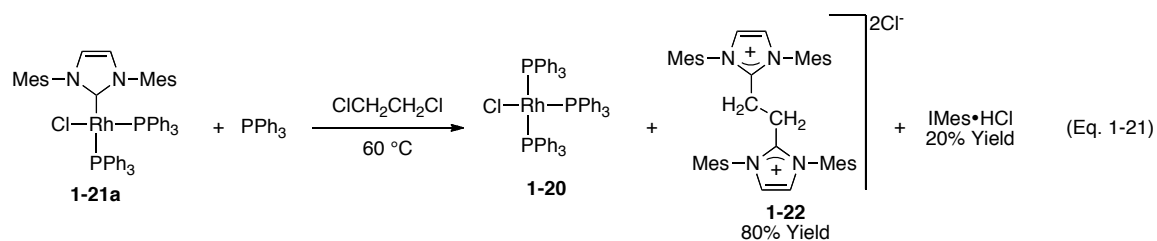


Entry	Catalyst (phosphine)	Substrate	TOF (h ⁻¹) and Additive Effects		
			none	CuCl	DCE
1	1-21a (PPh ₃)	(<i>E</i>)-β-methylstyrene	24	331	–
2	1-21a (PPh ₃)	isosafrole ^a	50	430	110
3	1-21b (P-(<i>p</i> -F-C ₆ H ₄) ₃)	(<i>E</i>)-β-methylstyrene	43	161	–
4	1-21c (P-(<i>p</i> -OMeC ₆ H ₄) ₃)	(<i>E</i>)-β-methylstyrene	5	417	–
5	1-20 (PPh ₃)	(<i>E</i>)-β-methylstyrene	297	243	–
6	1-20 (PPh ₃)	isosafrole ^a	250	300	–

^aReaction performed with 200 psi H₂.

Initial studies indicated that complex **1-21a** (R = Ph) was less active than **1-20** due to slower dissociation of the phosphine *trans* to IMes, which generates the active catalyst (compare entries 2 and 6, Table 1-2).¹⁰⁷ Addition of CuCl, a known phosphine scavenger, to the catalytic reaction caused a dramatic increase in the rate of hydrogenation and ultimately yielding better results than obtained with Wilkinson's catalyst **1-20**. The *p*-fluorophenyl derivative **1-21b** was found to have the highest inherent activity, however, addition of CuCl gave only a modest four-fold rate increase (entry 3). Conversely, the *p*-methoxyphenyl derivative **1-21c** showed a greater than 80-fold rate increase upon addition of CuCl (entry 4).¹⁰⁸

Interestingly, during the course of our laboratory's study on the exchange rate of the phosphine *trans* to IMes, heating of **1-21a** in DCE resulted in formation of [ClRh(PPh₃)₃] (**1-20**), IMes•HCl and dication **1-22**, resulting from the reaction of two equivalents of IMes with the chlorinated solvent (Eq. 1-21).¹⁰⁷

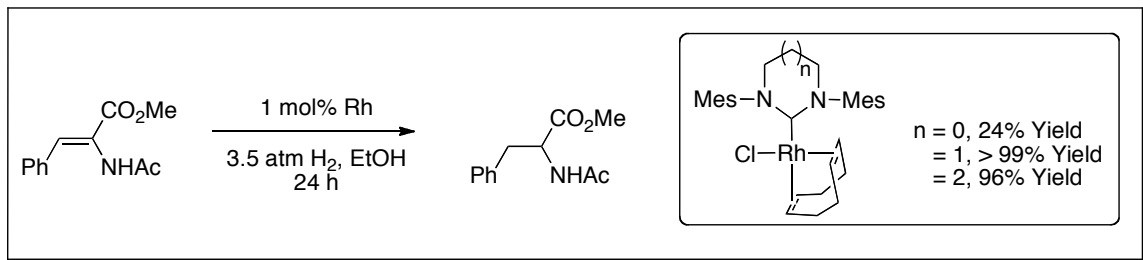


This has significant implications for reactions employing M(NHC)-based catalysts of unknown stability, because in this case a more active catalyst (**1-20**) is generated by loss of the carbene ligand. Consistent with this hypothesis, use of DCE as an additive in the hydrogenation of isosafrole with complex **1-21a** resulted in increased activity (entry 1, Table 1-2), presumably due to formation of **1-20**, and elimination of IMes as **1-22**. Thus, while M(NHC) complexes are typically seen as robust, stable alternatives to their phosphine analogues, they are still prone to degradation and

decomposition reactions under catalytic conditions that warrant serious consideration during catalytic studies.¹¹⁰

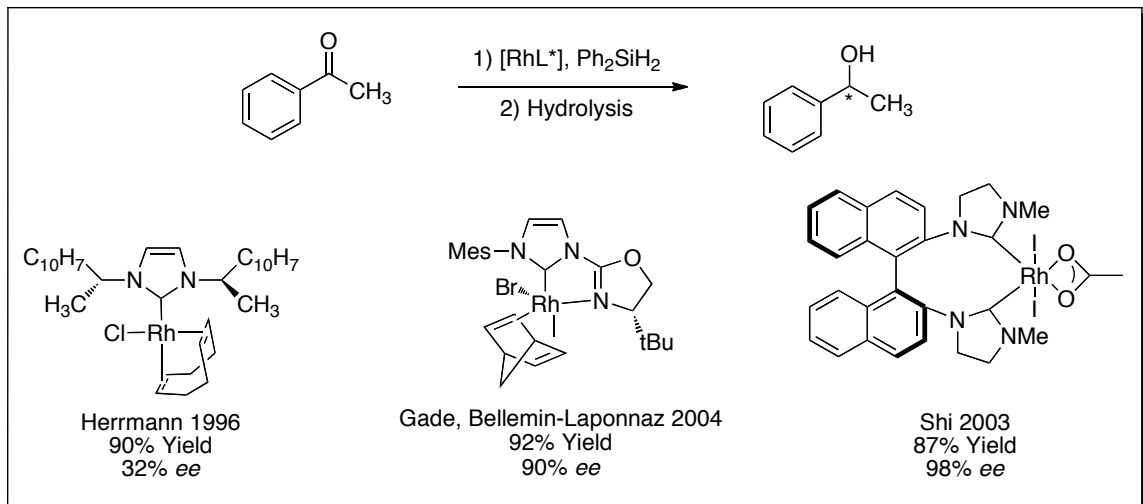
Other laboratories have reported the use of Rh(NHC) complexes as hydrogenation catalysts. Herrmann performed a systematic optimization of [CIRh(ICy)(COD)] (**1-23**) for the hydrogenation of cyclohexene.¹¹¹ The use of additive amounts of phosphine was necessary to prevent degradation of the catalyst, as hydrogenation of the COD ligand results in reactive, coordinatively unsaturated Rh(NHC) complexes prone to decomposition. Consistent with this, the use of a coordinating solvent such as ethanol often yields improved results. As seen with our catalyst **1-21**, under optimized conditions **1-23** was still an inferior catalyst to Wilkinson's catalyst **1-20**.

A recent report by Cavell and coworkers has looked at the use of 6- and 7-membered NHCs in complexes of the formula [CIRh(NHC)(COD)] as catalysts for the hydrogenation of alkenes.¹¹² The increased N-C-N angle in the larger ring sizes brings the *N*-R groups closer to the metal stabilizing these catalysts under hydrogenation conditions in the absence of additive phosphine ligands, resulting in improved activity *versus* their C-5 congeners (Scheme 1-9). Although decomposition was still observed in these reactions, this was avoided by employing an NHC featuring a weakly coordinating *ortho*-methoxy substituent on one or both of the *N*-aryl groups; this also concomitantly resulted in an even more active catalyst.



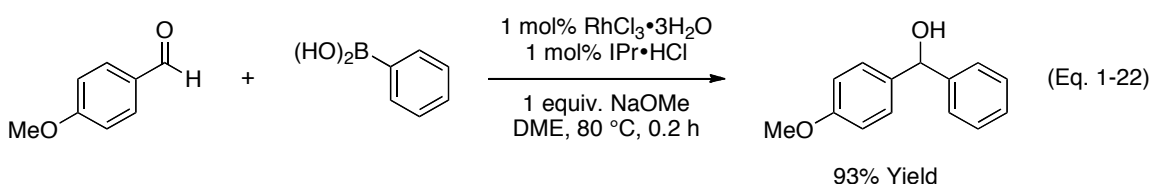
Scheme 1-9: Hydrogenation activity of rhodium catalysts with NHC ligands of increasing ring size.¹¹²

Another method for reducing organic compounds, that is probably the most studied Rh(NHC)-catalyzed reaction, is the hydrosilylation of unsaturated compounds, such as carbonyls, alkenes and alkynes. In this reaction, an inorganic or organic silicon hydride is added across the unsaturated bond of the substrate.¹¹³ Historically, it was one of the first catalytic reactions performed using a M(NHC) complex,¹¹⁴ and later became the first reported example of a M(NHC)-catalyzed reaction resulting in chiral induction.¹¹⁵ While enantioselectivities in this initial study by Herrmann were modest (32% *ee*), recent reports using axially chiral bis-NHC ligands¹¹⁶ and NHCs functionalized with chiral oxazolines¹¹⁷ have led to *ee*'s as high as 98% (Scheme 1-10). The hydrosilylation of alkenes and alkynes by Rh(NHC)-type complexes is considerably less well-represented than that of carbonyl compounds, however, a catalyst developed by Buchmeiser and co-workers featuring a tetrahydropyrimidine-based NHC was capable of reducing internal and external alkynes and alkenes at low catalyst loadings.¹¹⁸

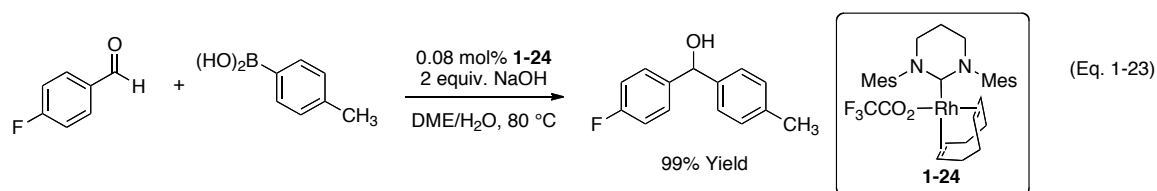


Scheme 1-10: Enantioselective hydrosilylation of ketones with chiral Rh(NHC) complexes.¹¹⁵⁻¹¹⁷

The transition metal catalyzed addition of organoboronic acids to aldehydes is a mild and efficient alternative to the use of organolithium and organomagnesium nucleophiles, and can be performed using a variety of late transition metals.¹¹⁹ Of the metals explored, rhodium has proven particularly useful in these catalytic reactions. Observing that sterically hindered, strongly basic alkyl phosphines often gave superior results,¹²⁰ Fürstner and co-workers investigated the application of Rh(NHC) complexes in these transformations.¹²¹ Comparable yields were obtained with NHCs relative to phosphines, however, the Rh(NHC) catalyzed reaction was much faster with rates five to eight times greater than the Rh(PR_3) catalyzed reaction. The optimized system, which employed equimolar amounts of $\text{RhCl}_3 \cdot 3\text{H}_2\text{O}$ and $\text{IPr} \cdot \text{HCl}$, was extremely efficient and exhibited a considerable substrate scope including aliphatic aldehydes and alkenyl boronic acids (Eq. 1-22).



Extensive investigation of various [XRh(NHC)(COD)] complexes as catalysts for this reaction have been undertaken by Özdemir and co-workers. A number of different NHC scaffolds were found to give satisfactory results including imidazolidinylidenes,^{122,123} tetrahydropyrimidinylidenes,¹²⁴ benzimidazolylidenes¹²⁵ and perhydrobenzimidazolylidenes.¹²³ Some of the highest TONs (up to 1230) for the Rh(NHC)-catalyzed transformation have come from the laboratory of Buchmeiser with catalyst **1-24**, which used a tetrahydropyrimidine-based NHC and replaced the halogen with trifluoroacetate (Eq. 1-23).¹²⁶ Enantioselective methods have also been explored, with a dicyclophane-containing NHC giving enantioselectivities up to 98%.¹²⁷



1.7 Conclusions

Originally thought of only as curiosities, the isolation of free carbenes, particularly NHCs, has led to a watershed of organometallic synthesis and homogeneous catalysis. The use of M(NHC) complexes in place of analogous phosphine-based catalysts has expanded the scope and efficiency of numerous reactions. Mechanistic studies of these transformations, with direct comparisons to the more common phosphine systems, have provided useful insight into the origin of these benefits. The quest for a fundamental understanding of the relationship between the electronics and sterics of NHC ligands and their respective effects on the fundamental steps in catalytic processes, combined with a comprehensive knowledge of the stability and decomposition pathways

of M(NHC) complexes, will surely lead to further important developments in this already burgeoning field.

1.8 Research Objectives

Recently, we have isolated dioxygen adducts of Rh(NHC)₂ complexes with relatively short O-O bond lengths and low coordination numbers. Chapter 2 describes our efforts to fully characterize this apparently unique binding mode and explain its origins. The coordination chemistry of [ClRh(IPr)₂] is further explored and its reactivity with N₂, CO and H₂ described. The catalytic activity of the dioxygen adducts was explored, with the hope of exploiting the unique binding mode for novel reactivity of the complex in oxidative transformations of organic molecules.

Chapter 3 will describe our efforts to synthesize Rh(NHC) hydroformylation catalysts with anionic ligands that are less inhibiting than the commonly employed halides. To this end, (OAc)Rh(NHC) complexes were synthesized and their ability to affect the hydroformylation of alkenes was optimized. Direct comparison of the catalyst to its chloro-containing analogue by comparing initial rates under standard conditions will be described.

Finally, efforts were made towards the synthesis of a Ru-based bifunctional hydrogenation catalyst featuring protic-NHC ligands in place of the commonly employed diamine ligands. The field of protic-NHC is relatively new, and this would represent the first example of a protic-NHC participating in a bifunctional catalytic reaction. In Chapter 4 these efforts are reported, and while we were unable to achieve the synthesis of

our desired catalyst, the N-bound tautomer was isolated and its catalytic activity investigated.

1.9 References

- (1) Bourissou, D.; Guerret, O.; Gabbai, F. P.; Bertrand, G. *Chem. Rev.* **1999**, *100*, 39-92.
- (2) de Fremont, P.; Marion, N.; Nolan, S. P. *Coord. Chem. Rev.* **2009**, *253*, 862-892.
- (3) Schuster, G. B.; Gold, V.; Bethell, D. In *Advances in Physical Organic Chemistry*; Academic Press: 1987; Vol. Volume 22, p 311-361.
- (4) Hoffmann, R. *J. Am. Chem. Soc.* **1968**, *90*, 1475-1485.
- (5) Schoeller, W. W. *J. Chem. Soc., Chem. Commun.* **1980**, 124-125. Pauling, L. *J. Chem. Soc., Chem. Commun.* **1980**, 688-689. Irikura, K. K.; Goddard, W. A.; Beauchamp, J. L. *J. Am. Chem. Soc.* **1992**, *114*, 48-51.
- (6) Igau, A.; Grutzmacher, H.; Baceiredo, A.; Bertrand, G. *J. Am. Chem. Soc.* **1988**, *110*, 6463-6466.
- (7) Soleilhavoup, M.; Baceiredo, A.; Treutler, O.; Ahlrichs, R.; Nieger, M.; Bertrand, G. *J. Am. Chem. Soc.* **1992**, *114*, 10959-10961.
- (8) Moss, R. A.; Huselton, J. K. *J. Chem. Soc., Chem. Commun.* **1976**, 950-951. Moss, R. A.; Wlostowski, M.; Terpinski, J.; Kmiciek-Lawrynowicz, G.; Krogh-Jespersen, K. *J. Am. Chem. Soc.* **1987**, *109*, 3811-3812. Moss, R. A.; Wlostowski, M.; Shen, S.; Krogh-Jespersen, K.; Matro, A. *J. Am. Chem. Soc.* **1988**, *110*, 4443-4444.
- (9) Moss, R. A.; Gerstl, R. *J. Org. Chem.* **1967**, *32*, 2268-2272. Moss, R. A.; Mallon, C. B. *J. Am. Chem. Soc.* **1975**, *97*, 344-347. Fedorynski, M. *Ç. Chem. Rev.* **2003**, *103*, 1099-1132.
- (10) Glorius, F. *N-Heterocyclic Carbenes in Transition Metal Catalysis*; Springer Verlag: Heidelberg, 2007; Vol. 21. Nolan, S. P. *N-Heterocyclic Carbenes in Synthesis*; Wiley-VCH: Weinheim, 2006.
- (11) Arduengo, A. J.; Harlow, R. L.; Kline, M. *J. Am. Chem. Soc.* **1991**, *113*, 361-363.
- (12) Arduengo, A. J.; Dias, H. V. R.; Harlow, R. L.; Kline, M. *J. Am. Chem. Soc.* **1992**, *114*, 5530-5534.
- (13) Wanzlick, H. W. *Angew. Chem., Int. Ed. Eng.* **1962**, *1*, 75-80.
- (14) Wanzlick, H. W.; Esser, F.; Kleiner, H. *J. Chem. Ber.* **1963**, *96*, 1208-1212.
- (15) Schonherr, H. J.; Wanzlick, H. W. *Liebigs Ann. Chem.* **1970**, *731*, 176-179. Schönherr, H.-J. R. S.; Wanzlick, H.-W. *Chem. Ber.* **1970**, *103*, 1037-1046.
- (16) Herrmann, W. A.; Elison, M.; Fischer, J.; Köcher, C.; Artus, G. R. *J. Chem.-Eur. J.* **1996**, *2*, 772-780.

- (17) Herrmann, W. A.; Köcher, C.; Gooflen, L. J.; Artus, G. R. J. *Chem.-Eur. J.* **1996**, *2*, 1627-1636.
- (18) Kuhn, N.; Kratz, T. *Synthesis* **1993**, *1993*, 561-562.
- (19) Enders, D.; Breuer, K.; Raabe, G.; Runsink, J.; Teles, J. H.; Melder, J.-P.; Ebel, K.; Brode, S. *Angew. Chem., Int. Ed. Engl.* **1995**, *34*, 1021-1023.
- (20) Hudnall, T. W.; Moerdyk, J. P.; Bielawski, C. W. *Chem. Commun.* **2010**, *46*, 4288-4290. Lavallo, V.; Canac, Y.; Präsang, C.; Donnadiou, B.; Bertrand, G. *Angew. Chem., Int. Ed.* **2005**, *44*, 5705-5709. Arduengo, A. J.; Goerlich, J. R.; Marshall, W. J. *J. Am. Chem. Soc.* **1995**, *117*, 11027-11028. Khramov, D. M.; Bielawski, C. W. *J. Org. Chem.* **2007**, *72*, 9407-9417. Hahn, F. E.; Wittenbecher, L.; Boese, R.; Blaser, D. *Chem.-Eur. J.* **1999**, *5*, 1931-1935. Guisado-Barrios, G.; Bouffard, J.; Donnadiou, B.; Bertrand, G. *Angew. Chem., Int. Ed.* **2010**, *49*, 4759-4762. Aldeco-Perez, E.; Rosenthal, A. J.; Donnadiou, B.; Parameswaran, P.; Frenking, G.; Bertrand, G. *Science* **2009**, *326*, 556-559. Hudnall, T. W.; Bielawski, C. W. *J. Am. Chem. Soc.* **2009**, *131*, 16039-16041.
- (21) Scott, N. M.; Dorta, R.; Stevens, E. D.; Correa, A.; Cavallo, L.; Nolan, S. P. *J. Am. Chem. Soc.* **2005**, *127*, 3516-3526.
- (22) Chugaev, L.; Skanavy-Grigorizeva, M. *J. Russ. Chem. Soc.* **1915**, *47*, 776. Tschugajeff, L.; Skanawy-Grigorjewa, M.; Posnjak, A. *Z. Anorg. Allg. Chem.* **1925**, *148*, 37-42.
- (23) Butler, W. M.; Enemark, J. H.; Parks, J.; Balch, A. L. *Inorg. Chem.* **1973**, *12*, 451-457.
- (24) Fischer, E. O.; Maasbol, A. *Angew. Chem., Int. Ed. Engl.* **1964**, *3*, 580-581.
- (25) Cardin, D. J.; Cetinkaya, B.; Lappert, M. F. *Chem. Rev.* **1972**, *72*, 545-574.
- (26) Taylor, T. E.; Hall, M. B. *J. Am. Chem. Soc.* **1984**, *106*, 1576-1584.
- (27) Lappert, M. F. *J. Organomet. Chem.* **1988**, *358*, 185-213.
- (28) Canac, Y.; Soleilhavoup, M.; Conejero, S.; Bertrand, G. *J. Organomet. Chem.* **2004**, *689*, 3857-3865. Whited, M. T.; Grubbs, R. H. *Acc Chem Res* **2009**, *42*, 1607-1616.
- (29) Öfele, K. *J. Organomet. Chem.* **1968**, *12*, P42-P43.
- (30) Wänzlick, H. W.; Schönherr, H. J. *Angew. Chem., Int. Ed. Engl.* **1968**, *7*, 141-142.
- (31) Cardin, D. J.; Cetinkay, B.; Lappert, M. F.; Manojlov, L.; Muir, K. W. *J. Chem. Soc. D-Chem. Commun.* **1971**, 400-401.
- (32) Cardin, D. J.; Cetinkay, B.; Cetinkay, E.; Lappert, M. F. *J. Chem. Soc., Dalton Trans.* **1973**, 514-522.

- (33) Lappert, M. F. *J. Organomet. Chem.* **1975**, *100*, 139-159.
- (34) Cetinkaya, B.; Hitchcock, P. B.; Lappert, M. F.; Pye, P. L. *J. Chem. Soc., Chem. Commun.* **1975**, 683-684.
- (35) Hitchcock, P. B.; Lappert, M. F.; Pye, P. L. *J. Chem. Soc., Dalton Trans.* **1977**, 2160-2172.
- (36) Jafarpour, L.; Stevens, E. D.; Nolan, S. P. *J. Organomet. Chem.* **2000**, *606*, 49-54.
- (37) Arduengo, A. J.; III Gamper, S. F.; Calabrese, J. C.; Davidson, F. *J. Am. Chem. Soc.* **1994**, *116*, 4391-4394.
- (38) Arduengo, A. J. III; Dias, H. V. R.; Calabrese, J. C.; Davidson, F. *Organometallics* **1993**, *12*, 3405-3409.
- (39) Arduengo, A. J. III; Dias, H. V. R.; Davidson, F.; Harlow, R. L. *J. Organomet. Chem.* **1993**, *462*, 13-18.
- (40) Arduengo, A. J. III; Dias, H. V. R.; Calabrese, J. C.; Davidson, F. *J. Am. Chem. Soc.* **1992**, *114*, 9724-9725. Arduengo, A. J. III; Dias, H. V. R.; Calabrese, J. C.; Davidson, F. *Inorg. Chem.* **1993**, *32*, 1541-1542.
- (41) Öfele, K.; Herrmann, W. A.; Mihalios, D.; Elison, M.; Herdtweck, E.; Scherer, W.; Mink, J. *J. Organomet. Chem.* **1993**, *459*, 177-184. Herrmann, W. A.; Kocher, C. *Angew. Chem., Int. Ed. Engl.* **1997**, *36*, 2162-2187. Herrmann, W. A. *Angew. Chem., Int. Ed.* **2002**, *41*, 1290-1309.
- (42) Lin, J. C. Y.; Huang, R. T. W.; Lee, C. S.; Bhattacharyya, A.; Hwang, W. S.; Lin, I. J. B. *Chem. Rev.* **2009**, *109*, 3561-3598.
- (43) Arnold, P. L.; Casely, I. J. *Chem. Rev.* **2009**, *109*, 3599-3611. Kuhn, N.; Al-Sheikh, A. *Coord. Chem. Rev.* **2005**, *249*, 829-857.
- (44) Herrmann, W. A.; Elison, M.; Fischer, J.; Köcher, C.; Artus, G. R. *J. Angew. Chem., Int. Ed. Engl.* **1995**, *34*, 2371-2374.
- (45) Köcher, C.; Herrmann, W. A. *J. Organomet. Chem.* **1997**, *532*, 261-265.
- (46) Voges, M. H.; Romming, C.; Tilset, M. *Organometallics* **1999**, *18*, 529-533. Abernethy, C. D.; Alan, H.; Cowley; Jones, R. A. *J. Organomet. Chem.* **2000**, *596*, 3-5.
- (47) Wang, H. M. J.; Lin, I. J. B. *Organometallics* **1998**, *17*, 972-975.
- (48) Lin, I. J. B.; Vasam, C. S. *Coord. Chem. Rev.* **2007**, *251*, 642-670.
- (49) Garrison, J. C.; Simons, R. S.; Tessier, C. A.; Youngs, W. J. *J. Organomet. Chem.* **2003**, *673*, 1-4. Kascatan-Nebioglu, A.; Panzner, M. J.; Garrison, J. C.; Tessier, C. A.;

Youngs, W. J. *Organometallics* **2004**, *23*, 1928-1931. Quezada, C. A.; Garrison, J. C.; Panzner, M. J.; Tessier, C. A.; Youngs, W. J. *Organometallics* **2004**, *23*, 4846-4848.

(50) Viciano, M.; Mas-Marzá, E.; Poyatos, M.; Sanaú, M.; Crabtree, R. H.; Peris, E. *Angew. Chem., Int. Ed.* **2005**, *44*, 444-447.

(51) Raynal, M.; Cazin, C. S. J.; Vallée, C.; Olivier-Bourbigou, H.; Braunstein, P. *Organometallics* **2009**, *28*, 2460-2470.

(52) McGuinness, D. S.; Cavell, K. J.; Yates, B. F. *Chem. Commun.* **2001**, 355-356.

(53) McGuinness, D. S.; Cavell, K. J.; Yates, B. F.; Skelton, B. W.; White, A. H. *J. Am. Chem. Soc.* **2001**, *123*, 8317-8328.

(54) Graham, D. C.; Cavell, K. J.; Yates, B. F. *Dalton Trans.* **2007**, 4650-4658.

(55) Grundemann, S.; Albrecht, M.; Kovacevic, A.; Faller, J. W.; Crabtree, R. H. *J. Chem. Soc., Dalton Trans.* **2002**, 2163-2167.

(56) Clement, N. D.; Cavell, K. J.; Jones, C.; Elsevier, C. J. *Angew. Chem., Int. Ed.* **2004**, *43*, 1277-1279.

(57) Mas-Marzá, E.; Sanaú, M.; Peris, E. *Inorg. Chem.* **2005**, *44*, 9961-9967.

(58) Trnka, T. M.; Morgan, J. P.; Sanford, M. S.; Wilhelm, T. E.; Scholl, M.; Choi, T.-L.; Ding, S.; Day, M. W.; Grubbs, R. H. *J. Am. Chem. Soc.* **2003**, *125*, 2546-2558.

(59) Arduengo, A. J. III; Calabrese, J. C.; Davidson, F.; Dias, H. V. R.; Goerlich, J. R.; Krafczyk, R.; Marshall, W. J.; Tamm, M.; Schmutzler, R. *Helv. Chim. Acta* **1999**, *82*, 2348-2364.

(60) Nyce, G. W.; Csihony, S.; Waymouth, R. M.; Hedrick, J. L. *Chem.-Eur. J.* **2004**, *10*, 4073-4079.

(61) Duong, H. A.; Tekavec, T. N.; Arif, A. M.; Louie, J. *Chem. Commun.* **2004**, 112-113.

(62) Voutchkova, A. M.; Appelhans, L. N.; Chianese, A. R.; Crabtree, R. H. *J. Am. Chem. Soc.* **2005**, *127*, 17624-17625.

(63) Voutchkova, A. M.; Feliz, M.; Clot, E.; Eisenstein, O.; Crabtree, R. H. *J. Am. Chem. Soc.* **2007**, *129*, 12834-12846.

(64) Hahn, F. E.; Langenhahn, V.; Meier, N.; Lügger, T.; Fehlhammer, W. P. *Chem.-Eur. J.* **2003**, *9*, 704-712. Hahn, F. E.; Langenhahn, V.; Lügger, T.; Pape, T.; Van, D. L. *Angew. Chem., Int. Ed.* **2005**, *44*, 3759-3763.

- (65) Hahn, F. E.; Plumed, C. G.; Münder, M.; Lügger, T. *Chem.-Eur. J.* **2004**, *10*, 6285-6293.
- (66) Kaufhold, O.; Flores-Figueroa, A.; Pape, T.; Hahn, F. E. *Organometallics* **2009**, *28*, 896-901.
- (67) Tolman, C. A. *Chem. Rev.* **1977**, *77*, 313-348.
- (68) Luo, L.; Nolan, S. P. *Organometallics* **1994**, *13*, 4781-4786.
- (69) Huang, J.; Stevens, E. D.; Nolan, S. P.; Petersen, J. L. *J. Am. Chem. Soc.* **1999**, *121*, 2674-2678.
- (70) Huang, J.; Schanz, H.-J.; Stevens, E. D.; Nolan, S. P. *Organometallics* **1999**, *18*, 2370-2375.
- (71) Hillier, A. C.; Sommer, W. J.; Yong, B. S.; Petersen, J. L.; Cavallo, L.; Nolan, S. P. *Organometallics* **2003**, *22*, 4322-4326.
- (72) Tolman, C. A. *J. Am. Chem. Soc.* **1970**, *92*, 2953-2956.
- (73) Dorta, R.; Stevens, E. D.; Hoff, C. D.; Nolan, S. P. *J. Am. Chem. Soc.* **2003**, *125*, 10490-10491. Dorta, R.; Stevens, E. D.; Scott, N. M.; Costabile, C.; Cavallo, L.; Hoff, C. D.; Nolan, S. P. *J. Am. Chem. Soc.* **2005**, *127*, 2485-2495.
- (74) Perrin, L.; Clot, E.; Eisenstein, O.; Loch, J.; Crabtree, R. H. *Inorg. Chem.* **2001**, *40*, 5806-5811. Tonner, R.; Frenking, G. *Organometallics* **2009**, *28*, 3901-3905. Gusev, D. G. *Organometallics* **2009**, *28*, 6458-6461.
- (75) Herrmann, W. A.; Schütz, J.; Frey, G. D.; Herdtweck, E. *Organometallics* **2006**, *25*, 2437-2448.
- (76) Clavier, H.; Nolan, S. P. *Chem. Commun.* **2010**, *46*, 841-861.
- (77) Poater, A.; Cosenza, B.; Correa, A.; Giudice, S.; Ragone, F.; Scarano, V.; Cavallo, L. *Eur. J. Inorg. Chem.* **2009**, *2009*, 1759-1766.
- (78) <http://www.molnac.unisa.it/OMtools/sambvca>
- (79) Diez-Gonzalez, S.; Marion, N.; Nolan, S. P. *Chem. Rev.* **2009**, *109*, 3612-3676.
- (80) Samojlowicz, C.; Bieniek, M.; Grela, K. *Chem. Rev.* **2009**, *109*, 3708-3742.
- (81) Kantchev, E. A. B.; O'Brien, C. J.; Organ, M. G. *Angew. Chem., Int. Ed.* **2007**, *46*, 2768-2813.
- (82) Praetorius, J. M.; Crudden, C. M. *Dalton Trans.* **2008**, 4079-4094.

- (83) *Handbook of Metathesis*; Grubbs, R. H., Ed.; Wiley-VCH: Weinheim, Germany, 2003; Vol. 1-3.
- (84) Chauvin, Y. *Adv. Synth. Catal.* **2007**, *349*, 27-33. Grubbs, R. H. *Adv. Synth. Catal.* **2007**, *349*, 34-40. Schrock, R. R. *Adv. Synth. Catal.* **2007**, *349*, 41-53.
- (85) Samojlowicz, C.; Bieniek, M. Ç.; Grela, K. *Chem. Rev.* **2009**, *109*, 3708-3742.
- (86) Schwab, P.; Grubbs, R. H.; Ziller, J. W. *J. Am. Chem. Soc.* **1996**, *118*, 100-110.
- (87) Dias, E. L.; Nguyen, S. T.; Grubbs, R. H. *J. Am. Chem. Soc.* **1997**, *119*, 3887-3897.
- (88) Sanford, M. S.; Ulman, M.; Grubbs, R. H. *J. Am. Chem. Soc.* **2001**, *123*, 749-750. Sanford, M. S.; Love, J. A.; Grubbs, R. H. *J. Am. Chem. Soc.* **2001**, *123*, 6543-6554. Love, J. A.; Sanford, M. S.; Day, M. W.; Grubbs, R. H. *J. Am. Chem. Soc.* **2003**, *125*, 10103-10109.
- (89) Weskamp, T.; Schattenmann, W. C.; Spiegler, M.; Herrmann, W. A. *Angew. Chem., Int. Ed.* **1998**, *37*, 2490-2493.
- (90) Weskamp, T.; Kohl, F. J.; Hieringer, W.; Gleich, D.; Herrmann, W. A. *Angew. Chem., Int. Ed.* **1999**, *38*, 2416-2419. Ackermann, L.; Fürstner, A.; Weskamp, T.; Kohl, F. J.; Herrmann, W. A. *Tetrahedron Lett.* **1999**, *40*, 4787-4790.
- (91) Scholl, M.; Trnka, T. M.; Morgan, J. P.; Grubbs, R. H. *Tetrahedron Lett.* **1999**, *40*, 2247-2250. Scholl, M.; Ding, S.; Lee, C. W.; Grubbs, R. H. *Org. Lett.* **1999**, *1*, 953-956.
- (92) Huang, J.; Schanz, H.-J.; Stevens, E. D.; Nolan, S. P. *Organometallics* **1999**, *18*, 5375-5380.
- (93) Kingsbury, J. S.; Harrity, J. P. A.; Bonitatebus, P. J.; Hoveyda, A. H. *J. Am. Chem. Soc.* **1999**, *121*, 791-799. Garber, S. B.; Kingsbury, J. S.; Gray, B. L.; Hoveyda, A. H. *J. Am. Chem. Soc.* **2000**, *122*, 8168-8179.
- (94) Sanford, M. S.; Love, J. A.; Grubbs, R. H. *Organometallics* **2001**, *20*, 5314-5318. Love, J. A.; Morgan, J. P.; Trnka, T. M.; Grubbs, R. H. *Angew. Chem., Int. Ed.* **2002**, *41*, 4035-4037.
- (95) Romero, P. E.; Piers, W. E.; McDonald, R. *Angew. Chem., Int. Ed.* **2004**, *43*, 6161-6165.
- (96) Barrios-Landeros, F.; Hartwig, J. F. *J. Am. Chem. Soc.* **2005**, *127*, 6944-6945.
- (97) Lewis, A. K. K.; Caddick, S.; Cloke, F. G. N.; Billingham, N. C.; Hitchcock, P. B.; Leonard, J. *J. Am. Chem. Soc.* **2003**, *125*, 10066-10073.
- (98) Green, J. C.; Herbert, B. J.; Lonsdale, R. *J. Organomet. Chem.* **2005**, *690*, 6054-6067. Lam, K. C.; Marder, T. B.; Lin, Z. *Organometallics* **2006**, *26*, 758-760.

- (99) Singh, R.; Viciu, M. S.; Kramareva, N.; Navarro, O.; Nolan, S. P. *Org. Lett.* **2005**, *7*, 1829-1832.
- (100) Hadei, N.; Kantchev, E. A. B.; O'Brien, C. J.; Organ, M. G. *J. Org. Chem.* **2005**, *70*, 8503-8507.
- (101) Stauffer, S. R.; Lee, S.; Stambuli, J. P.; Hauck, S. I.; Hartwig, J. F. *Org. Lett.* **2000**, *2*, 1423-1426.
- (102) Organ, M. G.; Çalimsiz, S.; Sayah, M.; Hoi, K. H.; Lough, A. J. *Angew. Chem., Int. Ed.* **2009**, *48*, 2383-2387.
- (103) Campeau, L.-C.; Thansandote, P.; Fagnou, K. *Org. Lett.* **2005**, *7*, 1857-1860.
- (104) Marion, N.; Nolan, S. P. *Acc. Chem. Res.* **2008**, *41*, 1440-1449.
- (105) Osborn, J. A.; Jardine, F. H.; Young, J. F.; Wilkinson, G. *J. Chem. Soc. (A)* **1966**, 1711-1732.
- (106) Jardine, F. H.; Osborn, J. A.; Wilkinson, G. *J. Chem. Soc. (A)* **1967**, 1574-1578.
Montelatici, S.; van der Ent, A.; Osborn, J. A.; Wilkinson, G. *J. Chem. Soc. (A)* **1968**, 1054-1058.
- (107) Allen, D. P.; Crudden, C. M.; Calhoun, L. A.; Wang, R. *J. Organomet. Chem.* **2004**, *689*, 3203-3209.
- (108) Allen, D. P.; Crudden, C. M.; Calhoun, L. A.; Wang, R.; Decken, A. *J. Organomet. Chem.* **2005**, *690*, 5736-5746.
- (109) Chen, A. C.; Allen, D. P.; Crudden, C. M.; Wang, R. Y.; Decken, A. *Can. J. Chem.-Rev. Can. Chim.* **2005**, *83*, 943-957.
- (110) Crudden, C. M.; Allen, D. P. *Coord. Chem. Rev.* **2004**, *248*, 2247-2273.
- (111) Herrmann, W. A.; Frey, G. D.; Herdtweck, E.; Steinbeck, M. *Adv. Synth. Catal.* **2007**, *349*, 1677-1691.
- (112) Binobaid, A.; Iglesias, M.; Beetstra, D. J.; Kariuki, B.; Dervisi, A.; Fallis, I. A.; Cavell, K. J. *Dalton Trans.* **2009**, 7099-7112.
- (113) Diez-Gonzalez, S.; Nolan, S. P. *Org. Prep. Proced. Int.* **2007**, *39*, 523 - 559.
- (114) Hill, J. E.; Nile, T. A. *J. Organomet. Chem.* **1977**, *137*, 293-300. Lappert, M. F.; Maskell, R. K. *J. Organomet. Chem.* **1984**, *264*, 217-228.
- (115) Herrmann, W. A.; Goossen, L. J.; Köcher, C.; Artus, G. R. J. *Angew. Chem., Int. Ed. Eng.* **1996**, *35*, 2805-2807.
- (116) Duan, W. L.; Shi, M.; Rong, G. B. *Chem. Commun.* **2003**, 2916-2917.

- (117) Gade, L. H.; César, V.; Bellemin-Laponnaz, S. *Angew. Chem. Int. Ed.* **2004**, *43*, 1014-1017.
- (118) Imlinger, N.; Wurst, K.; Buchmeiser, M. R. *Monatsh. Chem.* **2005**, *136*, 47-57.
Imlinger, N.; Wurst, K.; Buchmeiser, M. R. *J. Organomet. Chem.* **2005**, *690*, 4433-4440.
- (119) Miyaura, N. *Bull. Chem. Soc. Jap.* **2008**, *81*, 1535-1553.
- (120) Ueda, M.; Miyaura, N. *J. Org. Chem.* **2000**, *65*, 4450-4452.
- (121) Fürstner, A.; Krause, H. *Adv. Synth. Catal.* **2001**, *343*, 343-350.
- (122) Özdemir, I.; Demir, S.; Çetinkaya, B. *J. Mol. Catal. A* **2004**, *215*, 45-48.
- (123) Yiğit, M.; Özdemir, I.; Çetinkaya, E.; Çetinkaya, B. *Trans. Met. Chem.* **2007**, *32*, 536-540.
- (124) Özdemir, I.; Demir, S.; Çetinkaya, B.; Çetinkaya, E. *J. Organomet. Chem.* **2005**, *690*, 5849-5855.
- (125) Özdemir, I.; Gürbüz, N.; Gök, Y.; Çetinkaya, B.; Çetinkaya, E. *Trans. Met. Chem.* **2005**, *30*, 367-371.
- (126) Imlinger, N.; Mayr, M.; Wang, D.; Wurst, K.; Buchmeiser, M. R. *Adv. Synth. Catal.* **2004**, *346*, 1836-1843.
- (127) Ma, Y.; Song, C.; Ma, C.; Sun, Z.; Chai, Q.; Andrus, M. B. *Angew. Chem., Int. Ed.* **2003**, *42*, 5871-5874.

Chapter 2: Coordination Chemistry and Catalytic Activity of Rhodium bis-N-Heterocyclic Carbene Complexes

2.1 Introduction

2.1.1 Side-on Metal-Dioxygen Adducts

For 1:1 metal-dioxygen coordination complexes one of two possible binding approaches are observed: end-on (η^1) and side-on (η^2).¹⁻³ Metal-dioxygen complexes can be further differentiated as peroxo and superoxo depending on the O-O bond lengths and stretching frequencies observed by X-ray crystallography and vibrational spectroscopy, respectively.⁴ The η^2 -peroxo bonding mode, which is more common in side-on metal-dioxygen complexes, is characterized by longer bond lengths (~ 1.4 - 1.5 Å) and lower stretching frequencies (~ 800 - 930 cm^{-1}), while η^2 -superoxo complexes possess stronger O-O bonds and therefore have characteristically shorter bond lengths (~ 1.2 - 1.3 Å) and higher stretching frequencies (1050 - 1200 cm^{-1}).³ Examples of fully characterized η^2 -superoxo complexes in the literature are few, as exemplified by the short yet comprehensive list given in Table 2-1. To appreciate the data in Table 2-1, one should note that molecular oxygen (O_2) and the superoxide radical anion (O_2^-) have calculated O-O bond lengths of 1.220 and 1.363 Å, and stretching frequencies of 1550 and 1097 cm^{-1} , respectively.^{3,5} A report by Cramer et al. has demonstrated a direct correlation between these two characteristics of the O-O bond, and therefore given the lack of accuracy inherent in many of the reported X-ray structures of $\text{M}(\text{O}_2)$ complexes due to librational

motion and other issues (see below),^{3,6} it is important that the data obtained from the vibrational spectra also be considered.

Table 2-1: Previously reported transition metal η^2 -superoxo complexes.

Entry	Formula	Geometry	O-O Bond Length (Å)	$\nu(\text{O-O})$ (cm^{-1})
1	$[\text{Co}(\text{Tp}')(\text{O}_2)]^{3,7}$	Tetrahedral	1.355(3) ³	961 ⁷
2	$[\text{Sm}(\text{Tp}^{\text{Me}2})_2(\text{O}_2)]^8$	Pentagonal Bipyramidal	1.319	1124
3	$[\text{Cu}(\text{Tp}'')(\text{O}_2)]^9$	Tetrahedral	1.22(3)	1112
4	$[\text{Os}(\text{Cl})(\text{dcpe})_2(\text{O}_2)]^+^{10}$	Octahedral	1.315(5)	ND
5	$[\text{Cr}(\text{Cl})(\text{Tp}')(\text{O}_2)]^{11}$	Trigonal Bipyramidal	1.325(3)	1104

Tp' = hydridotris(3-tert-butyl-5-methylpyrazolyl)borate; Tp^{Me2} = hydridotris(3,5-dimethylpyrazolyl)borate; Tp'' = hydridotris(3-tert-butyl-5-isopropylpyrazolyl)borate

For example, $[\text{Cu}(\text{Tp}'')(\text{O}_2)]$ (entry 3, Table 2-1) has a reported bond length as short as molecular oxygen itself, but a stretching frequency typical of an η^2 -superoxo.⁹ Similarly, the original investigation of $[\text{Co}(\text{Tp}')(\text{O}_2)]$ (entry 1, Table 2-1) reported an O-O bond length of 1.262 Å, but a stretching frequency of 961 cm^{-1} suggesting superoxo electronic character.⁷ Cramer et al. have since redetermined the X-ray crystallographic structure of $[\text{Cu}(\text{Tp}'')(\text{O}_2)]$ at a lower temperature (-133 °C *versus* 22 °C), and found an O-O bond distance of 1.355 Å; a value more consistent with both the vibrational spectra and calculated values of the bond length (1.380 Å).³

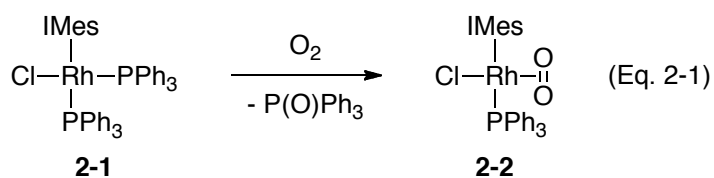
One of the difficulties with determining the O-O bond length in $\text{M}(\text{O}_2)$ complexes is that the O-O bond is actively oscillating and rotating about an axis defined by the metal atom and the middle of the O-O bond. This effect, called *librational motion*, is responsible for the discrepancy between the results of X-ray crystallography as a function of temperature as shown above. A well-documented phenomenon in X-ray

crystallography, librational motion always results in shortened bond distances, but the differences are usually less than 0.003 Å.¹² The observed difference of ~0.1 Å [Co(Tp')(O₂)] is largely because the constraints of the O₂ ligand are few, and its position, as represented by thermal ellipsoids, is an average of all orientations in all of the unit cells of the crystal. Thus as the temperature increases, which subsequently increases the thermal motion of the O₂ ligand, the approximation of the O atoms' positions becomes less accurate and the observed O-O bond length becomes shorter. It is therefore important to ensure that all X-ray data obtained of M(O₂) be performed at cryogenic temperatures to ensure maximal accuracy in the observed O-O bond length. Other difficulties such as degradation of the complex upon exposure to X-ray radiation have been reported to lead to incorrect O-O bond lengths.⁶

One further consideration when assigning an η²-dioxygen complex as peroxo or superoxo is the correct identification of the O-O stretch in the vibrational spectra. The presence of alkyl groups within organometallic coordination compounds can yield complicated fingerprint regions necessitating the synthesis of ¹⁸O₂-isotopomers for proper identification of the O-O stretching frequency. Comparing the spectra of the ¹⁸O₂-isotopomer to the initially synthesized ¹⁶O₂-isotopomer, the stretch from the latter complex should be replaced by a stretch at lower wave number due to the weaker O-O bond of the former.¹³ The use of a simple harmonic oscillator approximation for bond strengths in the two complexes can yield a useful predictive model to calculate the expected spectra of the isotopomer.¹³

2.1.2 [CIRh(L)(L')(O₂)] Complexes

As part of our laboratory's interest in the coordination chemistry of NHC-modified Rh complexes,¹⁴ former graduate student Daryl Allen found that reaction of [CIRh(IMes)(PPh₃)₂] (**2-1**) with oxygen or air results in a change of color of the solution from yellow to green. From this solution, the complex [CIRh(IMes)(PPh₃)(O₂)] (**2-2**) was isolated in small quantities as X-ray quality crystals, resulting from the replacement of a phosphine ligand by dioxygen (Eq. 2-1).



Despite considerable literature on the chemistry of Rh and Ir dioxygen complexes,¹⁵⁻²² compound **2-2** is a rare example of a formally square planar complex of molecular oxygen.²³⁻²⁷ In addition, the O-O bond length in **2-2**, an average of 1.26 Å over the three components of the crystal structure (Table 2-2, entry 1), is unusually short compared with typical peroxo species (1.4-1.5 Å). The closely related octahedral complexes [CIRh(NHC)(P-N)(O₂)] **2-3a** and **b** (where P-N = *o*-(diphenylphosphino)-*N,N*-dimethyl aniline, NHC = IPr (**2-3a**) or IMes (**2-3b**)) feature O-O bond lengths of 1.450(3) and 1.450(2) Å, respectively (Table 2-3, entry 5).²² Further oxidation of the remaining phosphine ligand upon exposure to air or oxygen made complex **2-2** difficult to handle and isolate in high yield. Thus, non-phosphine-containing analogs of **2-2** were prepared, replacing the phosphine with a second equivalent of the respective NHC.

Treatment of [CIRh(C₂H₄)₂]₂ with two equivalents of IPr or IMes under N₂ gave yellow solutions which were then exposed to air or oxygen. After several hours, the

reactions began to darken, resulting in deep blue solutions from which X-ray quality crystals of [ClRh(IPr)₂(O₂)] (**2-4**) and [ClRh(IMes)₂(O₂)] (**2-5**) were obtained (Eq. 2-2).²⁸ Complexes **2-4** and **2-5**, along with the mixed phosphine-NHC complex **2-2**, were atypical in both their coordination number and their short O-O bond distances as determined from X-ray crystallography (Table 2-2).

Table 2-2: O-O bond lengths of isolated Rh-(O₂) complexes in the Crudden laboratory from X-ray data collected at 180 K.

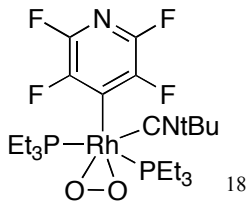
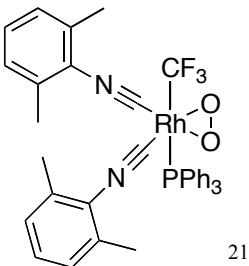
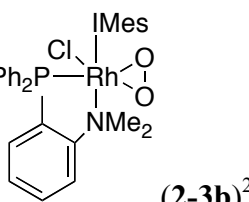
Entry	Complex	O-O (Å)
1	ClRh(IMes)(PPh ₃)(O ₂), 2-2	1.249(9), 1.298(9), 1.231(16)
2	ClRh(IPr) ₂ (O ₂), 2-4	1.323(3)
3	ClRh(IMes) ₂ (O ₂), 2-5	1.341(4)

The vast majority of previously reported Rh(O₂) complexes have been octahedral with O-O bond distances and stretching frequencies in the range typical of η^2 -peroxo complexes. Fully characterized examples are given in Table 2-3. The complexes synthesized in our laboratory, and shown in Table 2-2, however, are more characteristic of previously observed η^2 -superoxo complexes (Table 2-1) due to their shorter bond lengths. However as noted previously, the determination of bonding modes purely by crystallography, especially of O₂-complexes, is fraught with difficulties. In addition to librational motion, the accuracy of the O-O bond length in our complexes is compromised by positional disorder of the Cl-Rh-(O₂) within the unit cell.

With the large NHC and phosphine ligands of **2-2** dictating the overall packing within the unit cell, the relative placement of the chloro and O₂ ligands is apparently arbitrary. This results in half of the molecules within the crystal having the Cl-Rh-O₂ pointing in one direction, and the other half pointing in the opposite direction. The

original crystal structures of **2-4** and **2-5** also suffered from positional disorder, each possessing an equal number of the molecules within the crystal oriented in one of two opposite directions. The observed O-O bond lengths of **2-4** and **2-5** in these initial X-ray studies were as a result much shorter than those shown in Table 2-2 (**2-4**: 1.26(5), 1.24(6) Å; **2-5**: 1.207(7), 1.258(10) Å). Further crystallizations attempts yielded the results shown in Table 2-2, which did not possess any positional disorder within the crystal. Given the difficulties in acquiring reliable crystallographic data, alternative methods were sought in order to investigate and correctly assign the binding mode within these complexes.

Table 2-3: Typical examples of rhodium η^2 -peroxo complexes.

Entry	Formula	Geometry	O-O Bond Length (Å)	$\nu(\text{O-O})$ (cm^{-1})
1	$[\text{ClRh}(\text{PPh}_3)_3(\text{O}_2)]^{16,19}$	Octahedral	1.413 ¹⁶	890 ¹⁹
2	$[\text{Rh}(\text{pz}^{\text{iPr}}\text{H})(\text{Tp}^{\text{iPr}})(\text{O}_2)]^{20}$	Octahedral	1.467(5)	848
3	 $\text{Et}_3\text{P}-\text{Rh}(\text{CNtBu})(\text{PEt}_3)_2(\text{O}_2)$ ¹⁸	Octahedral	1.438(3)	882
4	 $\text{PPh}_3-\text{Rh}(\text{CF}_3)(\text{O}_2)$ ²¹	Octahedral	1.452(3)	852
5	 $\text{Ph}_2\text{P}-\text{Rh}(\text{Cl})(\text{IMes})(\text{NMe}_2)(\text{O}_2)$ ²² (2-3b)	Octahedral	1.450(2)	852

Tp^{iPr} = hydridotris(3,5-diisopropylpyrazolyl)borate; $\text{pz}^{\text{iPr}}\text{H}$ = 3,5-diisopropylpyrazole

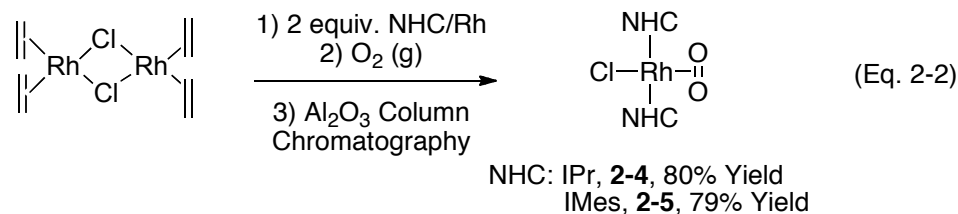
2.2 Results and Discussion

2.2.1 Characterization of [ClRh(NHC)₂(O₂)]

In order to fully characterize these unusual dioxygen complexes and better understand the binding mode of dioxygen, full NMR and IR spectra were obtained at Queen's, and through collaborations with Dr. Kennepohl (University of British Columbia) and Dr. Grein (University of New Brunswick) these complexes were also examined by XAS, Raman and DFT calculations. Conceivably three possible binding scenarios exist: a Rh^{III}-η²-peroxo resulting from full oxidative addition of dioxygen to the metal; a Rh^{II}-η²-superoxo resulting from a single-electron transfer from the metal to dioxygen; and a Rh^I-dioxygen complex resulting from coordination of dioxygen to the metal without the occurrence of an oxidation/reduction process between rhodium and dioxygen.¹ By using this combination of techniques we were able to elucidate what we believe to be the true nature of this unprecedented binding interaction. As noted previously, over oxidation of the remaining phosphine ligand in **2-2** upon exposure to air or oxygen made complex **2-2** difficult to handle and isolate in high yield. Thus, only complexes **2-4** and **2-5** were subjected to full characterization in this study.

The synthesis of these complexes was first optimized: the yellow solution obtained from stirring [ClRh(C₂H₄)₂]₂ and two equivalents of IPr or IMes in THF under a nitrogen atmosphere was degassed and stirred in the presence of oxygen gas for 24 – 48 h. The stability of the resulting complexes then allowed for purification by column

chromatography through neutral Al₂O₃. By collecting the blue fractions, complexes **2-4** and **2-5** were obtained in 80% and 79% yield, respectively (Eq. 2-2).



Both complexes were fully characterized by ¹H and ¹³C NMR spectroscopy yielding clean, sharp spectra consistent with a diamagnetic species. The structure of **2-4** showed restricted rotation on the NMR timescale, with the isopropyl methines appearing as a broad signal at 2.81 ppm. Cooling of the *d*₈-toluene solution of **2-4** to 233 K caused complete resolution of this broad signal to a pair of multiplets, indicative of restricted rotation about the Rh-C_{NHC} bond at this temperature.²⁹ Coincident with this phenomenon was resolution of the isopropyl methyl signals to a multiplet consistent with four chemically inequivalent doublets, although the separation of these peaks was not complete.

Considering the difficulties that can be associated with the accurate determination of O–O bond lengths with crystallography as discussed above,³ we next looked to assign the appropriate band in the IR spectrum, which would also provide an indication of bond strength and bonding mode. Our initial effort in lieu of available ¹⁸O₂ gas was substitution of the O₂ ligand by CO (see section 2.2.2 for further details on the synthesis and characterization of this complex). Although the relevant regions of the IR spectra were considerably complicated due to the alkyl groups of the IPr ligand, replacement of O₂ by CO at the metal centre resulted in the loss of a strong, broad stretch at 1021 cm⁻¹. Similar effects are observed when comparing the IR spectra of the related N₂ and H₂

complexes with **2-4** (section 2.2.2). While these results very strongly suggested the stretch at 1021 cm^{-1} was attributable to the O-O bond, the evidence was not unequivocal, and therefore the $^{18}\text{O}_2$ isotopomer was prepared ($^{18}\text{O}_2\text{-2-4}$). The IR spectra obtained was again complex, but the broad stretch at 1021 cm^{-1} was replaced by a weak stretch of 958 cm^{-1} . A simple harmonic oscillator calculation predicts that the O-O stretch should appear at 962 cm^{-1} , which is the same as the experimentally observed signal within experimental error.¹³

To further validate the assignment of the O-O stretching frequencies the $^{16}\text{O}_2$ and $^{18}\text{O}_2$ isotopomers of **2-4** were compared by Raman spectroscopy (Figure 2-1). Initial attempts at obtaining the Raman spectra resulted in decomposition of the sample, likely due to Raman excitation at excessively high energy. Raman excitation at 568 nm , however, into a low-energy adsorption of complex **2-4** did not damage the sample, and provided resonance enhancement of a band at 1010 cm^{-1} . This band was absent in the analogous Raman spectra of $^{18}\text{O}_2\text{-2-4}$, which possessed a new band at roughly 960 cm^{-1} . Although this signal is difficult to observe due to the presence of an existing signal in the $^{16}\text{O}_2$ -isotopomer, the signal at 1010 cm^{-1} is clearly absent, and is consistent with the loss of the band at 1021 cm^{-1} in the IR of **2-4** upon substitution with CO. This value is again within error of the predicted value from a simple harmonic oscillator calculation. Given the consistency of all the data from IR and Raman studies, we confidently assigned the stretch at 1021 cm^{-1} in the IR and 1010 cm^{-1} in the Raman as the O-O stretching frequency.

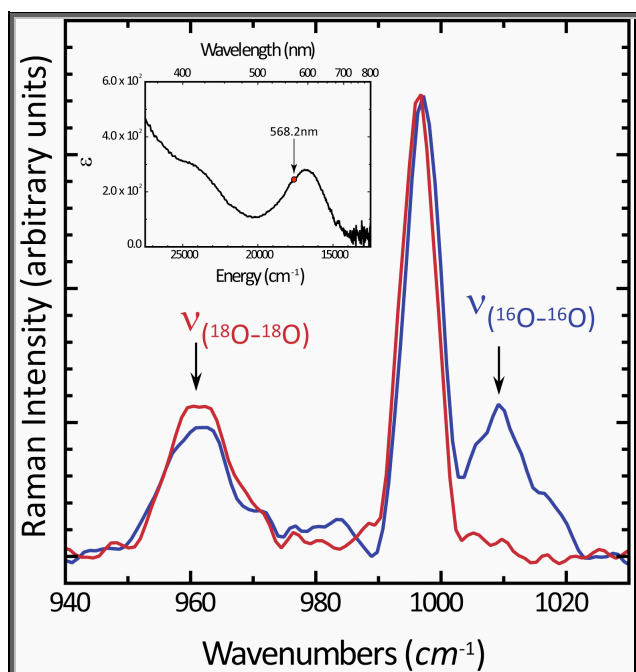


Figure 2-1: Raman spectra of complex 2-4 and its $^{18}\text{O}_2$ isotopomer.

The data from the IR/Raman study and the observed O-O bond lengths both support a stronger O-O bond and are not consistent with assignment of the complexes as Rh^{III} -peroxo complex such as those shown in Table 2-3. Instead, the data was more comparable to previously isolated superoxo complexes, and therefore was suggestive of a Rh^{II} -superoxo electronic structure. This appeared to be a confounding possibility since both rhodium(II) and superoxide radical anions are expected to be paramagnetic, which would contradict the NMR spectra of **2-4** and **2-5** that clearly suggest these are diamagnetic species. Singlet ground states of paramagnetic metal and dioxygen fragments can however form singlet ground states through either anti-ferromagnetic coupling or purely covalent interactions,³⁰ and thus the possibility of a $\text{Rh}^{\text{II}}-\eta^2$ -superoxo could not be excluded at this point.

Interested in determining the true binding mode of our complexes, we began a collaboration with Dr. Pierre Kennepohl at UBC in which the electronic structure of **2-4** was examined by Rh L-edge X-ray Absorption Spectroscopy (XAS).³¹ This methodology allowed us to evaluate the 4d occupancy of the complex and therefore provided significant insight into the binding mode of dioxygen by revealing the oxidation state of the metal.

XAS is a widely used technique, performed using synchrotron radiation sources, which is able to determine the electronic structure of matter, including organometallic transition metal complexes.³¹ Data are obtained by tuning the photon energy of the X-ray to a range where interaction of the electromagnetic radiation with the bound electrons is adsorbed causing excitation. At certain energies adsorption is observed to increase drastically giving rise to an *adsorption edge*. Each edge occurs when the energy of the incident photons is just sufficient to cause excitation of a core electron to the continuum state and produce a photoelectron. The adsorption edges are labeled based on the core electron that has been ejected at that energy with principal quantum numbers $n = 1, 2$ and 3 corresponding to the K-, L- and M-edges, respectively.

The L-edge of complex **2-4** was examined by XAS and compared to known rhodium(I) and rhodium(III) complexes (Figure 2-2). The intensity of the dipole-allowed $2p \rightarrow 4d$ transition in compound **2-4** when compared to the known standards was found to be consistent with a rhodium(I) $4d^8$ species. Therefore, a single unoccupied 4d orbital [Rh $4d_{xy}(x^2-y^2)$] should exist in the complex, and thus a single feature was expected at the L-edge, however a shoulder was observed about 2 eV below the main feature.

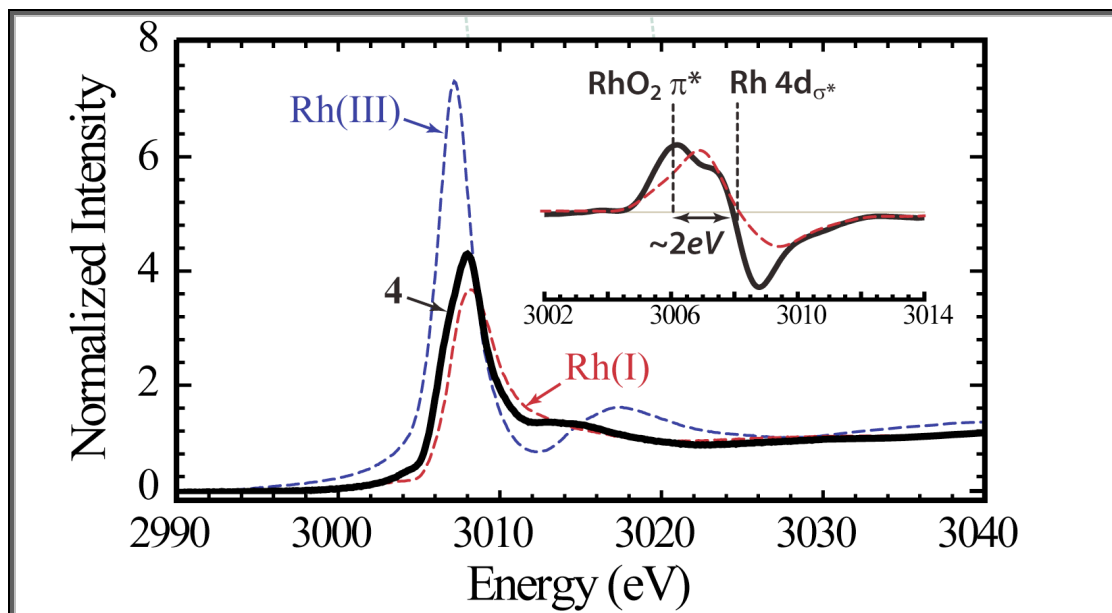


Figure 2-2: Rh L-edge XAS spectra of **2-4** (black), RhCl₃-hydrate (blue) and Rh(IPr)(CO)₂(OAc) (red). Inset: first derivative plot of data for **2-4** and Rh(IPr)(CO)₂(OAc).

To help explain the obtained XAS data, DFT calculations were performed in collaboration with Dr. Friedrich Grein at UNB on a simplified version of **2-4**, in which the *N*-aryl groups were replaced by *N*-methyls (**2-4t**). The resultant valence MO diagram is consistent with a square-planar Rh 4d⁸ metal centre bound to *singlet dioxygen* (Figure 2-3). Stabilization of the singlet state of dioxygen by π -backbonding from Rh into one of the two degenerate π^* orbitals of the dioxygen ligand results in splitting of the dioxygen π^* orbitals by about 0.8 eV. This provides a rationale for the observed low-energy shoulder appearing about 2 eV below the main feature in the L-edge XAS spectra (Figure 2-2, inset), which is a result of the Rh 2p \rightarrow Rh(O₂) π^* transition. The calculated energy difference between the Rh(O₂) π^* (LUMO) and the Rh 4d_{xy}(x²-y²) is 1.7 eV, very close to the experimentally determined value of 2 eV.

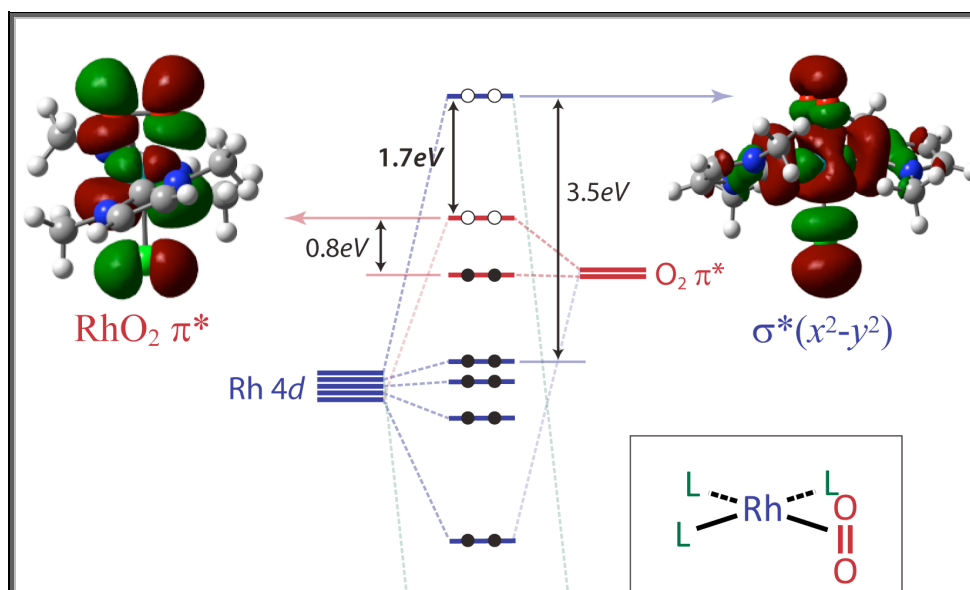


Figure 2-3: Energy level diagram of DFT-calculated MOs for 2-4t.

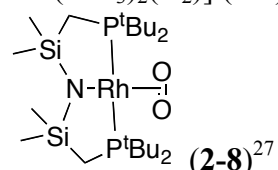
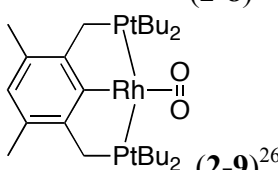
Thus, it appears the best description of **2-4**, and by analogy **2-2** and **2-5**, is a square-planar rhodium(I) complex of singlet oxygen ($^1\text{O}_2$). Unlike the addition of O_2 to a square-planar $\text{M}^{\text{n}}\text{L}_4$ fragment – which results in oxidative addition forming two M-O σ bonds and therefore, an octahedral $\text{M}^{\text{n}+2}(\text{O})_2$ complex – our complexes appear to be the result of π bonding between O_2 and the $\text{M}^{\text{n}}\text{L}_3$ fragment $[\text{ClRh}(\text{NHC})_2]$, resulting in a square-planar $\text{M}^{\text{n}}(\text{O}_2)$ complex. It would seem that formation of this $\text{Rh}^{\text{I}}-(^1\text{O}_2)$ adduct is a result of the large energy difference between filled Rh $4d_{\text{nb}}$ orbitals and the ligand-centred empty $\text{Rh}(\text{O}_2)$ π^* orbital, such that two electron transfer from Rh to O_2 is unfavorable. Thus, the splitting of the O_2 π^* orbitals by $\text{Rh}(\text{O}_2)$ π -backbonding not only makes the singlet state favorable, but inhibits reduction of the dioxygen molecule by rhodium.

Interestingly, there are a few reports of $\text{Rh}(\text{O}_2)$ complexes that possess properties uncharacteristic of Rh^{III} -peroxo compounds, and similar to **2-2**, **2-4** and **2-5** (Table 2-4).

Two complexes of the formula $[\text{ClRh}(\text{PR}_3)_2(\text{O}_2)]$ ($\text{R} = \text{Cy}$ (**2-6**)^{23,24} and ^iPr (**2-7**),²⁵ entries 1 and 2, respectively) were reported independently in the 1970s and both have conspicuously high O-O stretching frequencies. Interestingly, a crystal structure of **2-7** was obtained, but the reported O-O bond length is so short (1.03 Å) as to be unreliable. More recently, in separate reports, both Milstein²⁶ and Caulton²⁷ have described the isolation of square-planar $\text{Rh}(\text{O}_2)$ complexes sporting unusually short O-O bond distances (entries 3 and 4, Table 2-4).

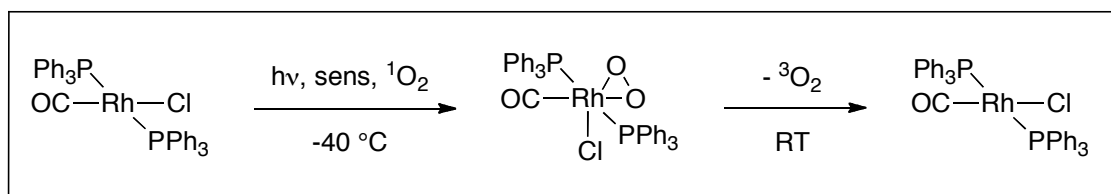
Given that these complexes are all square-planar and possess either a short O-O bond or a high O-O stretching frequency in the vibrational spectra, the complexes listed in Table 2-4 are likely also examples of $\text{Rh}^{\text{I}}-(^1\text{O}_2)$ complexes. Although XAS has not been performed on any of these structures, DFT calculations of **2-9** and observation of a large $J_{\text{Rh-P}}$ for **2-8** led the authors in both studies to speculate that these were dioxygen adducts of rhodium(I).

Table 2-4: Previously reported unusual $\text{Rh}(\text{O}_2)$ complexes.

Entry	Formula	Geometry	O-O Bond Length (Å)	$\nu(\text{O-O})$ (cm^{-1})
1	$[\text{ClRh}(\text{PCy}_3)_2(\text{O}_2)]$ (2-6) ^{23,24}	Square Planar	ND	993
2	$[\text{ClRh}(\text{P}^i\text{Pr}_3)_2(\text{O}_2)]$ (2-7) ²⁵	Square Planar	1.03 ^a	990
3	 (2-8) ²⁷	Square Planar	1.363	ND
4	 (2-9) ²⁶	Square Planar	1.365	ND

^aThe O-O bond length of unbound molecular oxygen is calculated to be 1.22 Å.

No other accounts of M-(¹O₂) species appear in the literature, so this binding mode is apparently unusual. Foote et al. have however, reported the reactions of pre-generated ¹O₂ with Vaska's complex ([ClIr(PPh₃)₂(CO)]) and its rhodium analogue.^{17,32} From these reactions Foote isolated [ClIr(PPh₃)₂(CO)(O₂)],³³ which is formed at a significantly faster rate when singlet oxygen is employed compared with triplet oxygen (³O₂). The previously unreported complex [ClRh(PPh₃)₂(CO)(O₂)] was also obtained (Scheme 2-1).



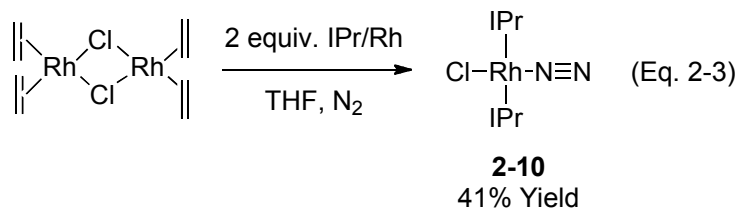
Scheme 2-1: Reaction of [ClRh(PPh₃)₂(CO)] with ¹O₂, and release of ³O₂.^{17,32}

Both of these were η^2 -peroxo complexes resulting from the oxidative addition of ¹O₂ to the metal. The iridium complex obtained was identical to that obtained through reaction with ³O₂ and both complexes bound oxygen reversibly, releasing oxygen in its triplet state. Thus, it appeared that singlet oxygen's abnormal reactivity was merely a result of its excited state, which gave the molecule sufficient energy to overcome the reaction barrier for peroxo formation, and did not in fact result in unusual binding in the resulting complexes.

2.2.2 Coordination of N₂, CO and H₂ to [ClRh(IPr)₂]

Intrigued by the unique binding properties of the rhodium-O₂ complex [ClRh(IPr)₂(O₂)] (**2-4**), we next decided to investigate the reactivity of the metal in the absence of oxygen. As mentioned above, the synthesis of **2-4** is achieved by reacting a

THF solution of $[\text{ClRh}(\text{C}_2\text{H}_4)_2]_2$ with IPr in a nitrogen atmosphere glove-box, and then exposing the resulting yellow reaction mixture to an atmosphere of air or oxygen. To determine the identity of this intermediate, the yellow complex was isolated prior to oxygen exposure, and was found to be an end-on $\text{Rh}(\eta^1\text{-N}_2)$ complex with the formula $[\text{ClRh}(\text{IPr})_2(\text{N}_2)]$ (**2-10**) (Eq. 2-3).



This compound was isolated in 41% yield following filtration through Celite to remove colloidal rhodium, evaporation of the volatiles and trituration of the resulting yellow solid with cold hexanes to remove unreacted IPr and any other non-volatile organic contaminants. X-ray quality crystals of this dinitrogen compound were obtained by slow diffusion of hexanes into a concentrated THF solution of **2-10**, the structure of which is given in Figure 2-4 along with relevant bond lengths and bond angles.

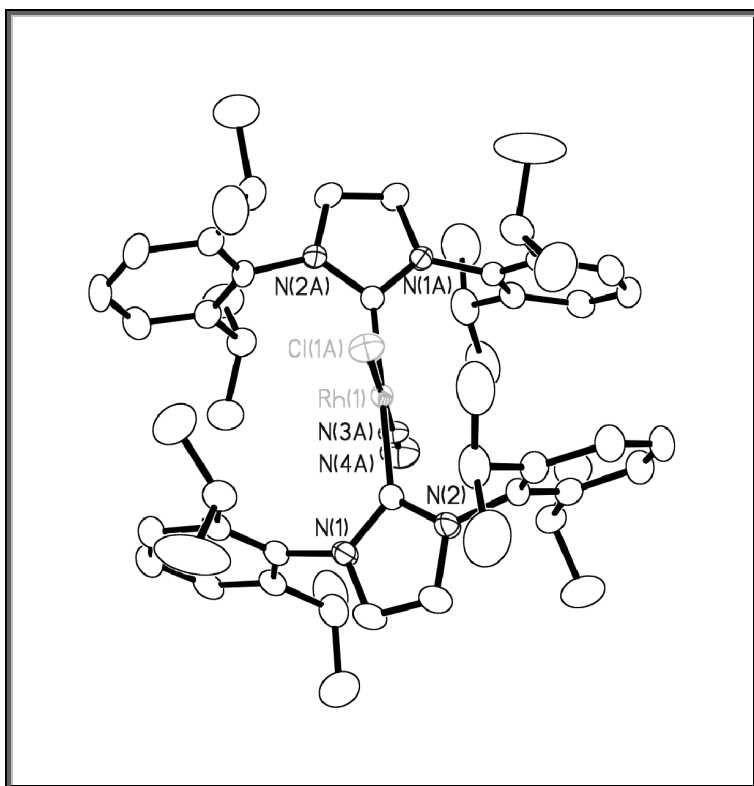


Figure 2-4: Crystallographically determined structure of **2-10**, displaying thermal ellipsoids drawn at the 50% confidence level. Hydrogen atoms removed for clarity. Selected interatomic distances (Å) and angles (deg): Rh(1)-N(3A), 1.892(7); Rh(1)-C(1), 2.0519(13); Rh(1)-Cl(1A), 2.2882(11); N(3A)-N(4A), 1.100(6); N(3A)-Rh(1)-C(1), 90.95(4); N(3A)-Rh(1)-C(1)#1, 90.95(4); C(1)-Rh(1)-C(1)#1, 178.10(8); N(3A)-Rh(1)-Cl(1A), 180.0; C(1)-Rh(1)-Cl(1A), 89.05(4); C(1)#1-Rh(1)-Cl(1A), 89.05(4).

The bound nitrogen in **2-10** has an N-N bond length of 1.100(6) *versus* 1.0975 Å in free nitrogen,³⁴ and the $\nu(\text{N-N})$ appears in the IR at 2103 cm^{-1} . Binding of N_2 to rhodium appears to have caused only a slight lengthening of its interatomic distance, a phenomenon similar to that observed in the dioxygen complex **2-4**, likely resulting from poor overlap of d_{xz} and d_{xy} orbitals on Rh with available π^* orbitals of the dinitrogen ligand. The very slight elongation of the N-N bond seems to contradict the relatively strong π back-donation indicated by the vibrational spectra compared to an analogous compound reported by Stephan and coworkers.^{35,36} The isolated compound

[CH{C(Me)(NⁱPr₂C₆H₃)₂Rh(N₂)(COE)}], is also a square-planar Rh^I-N₂ complex, and has a nearly identical bond length (1.091 Å), but an N-N stretching frequency of 2175 cm⁻¹, indicating weaker back-donation.³⁶ It has been noted however, that the correlation between the bond lengths observed by X-ray analysis and the N-N stretching frequency is not very precise.³⁵ It is generally accepted, however, that the qualitative information obtained from the vibrational spectra is more informative,³⁷ and the charge distribution within M(N₂) complexes is often evaluated using a resonance structure model analogous to that applied to M(CO) complexes.³⁵

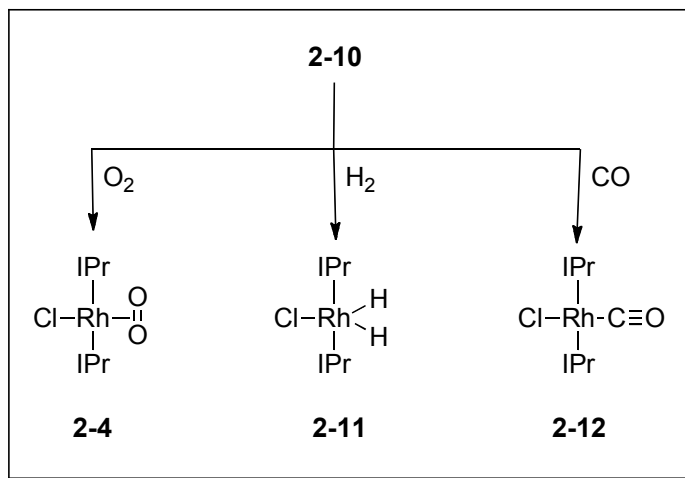
As with **2-4**, four-coordinate square planar rhodium complexes of molecular nitrogen bound end-on are quite rare, and typically involve ancillary ligands that are bulky and electron-rich. Some of these previously reported structures are analogous to the one which we report here, having the general formula *trans*-[XRhL₂(N₂)] (X = halogen or hydrogen), where in our case L is the NHC ligand IPr. When L = PⁱPr₃^{25,38} or PCy₃,^{24,39} and X = Cl the reported structures have nearly identical ν(N-N) stretches to those found in this investigation (2100 and 2103 cm⁻¹, respectively). In the case of the PⁱPr₃ complex, the Rh-N and N-N bond lengths (1.885(4) and 0.958(5)) are similarly reasonably close to those observed by us for compound **2-10**.³⁸ Milstein's group has reported a series of four-coordinate Rh-N₂ complexes featuring trivalent PCP ligands with ν(N-N) stretches ranging from 2110 to 2165 cm⁻¹.⁴⁰ One other example of a low-valent rhodium complex of molecular nitrogen was reported by Caulton's group featuring a unique PNP ligand, [(^tBu₂PCH₂SiMe₂)₂NRh(N₂)], which has a very low ν(N-N) of 2068 cm⁻¹.⁴¹ Interestingly, the 3-coordinate fragment of Caulton's complex²⁷ and the similar (PCP)Rh complex, [{Me₂C₆H(CH₂P^tBu₂)₂}Rh], reported by Milstein²⁶ are the

same ones mentioned previously in Section 2.2.1 that coordinate oxygen to give Rh(I)-O₂ complexes **2-8** and **2-9** similar to **2-4** with O-O bond lengths of 1.363 and 1.365 Å, respectively.

Compound **2-10** exhibits reasonable stability in the solid state and can be kept in a nitrogen atmosphere at room temperature for extended periods of time without noticeable decomposition. Furthermore, through introduction of other molecules, such as dioxygen, access to different coordination complexes are possible via complex **2-10**. In this way, **2-10** may act as a surrogate for the yet unreported coordinatively unsaturated species [ClRh(IPr)₂]. The analogous compound [ClRh(PCy₃)₂] was reported and used in the syntheses of N₂ complex [ClRh(PCy₃)₂(N₂)] and O₂ complex **2-6**, lending support to this hypothesis.^{23,24}

With this in mind, **2-10** was reacted independently with both H₂ and CO gases. Nolan and co-workers have previously shown that reacting a solution of [ClRh(COE)₂]₂ and two equivalents of IMes in THF with H₂ or CO gave complexes of the formula [ClRh(IMes)₂(XY)].⁴² Analogously, reaction of **2-10** with H₂ or CO gave [ClRh(IPr)₂(H)₂] (**2-11**) and [ClRh(IPr)₂(CO)] (**2-12**), respectively (Scheme 2-2).⁴³ Preparation of the two complexes is carried out similarly to the preparation of **2-4**: a THF solution of **2-10** (from a previously prepared sample or one prepared *in situ*) is degassed to remove the nitrogen atmosphere, which is then refilled with carbon monoxide or hydrogen. In the case of the carbon monoxide complex **2-12**, purification can be performed under aerobic conditions as the complex exhibits high stability. However, the dihydride appears to be oxidatively sensitive and upon exposure to oxygen reacts to form dioxygen complex **2-4**, necessitating anaerobic purification of **2-11**. Personal

communication with B.R. James indicated that a similar reaction was also observed in his laboratories; these findings were published concurrently with our own.^{43,44}



Scheme 2-2: Synthesis of bis-IPr rhodium complexes starting from complex **2-10**.

X-ray quality crystals of both **2-11** and **2-12** were obtained by diffusion of hexanes into concentrated THF solutions of the corresponding compounds, and are shown along with relevant bond lengths and bond angles in Figures 2-5 and 2-6, respectively (crystallographic parameters of **2-10**, **2-11** and **2-12** are presented in Table 2-5). The structural parameters of these three compounds possess a number of similarities as would be expected since their overall structure does not change significantly. All three of these structures are pseudo-square planar with slight distortions arising from a subtle tilting of the two rhodium-carbene bonds towards the chloro ligand. For each of these three compounds, as well as **2-4**, there is a dihedral angle of about 70° between the heterocyclic rings of the trans carbene ligands that minimizes steric interactions between the IPr ligands themselves and the *cis* chloro and (XY) ligands. The rhodium-carbene bonds are nearly identical for **2-10** and **2-12**, but slightly shorter in the case of **2-11**, a feature attributable to the difference in oxidation states between the former compounds

which are Rh(I), and the latter, which is formally Rh(III). Spectroscopically, however, no difference in this bonding can be detected, as for all three compounds the chemical shifts and $J_{\text{Rh-C}}$ of the carbene signal in the ^{13}C NMR spectra are quite similar. The ^{13}C resonances of the carbene carbons all appear between 189 and 193 ppm, and the $J_{\text{Rh-C}}$ values are about 40 Hz for each complex. While $J_{\text{Rh-P}}$ values are generally informative of the oxidation state of rhodium,⁴⁵ the same does not appear to be true for the $J_{\text{Rh-C}}$ of a Rh(NHC).⁴⁶ It also appears difficult to make assumptions about the electronic character of a rhodium complex based on the carbene carbon's chemical shift.⁴⁷

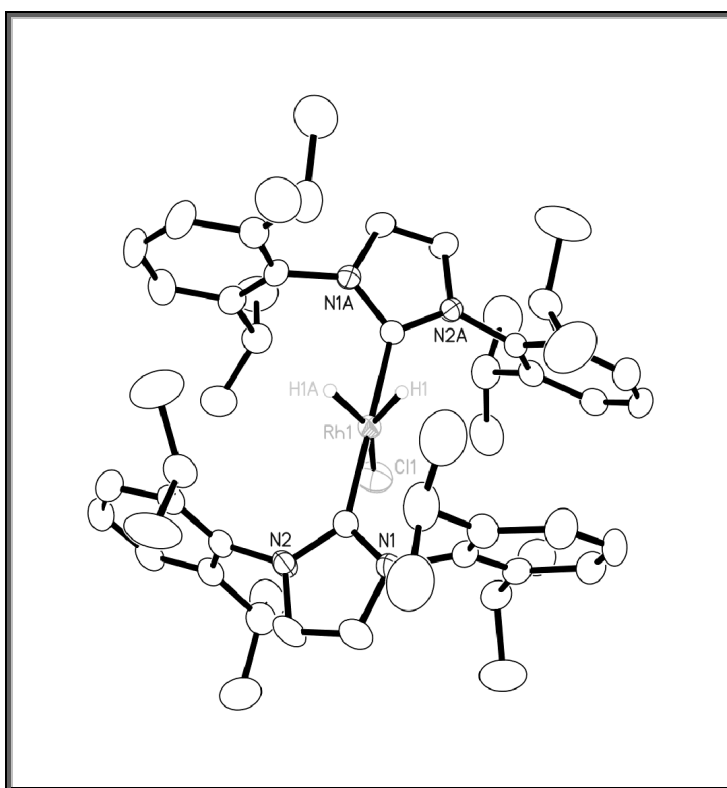


Figure 2-5: Crystallographically determined structure of the major component in the synthesis of $[\text{ClRh}(\text{IPr})_2(\text{H})_2]$ (**2-11**), displaying thermal ellipsoids drawn at the 50% confidence level. Selected interatomic distances (Å) and angles (deg): Rh(1)-H(1), 1.68(4); Rh(1)-C(1), 2.038(3); Rh(1)-Cl(1), 2.3628(12); H(1)-Rh(1)-Cl(1), 156.8(15); H(1)-Rh(1)-H(1A), 46.3(30); C(1)-Rh(1)-Cl(1), 90.91(8); C(1)#1-Rh(1)-Cl(1), 90.91(8); C(1)-Rh(1)-H(1), 93.0(18); C(1)#1-Rh(1)-H(1), 85.3(18); C(1)-Rh(1)-C(1)#1, 178.18(17).

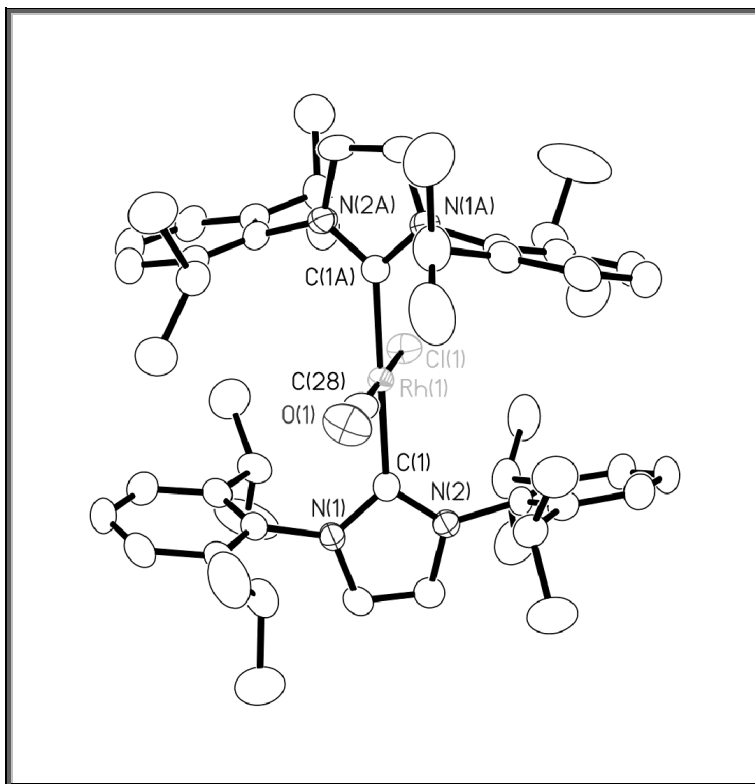


Figure 2-6: Crystallographically determined structure of $[\text{ClRh}(\text{IPr})_2(\text{CO})]$ (**2-12**), displaying thermal ellipsoids drawn at the 50% confidence level. Selected interatomic distances (Å) and angles (deg): Rh(1)-C(28), 1.839(11); Rh(1)-C(1), 2.0555(15); Rh(1)-Cl(1), 2.313(3); C(28)-O(1), 1.156(13); C(28)-Rh(1)-C(1), 90.66(4); C(28)-Rh(1)-Cl(1), 180.0; C(1)-Rh(1)-Cl(1), 89.34(4); C(1)#1-Rh(1)-C(1), 178.69(9).

The crystal packing of each structure is dictated almost entirely by the large carbene ligands positioned *trans* to one another, which is responsible for the high similarity between all the structures, and is a contributing factor in the positional disorder around the Cl-Rh-(XY) nucleus of the molecule. As was also observed in the initial crystal structures of Rh(O₂) complexes **2-4** and **2-5** (Section 2.1.2), the relative orientation of the Cl and XY groups within the crystal structures appears to be arbitrary with a nearly statistical distribution of these groups in either direction. The disorder observed in this area leads to some uncertainty in the X-Y bond lengths of these structures and may explain the considerably short N-N bond (1.100 Å) observed for **2-10**,

as crystals of **2-4** and **2-5** obtained without positional disorder had O-O bond lengths close to 0.1 Å longer than those that did (Section 2.1.2).

The crystal structure of dihydride **2-11** is characterized again by a *trans* relationship between the two carbene ligands, with the chloro and hydride ligands occupying the basal plane in this formally trigonal bipyramidal structure, similar to that observed by Nolan et al.⁴² Hydride ligands were observed crystallographically and have bond lengths of 1.68(4) Å, again consistent with the related Nolan complex prepared by an alternate route.

We were particularly interested in understanding the bonding in complex **2-11**, as it was shown that addition of oxygen to the [ClRh(IPr)₂] fragment *does not result in oxidation of the metal centre*, with both XAS and DFT studies suggesting that rhodium maintains a +1 oxidation state upon binding of O₂ (Section 2.2.1). For this reason, it was important to distinguish between classical dihydride [Rh^{III}-(H)₂] and non-classical dihydrogen [Rh^I-(H₂)] structures for complex **2-11**. This ambiguity can be resolved by measuring the relaxation time of the hydride signal in the ¹H NMR, as it has been shown that non-classical hydrides exhibit unusually short values because of increased physical relaxation imparted by the relatively close proximity of the hydrogen atoms to one another.⁴⁸ Determination of the *T*₁ time of the hydride signal in ¹H NMR by the typical method gave a value of 282 ms, indicative of a classical metal hydride. This leads to the interesting conclusion that hydrogen gas is able to oxidize the metal centre of [ClRh(IPr)₂], while oxygen is not.

Interestingly, the crystal structure of **2-11** also appears to contain the structure [Cl₂Rh(IPr)₂] (**2-13**), shown in Figure 2-7, in a relatively large abundance (~ 39 %). This

was somewhat surprising considering the very sharp NMR spectra of the bulk material, with no obvious indication of the presence of any paramagnetic material. However, closely related paramagnetic impurities have been observed and characterized in complexes derived from Wilkinson's complex,⁴⁹ and appear to result from incomplete reduction of rhodium in their synthesis from rhodium(III) starting materials.

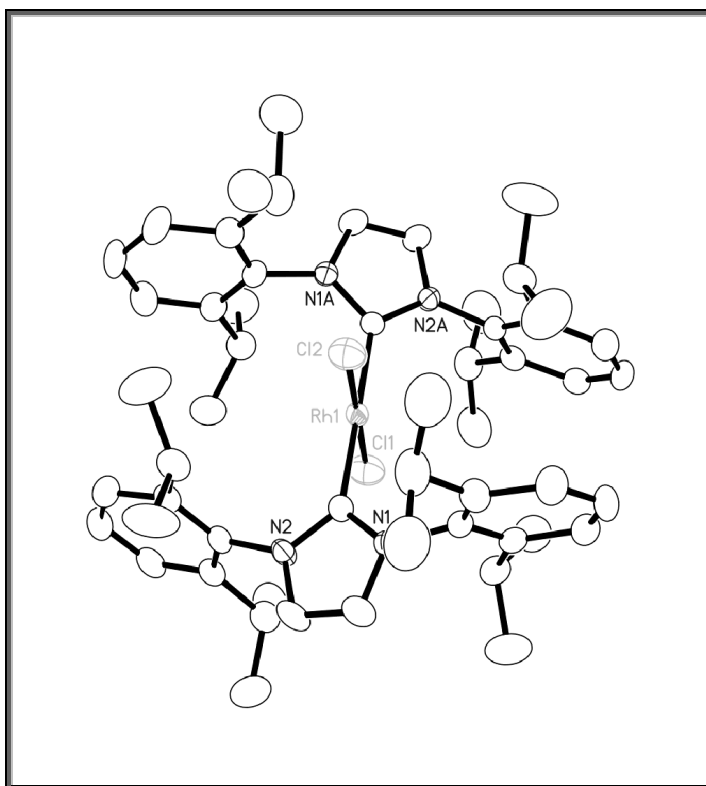


Figure 2-7: Crystallographically determined structure of the paramagnetic impurity $[\text{Cl}_2\text{Rh}(\text{IPr})_2]$ (**2-13**) in the synthesis of compound **2-11**, displaying thermal ellipsoids drawn at the 50% confidence level.

To gain some measure of the quantity of **2-13** in the bulk sample of **2-11**, EPR spectra were obtained and confirmed that a paramagnetic species was present in relatively low abundance within the sample ($< 0.1\%$). Considering the weakness of the EPR signal in the bulk material, it is likely that the small amounts of **2-13** present in bulk **2-11**

crystallized preferentially along with the structurally similar **2-11**, leading to enrichment in the crystalline form.

Table 2-5: Crystallographic parameters for compounds **2-10**, **2-11/2-13** and **2-12**.

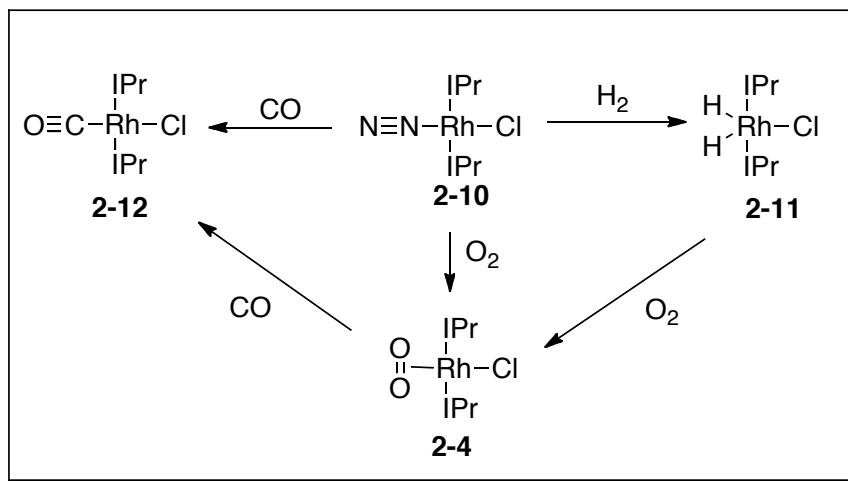
	2-10	2-11/2-13	2-12
Formula	C ₆₀ H ₈₆ N ₆ RhCl	C ₆₀ H _{87.21} N ₄ RhCl _{1.39}	C ₆₁ H ₈₆ N ₄ ORhCl
Fw	1029.74	1016.91	1029.70
Crystal dimensions (mm ³)	0.35 x 0.30 x 0.25	0.30 x 0.25 x 0.20	0.45 x 0.30 x 0.20
Crystal system	Orthorhombic	Orthorhombic	Orthorhombic
Space group	P2(1)2(1)2	P2(1)2(1)2	P2(1)2(1)2
<i>a</i> (Å)	13.0317(6)	13.00230(10)	13.0505(10)
<i>b</i> (Å)	20.6605(9)	20.6116(3)	20.6813(16)
<i>c</i> (Å)	10.6499(5)	10.63610(10)	10.6549(9)
<i>V</i> (Å ³)	2867.4	2850.46(5)	2877.0(4)
<i>Z</i>	2	2	2
<i>T</i> (K)	180(2)	180(2)	180(2)
<i>D</i> _{calcd} (g cm ⁻³)	1.196	1.184	1.189
<i>m</i> (mm ⁻¹)	0.386	0.405	0.385
<i>F</i> (000)	1106	1086	1100
<i>q</i> range (deg)	2.15-28.28	1.85-26.00	1.91-25.00
Index ranges (<i>h</i> , <i>k</i> , <i>l</i>)	±16, ±26, ±14	-16-14, -19-25, ±13	±15, ±24, ±12
No. of rflns collected	31416	14522	16993
No. of independent rflns/ <i>R</i> _{int}	6676/0.0234	5600/.0304	5073/0.0218
No. data/restraints/params	6676/0/297	5600/3/323	5073/0/306
<i>R</i> ₁ / <i>wR</i> ₂ (<i>I</i> > 2σ(<i>I</i>))	0.0227/0.0584	0.0373/0.0954	0.0210/0.0504
<i>R</i> ₁ / <i>wR</i> ₂ (all data)	0.0243/0.0590	0.0463/0.1003	0.0272/0.0688
GOF (on <i>F</i> ²)	1.053	1.055	1.017
largest diff peak/hole (e Å ⁻³)	0.352/-0.311	0.653/-0.438	0.279/-0.139

$$^a R_1 = \sum ||F_o| - |F_c|| / \sum |F_o|; \quad wR_2 = \{ \sum [w(F_o^2 - F_c^2)^2] / \sum [w(F_o^2)^2] \}^{1/2}; \quad \text{GOF} = \{ \sum [w(F_o^2 - F_c^2)^2] / (n - p) \}^{1/2}.$$

2.2.3 Relative Stability of [CIRh(IPr)₂(XY)] Complexes

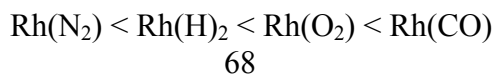
Through the study of compounds **2-4**, **2-10**, **2-11** and **2-12**, we have been able to gain an understanding of the relative stabilities of these complexes. Dinitrogen complex

2-10 can be used as a precursor to all other compounds described herein, which is an indication of the lability of this ligand with respect to the other ligands tested. Dioxygen complex **2-4** can also be prepared from dihydride **2-11**, a reaction that takes place quickly in solution and over extended periods in the solid state. Exposure of the carbon monoxide complex **2-12** to oxygen, however, did not lead to dioxygen compound **2-4**. Remarkably, this complex has such high oxidative stability that even after refluxing a toluene solution of **2-12** in air for 24 hours, no formation of **2-4** was observed. Since Milstein has reported Rh(O₂) complexes in which N₂ can be used to displace oxygen,²⁶ we attempted to prepare **2-10** from **2-4** by refluxing a toluene solution of the oxygen adduct under a positive pressure of nitrogen gas, however no conversion to nitrogen complex **2-10** was observed (Scheme 2-3).



Scheme 2-3: Relative reactivity of the [ClRh(IPr)₂(XY)] complexes.

It therefore appears that the carbon monoxide adduct is the most stable, while nitrogen is the most reactive. From this study a trend of stability for this series of complexes can be stated as follows:



A similar series of stabilities has been previously proposed for molecules of the formula $[\text{CIRh}(\text{P}^i\text{Pr}_3)_2(\text{XY})]$, however, the oxygen complex was less stable in this series, likely due to the presence of oxidatively sensitive phosphine ligands.²⁵ Interestingly, we did observe slow exchange of the O_2 ligand in $^{18}\text{O}_2\text{-2-4}$ for the naturally occurring $^{16}\text{O}_2$ isotopomer; an IR spectrum of $^{18}\text{O}_2\text{-2-4}$ taken after a week of storage on the bench top yielded spectra identical to $^{16}\text{O}_2\text{-2-4}$.

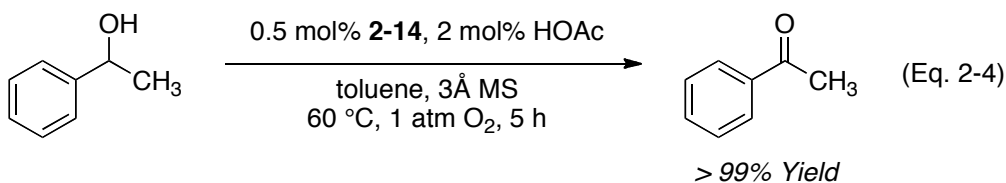
2.2.4 Oxidation/Reduction of C-O Bonds with $[\text{CIRh}(\text{IPr})_2(\text{XY})]$

The oxidation of alcohols is a reaction of great importance in organic synthesis and industrial processes, as the resulting carbonyl compounds are intermediates for medicines, agricultural chemicals, and fragrances.⁵⁰ Classical methods for the oxidation of alcohols to carbonyl compounds typically rely on stoichiometric oxidants, such as chromium oxide,⁵¹ dichromate⁵² or ruthenium oxide,⁵³ which are generally toxic and produce stoichiometric amounts of waste products. Thus recent efforts have been made to develop catalytic systems, preferably relying upon dioxygen as the terminal oxidant.

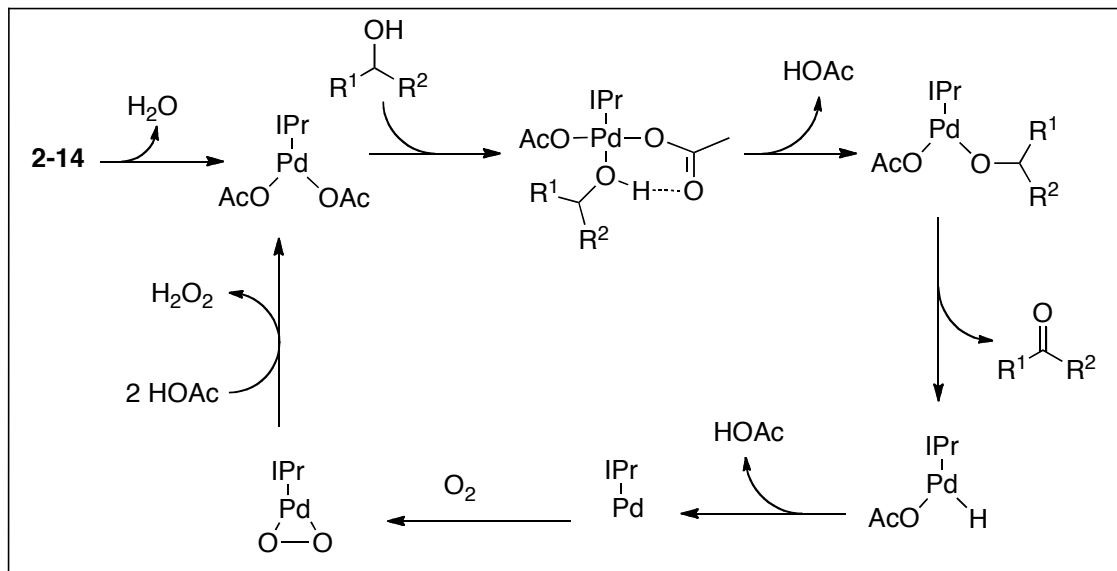
Examples of aerobic alcohol oxidation have been demonstrated for several transition metal systems, including those of ruthenium and copper. A number of copper complexes have been synthesized as biomimetic models of galactose oxidase, which selectively oxidizes primary alcohols to aldehydes in the presence of molecular oxygen.⁵⁴ Heterogeneous systems involving ruthenium hydroxide catalysts supported on aluminum and titanium oxides have also been developed and are capable of efficiently oxidizing a wide range of alcohols and amines.⁵⁵

We were particularly interested in catalytic systems employing palladium,⁵⁶ such as that shown in Eq. 2-4, as it was shown that Pd^{II} -peroxo complexes were likely

intermediates in the catalytic cycle. The specific catalyst employed in this case, [Pd(IPr)(OAc)₂(H₂O)] (**2-14**), also uses an N-heterocyclic carbene as the key ancillary ligand.⁵⁷



In the proposed catalytic cycle (Scheme 2-4) the alcohol replaces H₂O at the palladium center and is then deprotonated intramolecularly by an acetate ligand, releasing HOAc and generating a Pd-alkoxide. The Pd-alkoxide then undergoes β-hydride elimination giving the carbonyl product and a Pd-H, which after reductive elimination of another molecule of HOAc results in a coordinatively unsaturated Pd⁰ intermediate. Oxidation of the Pd⁰ intermediate by O₂ is followed by protonation to regenerate [Pd(IPr)(OAc)₂] and produce H₂O₂. The oxygen serves not only as the oxidant, but also removes the low-ligated Pd⁰ from the catalytic cycle preventing aggregation of palladium black.

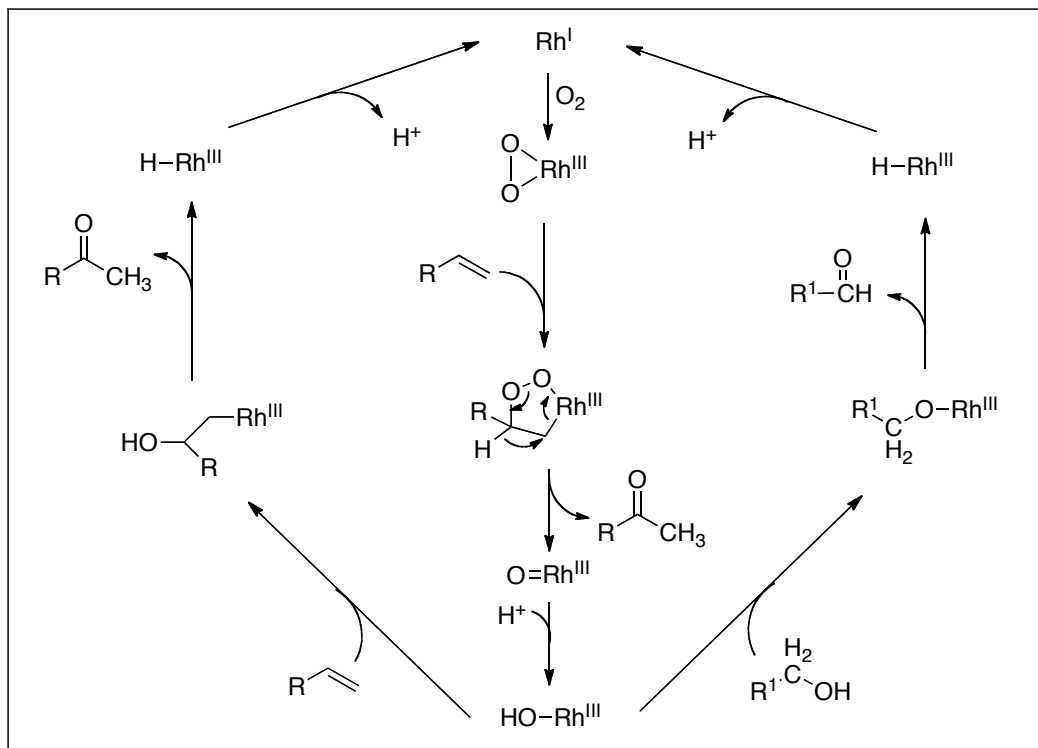


Scheme 2-4: Proposed mechanism for the aerobic oxidation of alcohols by **2-14**.⁵⁷

Of specific interest to us was an analogue of the proposed peroxo intermediate, $[\text{Pd}(\text{IMes})_2(\text{O}_2)]$, isolated by Stahl,⁵⁸ which inspired us to explore the possibility that our dioxygen complexes **2-4** and **2-5** may be capable of performing oxidation reactions analogous to those catalyzed by **2-14**. We therefore set out to optimize a rhodium-catalyzed aerobic oxidation of alcohols using $[\text{ClRh}(\text{IPr})_2(\text{O}_2)]$ (Table 2-6).

In terms of rhodium-catalyzed oxidation reactions, the O_2 -promoted conversion of alkenes to ketones has been previously reported.⁵⁹⁻⁶⁵ The reactions are thought to proceed through the Rh^{III} -peroxide, which reacts with the alkene to form a 5-membered metallocyclic intermediate, which then undergoes a β -hydride migration to yield the ketone and a Rh-oxo intermediate. Acid is required in the catalytic cycle to activate this $\text{Rh}(\text{O})$ intermediate, which oxidizes a second equivalent of alkene via a Wacker-type process, or oxidizes alcohol solvent via hydrogen transfer (Scheme 2-5).^{61,63,66} These transformations were often very sluggish, and required the addition of reducing

equivalents (such as primary or secondary alcohols),^{62,63} or oxidants (such as copper co-catalysts^{59,61} or *tert*-butylperoxide⁶⁵) to promote catalyst turn-over. Furthermore, side-products such as allylic ketones and epoxides were often observed.⁶⁴ Rhodium-catalyzed aerobic oxidation of secondary alcohols to ketones are, however, absent from the literature.

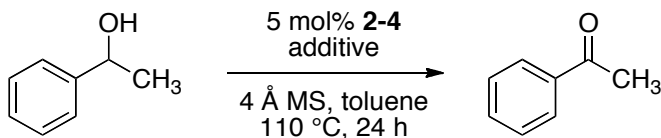


Scheme 2-5: Proposed catalytic cycle for Rh-catalyzed oxidation of alkenes to ketones.^{61,63,66}

We began our catalytic investigations by treating a 0.5 M solution of *sec*-phenethanol in toluene with 5 mol% **2-4** at 110 °C for 24 h under a positive pressure of air. While acetophenone was detected as the only product in the reaction, the reaction was not catalytic as only 4% conversion was observed (Table 2-6, entry 1). A series of additives, both acidic and basic, were then employed in an attempt to affect catalytic turnover. Addition of 20 mol% HOAc to the reaction gave a modest 29% yield,

corresponding to about 6 catalyst turnovers; the same amount of stronger acids such as trifluoroacetic acid (TFAA) and HCl gave much lower yields (entries 3 and 4, respectively). The IMes-containing dioxygen complex **2-5**, was also employed at 5 mol% with 20 mol% HOAc, but was not as effective as **2-4**, giving only a 10% yield of acetophenone after 24 h. Both organic and inorganic bases were employed with catalyst **2-4**, however, no noticeable advantage over HOAc was observed (entries 5-8). Sigman et al. have demonstrated that additive amounts of the naturally occurring (-)-sparteine used with an achiral $[\text{Cl}_2\text{Pd}(\text{NHC})]_2$ catalyst resulted in the oxidative kinetic resolution of racemic alcohol mixtures with k_{rel} values as high as 14.⁶⁷ Use of (-)-sparteine with our system (entry 6) gave identical yields to the same reaction with triethylamine (entry 7), and no optical enrichment of the remaining alcohol was observed.

Table 2-6: Optimization of Alcohol Oxidation with Catalyst **2-4**.^a



Entry	Additive	% Yield ^b
1	no additive	4
2	20 mol% HOAc	29
3 ^c	20 mol% HOAc	10
4	20 mol% TFAA	4
5	20 mol% HCl	3
6	20 mol% (-)-sparteine	22
7	20 mol% NEt ₃	22
8	1 equiv. Cs ₂ CO ₃	28
9	1 equiv. NaHCO ₃	22
10	5 mol% HOAc	55
11	5 mol% HOAc, 1 equiv. BzNEt ₃ ⁺ Cl ⁻	16

^aConditions: 5 mol% catalyst loading, additive, 4 Å molecular sieves, 0.5 M *sec*-phenethanol in toluene, 110 °C, 24 h under a positive pressure of air. ^bConversion determined by GC relative to hexamethylbenzene as an internal standard. ^cCatalyst **2-5** was employed.

As an additive HOAc appeared to give the best results in our catalytic reaction, so we next attempted to optimize its concentration (Figure 2-8). As noted above, the reaction is not catalytic in the absence of HOAc, however, as small amounts are added the yield incrementally increases, with a maximum yield of 55% achieved with 5 mol% HOAc (Table 2-7, entry 10). At 10 mol% the yield of acetophenone is halved, giving a nearly identical yield to that observed when 20 mol% HOAc is employed. Interestingly, the same reaction performed in the presence of a chloride source, BzNEt₃Cl, caused a dramatic decrease in the yield of the catalytic reaction (entry 11).

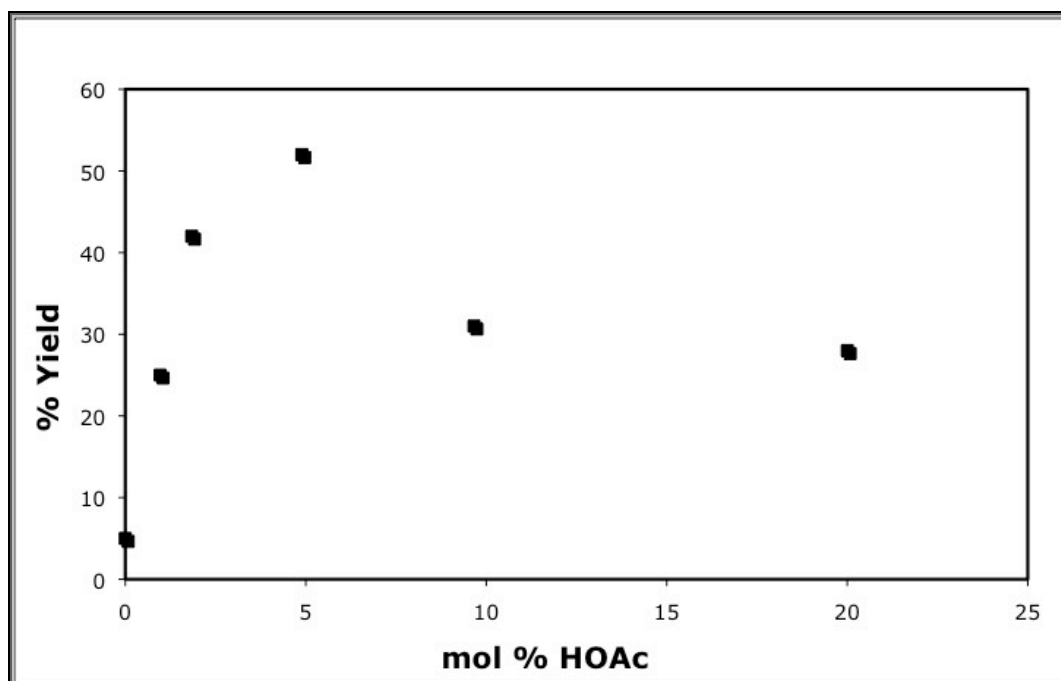
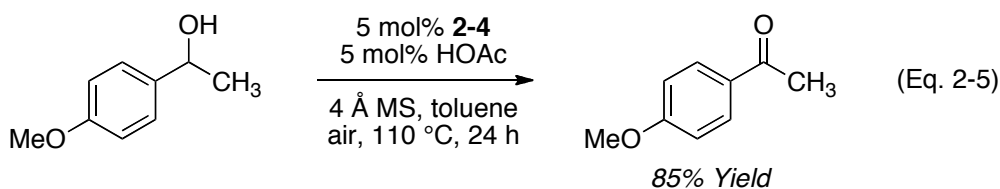


Figure 2-8: Effect of HOAc added on aerobic alcohol oxidation catalyzed by **2-4**. Catalytic runs were performed in duplicate and are presented as mean yields with errors of $\pm 2\%$.

Sigman's laboratory observed a similar effect of HOAc on yield in their mechanistic study of aerobic alcohol oxidation by **2-14**.⁵⁷ In their system, the rate acceleration at low concentrations HOAc was attributed to promoting the regeneration of

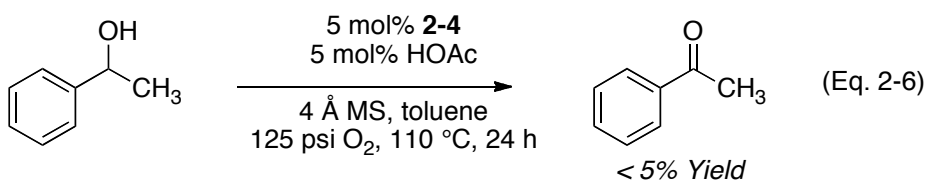
the active Pd^{II} catalyst via protonation of the Pd^{II}-(O₂) to yield [Pd(IPr)(OAc)₂] and H₂O₂. Rate retardation at higher [HOAc] was attributed to reprotonation of the Pd-alkoxide prior to β-hydride elimination, which shifts the equilibrium away from β-hydride elimination.

Employing our best conditions – 0.5 M *sec*-phenethanol in toluene, 5 mol% **2-4**, 5 mol% HOAc, 4 Å MS, reflux, air – for longer reaction times did not result in complete conversion, and significant production of colloidal rhodium was observed as the reaction progressed. In an attempt to achieve complete aerobic oxidation of an alcohol prior to catalyst decomposition, 1-(4-methoxyphenyl)ethanol was employed as a substrate, from which hydride abstraction would be expected to be more facile relative to *sec*-phenethanol based on Hammett studies of similar reactions.^{57,68} Gratifyingly, the product 4-methoxyacetophenone was obtained in 85% yield was obtained using our optimized conditions (Eq. 2-5). This result seemed to demonstrate the effect of the alcohol's electronic nature on the outcome of the catalytic reaction, and the importance of β-hydride elimination to overall reaction rate.

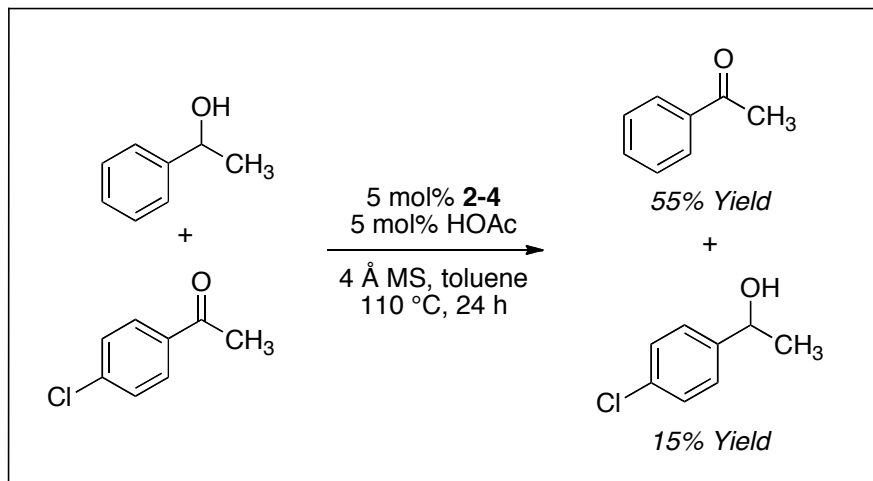


The deposition of rhodium black as the reaction proceeded was likely detrimental to catalytic activity, as the loss of activity coincided with the visual observation of colloidal metal formation. In the palladium-catalyzed reaction, the secondary role of oxygen was to limit the lifetime of palladium(0), preventing aggregation and precipitation of inactive colloidal species. Thus, we carried out the catalytic oxidation of *sec*-

phenethanol by **2-4** under 125 psi of O₂ gas in an attempt to prevent catalyst deactivation (Eq. 2-6). While the recovered reaction solution did not possess significant amounts of rhodium black, the catalytic activity was negatively affected, yielding less than 5% acetophenone after 24 h at 100 °C.

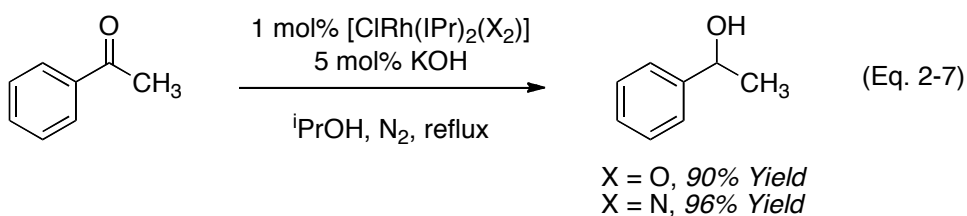


Unable to achieve complete conversion of our alcohol substrates to their corresponding ketones, we considered the possibility that these reactions were entirely reversible and that we were observing equilibrium yields. To test this hypothesis, a crossover experiment was performed in which both 4-chloro acetophenone and *sec*-phenethanol were submitted to our optimized conditions (Scheme 2-6). While the yield of acetophenone was the same as that observed in the absence of 4-chloro acetophenone (55%), under the oxidizing reaction conditions, the competing substrate was reduced to 1-(4-chlorophenyl)ethanol in about 15% yield. This proves the capability of the product ketone to intercept a rhodium-hydride and regenerate the starting alcohol at a competitive rate with respect to dioxygen.



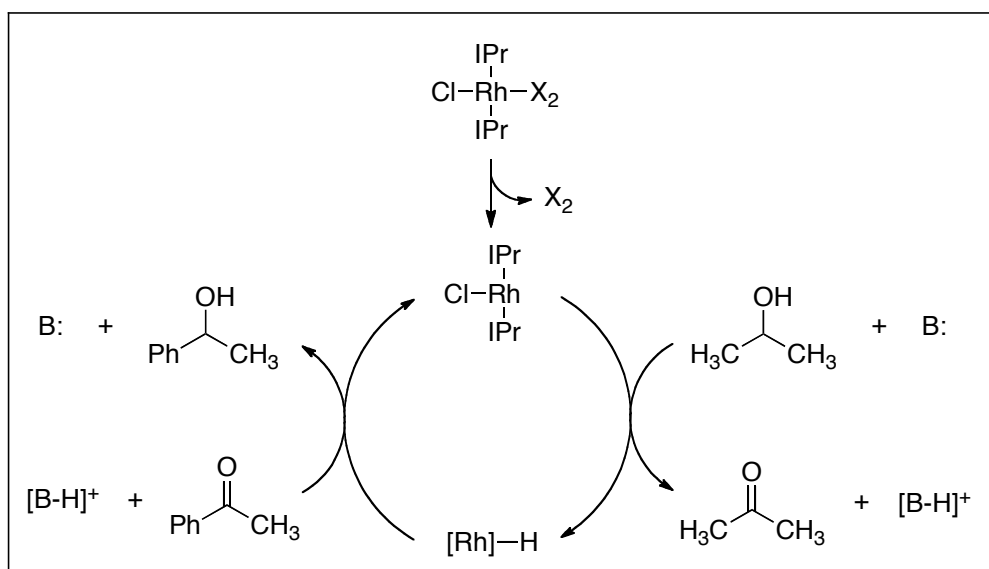
Scheme 2-6: Crossover experiment between *sec*-phenethanol and 4-chloroacetophenone.

Thus, we considered the possibility that our catalyst may prefer to *reduce* C-O bonds rather than oxidize them given the result of Scheme 2-6, which suggested a transfer hydrogenation occurring between the two substrates. To verify this hypothesis we next looked to catalytically reduce acetophenone under transfer hydrogenation conditions: 0.1 M acetophenone in isopropanol, 1 mol% **2-4**, 5 mol% KOH. Under these conditions, *sec*-phenethanol was obtained in 90% yield after 3 h at reflux under a nitrogen atmosphere (Eq 2-7, X = O).



A typical transfer hydrogenation mechanism would suggest that reaction of acetophenone is preceded by oxidation of isopropanol with rhodium to generate acetone and a rhodium-hydride. Acetophenone would then undergo a 1,2-insertion into the rhodium-hydride to generate a rhodium-alkoxide. To enter this catalytic cycle, which

requires no formal change in the oxidation state at rhodium, **2-4** likely dissociates the coordinated dioxygen to generate a coordinatively unsaturated complex capable of binding isopropanol (Scheme 2-7). Consistent with this hypothesis, employing the analogous dinitrogen compound **2-10** gave nearly identical results to **2-4** (Eq. 2-7).

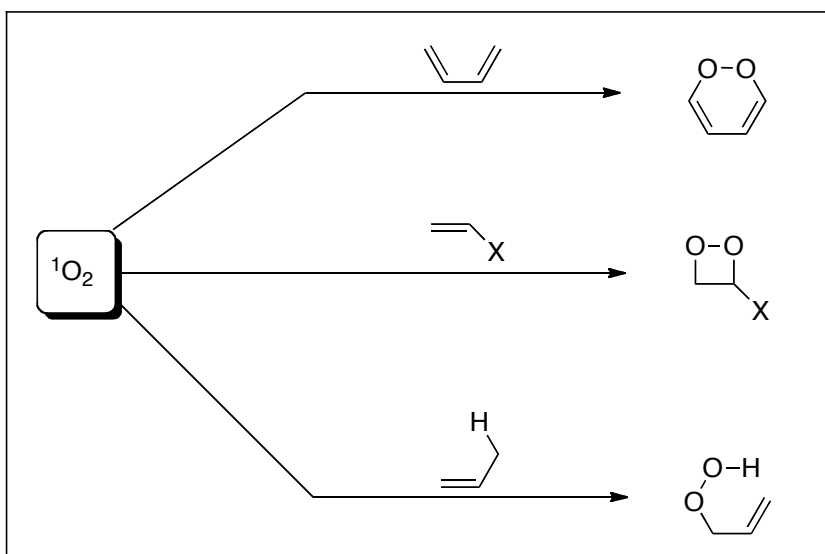


Scheme 2-7: Proposed transfer hydrogenation mechanism by **2-4** and **2-10**.

The fact that the catalytic reaction appears to proceed through a coordinatively unsaturated rhodium(I) intermediate may also explain the observed thermal decomposition under oxidative conditions. Furthermore, in both the reductive and oxidative processes it appears that no change in oxidation state at rhodium is required and that a rhodium(I) species likely predominates. This is consistent with our structural analysis of **2-4** which identified this species as a $\text{Rh}^{\text{I}}-(^1\text{O}_2)$ and not a Rh^{III} -peroxo, and in hindsight, it is therefore not surprising that **2-4** and **2-5** were inefficient oxidation catalysts.

2.2.5 Catalytic Generation of Singlet Oxygen

Since the initial discovery of the singlet oxygen by Foote et al. as the reactive species in photooxidation reactions,⁶⁹ it has been used as an atom-economical source for the introduction of oxygen atoms in organic synthesis.⁷⁰ Being isoelectronic to the carbon skeleton of ethylene, singlet oxygen exhibits similar reactivity undergoing [4 + 2] cycloadditions with conjugated dienes to form endoperoxides,⁷¹ [2 + 2] cycloadditions with electron-rich alkenes to form 1,2-dioxetanes⁷¹ and ene-type reactions with unactivated alkenes to form allylic hydroperoxides⁷² (Scheme 2-8).



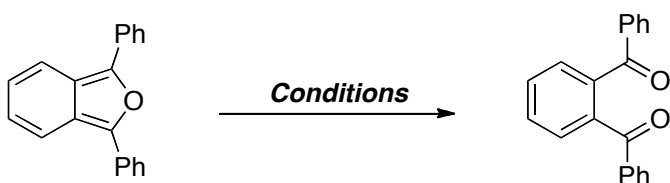
Scheme 2-8: Potential reactions of singlet oxygen with different alkene substrates.

These reactions, which are often quite selective, are in contrast to the reactions of triplet oxygen, which follows radical pathways. Generation of singlet oxygen for these reactions is usually performed by photosensitization, using a high-energy light source and a sensitizer such as rose bengal, methylene blue or porphyrins. Alternatively, chemical

sources can be used to generate singlet oxygen;⁷³ for example, hydrogen peroxide can be disproportionated to water and singlet oxygen using molybdenates.⁷⁴

There does not, however, exist a catalyst for the non-photosensitized generation of singlet oxygen. Given the unique structure of complex **2-4**, which is a coordination complex of singlet oxygen, we investigated whether or not it could be used as a source of singlet oxygen for organic synthesis. Based on our previous results, the thermal stability of complex **2-4** indicated that oxygen release does not occur below 80 °C and we were therefore limited to reactions whose products would be stable at this temperature.

Table 2-7: Catalytic Generation of Singlet Oxygen by **2-4**.



Entry	Conditions	% Yield
1	20 mol% 2-4 , refluxing toluene, 24 hr	52 ^a
2	20 mol% 2-4 , 20 mol% HOAc, refluxing toluene, 24 hr	78 ^a
3	20 mol% 2-4 , 20 mol% HOAc, MS, refluxing toluene, 24 hr	38 ^a
4	10 mol% 2-4 , refluxing toluene, 24 hr	16 ^a
5	10 mol% 2-4 , 10 mol% HOAc, refluxing toluene, 24 hr	20 ^a
6	10 mol% 2-4 , 20:1 DMF/H ₂ O, 120 °C, 7 hr	90 ^b
7	no catalyst, 20:1 DMF/H ₂ O, 120 °C, 7 hr	94 ^b

^aIsolated yield. ^bGC Yield.

A popular test substrate for investigating new sources of singlet oxygen is 1,3-diphenylisobenzofuran, which undergoes a [4 + 2] cycloaddition with singlet oxygen followed by a rearrangement to form *ortho*-dibenzoylbenzene. Using this as our test reaction, we began by probing conditions with 20 mol% of **2-4** in refluxing toluene (Table 2-7, entries 1–5). The reaction was accelerated by the presence of catalytic

amounts of HOAc, which gave the product in 78% isolated yield *versus* 52% yield with the use of **2-4** alone (entry 2). This was similar to the results obtained in alcohol oxidation reactions, so the addition of 4 Å molecular sieves was tested, however this appeared to retard the reaction, giving only a 38% yield (entry 3). Lowering the catalyst loading of **2-4** to 10 mol% gave significant decreases in the yield of *ortho*-dibenzoylbenzene: 20% and 16% yield with and without an equivalent amount of HOAc, respectively. An aqueous mixture of DMF was also tried as well (20:1 DMF/H₂O), giving nearly complete conversion in 7 h (entry 6), however, control reactions for these conditions gave nearly identical yields (entry 7).

A careful screen of the literature showed that 1,3-diphenylisobenzofuran undergoes autoxidation at elevated temperatures and control reactions are therefore imperative for such reactions.⁷⁵ Thus, while **2-4** may have potential as a catalytic source of singlet oxygen, its thermal stability is a liability for these types of reactions. Synthetic efforts should therefore be made towards analogous Rh^I-(¹O₂) complexes that are less thermally stable, and capable of releasing oxygen at lower temperatures.

2.3 Conclusions

The dioxygen complexes [ClRh(IPr)₂(O₂)] (**2-4**) and [ClRh(IMes)₂(O₂)] (**2-5**) were characterized by X-ray diffraction, NMR spectroscopy and DFT calculations; as well, complex **2-4** was characterized by IR, Raman, and XAS spectroscopy. The shorter O-O bond distances in the two complexes, atypical of common Rh(O₂) complexes, were corroborated by the high value for the corresponding O-O stretching frequencies in the vibrational spectrum of **2-4**. Analysis of complex **2-4**, by XAS and DFT calculations suggest that the best description of these compounds is a rhodium(I) coordination complex of singlet oxygen, which is consistent with all other data. The unique bonding mode appears to result from the interaction of a filled Rh d orbital with one of the two degenerate O₂ π* orbitals. This results in splitting of the O₂ π* orbitals, favoring spin pairing in the O₂ HOMO, and the inability of Rh to donate electron density to the empty π* orbital. The recent synthesis of [Rh(NHC)₂(RCN)₂(O₂)]⁺X⁻ complexes in our laboratory, which are octahedral Rh^{III}-peroxo complexes, seems to indicate that it is the low coordination number of **2-4** and its analogs that is responsible for its inability to effectively reduce O₂.⁷⁶

The coordination chemistry of the [ClRh(NHC)₂] fragment was also examined with simple diatomic molecules and was observed to bind dinitrogen end-on yielding [ClRh(IPr)₂(N₂)] (**2-10**). While this complex is very stable in the solid state, dinitrogen is easily displaced in solution by O₂, CO and H₂. For these complexes of the formula [ClRh(IPr)₂(XY)], the relative binding affinity of the diatomic molecules was qualitatively determined, and appears to follow the order: CO > O₂ > H₂ > N₂.

Finally, the ability of the dioxygen complexes, **2-4** and **2-5**, to catalytically oxidize secondary alcohols under aerobic conditions was assessed. Yields as high as 85% were achieved for the substrate 1-(4-methoxyphenyl)ethanol with a 5 mol% loading of catalyst **2-4**. By carrying out crossover studies, we were able to determine that incomplete conversion was due to a resulting equilibrium between the alcohol and its ketone. Thus, the ability of **2-4** and Rh(N₂) complex **2-10** to reduce acetophenone under transfer hydrogenation conditions was investigated, and the resulting alcohol isolated in up to 96% yield.

2.4 Experimental

General considerations: All manipulations were carried out in a nitrogen atmosphere glove box or using standard Schlenk techniques unless otherwise stated above. THF, toluene and hexanes were purified on a PureSolv Solvent Purification system, degassed by at least three freeze-pump-thaw cycles and stored over 4 Å molecular sieves prior to use. Deuterated solvents were distilled from CaH₂, degassed by at least three freeze-pump-thaw cycles and stored over 4 Å molecular sieves prior to use. [ClRh(C₂H₄)₂]₂,⁷⁷ IPr⁷⁸ and IMes⁷⁹ were prepared according to previously reported literature procedures. H₂, CO, and N₂ gases were purchased from Praxair and used without purification. ¹H NMR spectra were recorded on a 400 or 500 MHz spectrometer. Chemical shifts are reported in delta (δ) units, expressed in parts per million (ppm) downfield from tetramethylsilane using residual protonated solvent as an internal standard (C₆D₆, 7.15 ppm; CD₂Cl₂, 5.32 ppm). ¹³C NMR spectra were recorded on a 100 or 125 MHz spectrometer. Chemical shifts are reported as above using the solvent as an internal standard (C₆D₆, 128.0 ppm; CD₂Cl₂, 53.8 ppm). Elemental analyses were performed by Canadian Microanalytical Systems Ltd. X-ray data collection was performed on a Bruker SMART CCD 1000 X-ray diffractometer by Dr. Ruiyao Wang. EPR was performed courtesy of Dr. Sean McGrady and Aaron Matthews at the University of New Brunswick. XAS data was collected and analyzed by Dr. Pierre Kennepohl and Danielle Covelli of UBC at the Stanford Synchrotron Radiation Laboratory. DFT calculations were performed by Dr. Friedrich Grein of UNB and Dr. Pierre Kennepohl.

Synthesis of Organometallic Complexes:

Preparation of [ClRh(IPr)₂(O₂)] (**2-4**): An oven-dried round bottom flask containing a stir bar was brought into the glove box and charged with [ClRh(C₂H₄)₂]₂ (64.9 mg, 0.167 mmol), IPr (270.5 mg, 0.696 mmol) and 5 mL of THF. The reaction was allowed to stir for 10 minutes. The flask was removed from the glove box, frozen with liquid nitrogen, and the atmosphere removed by vacuum. After thawing, the yellow solution was purged twice with a balloon of oxygen gas, then left to stir under an atmosphere of oxygen. The volatiles were removed in vacuo, and the resulting blue/green residue dissolved in minimal CH₂Cl₂ and filtered through a short plug neutral Al₂O₃ collecting the blue fraction. Evaporation of the collected fraction yielded analytically pure [ClRh(IPr)₂(O₂)]. Yield 248 mg (80 %). Anal. Found (calcd) for RhC₅₄H₇₂N₄O₂Cl • 2H₂O: C 65.37 (65.80), H 5.81 (5.69), N 7.57 (7.98). IR (KBr): $\nu = 1021$ (O-O, s) cm⁻¹. ¹H NMR (298 K, 400 MHz, *d*₈-toluene) δ : 7.28 (t, J = 7.6 Hz, 4H), 7.07 (d, J = 7.6 Hz, 8H), 6.46 (s, 4H), 2.81 (m, br, 8H), 1.01 (m, 48H) ppm. ¹H NMR (233 K, 400 MHz, *d*₈-toluene) δ : 7.29 (t, J = 7.6 Hz, 4H), 7.07 (d, J = 7.6 Hz, 8H), 6.37 (s, 4H), 3.21 (m, 4H), 2.61 (m, 4H), 1.21-0.98 (m, 48H) ppm. ¹³C NMR (298 K, 400 MHz, *d*₈-toluene) δ : 180.8 (d, *J*_{Rh-C} = 40 Hz), 147.0 (br), 137.4, 129.4, 124.2, 123.6, 28.6, 26.3, 23.1 ppm.

Preparation of [ClRh(IPr)₂(¹⁸O₂)] (**¹⁸O₂-2-4**): A 25 mL Schlenk flask was charged with [ClRh(C₂H₄)₂]₂ (51.3 mg, 0.132 mmol) and IPr (206.7 mg, 0.532 mmol), and the solids dissolved in THF (10 mL). The resulting yellow solution was stirred for 10 min, a vacuum adaptor was attached to the top of the flask and the apparatus removed from the glovebox. The yellow solution was attached to the Schlenk line via the vacuum adaptor and to a lecture bottle of ¹⁸O₂ gas via the side arm; all joints were sealed with Teflon tape

then electrical tape. The reaction mixture was degassed through the vacuum adaptor via three freeze-pump-thaw cycles, the adaptor was closed and the flask back-filled with $^{18}\text{O}_2$ gas. The reaction was stirred for 8 h under $^{18}\text{O}_2$ gas, the volatiles removed and the sample stored in the glove box to prevent exchange with atmospheric O_2 . IR (KBr): $\nu = 958$ (^{18}O - ^{18}O , s) cm^{-1} .

Preparation of $[\text{ClRh}(\text{IMes})_2(\text{O}_2)]$ (**2-5**): An oven-dried round bottom flask containing a stir bar was brought into the glove box and charged with $[\text{ClRh}(\text{C}_2\text{H}_4)_2]_2$ (13.4 mg, 0.0344 mmol), IMes (46.0 mg, 0.151 mmol) and 5 mL of THF and the resulting yellow mixture was stirred for about ten minutes. The flask was removed from the glove box, frozen with liquid nitrogen, and the atmosphere removed by vacuum. After thawing, the yellow solution was purged twice with a balloon of oxygen gas, then left to stir under an atmosphere of oxygen. The volatiles were removed in vacuo, and the resulting blue/green residue dissolved in minimal CH_2Cl_2 and filtered through a short plug neutral Al_2O_3 collecting the blue fraction. Evaporation of the collected fraction yielded analytically pure $[\text{ClRh}(\text{IMes})_2(\text{O}_2)]$. Yield (79%). Anal. Found (calcd) for $\text{RhC}_{42}\text{H}_{48}\text{N}_4\text{O}_2\text{Cl} \cdot \text{H}_2\text{O}$: C 63.49 (63.28), H 6.01 (6.32), N 6.94 (7.03). IR (KBr): $\nu = 1020$ (O-O, s) cm^{-1} . ^1H NMR (400 MHz, d_8 -toluene) δ : 7.01 (s, 8H), 6.29 (s, 4H), 2.41 (s, 12H), 2.02 (s, 24H) ppm. ^{13}C NMR (400 MHz, d_8 -toluene) δ : 181.4 (d, $J_{\text{Rh-C}} = 39.9$ Hz), 137.1, 136.8, 136.7, 122.1, 30.4, 21.2 ppm.

Preparation of $[\text{ClRh}(\text{IPr})_2(\text{N}_2)]$ (**2-10**): A 25 mL Schlenk flask was charged with $[\text{ClRh}(\text{C}_2\text{H}_4)_2]_2$ (51.3 mg, 0.132 mmol) and IPr (206.7 mg, 0.532 mmol), and the solids dissolved in THF (10 mL). The resulting yellow solution was stirred for 4 hours and then the volatiles were removed in vacuo. The yellow residue was then triturated with cold

hexanes and collected by filtration. X-ray quality crystals were obtained by slow diffusion of hexanes into a concentrated THF solution of the product. Yield: 103 mg (41%). Anal. Found (calcd) for $\text{RhC}_{54}\text{H}_{72}\text{N}_4\text{Cl} \cdot 0.75\text{H}_2\text{O}$: C 70.16 (69.81), H 8.19 (7.97), N 5.63 (6.03). IR (KBr): $\nu = 2103$ (N-N, s) cm^{-1} . ^1H NMR (CD_2Cl_2 , 500 MHz): δ 7.31 (t, 4H, $J = 8$ Hz), 7.10 (d, 8H, $J = 8$ Hz), 6.62 (s, 4H), 3.14-2.54 (m, 8H), 0.98-0.79 (m, 48H) ppm. $^{13}\text{C}\{^1\text{H}\}$ NMR (CD_2Cl_2 , 100 MHz): δ 191.1 (d, $J_{\text{Rh-C}} = 40$ Hz), 147.9, 145.3, 137.9, 128.7, 123.9, 28.4, 25.8, 22.6 ppm.

Preparation of $[\text{ClRh}(\text{IPr})_2(\text{H})_2]$ (**2-11**): A 25 mL Schlenk flask was charged with $[\text{ClRh}(\text{C}_2\text{H}_4)_2]_2$ (51.0 mg, 0.131 mmol) and IPr (207.5 mg, 0.534 mmol), and the solids dissolved in THF (10 mL). The solution was frozen with liquid nitrogen, the atmosphere removed by vacuum and the flask charged with hydrogen gas. The reaction was stirred at room temperature for 16 hours and then the solvent was removed in vacuo to give a light brown solid. The residue was triturated with cold hexanes and collected by filtration. X-ray quality crystals were obtained by slow diffusion of hexanes into a concentrated THF solution of the product. Yield: 130.1 mg (54%). Anal. Found (calcd) for $\text{RhC}_{54}\text{H}_{74}\text{N}_4\text{Cl} \cdot 1\text{H}_2\text{O}$: C 69.14 (69.33), H 7.94 (8.19), N 5.89 (5.99). ^1H NMR (CD_2Cl_2 , 500 MHz): δ 7.31 (t, 4H, $J = 8$ Hz), 7.03 (d, 8H, $J = 8$ Hz), 6.75 (s, 4H), 2.72 (m, 8H), 0.91 (m, 48H), -23.51 (d, 2H, $J_{\text{Rh-H}} = 35$ Hz). $^{13}\text{C}\{^1\text{H}\}$ NMR (CD_2Cl_2 , 125 MHz): δ 193.7 (d, $J_{\text{Rh-C}} = 41$ Hz), 146.4, 137.6, 129.2, 124.0, 123.8, 28.4, 25.7, 23.1 ppm.

Preparation of $[\text{ClRh}(\text{IPr})_2(\text{CO})]$ (**2-12**): A 25 mL schlenk flask was charged with $[\text{Rh}(\text{C}_2\text{H}_4)\text{Cl}_2]_2$ (19.2 mg, 0.0494 mmol) and IPr (76.7 mg, 0.197 mmol), and the solids dissolved in THF (10 mL). The resulting yellow reaction mixture was stirred in the glovebox under nitrogen atmosphere and then removed to the schlenk line, degassed and

purged with an atmosphere of CO. An immediate colour change to a colourless reaction mixture is observed, signalling formation of **2-12**. The volatiles were then removed and the resulting beige solid triturated with cold hexanes and collected by filtration. X-ray quality crystals were obtained by slow diffusion of hexanes into a concentrated THF solution of the product. Anal. Found (calcd) for $\text{RhC}_{55}\text{H}_{72}\text{N}_4\text{OCl} \cdot 2\text{H}_2\text{O}$: C 66.40 (67.44), H 7.37 (7.82), N 5.44 (5.72). IR (KBr): $\nu = 1940$ (C-O, s) cm^{-1} . ^1H NMR (d_8 -toluene, 400 MHz): δ 7.26 (t, 4H, $J = 8$ Hz), 7.05 (d, 8H, $J = 8$ Hz), 6.50 (s, 4H), 3.06 (br, 8H), 1.04 (m, 48H) ppm. $^{13}\text{C}\{^1\text{H}\}$ NMR (d_8 -toluene, 100 MHz): δ 189.4 (d, $J_{\text{Rh-C}} = 42$ Hz), 187.5 (d, $J_{\text{Rh-C}} = 80$ Hz), 146.5, 137.8, 129.4, 124.2, 124.0, 28.7, 26.4, 23.1 ppm.

Catalytic Experiments:

Oxidation of *sec*-phenethanol. To a flame-dried 10 mL round-bottomed flask with a magnetic stirring bar was added $[\text{ClRh}(\text{IPr})_2(\text{O}_2)]$ (**2-4**) (23.7 mg, 25 μmol), *sec*-phenethanol (61.1 mg, 0.5 mmol), 0.25 mL of a 0.1 M solution of HOAc in toluene, hexamethylbenzene (16.2 mg, 0.1 mmol, internal standard) and a spatula tip of 4 Å MS. The reaction was diluted to 1 mL of toluene, a reflux condenser added and the reaction heated to 110 °C under a positive pressure of air. Small aliquots (~0.05 mL) were removed via syringe diluted in hexanes, dried over MgSO_4 and the yield determined by GC analysis.

Transfer Hydrogenation of Acetophenone. To a flame-dried 50 mL round-bottomed flask with a magnetic stirring bar was added $[\text{ClRh}(\text{IPr})_2(\text{O}_2)]$ (**2-4**) (9.4 mg, 10 μmol), KOH (2.8 mg, 50 μmol), hexamethylbenzene (16.2 mg, 0.1 mmol, internal standard) and acetophenone (120.1 mg, 1.0 mmol). The reagents were dissolved in 10 mL of isopropanol, the flask fitted with a reflux condenser and the solution heated to reflux

under an atmosphere of nitrogen for 3 h. The flask was then cooled in an ice bath for 1 h, the reaction concentrated, diluted in 5 mL of CDCl_3 , and the yield determined by ^1H NMR.

2.5 References

- (1) Valentine, J. S. *Chem. Rev.* **1973**, 73, 235-245.
- (2) Vaska, L. *Acc. Chem. Res.* **1976**, 9, 175-183. Jones, R. D.; Summerville, D. A.; Basolo, F. *Chem. Rev.* **1979**, 79, 139-179.
- (3) Cramer, C. J.; Tolman, W. B.; Theopold, K. H.; Rheingold, A. L. *Proc. Natl. Acad. Sci. U.S.A.* **2003**, 100, 3635-3640.
- (4) Instances occur in the literature in which bent, end-on dioxygen complexes are also referred to as 'super-oxo'. This chapter deals strictly with side-on dioxygen complexes, and so all mention of superoxo complexes will refer to these.
- (5) Rolfe, J.; Holzer, W.; Murphy, W. F.; Bernstein, H. J. *J. Chem. Phys.* **1968**, 49, 963-963. Andrews, L.; Smardzewski, R. R. *J. Chem. Phys.* **1973**, 58, 2258-2261.
- (6) Nolte, M. J.; Singleton, E.; Laing, M. *J. Am. Chem. Soc.* **1975**, 97, 6396-6400.
- (7) Egan, J. W.; Haggerty, B. S.; Rheingold, a. L.; Sendlinger, S. C.; Theopold, K. H. *J. Amer. Chem. Soc.* **1990**, 112, 2445-2446.
- (8) Zhang, X. W.; Loppnow, G. R.; McDonald, R.; Takats, J. *J. Am. Chem. Soc.* **1995**, 117, 7828-7829.
- (9) Fujisawa, K.; Tanaka, M.; Morooka, Y.; Kitajima, N. *J. Am. Chem. Soc.* **1994**, 116, 12079-12080.
- (10) Barthazy, P.; Worle, M.; Mezzetti, A. *J. Am. Chem. Soc.* **1999**, 121, 480-481.
- (11) Qin, K.; Incarvito, C. D.; Rheingold, A. L.; Theopold, K. H. *Angew. Chem. Int. Ed.* **2002**, 41, 2333-2335.
- (12) Cruickshank, D. W. J. *Acta Cryst.* **1956**, 9, 757-758. Busing, W. R.; Levy, H. A. *Acta Cryst.* **1964**, 17, 142-146. Dunitz, J. D. *X-Ray Analysis and the Structure of Organic Molecules*; Cornell Univ. Press: Ithaca, N.Y., 1979.
- (13) Nakamoto, K. *Infrared and Raman Spectra of Inorganic and Coordination Compounds; Part A: Theory and Application in Inorganic Chemistry*; 5th ed.; John Wiley & Sons: New York, 1997.
- (14) Chen, A. C.; Ren, L.; Decken, A.; Crudden, C. M. *Organometallics* **2000**, 19, 3459-3461. Chen, A. C.; Allen, D. P.; Crudden, C. M.; Wang, R. Y.; Decken, A. *Can. J. Chem.* **2005**, 83, 943-957. Allen, D. P.; Crudden, C. M.; Calhoun, L. A.; Wang, R. Y. *J. Organomet. Chem.* **2004**, 689, 3203-3209. Allen, D. P.; Crudden, C. M.; Calhoun, L. A.; Wang, R. Y.; Decken, A. *J. Organomet. Chem.* **2005**, 690, 5736-5746.

- (15) McGinnety, J. A.; Payne, N. C.; Ibers, J. A. *J. Am. Chem. Soc.* **1969**, *91*, 6301-6310. Bennett, M. J.; Donaldson, P. B. *Inorg. Chem.* **1977**, *16*, 1585-1589. Selke, M.; Rosenberg, L.; Salvo, J. M.; Foote, C. S. *Inorg. Chem.* **1996**, *35*, 4519-4522. Osakada, K.; Hataya, K.; Yamamoto, T. *Inorg. Chem.* **1993**, *32*, 2360-2365.
- (16) Bennett, M. J.; Donaldson, P. B. *Inorg. Chem.* **1977**, *16*, 1581-1585.
- (17) Selke, M.; Foote, C. S.; Karney, W. L. *Inorg. Chem.* **1993**, *32*, 5425-5426. Selke, M.; Karney, W. L.; Khan, S. I.; Foote, C. S. *Inorg. Chem.* **1995**, *34*, 5715-5720.
- (18) Ahijado, M.; Braun, T.; Noveski, D.; Kocher, N.; Neumann, B.; Stalke, D.; Stammler, H. G. *Angew. Chem. Int. Ed.* **2005**, *44*, 6947-6951.
- (19) Atlay, M. T.; Gahan, L. R.; Kite, K.; Moss, K.; Read, G. *J. Mol. Catal.* **1980**, *7*, 31-42.
- (20) Takahashi, Y.; Hashimoto, M.; Hikichi, S.; Akita, M.; Moro-oka, Y. *Angew. Chem. Int. Ed.* **1999**, *38*, 3074-3077.
- (21) Vicente, J.; Gil-Rubio, J.; Guerrero-Leal, J.; Bautista, D. *Organometallics* **2004**, *23*, 4871-4881.
- (22) Yu, X. Y.; Patrick, B. O.; James, B. R. *Organometallics* **2006**, *25*, 4870-4877.
- (23) Van Gaal, H. L. M.; Moers, F. G.; Steggerd, J. J. *J. Organomet. Chem.* **1974**, *65*, C43-C45.
- (24) Van Gaal, H. L. M.; Van den Bekerom, F. L. A. *J. Organomet. Chem.* **1977**, *134*, 237-248.
- (25) Busetto, C.; Dalfonso, A.; Maspero, F.; Perego, G.; Zazzetta, A. *J.C.S. Dalton Trans.* **1977**, 1828-1834.
- (26) Frech, C. M.; Shimon, L. J. W.; Milstein, D. *Helv. Chim. Acta* **2006**, *89*, 1730-1739.
- (27) Verat, A. Y.; Fan, H. J.; Pink, M.; Chen, Y. S.; Caulton, K. G. *Chem. Eur. J.* **2008**, *14*, 7680-7686.
- (28) Praetorius, J. M.; Allen, D. P.; Wang, R. Y.; Webb, J. D.; Grein, F.; Kennepohl, P.; Crudden, C. M. *J. Am. Chem. Soc.* **2008**, *130*, 3724-3725.
- (29) Winkelmann, O. H.; Riechstins, A.; Nolan, S. P.; Navarro, O. *Organometallics* **2009**, *28*, 5809-5813.
- (30) Chen, P.; Root, D. E.; Campochiaro, C.; Fujisawa, K.; Solomon, E. I. *J. Am. Chem. Soc.* **2002**, *125*, 466-474.

- (31) Zhang, H. In *Inorganic Electronic Structure and Spectroscopy, Volume I: Methodology*; Solomon, E. I., Lever, A. B. P., Eds.; John Wiley & Sons: New York, 2006.
- (32) Selke, M.; Foote, C. S. *J. Am. Chem. Soc.* **1993**, *115*, 1166-1167.
- (33) Vaska, L. *Science* **1963**, *140*, 809-810.
- (34) Chatt, J.; Leigh, G. J. *Chem. Soc. Rev.* **1972**, *1*, 121-144.
- (35) Holland, P. L. *Dalton Trans.* **2010**, *39*, 5415-5425.
- (36) Masuda, J. D.; Stephan, D. W. *Can. J. Chem.* **2005**, *83*, 324-327.
- (37) Hoffman, P. R.; Yoshida, T.; Okano, T.; Otsuka, S.; Ibers, J. A. *Inorg. Chem.* **1976**, *15*, 2462-2466.
- (38) Thorn, D. L.; Tulip, T. H.; Ibers, J. A. *J.C.S. Dalton Trans.* **1979**, 2022-2025.
- (39) Van Gaal, H. L. M.; Moers, F. G.; Steggerd, J. J. *J. Organomet. Chem.* **1974**, *65*, C43-C45.
- (40) Vigalok, A.; BenDavid, Y.; Milstein, D. *Organometallics* **1996**, *15*, 1839-1844. Vigalok, A.; Kraatz, H. B.; Konstantinovskiy, L.; Milstein, D. *Chem.-Eur. J.* **1997**, *3*, 253-260. Vigalok, A.; Milstein, D. *Organometallics* **2000**, *19*, 2061-2064.
- (41) Verat, A. Y.; Pink, M.; Fan, H.; Tomaszewski, J.; Caulton, K. G. *Organometallics* **2008**, *27*, 166-168.
- (42) Huang, J. K.; Stevens, E. D.; Nolan, S. P. *Organometallics* **2000**, *19*, 1194-1197.
- (43) Praetorius, J. M.; Wang, R.; Crudden, C. M. *Eur. J. Inorg. Chem.* **2009**, 1746-1751.
- (44) Yu, X.-Y.; Sun, H.; Patrick, B. O.; James, B. R. *Eur. J. Inorg. Chem.* **2009**, 1752-1758.
- (45) Ernsting, J. M.; Gaemers, S.; Elsevier, C. J. *Magn. Reson. Chem.* **2004**, *42*, 721-736.
- (46) Mas-Marzá, E.; Sanaú, M.; Peris, E. *Inorg. Chem.* **2005**, *44*, 9961-9967. Mata, J. A.; Chianese, A. R.; Miecznikowski, J. R.; Poyatos, M.; Peris, E.; Faller, J. W.; Crabtree, R. H. *Organometallics* **2004**, *23*, 1253-1263.
- (47) Herrmann, W. A.; Schütz, J.; Frey, G. D.; Herdtweck, E. *Organometallics* **2006**, *25*, 2437-2448.
- (48) Crabtree, R. H.; Lavin, M.; Bonneviot, L. *J. Am. Chem. Soc.* **1986**, *108*, 4032-4037. Crabtree, R. H. *Acc. Chem. Res.* **1990**, *23*, 95-101.

- (49) Osborn, J. A.; Jardine, F. H.; Young, J. F.; Wilkinson, G. *J. Chem. Soc. A* **1966**, 1711-1732. Ogle, C. A.; Masterman, T. C.; Hubbard, J. L. *Chem. Commun.* **1990**, 1733-1734. Harlow, R. L.; Thorn, D. L.; Baker, R. T.; Jones, N. L. *Inorg. Chem.* **1992**, *31*, 993-997.
- (50) Sheldon, R. A.; Kochi, J. K. *Metal-Catalyzed Oxidations of Organic Compounds*; Academic Press: New York, 1981. Trost, B. M.; Fleming, I.; Ley, S. V. In *Comprehensive Organic Synthesis*; Pergamon: Oxford, 1991; Vol. 7, p 251-325.
- (51) Holum, J. R. *J. Org. Chem.* **1961**, *26*, 4814-4816.
- (52) Lee, D. G.; Spitzer, U. A. *J. Org. Chem.* **1970**, *35*, 3589-3590.
- (53) Berkowitz, L. M.; Rylander, P. N. *J. Am. Chem. Soc.* **1958**, *80*, 6682-6684.
- (54) Kitajima, N.; Whang, K.; Morooka, Y.; Uchida, A.; Sasada, Y. *Chem. Commun.* **1986**, 1504-1505. Wang, Y.; Stack, T. D. P. *J. Am. Chem. Soc.* **1996**, *118*, 13097-13098. Wang, Y.; DuBois, J. L.; Hedman, B.; Hodgson, K. O.; Stack, T. D. P. *Science* **1998**, *279*, 537-540.
- (55) Yamaguchi, K.; Mizuno, N. *Angew. Chem. Int. Ed.* **2002**, *41*, 4538-4542. Yamaguchi, K.; Mizuno, N. *Chem. Eur. J.* **2003**, *9*, 4353-4361. Yamaguchi, K.; Kim, J. W.; He, J.; Mizuno, N. *J. Catal.* **2009**, *268*, 343-349.
- (56) Peterson, K. P.; Larock, R. C. *J. Org. Chem.* **1998**, *63*, 3185-3189. Nishimura, T.; Onoue, T.; Ohe, K.; Uemura, S. *J. Org. Chem.* **1999**, *64*, 6750-6755. Jensen, D. R.; Schultz, M. J.; Mueller, J. A.; Sigman, M. S. *Angew. Chem. Int. Ed.* **2003**, *42*, 3810-3813.
- (57) Mueller, J. A.; Goller, C. P.; Sigman, M. S. *J. Am. Chem. Soc.* **2004**, *126*, 9724-9734.
- (58) Konnick, M. M.; Guzei, I. A.; Stahl, S. S. *J. Am. Chem. Soc.* **2004**, *126*, 10212-10213.
- (59) Nyberg, E. D.; Drago, R. S. *J. Am. Chem. Soc.* **1981**, *103*, 4966-4968. Nyberg, E. D.; Pribich, D. C.; Drago, R. S. *J. Am. Chem. Soc.* **1983**, *105*, 3538-3544.
- (60) Collman, J. P.; Kubota, M.; Hosking, J. W. *J. Am. Chem. Soc.* **1967**, *89*, 4809-4811. Kurkov, V. P.; Pasky, J. Z.; Lavigne, J. B. *J. Am. Chem. Soc.* **1968**, *90*, 4743-4744.
- (61) Mimoun, H.; Perez Machirant, M. M.; Sere de Roch, I. *J. Am. Chem. Soc.* **1978**, *100*, 5437-5444.
- (62) Bressan, M.; Morandini, F.; Rigo, P. *J. Organomet. Chem.* **1983**, *247*, c8-c10.
- (63) Bressan, M.; Morandini, F.; Morvillo, A.; Rigo, P. *J. Organomet. Chem.* **1985**, *280*, 139-146.

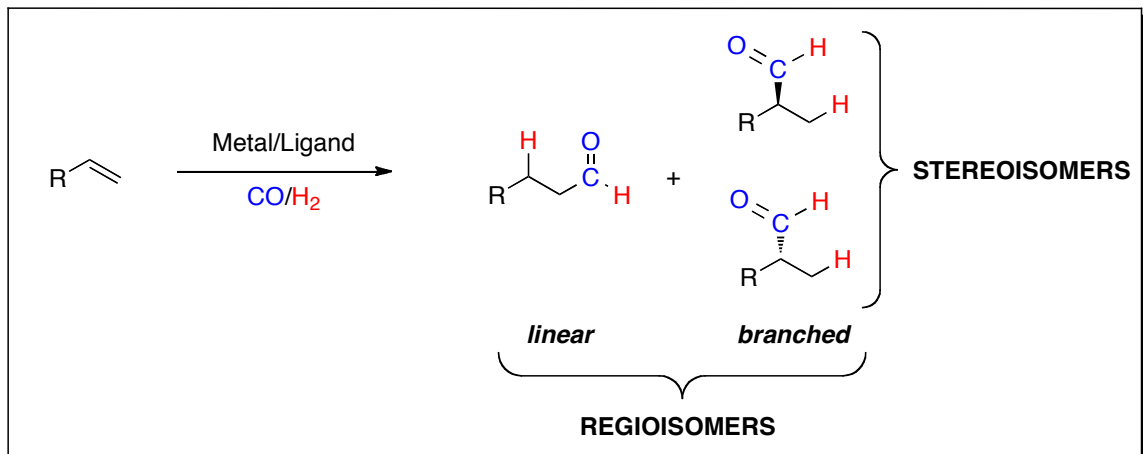
- (64) Morvillo, A.; Bressan, M. *J. Mol. Catal.* **1986**, *37*, 63-74.
- (65) Reuter, J. M.; Sinha, A.; Salomon, R. G. *J. Org. Chem.* **1978**, *43*, 2438-2442.
- (66) Bortolini, O.; Di Furia, F.; Modena, G.; Seraglia, R. *J. Mol. Catal.* **1984**, *22*, 313-317. Bruin, B. D.; Budzelaar, P. H. M.; Gal, A. W. *Angew. Chem. Int. Ed.* **2004**, *43*, 4142-4157.
- (67) Jensen, D. R.; Sigman, M. S. *Org. Lett.* **2002**, *5*, 63-65.
- (68) Spitzer, U. A.; Lee, D. G. *Can. J. Chem.* **1975**, *53*, 2865-2868. Lee, W.-O.; Che, C.-M.; Wong, K.-Y. *J. Mol. Catal.* **1994**, *89*, 57-62.
- (69) Foote, C. S.; Wexler, S.; Ando, W.; Higgins, R. *J. Am. Chem. Soc.* **1968**, *90*, 975-981. Foote, C. S. *Acc. Chem. Res.* **1968**, *1*, 104-110.
- (70) Wasserman, H. H.; Ives, J. L. *Tetrahedron* **1981**, *37*, 1825-1852.
- (71) Clennan, E. L. *Tetrahedron* **1991**, *47*, 1343-1382.
- (72) Schenck, G. O.; Eggert, H.; Denk, W. *Justus Liebigs Ann. Chem.* **1953**, *584*, 177-198.
- (73) Murray, R. W.; Kaplan, M. L. *J. Am. Chem. Soc.* **1969**, *91*, 5358-5364. Pierlot, C.; Nardello, V.; Schrive, J.; Mabile, C.; Barbillat, J.; Sombret, B.; Aubry, J.-M. *J. Org. Chem.* **2002**, *67*, 2418-2423. Wasserman, H. H.; Scheffer, J. R. *J. Am. Chem. Soc.* **1967**, *89*, 3073-3075.
- (74) Aubry, J. M.; Cazin, B. *Inorg. Chem.* **1988**, *27*, 2013-2014. Aubry, J. M.; Cazin, B.; Duprat, F. *J. Org. Chem.* **1989**, *54*, 726-728.
- (75) Howard, J. A.; Mendenhall, G. D. *Can. J. Chem.* **1975**, *53*, 2199-2201.
- (76) Cipot-Wechsler, J.; Covelli, D.; Praetorius, J. M.; Hearn, N.; Wang, R.; Kennepohl, P.; Crudden, C. M., *Manuscript in Progress* **2010**
- (77) van der Ent, A.; Onderdelinden, A. L. *Inorg. Synth.* **1981**, *27*, 92.
- (78) Jafarpour, L.; Stevens, E. D.; Nolan, S. P. *J. Organomet. Chem.* **2000**, *606*, 49-54.
- (79) Arduengo, A. J.; Dias, H. V. R.; Harlow, R. L.; Kline, M. *J. Am. Chem. Soc.* **1992**, *114*, 5530-5534.

Chapter 3: Synthesis of Rhodium-NHC Carboxylato Complexes For The Regioselective Hydroformylation of Terminal Alkenes

3.1 Introduction

3.1.1 Rhodium-Catalyzed Hydroformylation

The hydroformylation of alkenes is a well-known and industrially relevant catalytic reaction.¹ First discovered by Roelen in 1938, it is the metal-catalyzed addition of dihydrogen and carbon monoxide across carbon-carbon double bonds to form aldehydes.² Originally performed with osmium metals, the rhodium-catalyzed reaction has proven to be the most valuable and most commonly employed, and has since become one of the largest-volume industrial process involving homogeneous catalysts with production levels on the order of several million tons annually. Addition across asymmetrically substituted double bonds can occur to give two different regioisomers, and obviously enantiomers in the case of the branched isomer. Therefore, highly selective catalysts are extremely important (Scheme 3-1). The hydroformylation of terminal alkenes is typically more useful, as internal alkenes typically are orders of magnitude less reactive.³ The most commonly employed hydroformylation in industry is that of propylene, producing the commodity chemical butanol after reduction as described below.



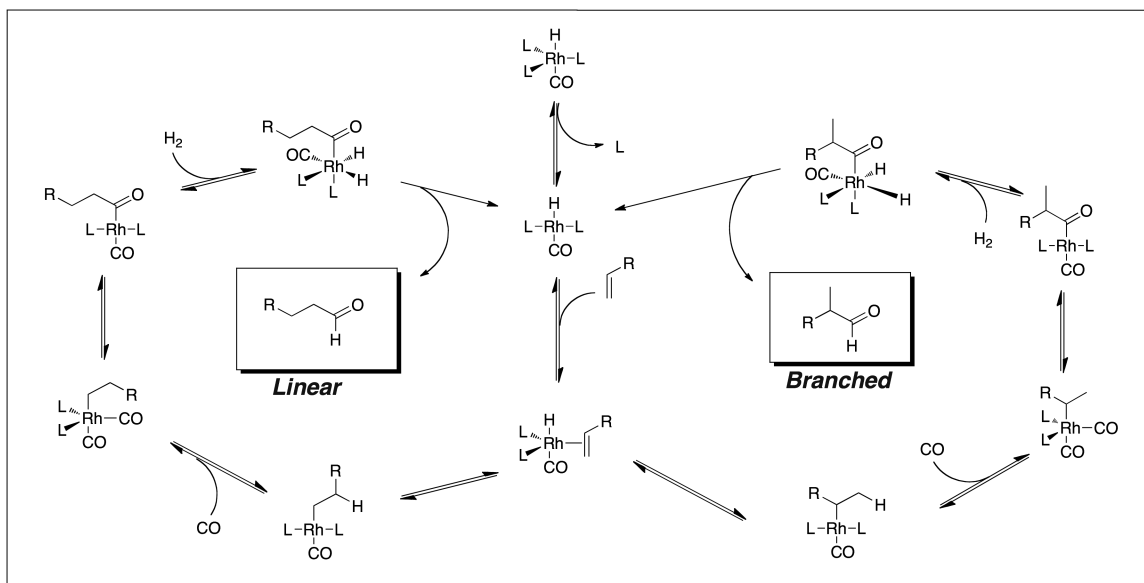
Scheme 3-1: Possible products in the hydroformylation of terminal alkenes.

Depending on the type of substrate employed, one of the two regioisomers is preferred. For example, high linear selectivity is desirable in the hydroformylation of propene since only *n*-butanal can be used in the preparation of a variety of high-volume commodity chemicals including paint solvents and plasticizers.⁴ Conversely, in the case of vinyl arenes, the branched products are more desirable since oxidation generates the corresponding 2-arylpropionic acids, which are important analgesic drugs including ibuprofen and naproxen. Although the active form of most profen drugs is the *S*-enantiomer, the largest volume of these (Ibuprofen/Advil™) is sold as the racemate since the inactive *R* form is converted into the *S*-enantiomer in the body.⁵ Therefore, stereocontrol is important in some cases, however, achieving high regioselectivity is essential in the hydroformylation of all alkenes.

Initial studies of the hydroformylation reaction focused primarily on unmodified cobalt catalysts obtained from either dicobalt-octacarbonyl or cobalt salts.⁶ Later studies by Shell demonstrated the benefits of phosphine ligands on the catalyst's reactivity and

selectivity;⁷ a feature that would hold true for all transition metals employed in this reaction, most notably rhodium. Studies from the Wilkinson laboratory in the late 1960s would establish phosphine-modified rhodium carbonyls as some of the most active and selective catalysts in the hydroformylation reaction and lead to greater understanding of this industrially important reaction.^{3,8-10}

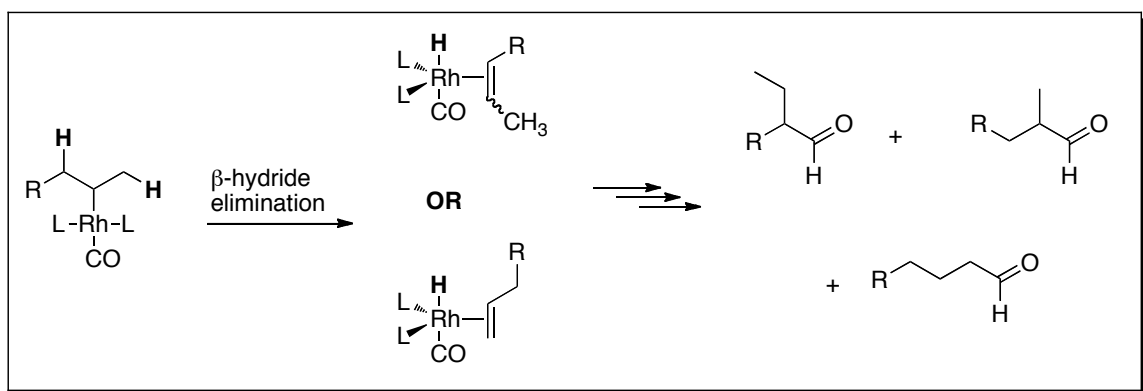
Breslow and Heck, having performed extensive studies on the cobalt-catalyzed reaction, were the first to propose the well-accepted “dissociative-mechanism” for the hydroformylation of alkenes.¹¹ This mechanistic interpretation is easily applicable to phosphine- or phosphite-modified rhodium-catalyzed reactions, and has been verified based on both experimental¹² and DFT studies^{13,14} (Scheme 3-2).



Scheme 3-2: Proposed dissociative mechanism for the rhodium-catalyzed hydroformylation of alkenes.

Starting from a coordinately saturated Rh-hydride, generally $\text{HRh}(\text{CO})_{4-n}(\text{L})_n$ where L = phosphine or phosphite, the true catalyst is generated by dissociation of a CO

or phosphorus ligand to open a coordination site for the alkene substrate. Following coordination to rhodium, the alkene undergoes regio-determining rhodium-hydride insertion to give one of two possible rhodium-alkyl intermediates. In the case of terminal alkenes, the outcome of this step will result in a linear or a branched aldehyde. The reverse of the alkene insertion is a β -hydride elimination, which in the case of aliphatic alkenes can result in isomerization to internal alkenes. Hydroformylation of these isomerization products leads strictly to branched aldehydes, degrading selectivities for the linear aldehyde which is typically the desired product in the case of the hydroformylation of aliphatic alkenes (Scheme 3-3).



Scheme 3-3: Mechanism for isomerization to internal alkenes and resulting aldehydes during hydroformylation.

Following alkene insertion, a molecule of carbon monoxide adds to the Rh complex, yielding a trigonal bipyramidal complex. 1,1-Insertion of carbon monoxide into the Rh-alkyl bond then occurs to give a Rh-acyl intermediate, which, following oxidative addition of dihydrogen, undergoes reductive elimination giving the corresponding aldehyde and regenerating $\text{HRh}(\text{CO})_{3-n}(\text{L})_n$.

Typical catalytic systems using rhodium, including a large portion of industrial processes, employ high concentrations of phosphine ligands to stabilize the metal centre and control regioselectivity, including up to 100:1 phosphine to Rh ratios, or even molten PPh_3 .¹⁵ In the case of propene hydroformylation, the requirement for such high concentrations of phosphine is related to the lability of the Rh-P bond, especially in the presence of CO, and the higher selectivities obtained with catalysts bearing more than one phosphine.^{9,10,16} Given the typically stronger bonds between transition metals and NHCs relative to phosphine ligands, Rh(NHC) complexes have been investigated in the hydroformylation reaction to try and alleviate the large excesses of ancillary ligands required in phosphine-based systems.¹⁷⁻²⁴

3.1.2 Rh(NHC) Hydroformylation Catalysts

Several research groups have explored the reactivity of NHC complexes in the hydroformylation of alkenes, and from this an interesting variety of Rh(NHC) catalysts have been reported (for selected examples see Figure 3-1), with the majority being of the general formula $[\text{XRh}(\text{NHC})(\text{COD})]$.^{17,19-23,25-27} Typically these catalysts have been tested in the hydroformylation of aliphatic alkenes (1-hexene, 1-octene or 1-decene), given the high value of linear, aliphatic aldehydes as commodity chemicals. With the strong desire to eliminate the need for any phosphines, the catalytic reactions are often performed without addition of exogenous ligands, however, in all of these studies isomerization of the alkene and lower regioselectivities ($\text{L/B} < 2:1$) are observed. While the addition of phosphines is not ideal, it has been shown that as low as three equivalents per rhodium can have dramatic effects on the propensity for isomerization and the observed regioselectivity ($\text{L/B} > 7$), without negatively effecting aldehyde yields.²⁴

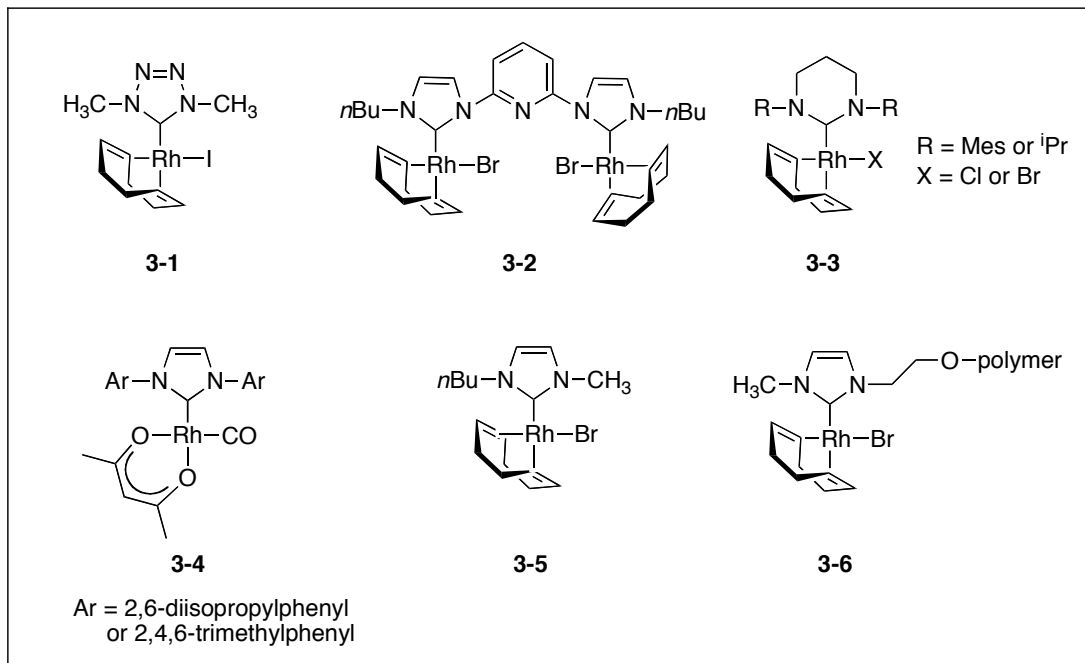


Figure 3-1: Examples of previously reported Rh(NHC) hydroformylation catalysts.^{18-21,24,28}

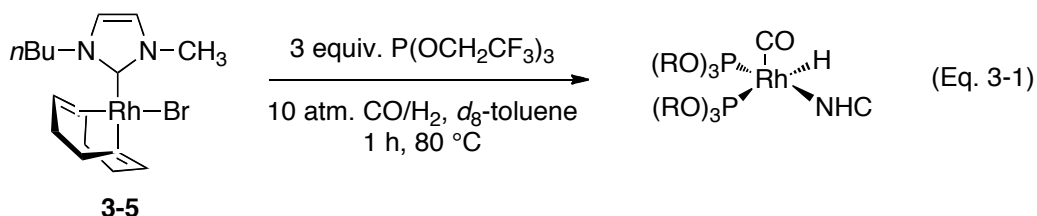
NHCs of various donating strength have been employed in this reaction, and it appears that the most active catalysts are the ones featuring the weakest donors. Weberskirch et al. described the most active catalyst which features a tetrazole-based NHC (**3-1**) and catalyzes the hydroformylation of aliphatic alkenes with 3500 turnovers per hour.²¹ This effect is similar to that observed with phosphine-based systems, in which electron-poor phosphites provide more active catalysts than phosphines. This trend has been predicted to extend to NHC-based systems by computational methods.¹⁴ Furthermore, the use of triphenylphosphite as an added donor ligand has been responsible for some of the highest linear selectivities observed with Rh(NHC) complexes.²⁴

Significant discussion has arisen as to the structure of the active catalyst in Rh(NHC) catalyzed hydroformylation, specifically whether or not the Rh-C_{NHC} bond is

retained throughout the catalytic cycle.²⁹ Fernandez and Peris demonstrated the stability of the Rh-C bond in their binuclear complex **3-2** under catalytically relevant conditions. Using high-pressure ¹³C NMR techniques, the Rh-C bond was still observed after 72 h at 40 °C and 30 atm CO/H₂.¹⁸ Furthermore, Nuyken and Buchmeiser were also able to observe the Rh-C bond of their catalyst **3-3** (R = ⁱPr, X = Br) by ¹³C NMR spectroscopy following a 4 h reaction at 100 °C and 50 bar CO/H₂.²⁰ While these observations are promising, they do not unequivocally identify a Rh(NHC) species as the active catalyst; other Rh species present at low concentrations with very high catalytic activities could be responsible for the observed reactivity. This contention has been made by Otto and co-workers who noted that their catalysts (**3-4**) were not active in the absence of added phosphines and the observed reactivity could be ascribed to [HRh(CO)₂(PPh₃)₂] generated via irreversible cleavage of the Rh-C_{NHC} bond.²⁸

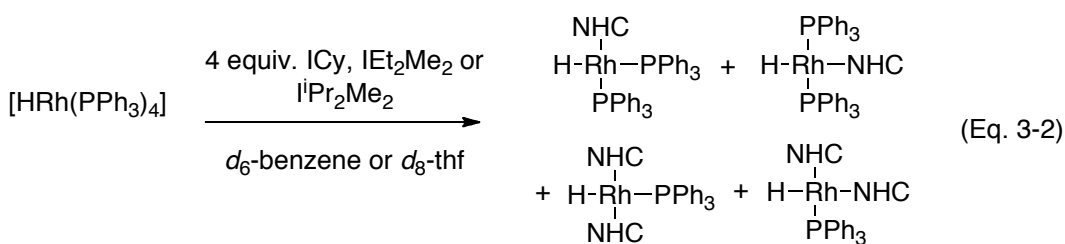
Full mechanistic investigations into Rh(NHC)-catalyzed hydroformylations have yet to be done, but a study by Trzeciak and co-workers has indicated that the active catalyst is likely a Rh(NHC)-hydride.²⁴ Although cleavage of the Rh-C_{NHC} bond was observed under stoichiometric conditions, hydroformylation of 1-hexene with [HRh(CO)(P(OPh)₃)₃] resulted in lower selectivity *versus* pre-catalyst **3-5** in the presence of P(OPh)₃, with L/B ratios of 1.3 and 7.9, respectively. This strongly suggested that a Rh(NHC) species was the highly selective active catalyst. Good evidence for the presence of the catalytically predominant Rh(NHC)-hydride was also obtained using a system consisting of **3-5**, 3 equiv. of P(OCH₂CF₃)₃ and CO/H₂. Analysis of the reaction mixture by ¹H and ³¹P NMR spectroscopy indicated the presence of the square-pyramidal complex assigned as [HRh(bmim-y)(CO)(P(OCH₂CF₃)₃)₂] (bmim-y = 1-butyl-3-

methylimidazol-2-ylidene) (Eq. 3-1).



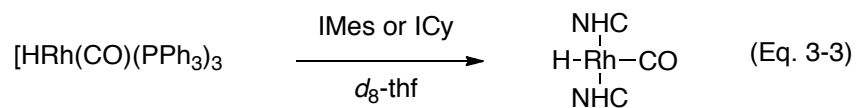
The formation of the observed Rh(NHC)-hydride from bromide **3-5** is consistent with the presence of induction periods when pre-catalysts are employed. Induction periods were not observed upon recycling of the catalyst. Given that all other reported Rh(NHC) hydroformylation catalysts are also halide-containing pre-catalysts, it is not surprising that induction periods have been observed by others.^{19-21,27}

Rh(NHC)-hydride complexes have been synthesized by Whittlesey et al. employing either [HRh(PPh₃)₄] or [HRh(CO)(PPh₃)₃] as the starting materials.³⁰ When [HRh(PPh₃)₄] was treated with ICy and other alkyl-substituted NHCs, mixtures of mono and bis, and *cis* and *trans* isomers were obtained (Eq. 3-2).



Treatment of [HRh(CO)(PPh₃)₃] with either IMes or ICy gave the corresponding Rh(NHC)₂-hydride carbonyl compounds (Eq. 3-3). The catalytic activity of these species has yet to be reported, however, given the inability to selectively synthesize mono-substituted Rh(NHC)-hydrides and the low activity of previously reported Rh(NHC)₂

complexes, the potential of these methods for the preparation of effective hydroformylation catalysts may be questionable.

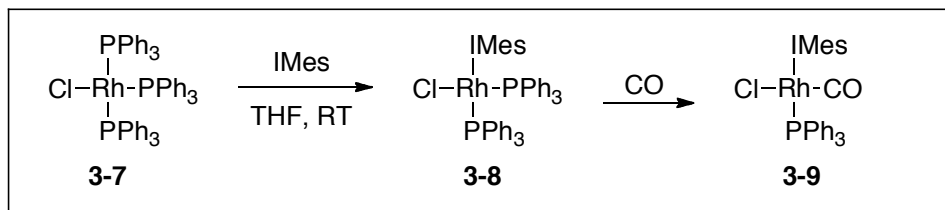


Apart from numerous catalysts of the general formula $[\text{Rh}(\text{NHC})(\text{COD})\text{X}]$, there have been examples of a binuclear dirhodium complex (**3-2**),¹⁸ an immobilized $\text{Rh}(\text{NHC})$ tethered to a water-soluble, amphiphilic block copolymer (**3-6**),¹⁹ and a rhodium complex featuring an imine-functionalized NHC chelate.²⁶ Cobalt-NHC complexes have also been examined in the hydroformylation of alkenes. Interestingly, the dimer $[\text{Co}(\text{CO})_3(\text{IMes})]_2$ showed no activity,³¹ while the related hydride $[\text{HCo}(\text{CO})_3(\text{IMes})]$ was catalytically active, although with modest turnover frequencies, for the hydroformylation of 1-octene. Again, isomerization of the alkene was observed.³²

3.1.3 Previous Endeavors From the Crudden Laboratory

Initial studies into the $\text{Rh}(\text{NHC})$ catalyzed hydroformylation in our laboratories began with $[\text{ClRh}(\text{IMes})(\text{PPh}_3)_2]$ (**3-8**), synthesized by direct substitution of one of the phosphine ligands of $[\text{ClRh}(\text{PPh}_3)_3]$ (**3-7**), known as Wilkinson's catalyst, with the free carbene IMes (Scheme 3-4).¹⁷ Compared to **3-7**, the carbene analog was both more active and more selective (78% conversion *versus* 35%; B:L ratios of 24:1 *versus* 7:1, see Table 3-1, entries 1 and 2). It was noted that during the reaction time, the initially bright yellow suspension of **3-8** was transformed into a pale yellow, homogeneous solution, which was identified as $[\text{ClRh}(\text{IMes})(\text{PPh}_3)(\text{CO})]$ (**3-9**). This complex, readily prepared by passing

a stream of carbon monoxide through a solution of **3-8**, was extremely stable, allowing it to be handled in air and purified by column chromatography.



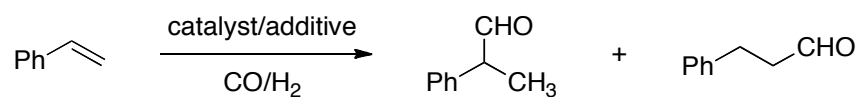
Scheme 3-4: Synthesis of IMes-containing analogues of Wilkinson's catalyst.¹⁷

Given its extreme stability relative to **3-8**, compound **3-9** was employed as the catalyst precursor (Table 3-1, entry 3). This species gave similar selectivities, yet roughly half the activity of derivative **3-8**. Since it was obvious that treatment of **3-8** with CO would generate a Rh carbonyl compound under reaction conditions, the difference between the use of **3-8** and **3-9** as a catalyst precursor was likely the presence of an extra equivalent of phosphine in the solution. Thus, an extra equivalent of triphenylphosphine was added per catalyst **3-9**, reestablishing the previous P/Rh ratio of catalyst **3-8**. This indeed gave essentially identical results to those observed with **3-8**. Further increases in the P/Rh ratio with catalyst **3-9** appeared to have little effect on the reaction (Table 3-1, entries 6 and 7).

Since previous results in the Crudden laboratory indicated that the carbene ligand can dissociate from the metal,³³ the activity of $[\text{ClRh}(\text{PPh}_3)_2(\text{CO})]$ with two equivalents of PPh_3 was also examined as a comparison (Table 3-1, entry 7). Use of this catalyst resulted in both lower yields and selectivities, indicating that the addition of IMes to coordination sphere of the metal was playing a role in these outcomes. Investigations of

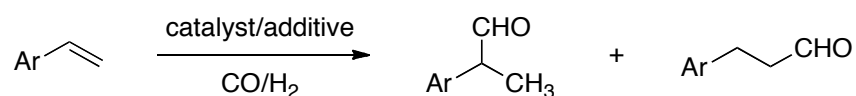
similar catalysts by the research groups of Fernandez/Peris¹⁸ and Nuyken/Buchmeiser,²⁵ both suggest its persistence during catalytic runs (vide supra) based on observed resonances in the ¹³C NMR spectra of their catalysts attributable to the Rh-C_{NHC} bond following hydroformylation conditions. As previously noted, these findings cannot exclude the possibility that undetectable amounts of carbene-free rhodium are responsible for the observed catalytic activity, but they provide compelling evidence for the thermodynamic stability of this bond under reaction conditions.

Table 3-1: Hydroformylation of styrenes with Rh phosphine and NHC catalysts.¹⁷



Entry	Catalyst	Additive (equiv/Rh)	Conversion ^a	B/L Ratio ^b
1	[ClRh(PPh ₃) ₃] (3-7)	None	35%	6.7
2	[ClRh(IMes)(PPh ₃) ₂] (3-8)	None	78%	24
3	[ClRh(IMes)(PPh ₃)(CO)] (3-9)	None	38%	16
4	[ClRh(IMes)(PPh ₃)(CO)] (3-9)	PPh ₃ (1 eq.)	74%	24
5	[ClRh(IMes)(PPh ₃)(CO)] (3-9)	PPh ₃ (2 eq.)	79%	24
6	[ClRh(IMes)(PPh ₃)(CO)] (3-9)	PPh ₃ (10 eq.)	80%	24
7	[ClRh(PPh ₃) ₂ (CO)]	PPh ₃ (2 eq.)	27%	7.3

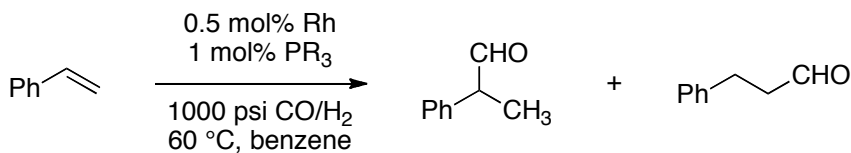
^aConversion determined by ¹H NMR of reaction solution after 19 h: 0.5% catalyst, 60°C, 1000 psi CO/H₂ (1:1). ^bBranched-to-linear ratio elucidated from ¹H NMR analysis of the crude mixture.

Table 3-2: Hydroformylation of vinyl arenes with NHC catalyst **3-9**.¹⁷

Entry	Ar	Catalyst ^a	Isolated yield	B/L Ratio ^b
1	<i>p</i> -C ₆ H ₄ -Me	3-9 /PPh ₃ (2eq.)	96%	24
2	<i>p</i> -C ₆ H ₄ -Cl	3-9 /PPh ₃ (2eq.)	94%	32
3	<i>p</i> -C ₆ H ₄ -Me	3-9 /PPh ₃ (2eq.)	98%	19
4	<i>p</i> -C ₆ H ₄ - ⁱ Bu	3-9 /PPh ₃ (2eq.)	93%	24

^aConversion determined by ¹H NMR of reaction solution after 19 h: 0.5% catalyst, 60°C, 1000 psi CO/H₂ (1:1). ^bBranched-to-linear ratio elucidated from ¹H NMR analysis of the crude mixture.

The hydroformylation of a variety of vinyl arenes was examined under “standard” conditions, yielding high selectivities for all of the substrates examined (Table 3-2). Although the activity of catalyst **3-9** was superior to the all phosphine derivatives (e.g. [CIRh(PPh₃)₂(CO)] or **3-7**), the absolute activity in terms of turnovers per hour was quite low (7 hr⁻¹) for a hydroformylation catalyst. Interestingly, substitution of the IMes ligand for the saturated analogue, SIMes, doubled the activity (Table 3-3, entry 2). A series of catalysts of the formula [CIRh(SIMes)(PR₃)(CO)] (**3-10**) were synthesized using a variety of phosphine ligands and their ability to hydroformylate styrene was assessed (Table 3-3).²² Changing the phosphine had a definite effect on activity, with tri-2-furylphosphine (**3-10f**) giving the most active catalyst. The largest increase in rate, however, was observed upon the addition of triethylamine.

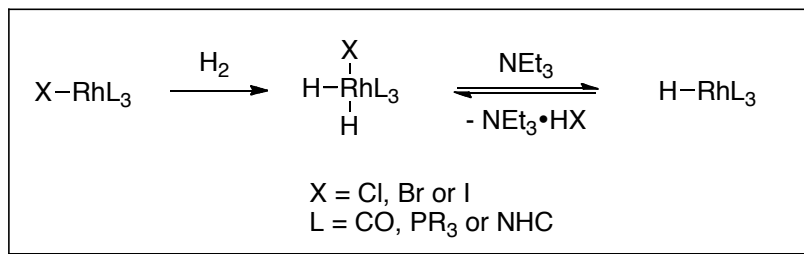
Table 3-3: Hydroformylation of Styrene with Rhodium-Carbene Catalysts.^{22a}

Entry	Catalyst	Phosphine	TOF ^b	B/L Ratio ^d	TOF ^b With NEt ₃ ^c
1	3-9	PPh ₃	8 ^e	96:4	
2	3-10a	PPh ₃	14	94:6	120
3	3-10b	P(OPh) ₃	0.5	65:35	14
4	3-10c	P(<i>p</i> -C ₆ H ₄ OMe) ₃	13	96:4	121
5	3-10d	P(<i>p</i> -C ₆ H ₄ F) ₃	31	95:5	125
6	3-10e	Ph-DBP ^e	3	93:7	9
7	3-10f	P(furyl) ₃	44 ^f	91:9	113 ^g
8	3-10g	PCy ₃	2	84:16	NR ^h
9	3-10h	P(<i>o</i> -tolyl) ₃	3	91:9	12 ⁱ

^aAt 0.5% catalyst loading (with 1% phosphine additive), 60 °C, 1000 psi CO/H₂ (1:1). ^bMeasured at 25-50% conversion unless otherwise noted. ^c0.5 mol% NEt₃ was employed. ^dBranched-to-linear ratio determined by ¹H NMR analysis of the crude mixture. ^ePhenyl dibenzophosphole. ^fMeasured at 70% conversion. ^gMeasured after 30 minutes. ^hNo reaction observed after 1 h. ⁱReduction to the alcohol was observed.

The addition of only one equivalent of NEt₃ gave an approximately nine-fold increase in activity for triphenylphosphine-based catalyst **3-10a**, with no appreciable loss of selectivity (Table 3-3, entry 2). Although similar increases in activity were observed for catalysts **3-10b-d** and **3-10f**, smaller effects were observed for catalysts modified by triphenylphosphite, benzophosphole and more sterically hindered phosphines. It is likely that the increase in turnover frequency can be ascribed to base-assisted generation of a Rh-hydride complex (Scheme 3-5). This in fact bodes well for the overall activity of a putative Rh-hydride NHC species, since stoichiometric studies carried out by former Crudden group member Yonek Hleba (*vide infra*) showed that the generation of this

hydride from the corresponding halide is not a high yielding reaction. Thus the rate acceleration observed is likely attributable to only a small amount of active catalyst.



Scheme 3-5: Base-assisted mechanism for the generation of a rhodium hydride in the hydroformylation reaction.

In the case of phosphine modified rhodium pre-catalysts containing halides, an induction period has been observed with the eventual rate of hydroformylation dependant on the identity of the halide, increasing in the order $\text{I} < \text{Br} < \text{Cl}$.³ It was also demonstrated that addition of a halide source inhibits the catalytic reaction. The order of reactivity of these halide-containing pre-catalysts is consistent with the relative Lewis basicities of the halides, with the softest halogen being the greatest inhibitor of the soft Lewis acid rhodium.³⁴ In the seminal publications of phosphine-modified rhodium hydroformylation catalysts by Wilkinson, the induction period was absent when organic bases, such as triethylamine were added or hydride-containing complexes were employed, such as $[\text{HRh}(\text{CO})(\text{PPh}_3)_3]$; supporting the identification of this compound as the active catalyst.³ Thus, added organic base enhances the reactivity of the catalyst by assisting the reductive elimination of HX, which generates the active catalyst.

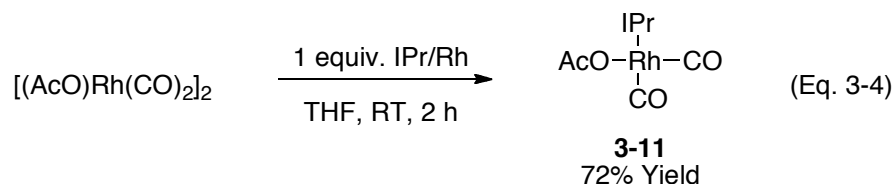
As noted previously, the requisite Rh(NHC)-hydride catalysts needed for hydroformylation have all been prepared *in situ* by elimination of HX from the

corresponding halide-containing Rh(NHC) pre-catalysts. Although Rh(NHC)-hydrides have been isolated by Whittlesey as previously mentioned,³⁰ all attempts to isolate or observe some type of Rh(NHC)-hydride by stoichiometric treatment of **3-9** with bases such as NEt₃ were unsuccessful.³⁵ Since attempts to prepare this species by other routes were also unsuccessful, we instead examined alternative precatalysts. It would be expected that relatively harder Lewis acids such as oxygen would be less inhibiting than the softer halide ligands, such as Cl. To this end, we embarked on the synthesis of carboxylate-containing Rh(NHC) precatalysts for the hydroformylation of alkenes.

3.2 Results and Discussion

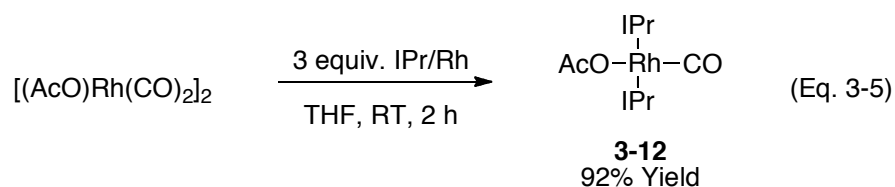
3.2.1 Synthesis and Characterization

Rh(NHC)-carboxylate complex, *cis*-[(AcO)Rh(IPr)(CO)₂] (**3-11**) was prepared by treating the previously reported rhodium dimer,³⁶ [(AcO)Rh(CO)₂]₂ with two equivalents of IPr in THF. This procedure afforded a red solution, which turned yellow within minutes (Eq. 3-4). Filtration over a bed of celite under aerobic conditions gave **3-11** as an air-stable complex in 72% yield. Crystallization of this compound was achieved by slow evaporation of hexanes into a concentrated THF solution.



Attempts were also made to prepare and isolate the bis-IPr analogue, *trans*-[(AcO)Rh(IPr)₂(CO)] (**3-12**), in which the second IPr ligand replaces a carbon monoxide ligand. This was done in a manner analogous to the preparation of **3-11**, however, in

order to obtain reasonable yields of **3-12**, three equivalents of IPr per rhodium were required (Eq. 3-5). Unfortunately under these conditions, large amounts of carbene by-products complicated the purification of **3-12**, and attempts at synthesis with less than three equivalents of IPr gave **3-12** as the major product, along with significant amounts of **3-11** detectable by ^1H NMR and IR spectroscopy that we were unable to be removed on bulk scale.



X-ray quality crystals of **3-12** could be obtained by crystallization from THF and hexanes; however, as **3-12** proved to be essentially inactive in the hydroformylation of alkenes (*vide infra*) its synthesis was not optimized further. The structures of **3-11** *cis*- $[(\text{AcO})\text{Rh}(\text{IPr})(\text{CO})_2]$ and **3-12**, *trans*- $[(\text{AcO})\text{Rh}(\text{IPr})_2(\text{CO})]$ are shown in Figures 3-2 and 3-3, respectively, and crystallographic parameters are presented in Table 4.

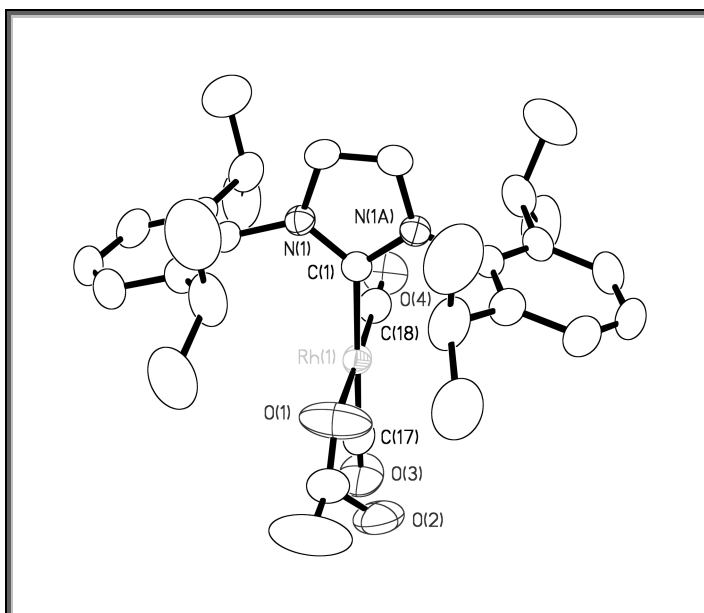


Figure 3-2: Crystallographically determined structure of **3-11**, displaying thermal ellipsoids drawn to the 50% confidence level. Hydrogen atoms have been removed for clarity. Selected interatomic distances (Å) and angles (°): Rh-C(1), 2.070(3); Rh-C(18), 1.813(4); C(18)-O(4), 1.151(4); Rh-C(17), 1.917(3); C(17)-O(3), 1.132(4); Rh-O(1), 2.043(3); O(1)-Rh-C(1), 86.95(11); O(1)-Rh-C(17), 93.66(15); O(1)-Rh-C(18), 176.60(12); C(18)-Rh-C(17), 89.75(15); C(1)-Rh-C(18), 86.95(12); C(1)-Rh-C(17), 176.70(13).

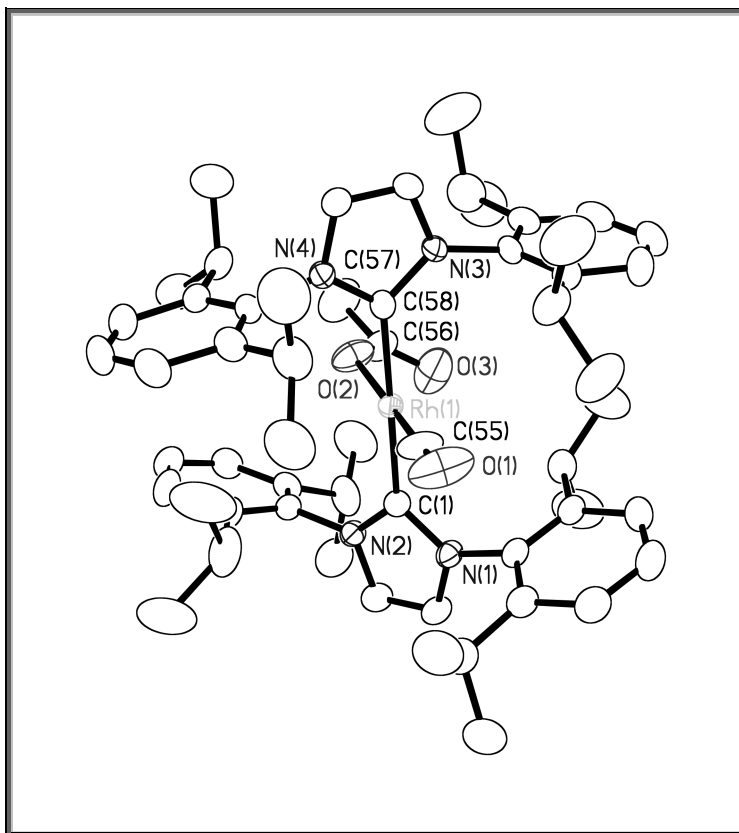


Figure 3-3: Crystallographically determined structure of **3-12**, displaying thermal ellipsoids drawn to the 50% confidence level. Hydrogen atoms have been removed for clarity Selected interatomic distances (Å) and angles (°): Rh-C(55), 1.789(3); Rh-C(58), 2.068(2); Rh-O(2), 2.07808(18); Rh-C(1), 2.078(2); C(55)-O(1), 1.151(3); C(55)-Rh-C(58), 87.94(10); C(55)-Rh-O(2), 174.04(10); C(58)-Rh-O(2), 87.01(8); C(55)-Rh-C(1), 91.58(10); C(58)-Rh-C(1), 179.14(8); O(2)-Rh-C(1), 93.43.

Table 3-4: Crystallographic Data for Compounds **3-11** and **3-12**.

	3-11	3-12
formula	C ₃₁ H ₃₉ N ₂ O ₄ Rh	C ₅₇ H ₇₅ N ₄ O ₃ Rh
fw	606.55	967.12
color/habit	yellow/block-shaped	yellow/block-shaped
cryst dimens (mm ³)	0.40 x 0.30 x 0.20	0.40 x 0.30 x 0.08
cryst syst	monoclinic	monoclinic
space group	<i>P</i> 2 ₁ / <i>m</i>	<i>P</i> 2 ₁ / <i>n</i>
<i>a</i> , Å	9.5386(8)	12.4289(8)
<i>b</i> , Å	17.4011(15)	21.2152(14)
<i>c</i> , Å	9.7950(9)	19.9599(13)
β , deg	111.0870(10)	93.3450(10)
<i>V</i> , Å ³	1516.9(2)	5254.1(6)
<i>Z</i>	2	4
<i>T</i> , K	180(2)	180(2)
D _{calcd} , g cm ⁻³	1.328	1.223
μ , mm ⁻¹	0.599	0.371
<i>F</i> (000)	632	2056
θ range, deg	2.29 - 25.00	1.40 - 25.00
index ranges (<i>h</i> , <i>k</i> , <i>l</i>)	±11, ±19, ±11	±14, ±25, ±23
no. of reflns collected	8 984	30 696
no. of indep reflns/ <i>R</i> _{int}	2765/0.0209	9249/0.0270
no. of data/restraints/params	2765/8/264	9249/0/846
<i>R</i> ₁ / <i>wR</i> ₂ (<i>I</i> > 2 σ (<i>I</i>)) ^a	0.0277/0.0716	0.0314/0.0832
<i>R</i> ₂ / <i>wR</i> ₂ (all data) ^a	0.0299/0.0729	0.0438/0.0894
GOF (on <i>F</i> ²) ^a	1.000	1.000
largest diff peak and hole (e Å ⁻³)	+0.558/-0.498	+0.903/-0.344

$$^a R_1 = \frac{\sum |F_o| - |F_c|}{\sum |F_o|}; \quad wR_2 = \left\{ \frac{\sum [w(F_o^2 - F_c^2)^2]}{\sum [w(F_o^2)^2]} \right\}^{1/2}; \quad \text{GOF} = \left\{ \frac{\sum [w(F_o^2 - F_c^2)^2]}{\sum [w(F_o^2)^2]} \right\}^{1/2}.$$

The crystal structures of the two complexes reveal that they are both pseudo-square planar, with the acetate ligands bound to the metal center in a unidentate manner. The X-ray structure of **3-11** (Figure 3-2) shows that the CO ligands are oriented *cis* to one another; which was confirmed in the bulk material by ¹³C{¹H} NMR and IR spectroscopy. The ¹³C{¹H} NMR was characterized by two carbonyl resonances at 187.1 and 185.8 ppm and two CO stretches at 2070 and 1990 cm⁻¹ were observed in the IR

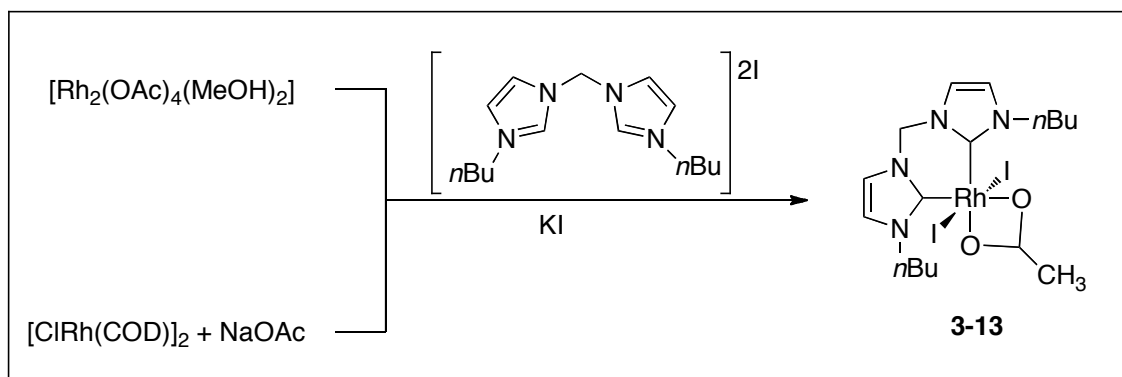
spectrum. The IR data for **3-11** are similar to those recently reported by Herrmann in analogous structures.³⁷ The *trans* geometry of **3-12** seen in the crystal structure of this compound (Figure 3-3), was also confirmed in solution by $^{13}\text{C}\{^1\text{H}\}$ NMR which featured only one carbene (190.6 ppm) and one carbonyl carbon resonance (191.8 ppm). The IR spectrum contained a single CO stretch at 1952 cm^{-1} consistent with the presence of only one CO ligand. Notably, the $\nu(\text{CO})$ value is at slightly higher wavenumber than the previously reported $\text{P}(\text{iPr})_3$ ³⁸ and IMes ³⁹ derivatives, and comparable to a previously reported bis-NHC rhodium-CO complex, $[\text{Rh}(\text{IMe})_2(\text{CO})\text{Cl}]$.⁴⁰ In addition, the Rh-C_{IPr} bond lengths of **3-11** and **3-12** are in the commonly observed range, and the C-O bond lengths of the carbonyl *cis* and *trans* to the carbene of **3-11** are 1.151(4) and 1.132(4) Å, respectively. As would be expected due to the larger *trans*-effect of the IPr ligand, the carbonyl in the *trans* position possesses a longer Rh-C bond and therefore a shorter C-O bond.

The hapticity of metal-carboxylate complexes can be spectroscopically probed by examining the difference between the $\nu(\text{OCO})_{\text{asym}}$ and $\nu(\text{OCO})_{\text{sym}}$ stretches (Δ), where it is believed that chelating ROCO groups have $\nu(\text{OCO})_{\text{asym}}$ and $\nu(\text{OCO})_{\text{sym}}$ very similar to the free ion.⁴¹ Unidentate ROCO groups, on the other hand, possess asymmetric stretches at higher frequencies and therefore larger Δ values than the free ions. The unidentate coordination of the acetate ligand observed crystallographically for both **3-11** and **3-12** is confirmed in the bulk material by the Δ values of 231 cm^{-1} and 259 cm^{-1} , respectively (Table 3-5). Interestingly, in the Rh^{III} -carboxylato complex **3-13** reported by Peris and co-workers containing a chelating bis-NHC ligand, the acetate is a bidentate ligand (Scheme 3-6).⁴² This might be due to the acetate satisfying the preference of Rh^{III} to

adopt an octahedral geometry, whereas in our case Rh^I would prefer to remain square planar.

Table 3-5: Selected IR Stretches of Compounds **3-11** and **3-12**.

Entry	Structure	$\nu(\text{CO})$ (cm ⁻¹)	$\nu(\text{OCO})_{\text{asym}}$ (cm ⁻¹)	$\nu(\text{OCO})_{\text{sym}}$ (cm ⁻¹)	Δ (cm ⁻¹)
1	NaOAc ⁴³	N/A	1578	1414	164
2	unidentate OCOR ⁴⁴	N/A	1580 - 1650	1310-1390	210-270
3	bidentate OCOR ⁴⁴	N/A	1490-1540	1400-1470	40-120
4	(3-11)	2070, 1990	1613	1382	231
5	(3-12)	1952	1619	1360	259



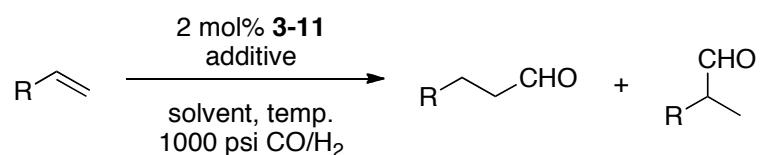
Scheme 3-6: Synthesis of a Rh^{III}(NHC) complex with a chelating acetate ligand.⁴²

3.2.2 Catalytic Activity

Given their similarity to catalytically active rhodium-NHC complexes previously reported by our group,^{17,22} we began our investigation by assessing the ability of complex **3-11** to hydroformylate vinyl arenes. An optimization study was initially undertaken, in which solvents, additives and reaction conditions were screened (Table 3-6). In the hydroformylation of styrene, complex **3-11** was shown to be a competent catalyst in a

variety of solvents including dichloromethane and hexanes, however, the highest regioselectivity in favour of the branched isomer was observed in benzene (Table 3-6, entry 5) and so this solvent was chosen for further optimization studies.

Table 3-6: Optimization of the Hydroformylation of Styrene Using **3-11**.^a



Entry	Solvent	Temp. (°C)	Additive	Yield (%) ^b	B/L Ratio
1	MeCN	60	None	<1	N/A
2	DCM	60	None	47	10
3	hexanes	60	None	9	14
4	THF	60	None	<1	N/A
5	benzene	60	None	27	22
6	benzene	40	None	8	>40
7	benzene	80	None	93	10
8	benzene	80	NEt ₃ (2%)	4	N/A
9	benzene	80	NEt ₃ (20%)	16	5
10	benzene	80	KI (2%)	7	6
11	benzene	80	KI (20%)	11	3
12	benzene	80	PPh ₃ (2%)	78	27
13	benzene	80	PPh ₃ (20%)	44	20

^a2 mol% catalyst loading in a 0.100 M solution of styrene for 17 h at various temperatures, under a 1000 psi (1:1) atmosphere of CO and H₂. ^bYields determined by ¹H NMR using an internal standard.

A number of different additives that have been shown to be effective with previous hydroformylation catalysts were tested. In the absence of any additives, complex **3-11** gave the corresponding aldehydes in 93% yield after 16 h with a B:L ratio of 10:1 (Table 3-6, entry 7). Interestingly, with this catalyst precursor, triethylamine had a detrimental effect on activity; in contrast to chloride-containing catalysts previously reported by our group, which gave significantly higher activity upon the addition of

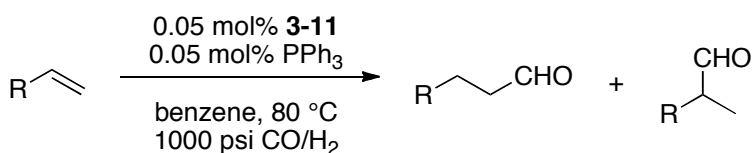
triethylamine (*vide supra*). As discussed in Section 1.2.3, this may be due to faster elimination of the acetate ligand and its insignificant inhibitory effect when compared to halides. Unlike a related complex synthesized by Otto and coworkers (**3-4**),²⁸ complex **3-11** is catalytically active in the absence of additional phosphine, however, the addition of one equivalent of PPh₃ per rhodium improved the selectivity to 27:1 with only a slight decrease in yield to 78% (entry 12).³² The addition of more than 1 equivalent of PPh₃ per rhodium (PPh₃/Rh = 10) did not lead to an improvement in yield or selectivity (compare entries 12 and 13 in Table 3-6).³⁷ The effect of additional halide anion on the reaction was also tested by adding one and ten equivalents of KI to the reaction (Table 3-6, entries 10 and 11 respectively). This appeared to inhibit the reaction, leading to lower yields and selectivities.

Examination of the progress of the reaction with high concentrations of substrate, 2.5 M, indicated that the turnover frequency of the catalyst was actually quite high; over 500 h⁻¹ depending on the substrate (Table 3-7). We were therefore able to lower the catalyst loading to 0.05 mol% and still achieve similar yields for a number of vinyl arenes. Regioselectivities in these reactions were quite high, with the branched aldehyde accounting for 90-96% of the product mixture depending on the substrate employed.

The ability of complex **3-11** to hydroformylate aliphatic alkenes was also investigated using allylbenzene, 4-phenyl-1-butene, 2-octene and 1-decene as substrates. As noted previously, the hydroformylation of aliphatic alkenes, a very important industrial process, is plagued by isomerization of the double bond, erosion of regioselectivity via hydroformylation of the resulting internal alkenes, and competitive hydrogenation to the corresponding alkane.¹⁰ Although Rh(NHC) complexes have been

previously reported as competent catalysts for the hydroformylation of terminal aliphatic alkenes, they are also plagued by these isomerization pathways, as well as hydrogenation of the substrates.

Table 3-7: Hydroformylation of Aromatic and Aliphatic Alkenes with **3-11**.^a



Entry	Substrate	TOF ^b	Yield ^c	B/L
1	styrene	338	75	21
2	4-Cl styrene	515	ND	23
3	4-OMe	334	ND	9
4	4-Me	426	ND	11
5	4-OAc	282	ND	15
6	4-phenyl-1-butene	725	96.5	1:2.3
7	allylbenzene	109	86	1:2
8	1-decene	345	78	1:3
9	2-octene	25	24	ND

^a0.05 mol% **1**, 0.05 mol% PPh₃ in a ca. 2.5 M benzene solution of substrate under a 1000 psi (1:1) atmosphere of CO and H₂. ^bTOF's determined after 1 h by ¹H NMR using an internal standard. ^cYields determined after 19 h by ¹H NMR using an internal standard.

The regioselectivity of the hydroformylation of allylbenzene and 4-phenyl-1-butene are interesting tests of the propensity for isomerization, as in these cases, isomerization gives the corresponding styrenes, which are more stable given the conjugation of the double bond to the phenyl ring. Subsequent hydroformylation of these isomerization products would then likely lead to 2-phenylbutanal and 2-phenylpentanal, respectively, because of the proposed high stability of the Rh-benzyl intermediate preceding the aldehyde product and the observed regiochemistry of the catalyst with the

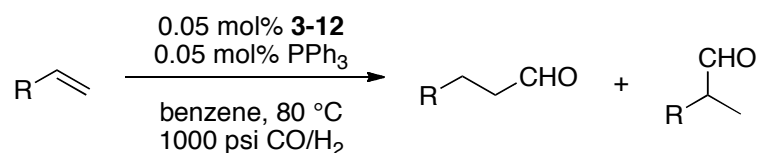
vinyl arene substrates.⁴⁵ Hydroformylation of 2-octene was also carried out to determine the relative rate of internal *versus* terminal alkenes.

For 4-phenyl-1-butene and allylbenzene, the linear aldehydes were obtained with moderate selectivities over the branched isomers (L/B = 2.3:1), and the reactions proceeded without any detectable isomerization or hydrogenation of either substrate (Table 3-7, entries 6 and 7). Yields and TOFs were reasonably high and importantly, the linear to branched selectivities were determined to be the same at 1 h and at 19 h. This is significant because isomerization of the terminal alkene to internal positions usually results in a degradation of linear to branched selectivity as the reaction proceeds through hydroformylation of the newly formed internal alkenes.²⁰ In the case of 1-decene (Table 3-7, entry 8), only the 1- and 2-aldehydes were detected, with no observable isomerization or hydrogenation of the double bond and again the B/L ratios were the same after 1 h or 19 h. In the case of 2-octene (Table 3-7, entry 9), although the reaction was quite slow,⁴⁶ less than 1% of the *n*-aldehyde was observed, which would have resulted from isomerization to the 1-alkene and hydroformylation. The high mass balance obtained (96%) implies that hydrogenation is not an issue with this substrate either.

Since high linear selectivity in the hydroformylation of aliphatic alkenes is generally attributed to complexes which have more than one phosphine ligand,^{9,10,16} bis-(NHC) complex **3-12**, bearing two IPr ligands in a *trans* relationship was examined in the hydroformylation of alkenes (Table 3-8). Low TOFs, on the order of 1-3 h⁻¹, were obtained using **3-12**. Although the dramatically lower activity of **3-12** relative to **3-11** may be due to the significant steric bulk of the second carbene ligand, the minimal

activity that was observed may reasonably be attributed to the presence of small amounts of complex **3-11** (*vide supra*). Since lability of the carbene-metal bond has been documented in the case of Rh and other metals,⁴⁷ it is also possible that the observed catalytic activity with **3-12** is a result of its decomposition to a mono-carbene species. Fernandez and Peris previously reported that the cationic rhodium complex (**3-13**) featuring a chelating bis-NHC ligand was catalytically inactive for the hydroformylation of styrene, consistent with the observed results for catalyst **3-12**.¹⁸

Table 3-8: Hydroformylation of Aromatic and Aliphatic Alkenes by **3-12**.^a



Entry	Substrate	Yield ^b	B/L
1	styrene	8.3	20
2	4-phenyl-1-butene	12	2.6
3	1-decene	32	2.0

^a0.05 mol% **1**, 0.05 mol% PPh₃ in a ca. 1.0 - 1.2 M benzene solution of substrate under a 1000 psi (1:1) atmosphere of CO and H₂. ^bYields determined after 19 h reaction time by ¹H NMR using an internal standard.

3.2.3 Initiation of [Rh(IPr)(CO)₂X]

In the classic mechanistic study reported by Wilkinson, the rate of hydroformylation of 1-pentene was monitored by GC for a series of analogous catalysts [XRh(CO)(PPh₃)₂], where X = Cl, Br, I.³ The first-order plots (ln([1-pentene]₀/[1-pentene]_t) by time) of these catalytic reactions did not pass through the origin, indicating an induction period in the reaction. This induction period was absent in the presence of

base or when the corresponding Rh-hydride catalyst was employed, indicating that hydrogenolysis of the halide-containing precatalyst to form a Rh-hydride precedes conversion of the alkene to aldehyde. The observed rates of the hydroformylation of 1-pentene with different $[\text{XRh}(\text{CO})(\text{PPh}_3)_2]$ catalysts were observed to increase in the series $\text{Cl} > \text{Br} > \text{I}$, which follows Pearson's Hard-Soft Lewis Acid-Base principle. We propose that the relatively harder acetate ligand would fall before chloride in this series, and therefore expect our catalyst **3-11** to hydroformylate alkenes at an increased rate compared to the analogous chloro-containing $[\text{ClRh}(\text{IPr})(\text{CO})_2]$ (**3-14**).

Induction periods have been noted in the hydroformylation of alkenes with Rh(NHC) catalysts. For example, Nuyken, Buchmeiser et al. have observed 30-60 minute induction periods in their study of an interesting class of tetrahydropyrimidin-2-ylidene complexes,²⁰ and the immobilized and recyclable Rh(NHC) catalyst developed by Weberskirch et al. required roughly four hours of reaction time before reaching maximal activity.¹⁹ Previous work in the Crudden laboratory with IMes-type ligands has also suggested that HX elimination was an important contributor to catalytic activity with turnover numbers increasing from about 10-30 h^{-1} to about 100-125 h^{-1} upon the addition of NEt_3 which is known to promote HX elimination.²²

To verify our hypothesis as to the increased activity of our catalyst **3-11**, the initial rate of the hydroformylation of 1-decene was determined and compared to that of the chloro-containing analogue $[\text{ClRh}(\text{IPr})(\text{CO})_2]$ (**3-14**). **3-14** was prepared in a manner analogous to **3-11**: equimolar amounts of $[\text{Rh}(\text{CO})_2\text{Cl}]_2$ and IPr were dissolved in THF and stirred for two hours giving a yellow reaction mixture. This mixture was concentrated under high vacuum, dissolved in DCM and filtered through a plug of Celite.

Evaporation of the DCM then gave analytically pure yellow solid in near quantitative yield, with the ^1H and ^{13}C NMR spectra matching those later reported by James et al.⁴⁸ The activity of this catalyst was then tested relative to **3-11** for the hydroformylation of 1-decene (1.0 M in benzene, 2000:1:1 alkene/Rh/PPh₃, 80 °C, 1000 psi CO/H₂), with yields of aldehydes determined at different points during the reaction.

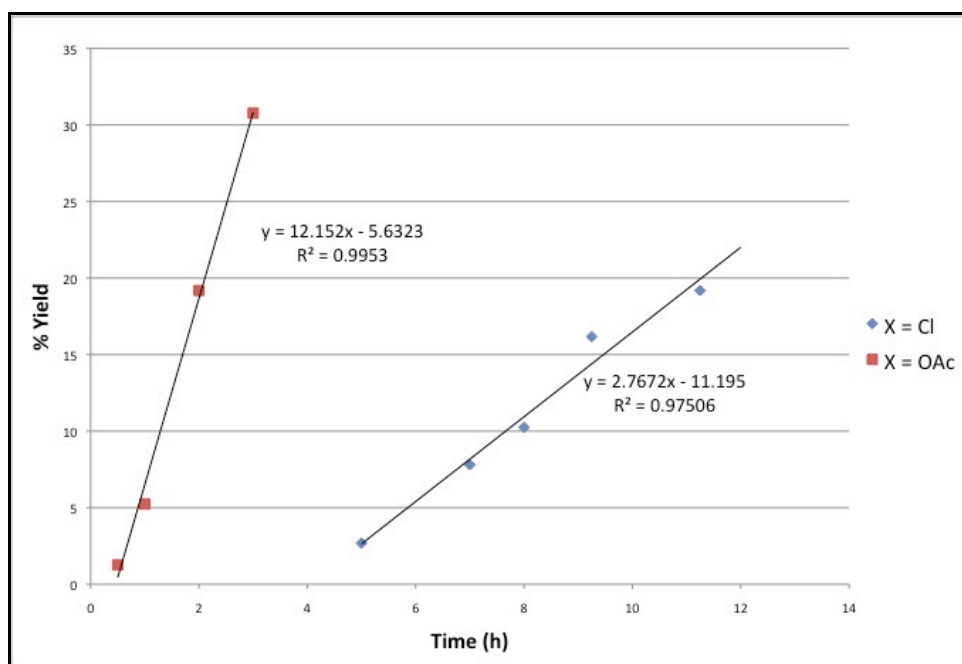
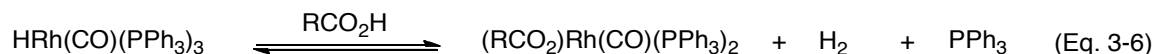


Figure 3-4: Hydroformylation of 1-decene with $[\text{XRhIPr}(\text{CO})_2]$.

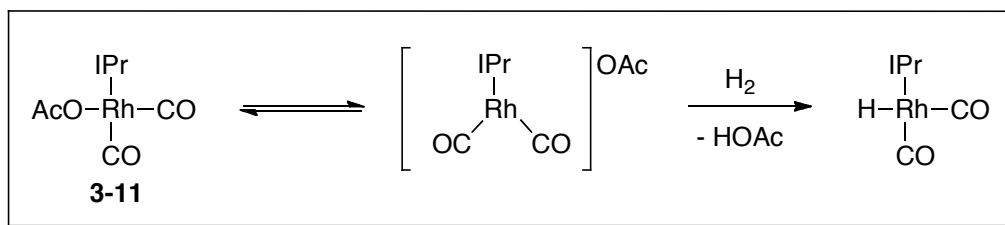
Plotting the total yield of aldehydes *versus* time, which accounts for all consumed alkene, gave linear plots for both catalysts **3-11** and **3-14** at low conversion (Figure 3-4). Of the two catalysts, **3-11** was both considerably faster and possessed a significantly shorter inhibition period. Extrapolating the plot of yield *versus* time for catalyst **3-11** approximates an inhibition period of roughly 40 min. Using the slope of the line to determine the rate, the turnover frequency was calculated to be 204 h^{-1} . Under nearly identical conditions, the observed inhibition period for catalyst **3-14** is roughly 4 h; six

times longer than that observed for **3-11**. Furthermore, the observed rate of aldehyde production after this period is about 4.5 times slower than that of the analogous carboxylato catalyst **3-11**, with an observed TOF of 47 h^{-1} . The identity of the catalyst, as well as the lower concentration used in these experiments, had little effect on the regioselectivity of the reaction giving similar percentages ($73 \pm 2\%$ linear aldehyde) for both catalysts at all time points. Most importantly, the selectivity was maintained at higher conversions with no indication of alkene isomerization, concomitant erosion of selectivity or formation of aldehydes at internal positions of the C-10 chain beyond C-2.

The inhibiting effect of added carboxylic acids on the hydroformylation ability of phosphine-modified rhodium hydroformylation catalysts has been previously described by Ziolkowski, Trzeciak and co-workers.⁴⁹ In this study, it was shown that the addition of carboxylic acids to the rhodium-catalyzed hydroformylation of 1-hexene using $[\text{Rh}(\text{acac})(\text{CO})(\text{PPh}_3)]$ can inhibit the reaction, however in the case of propionic acid, large $[\text{R-CO}_2\text{H}]/[\text{Rh}]$ ratios (> 450) were required. At lower ratios, no observable differences in yield, linear/branched ratios or isomerization rates were observed. The inhibition by the carboxylic acid at high concentrations was stated to be the same as that observed with halides, in which active hydroformylation catalysts are removed from the catalytic cycle by an equilibrium reaction with the carboxylic acid (Eq. 3-6). This was demonstrated by the stoichiometric reaction of $[\text{HRh}(\text{CO})(\text{PPh}_3)_3]$ with propionic acid to form $[\text{Rh}(\text{O}_2\text{C-C}_2\text{H}_5)(\text{CO})(\text{PPh}_3)_2]$, which itself is an effective pre-catalyst for 1-hexene hydroformylation. Given the lack of inhibition observed at low $[\text{R-CO}_2\text{H}]/[\text{Rh}]$ ratios in their study, the sub-millimolar concentrations of both Rh and the liberated HOAc likely render this effect negligible in our catalytic system.



The carboxylato-containing Rh(NHC) catalyst, however, seems to differ from its chloro analogue in both the length of the inhibition period *and* the relative rate of hydroformylation after catalyst activation. While the latter observation was anticipated, the very different initial inhibition period is somewhat surprising; the inhibition period for **3-11** is almost negligible and may possibly be attributed to the time required for the internal temperature to equilibrate to 80 °C. Activation of dihydrogen by a cationic rhodium species generated by dissociation of the anionic ligand has been previously invoked,²⁴ and could be operating in our system. Although we did not observe fluxional coordination behaviour of the acetate ligand by ¹H NMR, at catalytically relevant concentrations and temperatures dissociation of this ligand could be favourable. Thus, dissociation of AcO⁻ followed by activation of dihydrogen could yield the active Rh(NHC)-hydride catalyst and liberate HOAc (Scheme 3-7). This would also be consistent with the inability of low concentrations of HO₂C-R additives to inhibit the reaction as observed by Ziólkowski et al. and in these studies.



Scheme 3-7: Possible mechanism for the activation of pre-catalyst **3-11**.

These observations may also explain the differing effects of added triethylamine in the hydroformylation of alkenes catalyzed by **3-10** *versus* **3-11**, which benefitted the former while inhibiting the latter. While AcO^- can readily dissociate from **3-11** under catalytic conditions, the stronger binding Cl^- requires the assistance of an organic base to promote elimination of HCl and generate the active hydride catalyst. This may also explain the difficulties of synthesizing a $\text{Rh}(\text{NHC})$ -hydride from **2-10** experienced by previous graduate student Yonek Hleba.³⁵

3.3 Conclusions

In conclusion, two new rhodium *N*-heterocyclic carbene complexes have been prepared, which represent the first examples of such complexes possessing unidentate carboxylato ligands. Complex **3-11** represents one of the most active NHC-modified rhodium catalysts reported to date for the hydroformylation of styrene derivatives. High regioselectivity, up to 40:1 in favour of the branched isomer, was observed in the hydroformylation of vinyl arenes with **3-11**. Complex **3-11** also shows good activity in the hydroformylation of terminal aliphatic alkenes, with TOFs of up to 725 h⁻¹, and turnover numbers as high as 1900 h⁻¹. Most importantly, the reactions of these substrates occur without concomitant isomerization of the alkene.

The inhibiting effects of the carboxylate ligand were also probed, and compared to the chloro-containing analogue **3-14**. By monitoring the production of aldehydes with respect to time, it was demonstrated that catalyst **3-11** was not only a more efficient catalyst than **3-14**, with an observed TOF nearly five times greater than **3-14**, but it also generated the active catalyst over five times faster. Thus, it may be beneficial for future researchers to explore rhodium pre-catalysts (or other soft late transition metals) containing carboxylates as sacrificial ligands in other catalytic processes given their facile expulsion from the coordination sphere and low inhibitory effects.

3.4 Experimental

General Considerations: Both the rhodium dimer, $[\text{Rh}(\text{CO})_2(\text{OAc})]_2$,³⁶ and the free carbene, IPr⁵⁰ were prepared according to literature procedures. Benzene and triethylamine were each distilled under an argon atmosphere from calcium hydride. All other solvents (THF, DCM, hexanes, MeCN) were purified using an MBraun SPS solvent system. All solvents were purged of oxygen using a minimum of three freeze-pump-thaw cycles before being brought into a nitrogen-atmosphere glovebox. All alkene substrates were purchased from commercial sources and distilled under vacuum via bulb-to-bulb distillation and deoxygenated using a minimum of three freeze-pump-thaw cycles and stored in the glovebox at -20 °C. Triphenylphosphine was obtained from commercial sources and recrystallized from absolute ethanol prior to use. KI was recrystallized from boiling distilled water and dried under vacuum over P_2O_5 . ^1H and $^{13}\text{C}\{^1\text{H}\}$ NMR spectra were performed using Bruker Avance 400 and 500 MHz spectrometers. Mass spectra were determined by TOF-EI mass spectrometry on a Biosystems/MDS Sciex QSTAR XL Q-TOF mass spectrometer. Elemental analysis was performed by Canadian Microanalytical Systems Ltd. X-ray data collection was performed on a Bruker SMART CCD 1000 X-ray diffractometer and all structures were solved by Ruiyao Wang.

Synthesis of Catalysts

Preparation of $[(\text{AcO})\text{Rh}(\text{IPr})(\text{CO})_2]$ (**3-11**): An oven-dried round bottomed flask containing a stir bar was brought into the glove box and to it was added $[\text{Rh}(\text{CO})_2(\text{OAc})]_2$ (19.5 mg, 44.7 μmol), IPr (34.9 mg, 89.8 μmol) and 5 mL of THF. The reaction was

stirred for two hours, after which time the solution had turned from red/orange to yellow. After two hours the flask was removed from the glovebox and the reaction mixture filtered through a plug of celite under aerobic conditions. The filtrate was concentrated in vacuo to give a fine yellow, air stable powder. X-ray quality crystals were obtained by slow diffusion of hexanes into a THF solution of the complex. (Yield 39.0 mg, 72 % Yield). Anal. Found (calcd) for $\text{RhC}_{31}\text{H}_{39}\text{O}_4\text{N}_2$: C 61.62 (61.37), H 6.63 (6.48), N 4.56 (4.62). ^1H NMR (CDCl_3 , 400 MHz): δ 7.51 (t, 2H), 7.32 (d, 4H), 7.16 (s, 2H), 2.84 (septet, 4H), 1.85 (s, 3H), 1.32 (d, 12H), 1.12 (d, 12H) ppm. $^{13}\text{C}\{^1\text{H}\}$ NMR (CDCl_3 , 100 MHz): δ 187.1 (d, $J_{\text{C-Rh}} = 69$ Hz, Rh-CO), 185.8 (d, $J_{\text{C-Rh}} = 58$ Hz, Rh-CO), 181.8 (d, $J_{\text{C-Rh}} = 48$ Hz, Rh-C_{IPr}), 176.3, 146.2, 135.3, 130.7, 125.3, 124.1, 68.29, 28.8, 26.5, 22.9 ppm. IR (KBr, cm^{-1}): 2070, 1990, 1613, 1382 cm^{-1} .

Preparation of $[(\text{AcO})\text{Rh}(\text{IPr})_2(\text{CO})]$ (**3-12**): A solution of IPr (56.0 mg, 0.144 mmol) in THF (3 mL) was prepared in the glove box. To this was added a solution of $[(\text{AcO})\text{Rh}(\text{CO})_2]_2$ (15.7 mg, 0.036 mmol) in THF (2 mL) dropwise. The resulting orange solution was allowed to stir for 4 hours then removed from the box and filtered through celite under aerobic conditions. The orange filtrate was concentrated and the resulting solid recrystallized from hexanes and THF. Slow diffusion of hexanes into a THF solution of the yellow powder gave X-ray quality crystals. (Yield 42.7 mg, 92% Yield, contaminated with 10-15% of **3-11**). ^1H NMR (C_6D_6 , 400 MHz): δ 7.29 (t, 4H), 7.14 (d, 8H), 6.54 (s, 4H), 3.21 (m, 8H), 1.99 (s, 3H), 1.12 (d, 24H), 0.97 (d, 24H). $^{13}\text{C}\{^1\text{H}\}$ NMR (CDCl_3 , 100 MHz): δ 191.8 (d, $J_{\text{C-Rh}} = 70$ Hz, Rh-CO), 190.6 (d, $J_{\text{C-Rh}} = 44$ Hz, Rh-C_{IPr}), 172.9, 146.8, 137.9, 129.1, 126.1, 124.0, 34.4, 30.5, 28.2, 26.7, 23.2. IR (KBr): 1952, 1619, 1360 cm^{-1} . EI MS: m/z 966.49 [M^+].

Preparation of [ClRh(IPr)(CO)₂] (**3-14**): A solution of IPr (66.4 mg, 0.171 mmol) in THF (3 mL) was prepared in the glove box. To this was added a solution of [ClRh(CO)₂]₂ (32.8 mg, 0.085 mmol) in THF (2 mL) dropwise. The resulting orange solution was allowed to stir for 2 hours then removed from the box, concentrated to about 1 mL and filtered through celite under aerobic conditions. The orange filtrate was concentrated and the resulting yellow solid recrystallized from hexanes and THF. (Yield 73 mg, 74%). ¹H NMR (CDCl₃, 400 MHz): δ 7.50 (t, 2H, *J* = 8 Hz), 7.32 (d, 4H, *J* = 8Hz), 7.18 (s, 2H), 2.90 (septet, 4H, *J* = 7 Hz), 1.39 (d, 6H, *J* = 7 Hz), 1.11 (d, 6H, *J* = 7 Hz) ppm. ¹³C NMR (CDCl₃, 100 MHz): δ 185.2 (d, *J*_{C-Rh} = 54 Hz, Rh-CO), 182.9 (d, *J*_{C-Rh} = 73 Hz, Rh-CO), 180.6 (d, d, *J*_{C-Rh} = 45 Hz, Rh-C_{IPr}), 146.4, 135.2, 130.7, 125.1, 124.4, 29.1, 26.7, 23.0 ppm.

Representative hydroformylation experiment

Preparation of (+/-)-2-phenylpropanal: In the glove box, a glass liner was charged with **3-11** (4.3 mg, 7.1 μmol), PPh₃ (1.8 mg, 7.1 μmol) and styrene (38.0 mg, 0.365 mmol). The mixture was dissolved in 5 mL of benzene, and the solution stirred to mix. The liner was placed in the autoclave, which contained an additional 2 mL of benzene to prevent unwanted movement of the glassliner. The autoclave was removed from the box, the gauge block assembly attached and the system pressurized with 500 psi of CO(g) followed by 500 psi of H₂(g). The reaction was allowed to equilibrate to the desired temperature without stirring for 15 min, then stirred at the desired reaction temperature for 19 h, after which the reaction was immediately cooled in an ice bath for one hour and the pressure released from the autoclave. The contents of the autoclave were transferred to a round-bottomed flask containing a known amount of hexamethylbenzene, as an

internal standard, and the liner and autoclave rinsed with CDCl_3 . The yield of the reaction was determined ^1H NMR using solvent suppression techniques to remove the signals for benzene from the spectra.

Representative time-course experiment.

In the glove box, duplicate reactions were prepared in a manner analogous to above: two glass liners were each charged with **3-11** or **3-14** (5 μmol), PPh_3 (1.3 mg, 5 μmol) and 1-decene (1.403 g, 10 mmol). The mixtures were each dissolved in 10 mL of benzene, and the solutions stirred to mix. The liners were placed in autoclaves, which each contained an additional 2 mL of benzene to prevent unwanted movement of the glass liners. The autoclaves were removed from the box, the gauge block assemblies attached and the systems pressurized with 500 psi of $\text{CO}(\text{g})$ followed by 500 psi of $\text{H}_2(\text{g})$. The reactions were allowed to equilibrate to 80 $^\circ\text{C}$ without stirring for 15 min, then stirred at the desired reaction temperature for an equal amount of time. Afterwards, the reactions were immediately cooled in an ice bath for one hour and the pressure released from the autoclaves. The contents of the autoclaves were transferred to round-bottomed flasks containing known amounts of hexamethylbenzene, as an internal standard; each liner and autoclave was rinsed with CDCl_3 . The yield of the reactions were determined ^1H NMR using solvent suppression techniques to remove the signals for benzene from the spectra.

3.5 References

- (1) Leeuwen, P. W. N. M. v.; Claver, C. *Rhodium Catalyzed Hydroformylation*; Kluwer Academic Publishers: Boston, 2000; Vol. 22.
- (2) Roelen, O. Germany 849548, 1938.
- (3) Evans, D.; Osborn, J. A.; Wilkinson, G. *J. Chem. Soc. A* **1968**, 3133-3142.
- (4) Coloquhuon, H. M.; Thompson, D. J.; Twigg, M. V. *Carbonylation: Direct Synthesis of Carbonyl Compounds*; Plenum Press: New York, 1991.
- (5) Kaiser, D. G.; Vangiessen, G. J.; Reischer, R. J.; Wechter, W. J. *J. Pharm. Sci.* **1976**, *65*, 269-273. Bhattacharya, A.; Murphy, D. *Org. Process Res. Dev.* **2003**, *7*, 717-722.
- (6) Adkins, H.; Krsek, G. *J. Am. Chem. Soc.* **1948**, *70*, 383-386.
- (7) Slaugh, L. H.; Mullineaux, R. D. US 3239570, 1966. Slaugh, L. H.; Mullineaux, R. D. US 3239569, 1966. Slaugh, L. H.; Mullineaux, R. D. *J. Organomet. Chem.* **1968**, *13*, 469-477.
- (8) Evans, D.; Yagupsky, G.; Wilkinson, G. *J. Chem. Soc. A* **1968**, 2660-2265. Yagupsky, G.; Brown, C. K.; Wilkinson, G. *J. Chem. Soc. D - Chem. Comm.* **1969**, 1244-1245.
- (9) Brown, C. K.; Wilkinson, G. *Tetrahedron Lett.* **1969**, *10*, 1725-1726.
- (10) Brown, C. K.; Wilkinson, G. *J. Chem. Soc. A* **1970**, 2753-2764.
- (11) Heck, R. F.; Breslow, D. S. *J. Am. Chem. Soc.* **1961**, *83*, 4023-4027.
- (12) Kamer, P. C. J.; van Rooy, A.; Schoemaker, G. C.; van Leeuwen, P. W. N. M. *Coord. Chem. Rev.* **2004**, *248*, 2409-2424.
- (13) Matsubara, T.; Koga, N.; Ding, Y.; Musaev, D. G.; Morokuma, K. *Organometallics* **1997**, *16*, 1065-1078. Decker, S. A.; Cundari, T. R. *Organometallics* **2001**, *20*, 2827-2841.
- (14) Sparta, M.; Børve, K. J.; Jensen, V. R. *J. Am. Chem. Soc.* **2007**, *129*, 8487-8499.
- (15) Pruet, R. L.; Stone, F. G. A.; Robert, W. In *Advances in Organometallic Chemistry*; Academic Press: 1979; Vol. Volume 17, p 1-60.
- (16) Hjortkjaer, J. *J. Mol. Catal.* **1979**, *5*, 377-384.
- (17) Chen, A. C.; Ren, L.; Decken, A.; Crudden, C. M. *Organometallics* **2000**, *19*, 3459-3461.

- (18) Poyatos, M.; Uriz, P.; Mata, J. A.; Claver, C.; Fernandez, E.; Peris, E. *Organometallics* **2003**, *22*, 440-444.
- (19) Zarka, M. T.; Bortenschlager, M.; Wurst, K.; Nuyken, O.; Weberskirch, R. *Organometallics* **2004**, *23*, 4817-4820.
- (20) Bortenschlager, M.; Mayr, M.; Nuyken, O.; Buchmeiser, M. R. *J. Mol. Catal. A: Chem.* **2005**, *233*, 67-71.
- (21) Bortenschlager, M.; Schütz, J.; von Preysing, D.; Nuyken, O.; Herrmann, W. A.; Weberskirch, R. *J. Organomet. Chem.* **2005**, *690*, 6233-6237.
- (22) Chen, A. C.; Allen, D. P.; Crudden, C. M.; Wang, R. Y.; Decken, A. *Can. J. Chem.* **2005**, *83*, 943-957.
- (23) Praetorius, J. M.; Kotyk, M. W.; Webb, J. D.; Wang, R.; Crudden, C. M. *Organometallics* **2007**, *26*, 1057-1061.
- (24) Gil, W.; Trzeciak, A. M.; Ziólkowski, J. J. *Organometallics* **2008**, *27*, 4131-4138.
- (25) Poyatos, M.; Uriz, P.; Mata, J. A.; Claver, C.; Fernandez, E.; Peris, E. *Organometallics* **2002**, *22*, 440-444.
- (26) Dastgir, S.; Coleman, K. S.; Cowley, A. R.; Green, M. L. H. *Organometallics* **2005**, *25*, 300-306.
- (27) Neveling, A.; Julius, G. R.; Cronje, S.; Esterhuysen, C.; Raubenheimer, H. G. *Dalton Trans.* **2005**, 181-192.
- (28) Datt, M. S.; Nair, J. J.; Otto, S. *J. Organomet. Chem.* **2005**, *690*, 3422-3426.
- (29) Veige, A. S. *Polyhedron* **2008**, *27*, 3177-3189.
- (30) Douglas, S.; Lowe, J. P.; Mahon, M. F.; Warren, J. E.; Whittlesey, M. K. *J. Organomet. Chem.* **2005**, *690*, 5027-5035.
- (31) van Rensburg, H.; Tooze, R. P.; Foster, D. F.; Slawin, A. M. Z. *Inorg. Chem.* **2004**, *43*, 2468-2470.
- (32) Llewellyn, S. A.; Green, M. L. H.; Cowley, A. R. *Dalton Trans.* **2006**, 4164-4168.
- (33) Allen, D. P.; Crudden, C. M.; Calhoun, L. A.; Wang, R. *J. Organomet. Chem.* **2004**, *689*, 3203-3209.
- (34) Pearson, R. G. *J. Am. Chem. Soc.* **1963**, *85*, 3533-3539.
- (35) Hleba, Y.B. Unpublished results.
- (36) Lawson, D. N.; Wilkinson, G. *J. Chem. Soc.* **1965**, 1900.

- (37) Herrmann, W. A.; Schütz, J.; Frey, G. D.; Herdtweck, E. *Organometallics* **2006**, *25*, 2437-2448.
- (38) Wang, K.; Rosini, G. P.; Nolan, S. P.; Goldman, A. S. *J. Am. Chem. Soc.* **1995**, *117*, 5082-5088.
- (39) Huang, J.; Stevens, E. D.; Nolan, S. P. *Organometallics* **2000**, *19*, 1194-1197.
- (40) Herrmann, W. A.; Fischer, J.; Öfele, K.; Artus, G. R. J. *J. Organomet. Chem.* **1997**, *530*, 259-262.
- (41) Nakamoto, K. *Infrared Spectra of Inorganic and Coordination Compounds*; Wiley: New York, 1970.
- (42) Poyatos, M.; Sanau, M.; Peris, E. *Inorg. Chem.* **2003**, *42*, 2572-2576.
- (43) Ito, K.; Bernstein, H. J. *Can. J. Chem.* **1956**, *34*, 170-178.
- (44) Robinson, S. D.; Uttley, M. F. *J. Chem. Soc., Dalton Trans.* **1973**, 1912-1920.
- (45) Tanaka, M.; Watanabe, Y.; Mitsudo, T.; Takegami, Y. *Bull. Chem. Soc. Jpn.* **1974**, *47*, 1698-1703.
- (46) This is consistent with the previous study by Wilkinson demonstrating that the hydroformylation of internal alkenes are 1-2 orders of magnitude slower than terminal alkenes; see ref. 10.
- (47) Crudden, C. M.; Allen, D. P. *Coord. Chem. Rev.* **2004**, *248*, 2247-2273.
- (48) Yu, X.-Y.; Sun, H.; Patrick, B. O.; James, B. R. *Eur. J. Inorg. Chem.* **2009**, *2009*, 1752-1758.
- (49) Mieczynska, E.; Trzeciak, A. M.; Ziolkowski, J. J. *J. Mol. Catal.* **1993**, *80*, 189-200.
- (50) Jafarpour, L.; Stevens, E. D.; Nolan, S. P. *J. Organomet. Chem.* **2000**, *606*, 49-54.

Chapter 4: Ruthenium-Catalyzed Enantioselective Hydrogenation of Ketones Without the Use of Protic Amino Ligands

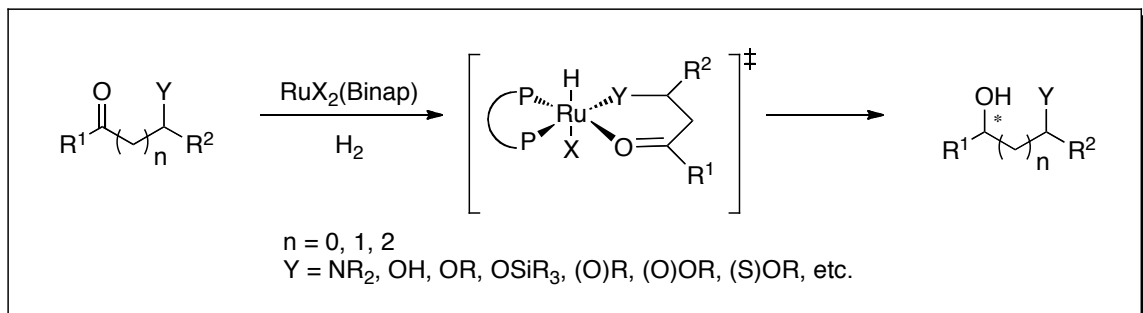
4.1 Introduction

4.1.1 Noyori-Type Hydrogenations

The reduction of carbonyl compounds to their respective alcohols is an important reaction both on laboratory¹ and industrial² scales. Considering the complexity and functional group density of common synthetic targets, efficient and chemoselective methods to affect this transformation are necessary.³ Furthermore, the development of enantioselective methods to yield chiral secondary alcohols via the reduction of ketones is highly desirable.⁴

The greatest breakthroughs in this field have come from the Noyori laboratory where systematic investigations of $[X_2Ru(\text{Binap})]$ (Binap = 2,2'-bis(diphenylphosphino)-1,1'-binaphthyl) complexes have led to highly efficient and selective catalytic methods for the reduction of carbonyl compounds.⁵ Initial success was found in the asymmetric hydrogenation of functionalized ketones with pendant heteroatoms capable of forming five- to seven-membered chelate intermediate complexes in which the ruthenium(II) atom interacts with the carbonyl oxygen and the heteroatom (Scheme 4-1). A wide variety of heteroatom-containing functionalities are capable of activating these substrates towards hydrogenation including dialkyl amino, hydroxyl, alkoxy, siloxy, keto, alkoxythiocarbonyl and carboxyl groups, with β -ketoesters generally being the best substrates in this reaction.⁶ Notably, these reactions can be performed in aqueous acetone

with no observable reduction of the solvent, demonstrating the inertness of simple ketones towards reduction by $[X_2Ru(\text{Binap})]$ catalysts.⁵



Scheme 4-1: Ru(Binap) catalyzed hydrogenation of heteroatom functionalized ketones.

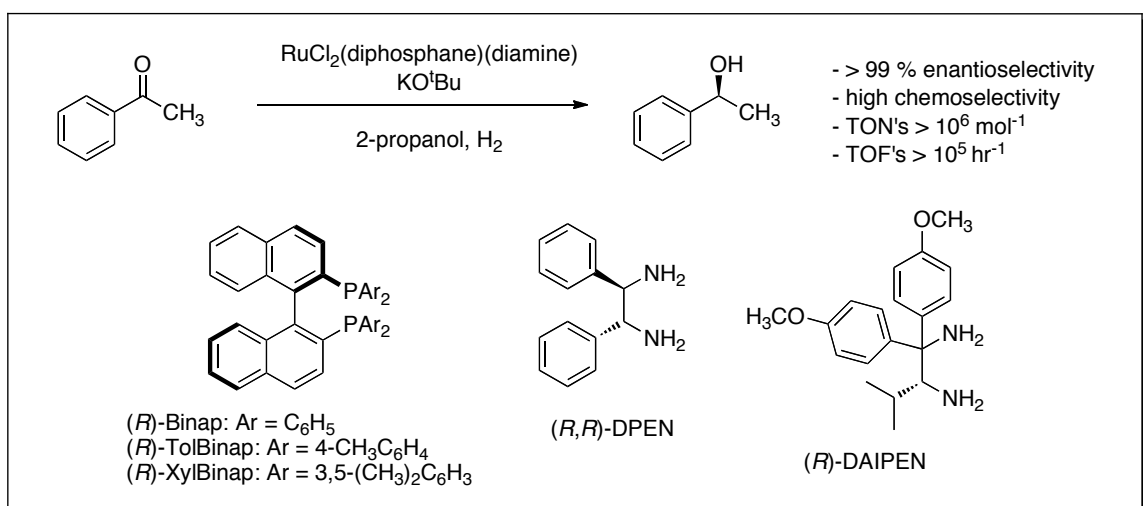
Given the relative ease with which these ruthenium complexes activate hydrogen gas, the lack of reactivity towards simple ketones, such as acetone or acetophenone, is apparently due to a lack of ancillary coordinating heteroatoms in the substrate. Thus, in order to expand the scope of this reaction to other substrates in which the carbonyl group is isolated, other routes for coordination and activation of the substrate had to be explored. Generally, carbonyls tend to form σ complexes with electrophilic metal centers through coordination of the oxygen atom rather than the π system, in contrast to alkenes, which readily form π complexes with late transition metal complexes and are typically hydrogenated under relatively mild conditions. While coordination of the carbonyl oxygen to an electrophilic metal activates the π system towards nucleophilic attack at carbon, it places the carbon further away from the metal-hydride making reaction between the two problematic. The simplest electrophile, a proton, could be used to promote the hydrogenation of the ketone, however, even with the use of a strong acid the low concentration of both the protonated ketone and ruthenium hydride under catalytic

conditions make this strategy impractical. Instead, Noyori's lab sought to place a protic moiety within the catalyst, such that activation of the carbonyl could be achieved in close proximity to the metal-hydride.

Thus, it was discovered that the use of a ruthenium phosphine species bearing a protic amine as part of the ligand system results in catalysts that are extraordinarily active under relatively mild hydrogenation conditions.^{7,8} Coordination of the diamine to ruthenium increases the acidity of the NH protons and places them in close proximity to the metal centre. The coordinated diamine, now sufficiently protic to activate the carbonyl oxygen, subsequently activates the carbon towards nucleophilic attack, near the nucleophilic the metal-hydride. This cooperation between the ruthenium-hydride and the protic diamine ligand to activate and reduce unfunctionalized carbonyl substrates is known as bifunctional catalysis.^{5,9,10}

In addition to being an extremely efficient reaction, it was found that proper matching of a chiral diamine, for example (*R,R*)-diphenylethylenediamine (dpem), with the correct enantiomer of a chiral ruthenium diphosphine (e.g. [Cl₂Ru(*R*)-Binap]) can produce an exceptionally enantioselective precatalyst, with high turnover numbers and frequencies (Scheme 4-2).¹¹⁻¹³ While the chiral complex [Cl₂Ru(*R*)-Binap](*R,R*-dpem) and its (*S,S*)-enantiomer were not always exceptionally enantioselective, [Cl₂Ru(*R*)-XylBinap](*R*-daipen) (XylBinap = 2,2'-bis(3,5-xylylphosphino)-1,1'-binaphthyl; daipen = 1,1-dianisyl-2-isopropyl-1,2-ethylenediamine) consistently gave better results. Thus, highly enantioselective hydrogenation of a number of ketonic substrates can be affected with this system including hetero-aromatic,¹⁴ cyclopropyl,¹² dialkyl,¹² *tert*-alkyl,¹⁵ α -amino¹⁶ and α -alkoxy ketones, as well as *ortho*-substituted benzophenones¹³ and

tetralone derivatives.¹⁷ Furthermore, the coordinatively saturated ligand sphere of ruthenium prevents coordination of alkenyl π systems to the metal, making these catalysts highly chemoselective for carbonyls *versus* olefins, and capable of producing chiral allylic alcohols from α,β -unsaturated ketones;^{8,12} an otherwise daunting task for transition metal catalyzed hydrogenation reactions.

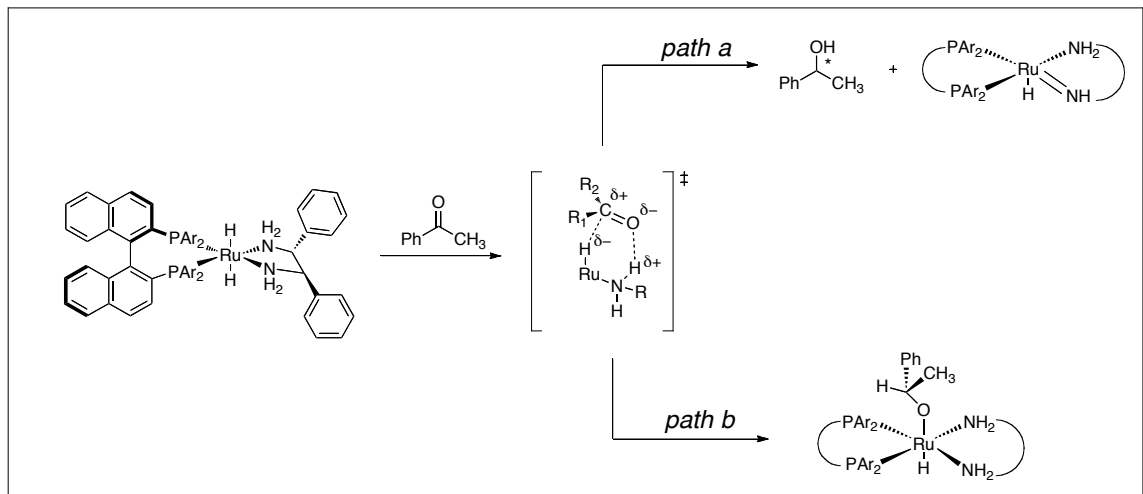


Scheme 4-2: Representative hydrogenation of a simple ketone using Noyori's bifunctional catalyst.

Noyori's research group,¹⁸ and others,^{19,20} have investigated the mechanism of this reaction, with the aim to explain its remarkable reactivity and selectivity. It is clear from numerous studies that the presence of a diamine ligand bearing at least one N–H bond is critical for high activity and chemoselectivity,^{7,21} however, the precise explanation of this effect has been the subject of recent debate.

The most commonly accepted mechanism has the reaction occurring through a six-membered, concerted transition state, in which the coordinatively saturated metal center promotes an outer-sphere mechanism that never involves direct interaction of the

substrate with the ruthenium atom.^{18,20,22} Instead, the protic amine is believed to act as a Brønsted acid, which adds to the carbonyl carbon simultaneously with the metal-hydride releasing the secondary alcohol without the intermediacy of a ruthenium-alkoxide (Scheme 4-3, path a). The resulting Ru-amide formed as a result of hydrogenation of the ketone, has been shown through kinetic experiments to be the resting state of the catalytic cycle, with regeneration of the active species *via* addition of a molecule of hydrogen gas being the rate-determining step. Mechanistic studies and computational analysis of a related [Ru(arene)(diamine)] system are consistent with the concerted, six-membered transition state as a likely mechanism in the enantioselective transfer hydrogenation of ketones.^{9,23} This has, by extension, been applied to the [Cl₂Ru(diphosphine)(diamine)] system. This mechanism also explains the chemoselectivity of this system for carbonyls *versus* alkenes. The coordinatively saturated ruthenium catalyst prevents coordination of the alkene through its C-C double bond and the less basic, electronically symmetrical π -system of the alkene interacts poorly with the weakly acidic bound amine. Conversely, carbonyl substrates are activated by interaction of the oxygen atom with the protic hydrogen and also appropriately positioned for addition of the hydride to the electrophilic carbon.



Scheme 4-3: Opposing mechanisms proposed by Noyori (path a) and Bergens (path b) for the enantiodetermining step in Noyori's bifunctional hydrogenation of ketones.

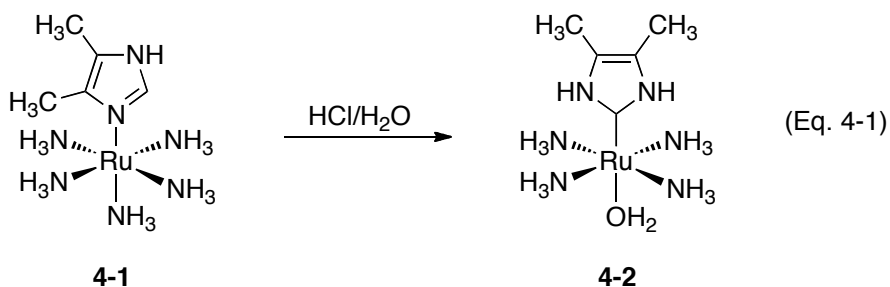
Stoichiometric studies by Bergens on this system, however, have suggested that while the protic diamine may act as a binding point for the nucleophilic oxygen atom, thereby activating the π -bond towards attack of the hydride, its addition to the carbonyl does not occur simultaneously with hydride addition (Scheme 4-3, path b).²⁴ Instead, the carbonyl first undergoes a metal-hydride insertion to afford a ruthenium alkoxide intermediate. As evidence for this alternative mechanism, they were able to isolate a ruthenium-alkoxide resulting from a 1,2-addition of the carbonyl to *trans*- $[(\text{H})_2\text{Ru}((R)\text{-Binap})((R,R)\text{-dpen})]$. After hydride addition, the amine ligand is deprotonated by the alkoxide base present in solution, generating a lone pair that ejects the alkoxide and forms the ruthenium-amide complex proposed by Noyori to be the catalyst resting state.

4.1.2 Protic N-Heterocyclic Carbene Ligands

The organometallic chemistry of NHC ligands, despite great exploration in terms of inorganic synthesis, stoichiometric reactivity, stability and catalytic applications, has dealt almost entirely with NHCs bearing alkyl or aryl wingtips at *both* nitrogens.

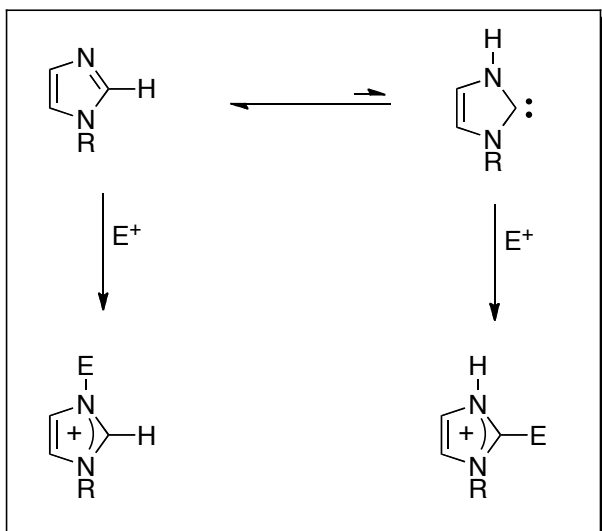
Although their numbers are limited, several structures of M(NHC) complexes in which *one* of the carbene nitrogens has a hydrogen wingtip have been reported.²⁵ These protic-NHC ligands are the high-energy tautomers of simple N-containing heterocycles, such as imidazoles, benzimidazoles or pyridines achieved by *C,N*-1,2-hydrogen rearrangements. Many M(protic-NHC) complexes are therefore synthesized via tautomerization of these stable starting materials. Furthermore, this type of tautomerization may be relevant to biological processes, where the high-energy tautomer is often an active intermediate that dictates reaction mechanisms and product distributions.²⁶

The first isolation of a M(protic-NHC) complex was reported by Taube in 1974 by reaction of ruthenium imidazole complex **4-1** in dilute aqueous HCl under aerobic conditions to yield **4-2** (Eq. 4-1).²⁷ Given the presence of imidazole groups in biological systems as the functional side-chain in the amino acid histidine, the biological relevance of such a tautomerization was brought into question. Further forays into the synthesis of protic-NHC complexes of transition metals via the NH-tautomerization of nitrogen heterocycles were preceded by a theoretical study by Crabtree, Eisenstein and Sini, which sought to determine if binding through the imidazol-2-ylidene tautomer could be thermodynamically favourable.²⁸



Addition of a proton to the nitrogen of imidazole or the carbene of its tautomer is isoenergetic, as protonation of both yields an imidazolium cation (Scheme 4-4, E = H).

When hydrogen is substituted for other electrophiles, such as transition metal centers, these two sites are differentiated and could potentially lead to situations in which the C-bound tautomer is favoured.



Scheme 4-4: C,N-1,2-tautomerization of imidazole and reaction of the conformers with an electrophile.

The ΔE of the tautomerization for imidazole was calculated to be 28.9 kcal/mol indicating insignificant quantities of the carbene at equilibrium, yet numerous metal fragments were identified that compensated for this difference and stabilized the carbene complex. Trends seemed to favour stabilization of the carbene tautomer with softer late transition metals (for example, Au *versus* Cu or Pt *versus* Ni); sterically demanding larger ligand systems; the presence of a hydrogen-bond acceptor *cis* to the protic-NHC; and complexes containing ligands with a weaker trans-influence *trans* to the imidazole.

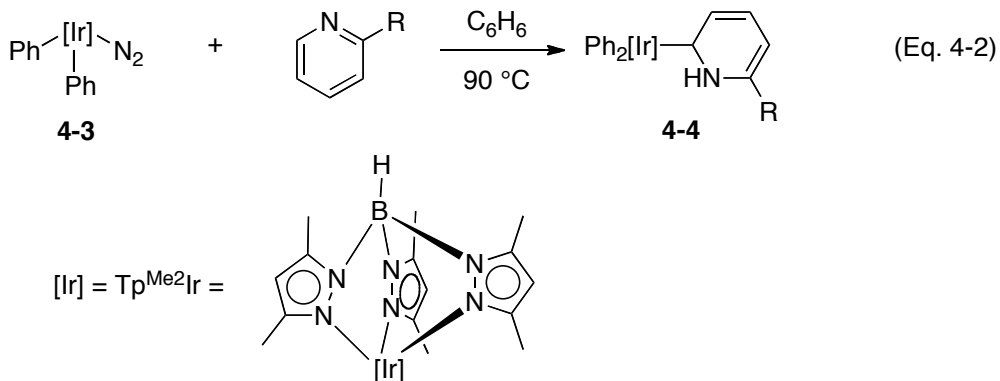
Since this report, M(protic-NHC) complexes have been described for variety of transition metals including iridium, rhodium, ruthenium, osmium, rhenium, chromium, platinum and manganese.²⁹⁻⁴⁷ There are numerous strategies for the synthesis of these

complexes including metal-mediated tautomerization of N-heterocycles, acid/base induced tautomerizations, or templated synthesis of the M(protic-NHC) by intramolecular attack on a coordinated isonitrile by an *in situ* generated, pendant amine or alkoxide. Also, examples have been reported of M(protic-NHC) formation via cleavage of an N-C or N-Si bond within the NHC unit.⁴⁸⁻⁵⁰

Recent reports by Bergman and Ellman have shown that Rh(protic-NHC) complexes of various N-heterocycles are the catalytically competent intermediates in the coupling reaction of these substrates with alkenes and aryl halides.⁵¹ Additionally, there are a number of accounts detailing the stoichiometric reactions of M(protic-NHC) complexes including transmetallation reactions,^{36,37} dehydrative additions of allyl alcohol to N-heterocycles,⁴⁷ and reactions demonstrating the bifunctional nature of M(protic-NHC) complexes.⁴⁶ Given the great potential of these complexes to perform novel catalytic transformations, experimental and theoretical studies have been performed to ascertain the mechanism of their formation.^{32,38,39,44,45}

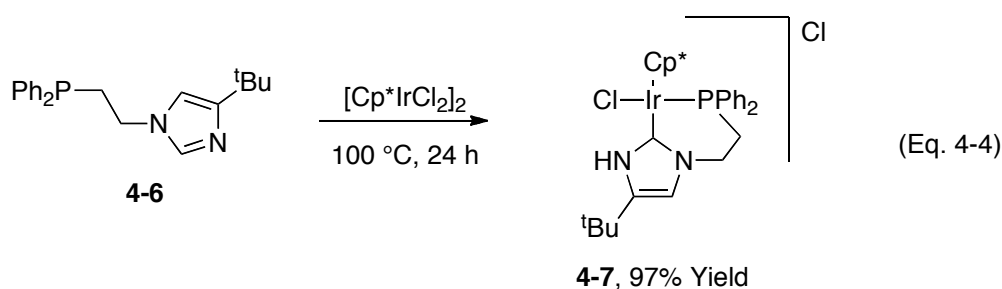
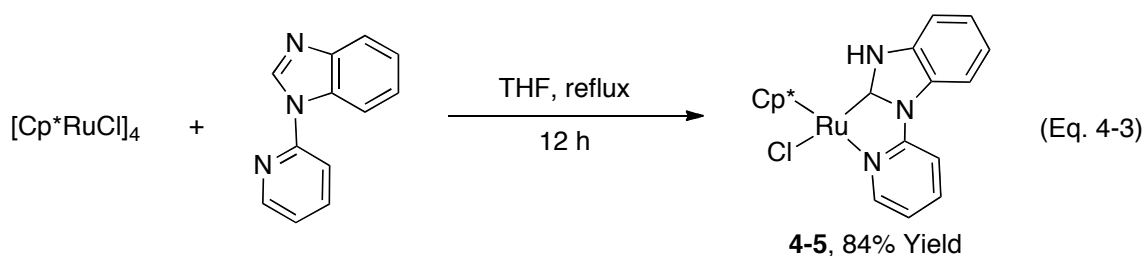
4.1.3 Synthesis of M(protic-NHC) Complexes

The most direct route to the formation of M(protic-NHC) complexes is by reaction of the CH-tautomer of a common aromatic N-heterocycle, such as pyridine or imidazole, with transition metal complexes. For example, Carmona and Poveda demonstrated the synthesis of Ir(protic-NHC) complexes **4-4** resulting from heating [Ir(Tp^{Me2})] complex **4-3** (Tp^{Me2} = hydrotris(3,5-dimethylpyrazolyl)borate) with 2-substituted pyridines (Eq. 4-2).²⁹

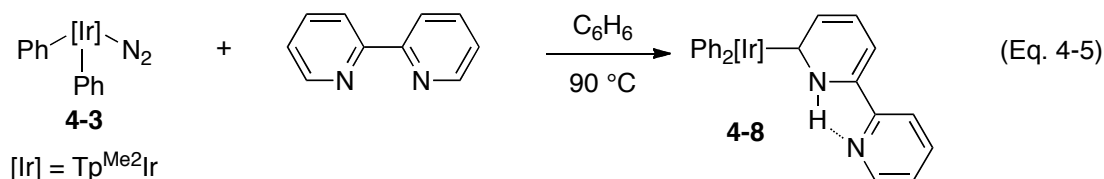


Despite the high energy of the pyridine NH-tautomer, calculated to be more than 40 kcal/mol less stable,⁵² reaction of 2-substituted pyridines with the metal stabilized this conformation, resulting in formation of a M(protic-NHC) complex. Interestingly, the analogous reaction with pyridine or 4-dimethylaminopyridine results in coordination of the pyridine at nitrogen. Thus, increasing the bulkiness at the 2-substituted pyridines destabilizes the *N*-adduct, favoring tautomerization of the pyridine and migration of the metal to the carbene, which relieves the steric repulsion imparted by the 2-substituent. Studies by Esteruelas et al., extended the metal-mediated tautomerization of 2-substituted pyridines to the synthesis of complexes of Os and Ru,^{43,44} and also demonstrated analogous reactions with quinolines^{44,45} and benzoquinolines.⁴²

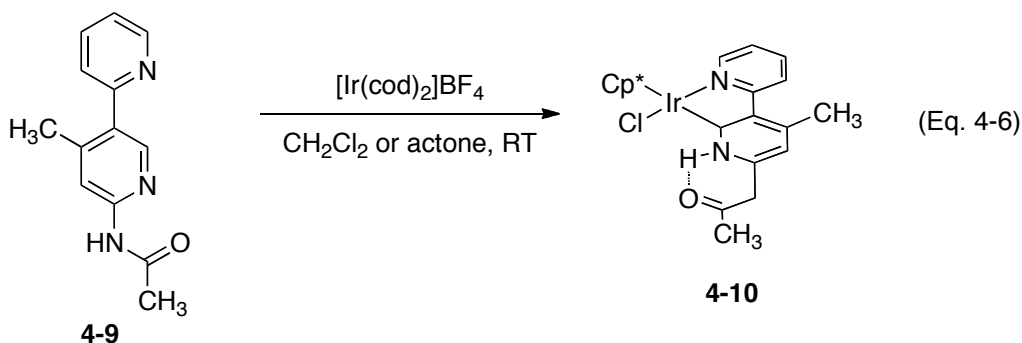
M(protic-NHC) is favoured in cases where the heterocycle contains pendant functionality capable of coordinating the metal center to form a chelate complex. For example, reaction of *N*-(2-pyridyl)benzimidazole with [Cp**RuCl*]₄ gave the chelate complex **4-5** in 84 % yield after 12 hours in refluxing THF (Eq. 4-3).⁴⁷ Similarly, phosphine functionalized imidazole **4-6**, which reacted with [Cp**IrCl*]₂ through coordination of phosphorous at ambient temperature, gave the chelating carbene complex **4-7** upon heating (Eq. 4-4).⁴⁶



Formation of NH tautomers is also favoured in cases where the NH participates in hydrogen bonding with a hydrogen bond acceptor within the metal complex. This type of stabilization has been demonstrated by Carmona and Poveda in the synthesis of iridium complex **4-8**, obtained by reaction of **4-3** with 2,2'-bipyridine, which is stabilized by a hydrogen bond between the NH and the pyridyl nitrogen on the adjacent ring (Eq. 4-5).³⁰ This result is surprising, as a chelate complex might typically be expected to result from either coordination of the second nitrogen to the metal or C-H activation at the 3'-position.



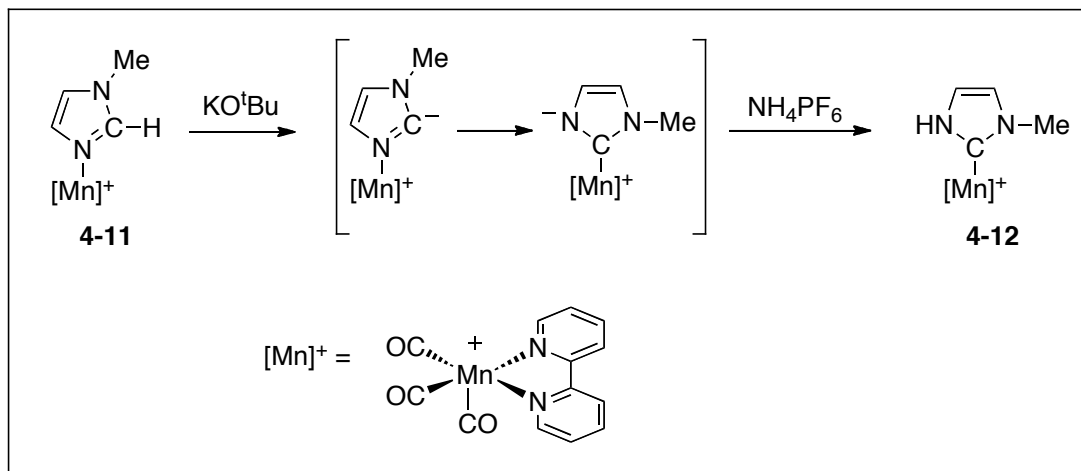
A similar reaction was investigated by Li et al., in which 2,3'-bipyridines were reacted with $[\text{Ir}(\text{cod})_2]\text{BF}_4$, to give the corresponding CN-chelate complexes via tautomerization of the 3'-pyridyl ring (Eq. 4-6).³¹ While the reaction of unfunctionalized 2,3'-bipyridine gave complex mixtures, amide functionalized ligand **4-9** reacted cleanly to give the desired complex **4-10**, presumably because of the stabilization provided by the hydrogen-bond accepting carbonyl of the amide.



Like the first reported synthesis of a $\text{M}(\text{protic-NHC})$ complex by Taube,²⁷ acid/base mediated processes have been reported as viable methods for the isolation of related compounds. Unlike, the initial report of Taube which utilized a substoichiometric amounts of acid to catalyze the C,N -1,2-tautomerization of imidazole, recent reports have focused on complete deprotonation of bound^{36,37,53} or unbound³⁵ imidazole derivatives.

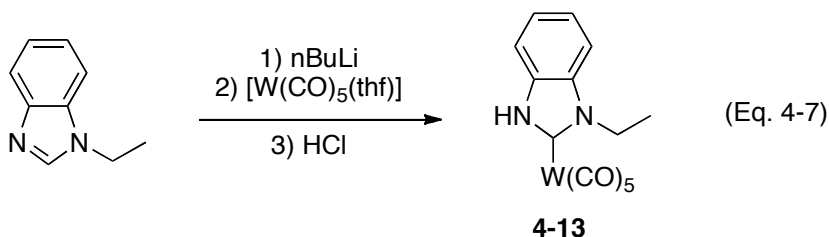
Ruiz et al., have developed a method in which manganese-imidazole complex **4-11** is stoichiometrically deprotonated by KO^tBu , followed by rearrangement to give the imidazolyl complex; protonation of this intermediate yields the corresponding NH-tautomer **4-12** (Scheme 4-5).³⁶ A similar procedure was recently applied to the synthesis of oxazole- and thiazole-based $\text{Mn}(\text{protic-NHC})$ complexes.³⁷ The resulting carbene compounds may prove to be useful transmetallating reagents for a general synthesis of

M(protic-NHC) complexes, but to date have only been effective in the transfer of the NHC ligand to gold complexes.



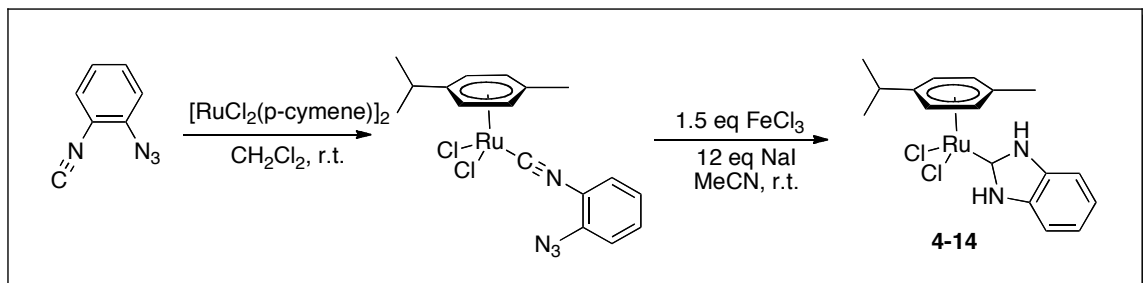
Scheme 4-5: Formation of an Mn(protic-NHC) via the base-promoted tautomerization of an imidazole ligand.³⁶

Similar results can be achieved via deprotonation of imidazoles prior to metal coordination: Hahn and Waldvogel reported the synthesis of a W(protic-NHC) compound **4-13** by first deprotonating 1-ethylbenzimidazole with *n*BuLi, reacting the resulting benzimidazolate with $[W(CO)_5(thf)]$ and then protonating with HCl (Eq. 4-7).³⁵



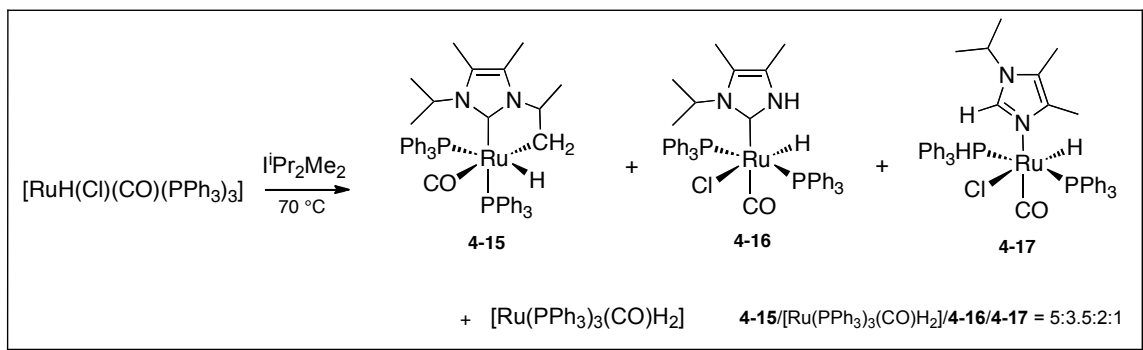
As mentioned in Section 1.4, the templated synthesis of NHCs via intramolecular attack of a pendant amine on a coordinated isonitrile ligand is a viable method for the synthesis of M(NHC) complexes. The immediate product of such a reaction is necessarily a protic carbene, bearing at least a single hydrogen wingtip. For example,

Hahn et al. demonstrated that using 2-azidophenyl isocyanide^{33,54} or 2-nitrophenyl isocyanide⁵⁵ as synthons for the unstable 2-amino isocyanide, diprotic benzannulated NHC-metal complexes, such as **4-14**, can be obtained (Scheme 4-6).



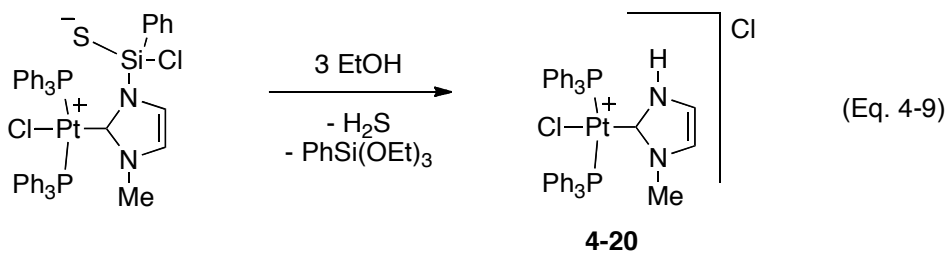
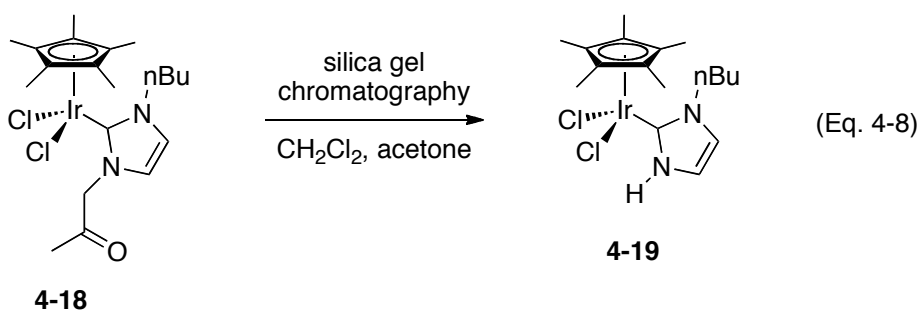
Scheme 4-6: Templated synthesis of a Ru(protic-NHC) via annulation of a coordinated 1,2-azidoisocyanide.⁵⁵

Formation of M(protic-NHC) complexes has also been achieved by cleavage of one of the nitrogen substituents of a preexisting M(NHC) complex. Reaction of $[\text{ClRu}(\text{H})(\text{CO})(\text{PPh}_3)_3]$ with two equivalents of $\text{I}^i\text{Pr}_2\text{Me}_2$ resulted in a mixture of products including complexes resulting from C-H activation of the N-isopropyl group (**4-15**), N-C activation with loss of propylene to form protic-NHC complex **4-16**, and tautomerization of **4-16** to N-bound C-H tautomer **4-17** (Scheme 4-7).⁴⁸ The ability of the carbene ligand to undergo spontaneous C-H activation appears to be important in formation of the protic-NHC complex, as the corresponding N-ethyl derivatives did not undergo this reaction.



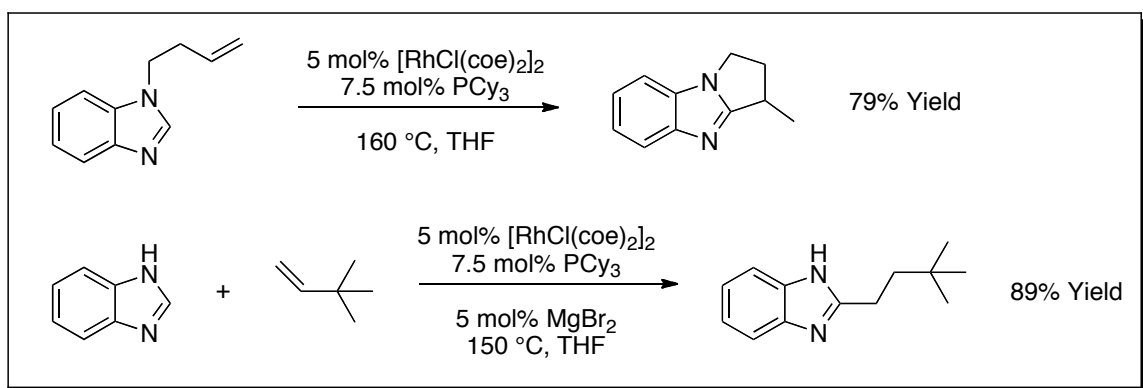
Scheme 4-7: Formation of Ru(protic-NHC) complex via tandem C-H, N-C activation.⁴⁸

In another example of serendipitous protic-NHC formation, attempts to purify **4-18** by column chromatography resulted in loss of the pendant ketone functionalized wing tip and formation of Ir(protic-NHC) **4-19** (Eq. 4-8).⁴⁹ In a separate instance, N-Si cleavage was observed to yield the Pt(protic-NHC) complex **4-20** (Eq. 4-9).⁵⁰



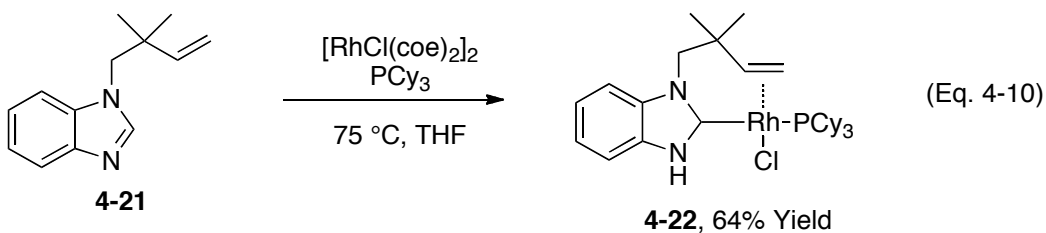
4.1.4 Reactivity of M(protic-NHC) Complexes

The research groups of Bergman, Ellman et al. have described the intramolecular rhodium-catalyzed annulation of alkene-substituted heterocycles and intermolecular alkene/heterocycle cross-coupling, both proceeding through regioselective C-H activation of the heterocycle (Scheme 4-8).^{51,56}

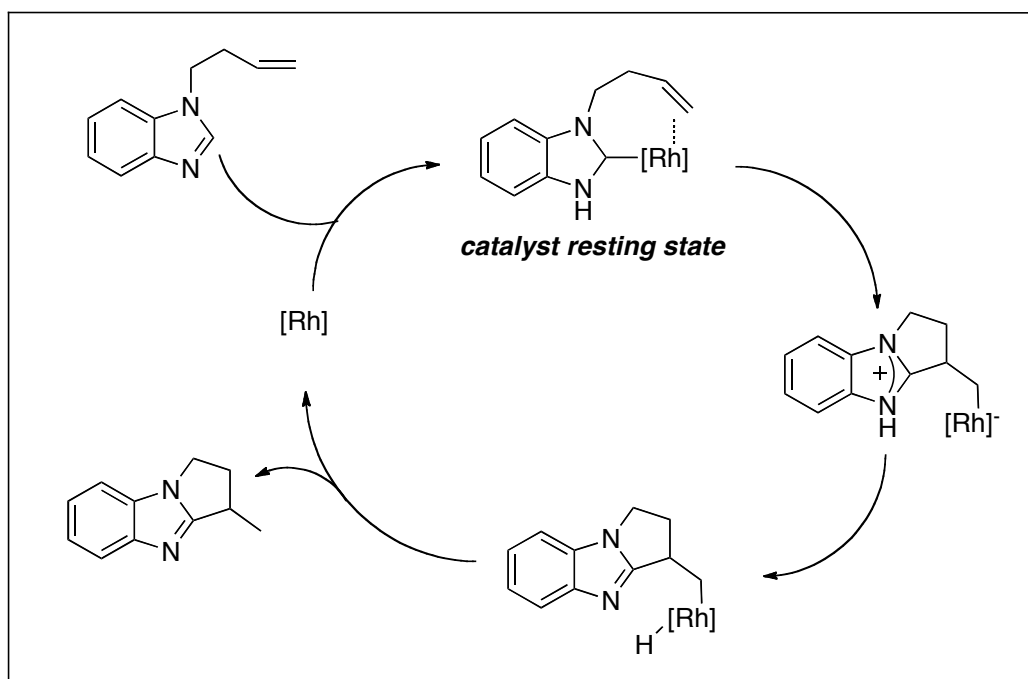


Scheme 4-8: Rhodium-catalyzed intra- and intermolecular coupling of olefins to heterocycles.^{51,56}

Given the high synthetic utility of these transformations, mechanistic studies were undertaken with the hope of further expanding their scope. During these studies, stoichiometric reaction of alkene-substituted benzimidazole **4-21** with [ClRh(COE)₂]₂ and tricyclohexylphosphine (PCy₃) at 75 °C, considerably below the temperatures required for coupling (135-165 °C), resulted in formation of the corresponding Rh(protic-NHC) complex **4-22** (Eq. 4-10).³⁸



At the higher temperatures required for cyclization, **4-22** was found to be a competent catalyst, and proposed to be the resting state of the catalytic cycle based on kinetic studies.³⁸ The proposed catalytic cycle (Scheme 4-9), based on experimental and computational studies, then proceeds via alkenyl C-C insertion into the Rh-C_{carbene} bond of the Rh(protic-NHC) intermediate, followed by hydrogen transfer to Rh and reductive elimination to give the product and [ClRh(PCy₃)₂]. C-H activation of another substrate molecule regenerates the Rh(protic-NHC) intermediate and completes the catalytic cycle. Thus, the catalytic reaction is a unique example in which the isolable M(protic-NHC) complex of the heterocyclic substrate is an active species.

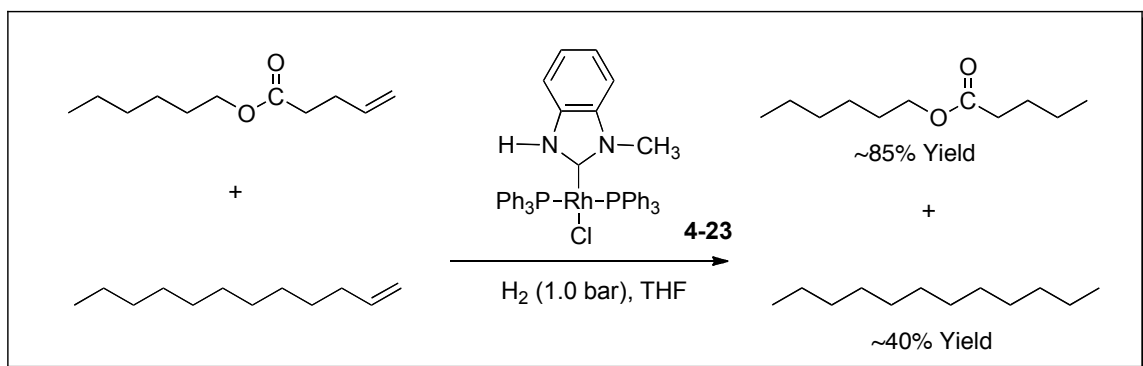


Scheme 4-9: Proposed catalytic cycle for the rhodium-catalyzed annulation of alkene-substituted benzimidazoles.³⁸

As a result of these mechanistic studies, the scope of this transformation was expanded to intramolecular coupling of alkenes with azoles,⁵⁷ oxazolines,⁵⁸

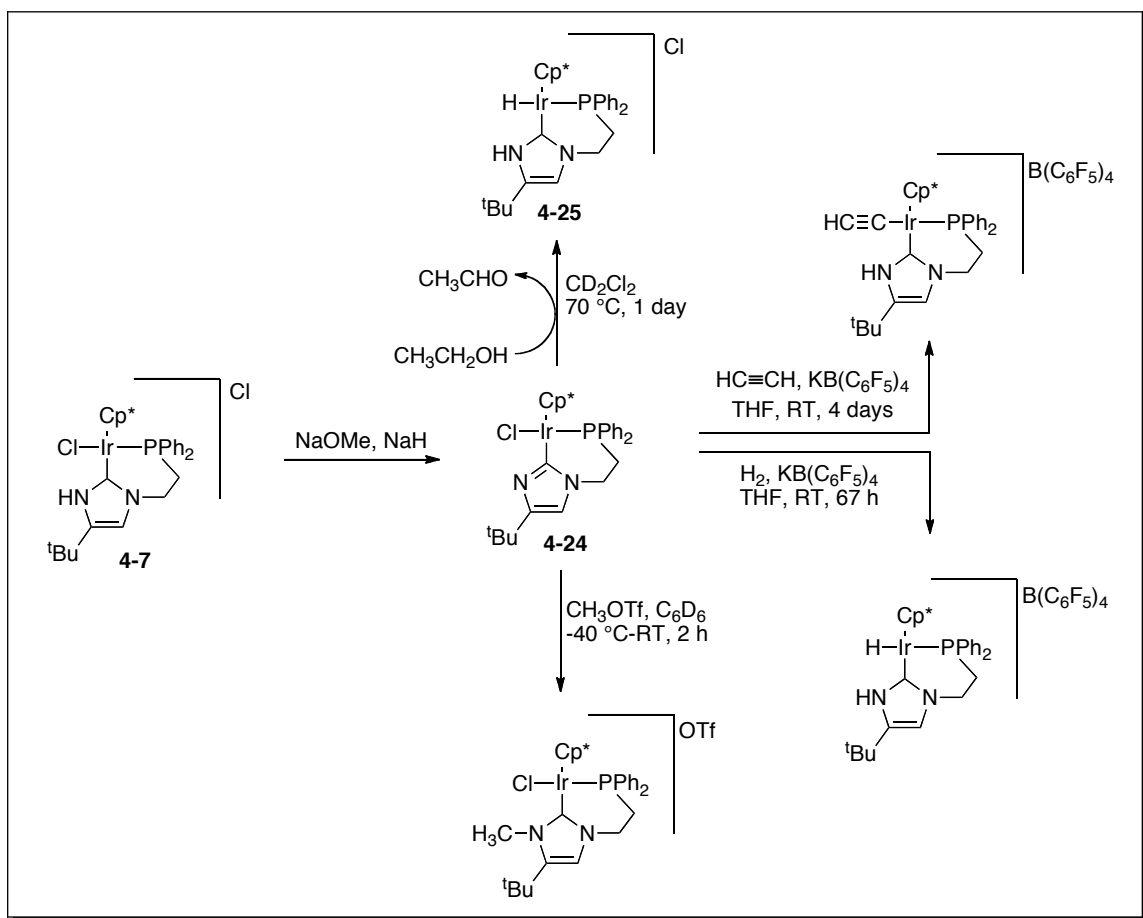
dihydroquinazolines,⁵⁹ pyridines and quinolines.⁶⁰ This reaction class was also further elaborated to include the direct arylation of these heterocycles with aryl halides.^{61,62} Concomitant with the development of these methodologies, Rh(protic-NHC) complexes of *N*-methylbenzimidazole,⁶³ 3-methyl-3,4-dihydroquinazoline³⁹ and 1-methyl-1,4-dimethyl-benzodiazepine-2-one⁴⁰ were also isolated and characterized.

In a report by Hahn, Waldvogel et al., the protic nature of W(protic-NHC) compound **4-13** was demonstrated by titration with the hydrogen-bond acceptor *N,N*-dimethyl-3,4,5,6-tetrahydropyrimidin-2(1*H*)-one (DMPU) and monitored by ¹H NMR. Downfield shifting of the NH signal upon addition of DMPU indicated a hydrogen-bonding interaction, which was assigned a binding constant of roughly 40 M⁻¹ or $\Delta G = 2.2$ kcal/mol. On the basis of this interaction, Rh(protic-NHC) catalyst **4-23** was submitted to a competitive hydrogenation reaction of dodecene *versus* pentyl but-3-enoate, which showed a slight preference for the carbonyl containing substrate (Scheme 4-10).³⁵ It should be noted that **4-23** was contaminated with the N-bound tautomer as a minor component, which appeared to interconvert in solution, obviously complicating the interpretation of these results.



Scheme 4-10: Competitive hydrogenation of a carbonyl containing alkene and a simple alkene with a Rh(protic-NHC) complex.³⁵

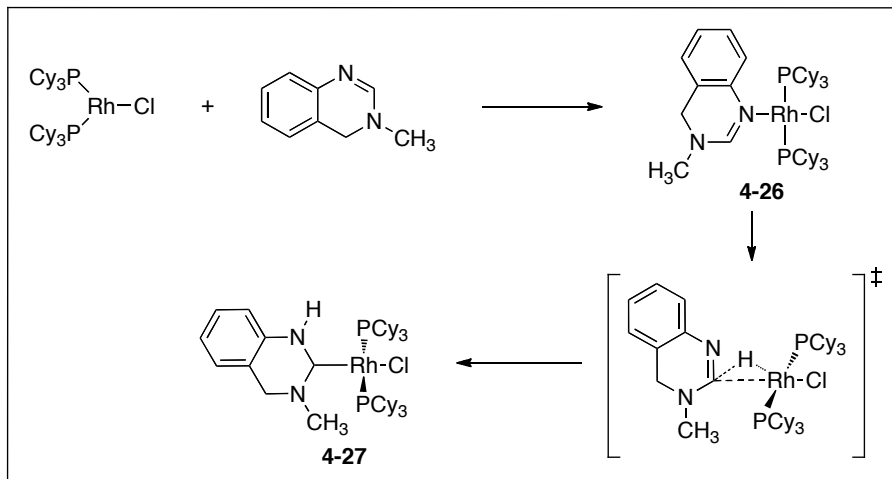
The report from the laboratories of Grotjahn and Rheingold of Ir(protic-NHC) complex **4-7**, included a number of stoichiometric reactions demonstrating its bifunctional behaviour.⁴⁶ Deprotonation of the cationic complex **4-7** led to the neutral imidazolyl complex **4-24**, which was shown to: dehydrogenate ethanol yielding acetaldehyde and generating **4-25** the metal hydride analogue of **4-7**; activate hydrogen gas and acetylene to give the corresponding hydride and acetylide Ir(protic-NHC) complexes, respectively; and undergo alkylation at the basic nitrogen by methyl triflate (Scheme 4-11).



Scheme 4-11: Stoichiometric reactions demonstrating the bifunctional behaviour of **4-7**.⁴⁶

4.1.5 Mechanistic Aspects of the Formation of M(protic-NHC) Complexes

The coupling of N-heterocycles with olefinic partners is a unique example of a catalytic reaction involving a protic-NHC metal complex as a catalytic intermediate. This fact, and the synthetic utility of the products inspired Bergman and Ellman to undertake mechanistic investigations to determine the mechanism of *N*-heterocycle C-H activation, which ultimately leads to formation of the Rh(protic-NHC) complex.^{38,39} Using 3-methyl-3,4-dihydroquinazoline, the formation of complex **4-27** was achieved with various similarities to the previously isolated **4-22**: **4-27** formation is observed at temperatures below those required for the coupling of the heterocycle to olefins; **4-27** is capable of acting as an effective catalyst in the coupling reaction; and **4-27** was determined to be the resting state of the catalytic cycle. The studies revealed that formation of the protic-NHC complex was preceded by coordination of sp^2 hybridized N1 of the heterocycle to rhodium to form **4-26**. Complex **4-26** was then shown undergo an intramolecular C-H activation/proton transfer pathway to give **4-27** (Scheme 4-12). This is one of the few examples in which formation of a protic-NHC metal complex has been studied.

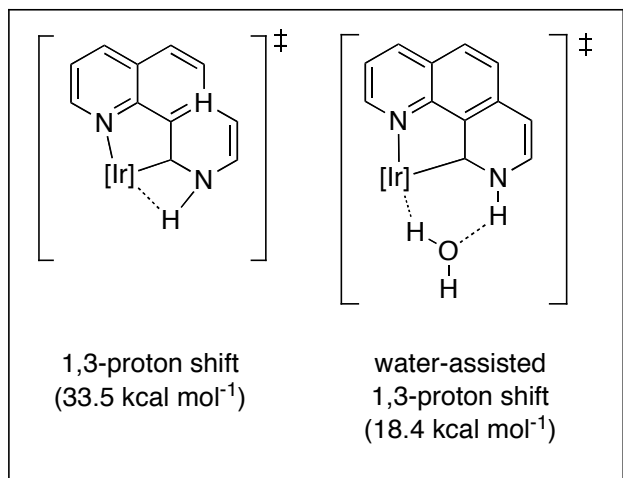


Scheme 4-12: Proposed mechanism for the formation of Rh(protic-NHC) in catalytic heterocycle olefination.^{38,39}

A recent study on the formation of Ir^I(protic-NHC) complexes by C-H activation of 1,9-phenanthroline provided further insights into factors controlling the formation of protic-NHC complexes.³² Reaction of phenanthroline with [ClIr(coe)₂]₂ followed by treatment with various triarylphosphines gave protic-NHC complexes of the general structure **4-28-Cl**. The stability of these complexes was provided by the existing hydrogen bond between the protic N-H of the carbene and the chloride counterion. Interrupting this interaction by halide exchange using various thallium and sodium salts gave equilibrium mixtures of **4-28-X** and the corresponding Ir^{III}-hydride **4-29-X**, with K_{eq} being strongly dependant on the counterion and solvent employed (Scheme 4-13).

donors to provide greater stabilization of the transformation from the Ir^I(NHC) to the Ir^{III}-hydride species in this process, as the higher oxidation state of the metal afforded greater stabilization by electron-rich phosphines.

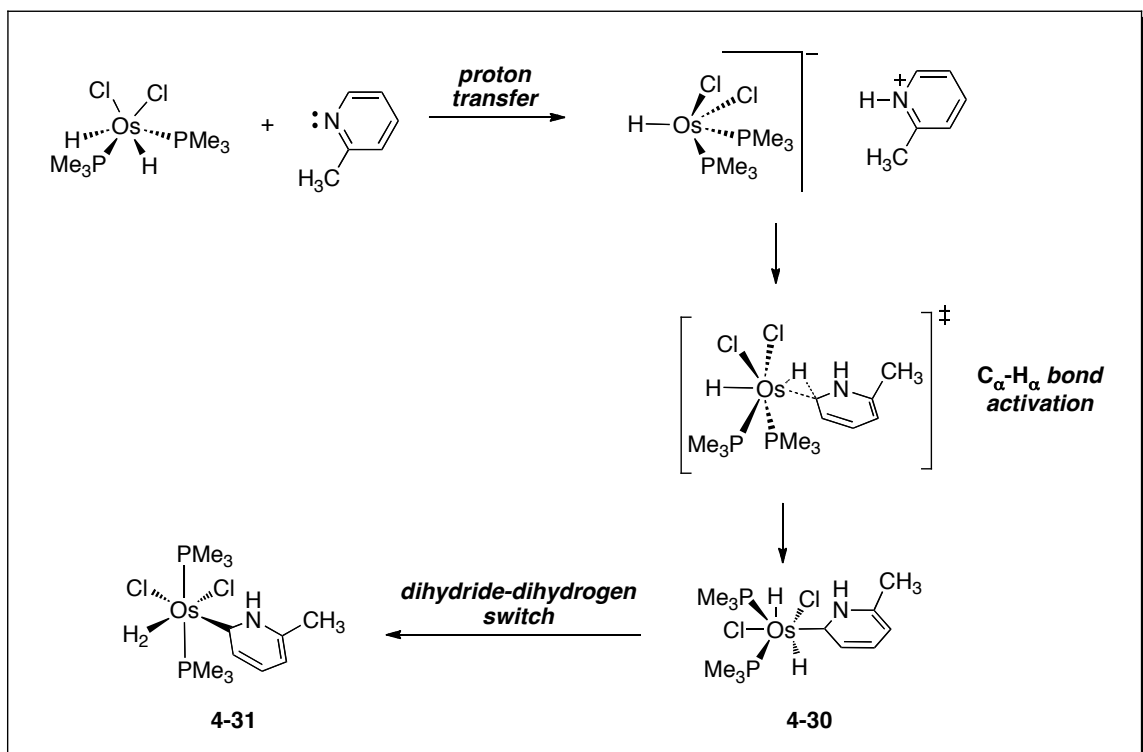
The equilibrium process was also studied by DFT calculations, which, in addition to revealing a 1,3-hydrogen shift mechanism analogous to the one reported by Bergman and Ellman, also resulted in a proposed mechanism in which the hydrogen shift was assisted by the presence of a water molecule (Scheme 4-14). This water-assisted pathway involves a six-membered metallocyclic transition state as compared to the four-membered transition state of the unassisted pathway, and as a result has a lower overall reaction barrier (ΔG^\ddagger). Experimental studies showed a strong kinetic dependence on the water concentration in the reaction mixture, corroborating the theoretical study and indicating the probable involvement of the water-assisted mechanism in this system.



Scheme 4-14: Calculated transition states for the tautomerization of 4-28, and their ΔG^\ddagger .³²

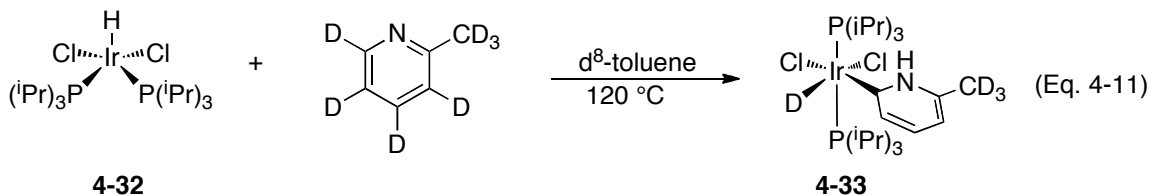
The mechanism of NH-tautomerization of 2-methylpyridine and quinoline upon addition to osmium dihydride complex $[\text{Cl}_2\text{Os}(\text{H})_2(\text{PMe}_3)_2]$ was studied using DFT

calculations (Scheme 4-15), revealing a common mechanism for the two related aromatic heterocycles.⁴⁴ In the initial step with 2-methylpyridine, although coordination of the aromatic nitrogen to osmium was determined to be an exergonic process (-3.2 kcal/mol) the ensuing hydride transfer from osmium to nitrogen was extremely endergonic (+45.7 kcal/mol). Instead a more favorable process initiating through hydrogen transfer from osmium to nitrogen was revealed. This cation-anion pair then undergoes C-H bond activation to give the Os(protic-NHC) intermediate **4-30**, followed by a dihydride-dihydrogen tautomerization to give product **4-31**. The calculated reaction pathway was analogous on moving from 2-methylpyridine to quinoline, however, C-H activation for quinoline is shown to be a more facile process due to the capacity of the extended aromatic system to stabilize intermediates involved in this process.

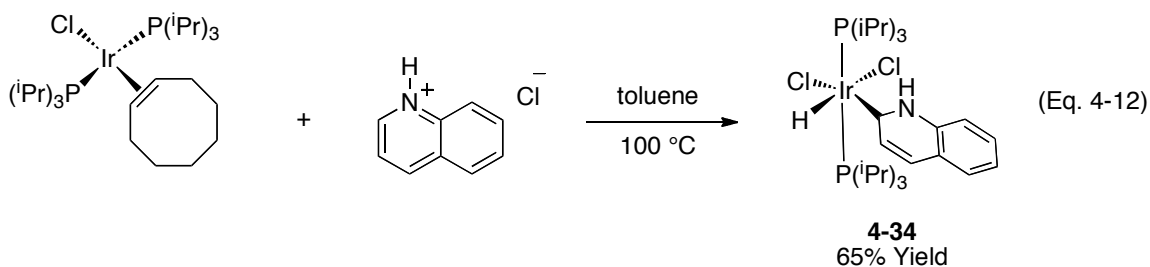


Scheme 4-15: DFT calculated mechanism for the NH-tautomerization of 2-methylpyridine in the presence of $[\text{Cl}_2\text{Os}(\text{H})_2(\text{PMe}_3)_2]$.⁴⁴

Esteruelas et al. also carried out experimental studies to gain evidence for the proposals made in the DFT study. Reaction of dideuterated complex $[\text{Cl}_2\text{Os}(\text{D})_2(\text{P}^i\text{Pr}_3)_2]$ with 2-methylpyridine and quinoline gave the expected complexes but with significant loss of deuterium at osmium, indicating involvement of the metal in tautomerization. A similar reaction between perdeuterated 2-methylpyridine and $[\text{Cl}_2\text{IrH}(\text{P}^i\text{Pr}_3)_2]$ (**4-32**) showed incorporation of deuterium at iridium in product **4-33**, further justifying the proposed metal-mediated C-H activation (Eq. 4-11).⁴⁵ Furthermore, in all the isolated Ir(protic-NHC) complexes of this study, the carbene was positioned *cis* to the hydride ligand, likely a consequence of the mechanism of NC-H bond activation of the protonated heterocycle.



In this study, the mechanism of the proposed activation of the heterocycle by hydrogen transfer to nitrogen from the metal was also probed. During the hydrogen transfer from **4-32** to quinoline, the abstraction of the metal-hydride as a proton would result in reduction of the metal center and formation of an iridium(I)-quinolinium counter-ion pair. Reaction of iridium(I) complex, $[\text{ClIr}(\text{coe})(\text{P}^i\text{Pr}_3)_2]$, with quinoline does not give the desired NH-tautomerization product, likely due to its lack of a hydride ligand. Reaction of the same iridium complex with quinolinium chloride, however, gave **4-34** in 65% yield; the same product obtained with iridium(III)-hydride **4-32** (Eq. 4-12), consistent with the mechanism proposed in Scheme 4-15.



Thus, it is obvious that M(protic-NHC) complexes represent a unique sub-section of the now ubiquitous M(NHC) complexes present in the literature. Although they are a very recent development in the field, there already exist a considerable number of examples synthesized utilizing a number of different methods. The serendipitous discovery of the involvement of M(protic-NHC)s as the active species in the catalytic coupling of N-heterocycles and alkenes by Bergman and Ellman, as well as some initial reports on the stoichiometric reactivity of M(protic-NHC) complexes points towards their strong potential as bifunctional catalysts in organic transformations. With the development of new and generally applicable synthetic strategies for the formation of M(protic-NHC) complexes aided by the initial mechanistic investigations described above, this relatively new field will surely flourish in the near future.

4.2 Results & Discussion

4.2.1 Attempted Synthesis of [Cl₂Ru(diphosphine)(protic-NHC)₂] Complexes

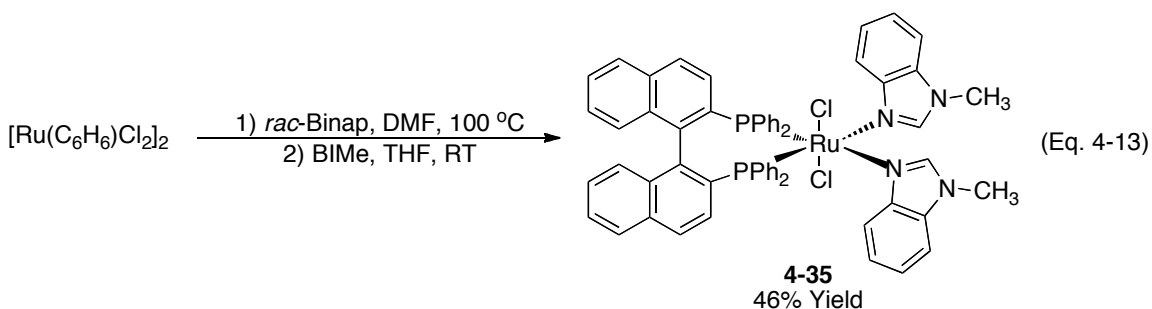
Our catalyst design focused on direct analogues of Noyori's Ru(diphosphine)(diamine) catalysts, with replacement of the diamine ligand by two monodentate protic-NHCs. Previous reports have demonstrated both the truly protic nature of M(protic-NHC) complexes,³⁵ as well as their bifunctional behaviour.⁴⁶ We believed this proved the great potential of this ligand class for affecting chemoselective

hydrogenation of simple aromatic ketones via a bifunctional mechanism analogous to the Noyori system. In addition, this would provide one of the first examples of a protic-NHC as a participatory ligand in a transition metal catalyzed reaction. Employing two protic-NHC ligands per ruthenium would generate an octahedral coordination environment and the chemoselective reduction of carbonyls over alkenes should be achieved by promoting an outer-sphere reduction mechanism.

Initial attempts at preparing the desired catalyst focused on trying to access the 2-ylidene tautomer of 1-methylbenzimidazole (BIMe) through heating. Inputting heat to overcome the thermodynamic barrier to tautomerization should allow complexation of the metal to the carbene, however, as postulated by Crabtree and Eisenstein, the major product of such a reaction would be dictated by the relative stability of the M-N *versus* the M-C bond.²⁸

Thus, a solution of $[\text{Cl}_2\text{Ru}(\textit{rac}\text{-Binap})]$ and 2.2 equivalents of BIMe were heated in THF for 16 hours at various temperatures from 20 to 100 °C. All reactions regardless of temperature gave the same ^{31}P NMR spectra. On a preparatory scale, $[\text{Cl}_2\text{Ru}(\textit{rac}\text{-Binap})]$ was reacted overnight with two equivalents of methylbenzimidazole (BIMe) to give $[\text{Cl}_2\text{Ru}(\textit{rac}\text{-Binap})(\text{BIMe})_2]$ (**4-35**) in 46% yield after recrystallization (Eq. 4-13). ^{31}P NMR of a pure sample of the orange solid in C_6D_6 showed signals attributable to a mixture of three different diastereomeric conformers: two singlets (one sharp and one broad) and a pair of doublets. The two conformers represented in the ^{31}P NMR by singlets stem from two C_2 -symmetric systems in which the phosphorous atoms of the Binap ligand are magnetically equivalent. The other conformer is characterized by a pair of doublets in the ^{31}P NMR, indicating that the two phosphorous atoms of the Binap

ligand are inequivalent in this conformer. Integration of the signals in the ^1H NMR attributable to the Binap ligand *versus* coordinated methylbenzimidazole indicates that two benzimidazoles are bound to a single ruthenium center, resulting in coordinatively saturated and octahedral complexes. Interestingly, addition of a single equivalent of methyl benzimidazole results only in the formation of complex **4-35** and $[\text{Cl}_2\text{Ru}(\text{rac-Binap})]$; no other species could be detected by ^{31}P NMR, illustrating the strong preference in this system for coordinative saturation.



Once bound to Ru, the benzimidazole ligands can exist in two possible conformations: *syn* and *anti* relative to each other with the *N1* methyl substituents on the same or opposite sides of the plane defined by P-Ru-P, respectively. In addition, the presence of the C_2 symmetric Binap ligand further differentiates these planes into two inequivalent quadrants, allowing for two possible *anti* conformations, both of which have overall C_2 symmetry (Figure 4-1). Based on the ^{31}P NMR spectra, **4-35** appears to exist as a mixture of all three of these conformations. Analysis of a related compound by X-ray crystallography confirms this hypothesis (*vide infra*), however, it also showed the benzimidazoles to be bound to metal through the aromatic nitrogen (Eq. 4-13).

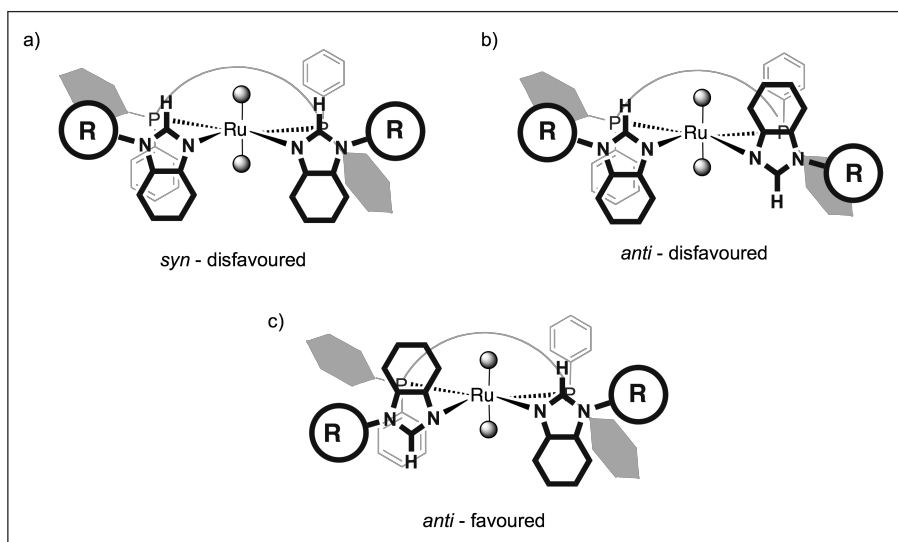


Figure 4-1: Possible conformations of **4-35** and related complexes.

Since the protic-NHC appeared to be inaccessible through heating the benzimidazole in the presence of $[\text{Cl}_2\text{Ru}((rac)\text{-Binap})]$, we next sought to catalyze this interconversion through the use of base. Heating a THF solution of $[\text{Cl}_2\text{Ru}((rac)\text{-Binap})]$ and 2.2 equiv of benzimidazole to reflux in the presence of 10 mol% KO^tBu again gave $[\text{Cl}_2\text{Ru}(rac\text{-Binap})(\text{BIME})_2]$ as the only observable product by ^{31}P NMR. An analogous procedure was attempted with catalytic amounts of NH_4Cl , yielding similar results. These attempts seem to suggest that the *N*-bound tautomer is favoured thermodynamically, and our next attempts focused on trying to trap the *C*-bound tautomer kinetically.

Ruiz et al., recently reported the clean conversion of a manganese(I) imidazole complex to its protic-NHC derivative via a base-promoted tautomerization.³⁶ Treatment of $fac\text{-}[\text{Mn}(\text{L})(\text{CO})(\text{bipy})]^+$ with a stoichiometric amount of KO^tBu gave complete $\text{C}2$ deprotonation of the imidazoles as observed by IR. Protonation of these intermediates with NH_4PF_6 yielded the corresponding *C*-bound tautomer believed to result from a

preferred C-bound *versus* N-bound imidazolate, with the more electronegative nitrogen forming the more thermodynamically favourable anion; trapping of this intermediate by protonation gives the protic-NHC compound (Scheme 4-5).

In this vein, similar deprotonation/protonation strategies were attempted with $[\text{Cl}_2\text{Ru}(\text{rac-Binap})(\text{BIME})_2]$. Thus, $[\text{Cl}_2\text{Ru}(\text{Binap})]$ and 2 equiv of BIME were stirred in THF for 20 min, allowing *in situ* formation of **4-35**, followed by addition of excess KO^tBu or NaH. Again monitoring by ^{31}P NMR, the deprotonation reaction was considered complete once **4-35** had been consumed; the disappearance of this complex appeared concomitant with the formation of a new complex as the major product, represented by a pair of doublets at 40.1 and 49.4 ppm. While deprotonation appeared successful, protonation of the observed intermediate (with NH_4Cl , $\text{HCl}/\text{Et}_2\text{O}$ or TsOH) resulted only in the formation of complex **4-35**. Similar results were obtained when deprotonation of the benzimidazole was performed prior to addition of $[\text{Cl}_2\text{Ru}(\text{Binap})]$. It is worth noting that inadvertent addition of excess HCl in the final step resulted in the formation of an anionic chloride bridged Ru(diphosphine) dimer with a protonated benzimidazolium counterion $\text{HBI}^t\text{Bu}^+[(\mu\text{-Cl}_3)\{\text{ClRu}(\text{Binap})\}_2]^-$ (**4-36**), whose structure was determined by X-ray crystallography (Figure 4-2).

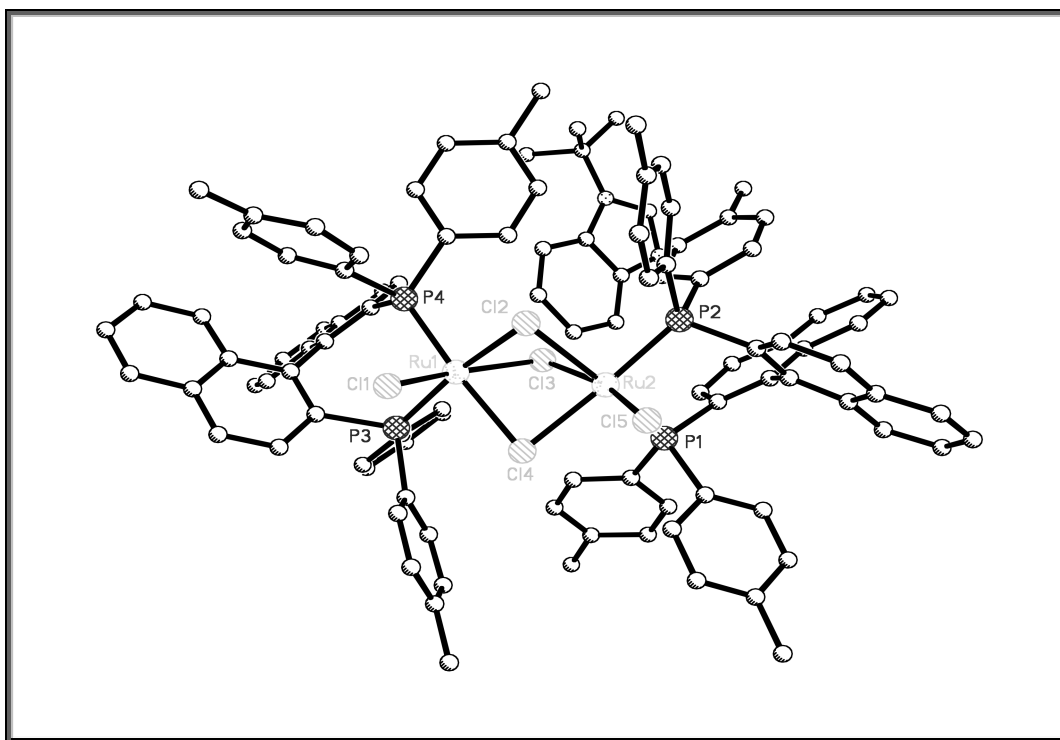


Figure 4-2: Crystallographically determined structure of **4-36**, displaying thermal ellipsoids drawn at the 50% confidence level. Selected interatomic distances (Å) and angles (deg): Ru(1)-P(4), 2.2632(9); Ru(1)-Cl(1), 2.3777(9); Ru(1)-Cl(4), 2.5085(8); Ru(2)-P(2), 2.2740(9); Ru(2)-Cl(5), 2.4044; Ru(2)-Cl(4), 2.4432; P(4)-Ru(1)-P(3), 93.70(3); P(1)-Ru(2)-P(2), 92.15(3); P(4)-Ru(1)-Cl(4), 175.56; P(2)-Ru(2)-Cl(4), 170.64(3).

Based on the above experiments, it appears that $[\text{Cl}_2\text{Ru}(\text{diphosphine})(\text{benzimidazole})_2]$ systems strongly favour the *N*-bound tautomer. Ruthenium complexes featuring protic-NHCs have been reported, so this does not appear to be an effect directly attributable to the metal itself, however, given the very specific design we required, the failure of this reaction may be a result of the other ancillary ligands and their respective positioning. Considering specifically octahedral late transition metal complexes of non-chelating protic-NHCs, *in all instances the protic-NHC is positioned trans to ligands of low trans-effect* (e.g. chloride or carbon monoxide, but not phosphine). The most favourable conformation of $[\text{Cl}_2\text{Ru}(\text{diphosphine})(\text{L})_2]$ complexes appears to be one in

which the chloro ligands are positioned *trans* to one another, thus, necessarily positioning the other two non-phosphines ligands *cis* to one another. The propensity for the benzimidazole ligands to remain bound by nitrogen may therefore be a result of its position *trans* to phosphorous, which has a higher trans-effect relative to chloride.

4.2.2 Different Approach to Bifunctional Catalysis Without Amines

While attempts to make analogues of Noyori's bifunctional hydrogenation catalyst featuring protic-NHCs were largely unsuccessful, the isolation of a well-defined ruthenium complex featuring 1-substituted benzimidazoles had been achieved and thus we set out to determine whether these complexes could be effective catalysts for the hydrogenation of carbonyl compounds. The mechanistic studies by Bergens on Noyori's bifunctional catalyst noted that direct transfer of a proton from the diamine ligand was not simultaneous with insertion of the carbonyl into the ruthenium hydride (Section 4.1.1, Scheme 4-3). The implication of this is that ligands featuring Brønsted acids are not required by Noyori-type hydrogenation catalysts to affect reduction and that replacement of the diamine with another ligand featuring a Lewis acidic functionality capable of activating the C-O π -bond could be successful. On this basis, we predicted that our newly synthesized benzimidazole substituted ruthenium complex might be capable of catalyzing the chemoselective hydrogenation of carbonyl compounds.

It is well known from *N*-heterocyclic carbene chemistry that the C2 position of *N,N'*-disubstituted imidazolium⁶⁴ and benzimidazolium⁶⁵ salts are sufficiently acidic to be deprotonated by relatively mild alkoxide bases (Figure 4-3). In analogy with benzimidazolium cations, coordination of the basic nitrogen of 1-substituted benzimidazoles results in polarization of the C2-H bond in a manner similar to alkylation

at this position. Furthermore, in studies of ionic liquids, α -values of Kamlet-Taft parameters for imidazoliums have been determined and these solvents are about as protic as *tert*-butanol (0.627⁶⁶ versus 0.68,⁶⁷ respectively). A recent example in the literature has also shown that imidazolium-based ionic liquids are capable of acting as protic catalysts in the BOC protection of phenols.⁶⁸ Catalytic studies were therefore undertaken in light of the inability to isolate a protic-NHC compound, postulating that polarization of the C-H bond of benzimidazole upon binding to ruthenium might furnish a Lewis acid capable of activating the C-O bond of the ketone towards reduction.

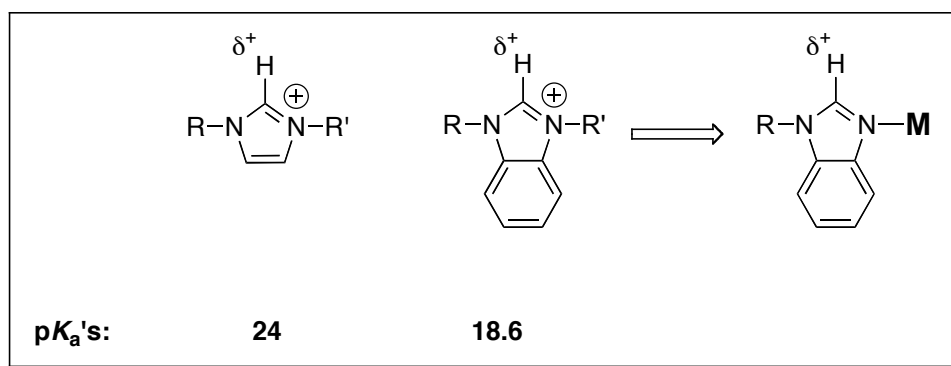


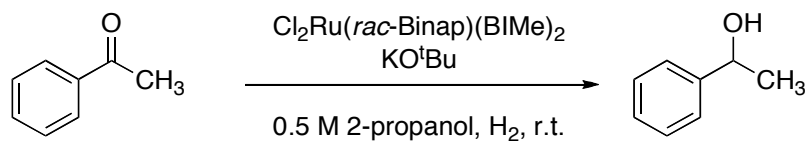
Figure 4-3: Relative acidities of imidazolium and benzimidazolium cations in DMSO and representative polarization of the C2-H bond by coordination of benzimidazole to a metal.^{64,65}

4.2.3 Catalytic Studies

In order to test the catalytic activity of our initially prepared benzimidazole-containing Ru complex, acetophenone was exposed to catalyst **4-35** in basic 2-propanol at room temperature. The reduction of acetophenone was complete in 3 h under mild conditions (100:10:1 substrate/KO^tBu/Ru, 0.5 M in 2-propanol, 20 °C, 10 atm H₂). This is in stark contrast to [Cl₂Ru(Binap)] itself, which gives no detectable product under

identical conditions, without the addition of a diamine or benzimidazole. To further test the ability of **4-35** as a hydrogenation catalyst, its loading was decreased to 0.1 mol% and the pressure of hydrogen gas in the reactions reduced. The turnover frequency was greatly reduced upon lowering the pressure of hydrogen from 5 to 1 atm (Table 4-1, entries 2 and 3), and very little conversion was observed (< 10% after 16 h) when the reaction was performed under an atmosphere of argon.

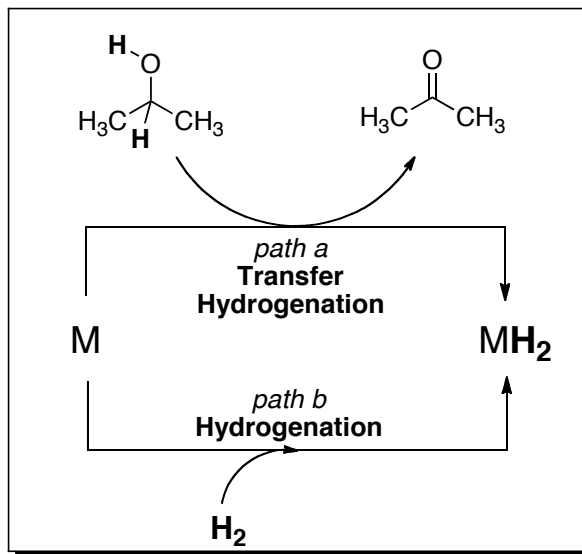
Table 4-1: Catalytic results in the hydrogenation of acetophenone with $[\text{Cl}_2\text{Ru}(\text{rac}\text{-Binap})(\text{BIME})_2]$ (**4-35**).



Entry	Amt of Ru (mol %)	Amt of KO ^t Bu (mol %)	Time (h)	H ₂ (atm)	% Yield ^a
1	1	10	3	10	> 98
2	0.1	1	3	5	50
3	0.1	1	3	1	14
4	0.1	1	16	0	9

^aYields determined by ¹H NMR with an internal standard (1,4-dimethoxybenzene).

The dependence of the reaction rate on hydrogen pressure suggests that the primary mechanism of ketone reduction is hydrogenation and not transfer hydrogenation as might be expected from the use of a solvent like 2-propanol. In the latter case hydrogen gas would not be required, and the metal-hydride would be regenerated by oxidation of the solvent to acetone (Scheme 4-16).



Scheme 4-16: Possible mechanisms for regeneration of MH_2 during hydrogenation in 2-propanol.

On the basis of our initial hypothesis, after formation of a ruthenium hydride coordination of the carbonyl oxygen to the C2-H of one of the benzimidazoles may occur, orientating and activating the carbonyl towards insertion forming a ruthenium alkoxide. Unlike Noyori's catalysts, however, deprotonation of the assisting ligand (in our case the benzimidazole, in Noyori's the diamine) likely does not occur, and release of the product molecule is instead accomplished via the protic solvent. It is also possible that these complexes function by an alternative mechanism of hydrogenation, since there have been other reports of hydrogenations by Ru(diphosphine) complexes without protic amine ligands.⁶⁹ Bergens has previously demonstrated that Ru(diphosphine) catalysts modified with pyridyl ligands instead of protic diamines are capable of hydrogenating ketones with enantioselectivities up to 49% *ee*.⁶⁹

Although complex **4-35** obviously displayed the desired catalytic activity, the presence of multiple conformations did not bode well for eventual enantio-

discrimination. In fact, C_2 -symmetric metal-BINAP complexes are known to react with high enantioselectivity in a variety of processes since the number of possible diastereomeric transition states is reduced by a factor of two. In the case of Binap-derived and related ligands, the remaining binding sites on the metal are differentiated into pairs of sterically hindered and open quadrants by the edge-on and face-on phenyl groups of the chelating diphosphine.⁷⁰ Thus, it was hypothesized that if a large substituent was employed on the benzimidazole, steric interactions between this group and the phenyl substituents of BINAP might enforce only one binding mode of the benzimidazole, resulting in a compound with overall C_2 -symmetry (Figure 4-1c). If steric congestion in the quadrant is not great enough, the two substituents can face the same way (Figure 4-1, *syn* conformation a) or even adopt an *anti* conformation with the substituents of both benzimidazoles in unfavourable quadrants (Figure 4-1b). As mentioned above, this is believed to be the case for 1-methylbenzimidazole substituted compound **4-35**, whose ^{31}P NMR spectrum is consistent with a near equal mixture of all possible conformations. Based on this hypothesis, complexes with larger substituents at this position were prepared.

Thus, $[\text{Cl}_2\text{Ru}((R)\text{-TolBinap})]$ was reacted with a number of different benzimidazoles substituted at *N1* with alkyl groups of increasing size (BIR: where R = Me, Et, Ph, Bz, and CPh₃) and the resulting solids analyzed by ^{31}P NMR in C_6D_6 . Compound **4-37a** (R = Me) yielded a ^{31}P NMR spectrum nearly identical to its racemic counterpart **4-35**, again consisting of a mixture of diastereomers (*vide supra*). Increasing the size of the substituent at *N1* on the benzimidazole had little effect on the distribution of the mixture of diastereomers for compounds BI_{Et}, BI_{Ph}, BI_{Bz} or BI^tBu as observed

by ^{31}P NMR, however, **4-37b** ($\text{R} = \text{CPh}_3$) exhibits only a single resonance in the ^{31}P NMR with no evidence of any other diastereomer. This indicates that the very large R-substituent at *N1* has induced only the favourable C_2 -symmetric conformation in which the R substituents on the two *cis* benzimidazoles are oriented anti to one another. The ^1H NMR spectra are also consistent with the existence of a single species in solution. A similar synthesis was performed with $[\text{Cl}_2\text{Ru}((R)\text{-XylBinap})]$ to prepare $[\text{Cl}_2\text{Ru}((R)\text{-Xylbinap})(\text{BIME})_2]$ (**4-38a**) and $[\text{Cl}_2\text{Ru}((R)\text{-XylBinap})(\text{BICPh}_3)_2]$ (**4-38b**) in 23 and 28% yields, respectively, after recrystallization. Apart from the additional methyl signals attributable to the xylyl groups, the spectra were analogous to those of the TolBinap-based complexes. The ^{31}P NMR spectra of $[\text{Cl}_2\text{Ru}(\text{XylBinap})]$ after reaction with two equivalents of BIME (**4-38a**) and BICPh_3 (**4-38b**) are shown in Figure 4-4.

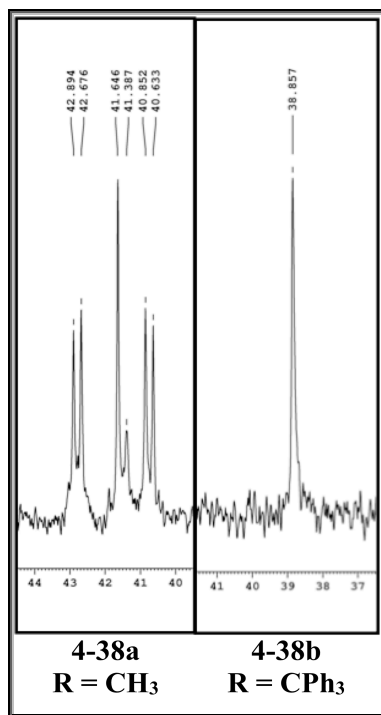


Figure 4-4: Relevant areas of the ^{31}P spectra of compounds **4-38a** and **4-38b**.

X-ray quality crystals of **4-38a** were obtained by slow diffusion of hexanes into a dichloromethane solution of **4-38a**, confirming the overall connectivity of the complex. The solid-state structure is a distorted octahedron about Ru, with the two benzimidazoles bound through the aromatic nitrogen and positioned *cis* to one another, while the chlorines are situated *trans*. Consistent with our interpretation of the NMR spectra of this and related compounds, the crystal is a statistical mixture of three conformational diastereomers, one *syn* and two *anti*. The two *anti* conformations are non-identical C_2 symmetric structures. The benzimidazoles are canted slightly and appear nearly parallel to the axial xylyl rings of the XylBinap ligand, possibly as a result of π -stacking between the two aromatic groups. Two of the possible conformers are displayed in Figure 4-5 and the crystallographic data of **4-38a**, as well as **4-36**, is presented in Table 4-2.

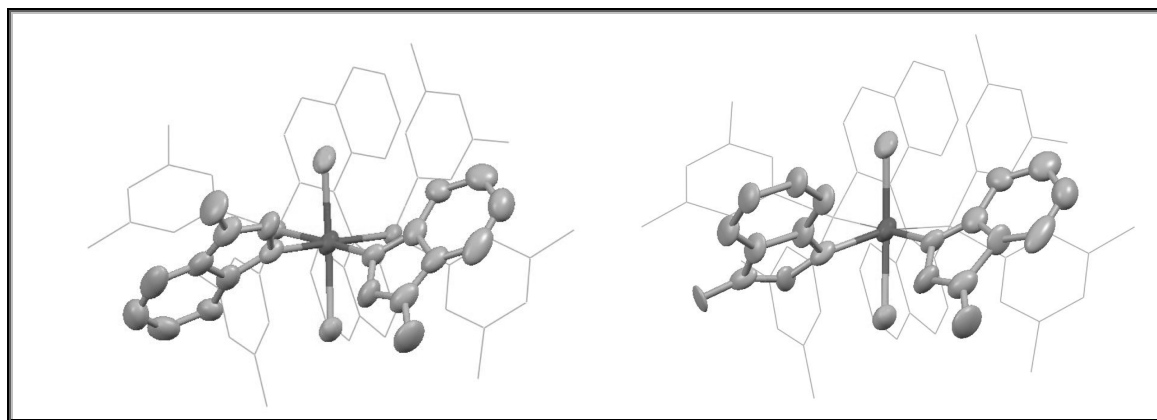


Figure 4-5: Crystallographically determined structure of **4-38a** with selected atoms displayed as ellipsoids at the 50 % confidence level. Hydrogen atoms have been omitted for clarity. Two of the three different diastereomeric conformations present in the unit cell are shown below. Selected interatomic distances (Å) and angles (deg) are: Ru(1)-N(1A), 2.187(6); Ru(1)-N(1B), 2.20(2); Ru(1)-P(1), 2.3042(11); Ru(1)-Cl(1), 2.4206(12); N(1A)-Ru(1)-N(1A)#1, 81.9(3); N(1B)-Ru(1)-N(1B)#1, 104.3(10); N(1B)-Ru(1)-(N1A)#1, 91.5(5); N(1A)#1-Ru(1)-P(1), 94.28(14); N(1B)#1-Ru(1)-P(1), 84.8(5); N(1A)-Ru(1)-P(1)#1, 94.28(14); P(1)-Ru(1)-P(1)#1, 89.52(5); Cl(1)-Ru(1)-Cl(1)#1, 166.76(6).

Table 4-2: Crystallographic information for compounds **4-36** and **4-38a**.

	4-36	4-38a
Formula	C ₁₀₇ H ₉₅ N ₂ P ₄ Ru•3.25CH ₂ Cl ₂	C ₆₈ H ₆₄ Cl ₂ N ₄ P ₂ Ru•C ₄ H ₈ O
Fw	2188.13	1243.25
Color/habit	orange/block-shaped	orange/prism shaped
Cryst dimens (mm ³)	0.35 x 0.20 x 0.18	0.25 x 0.16 x 0.08
Cryst syst	monoclinic	orthorhombic
space group	<i>P</i> 2(1)	<i>C</i> 222(1)
<i>a</i> (Å)	13.9377(6)	12.5121(16)
<i>b</i> (Å)	23.5407(10)	22.639(3)
<i>c</i> (Å)	17.4111(7)	21.746(3)
β (deg)	108.2030(10)	90
<i>V</i> (Å ³)	5426.8(4)	6162.6(13)
<i>Z</i>	2	4
D _{calcd} (Mg/m ³)	1.339	1.34
μ (mm ⁻¹)	Multi-scan	0.441
<i>F</i> (000)	2241	2592
θ range (deg)	1.76 - 26.00	1.80 - 25.99
index ranges (<i>h,k,l</i>)	-16-17, -29-27, ±21	±15, ±27, ±26
no. of rflns collected	29532	30803
no. of indep rflns/ <i>R</i> _{int}	19575/0.0184	6045/0.0783
no. of data/restraints/parameters	19575/11/1243	6045/12/436
<i>R</i> ₁ / <i>wR</i> ₂ (<i>I</i> > 2σ(<i>I</i>)) ^a	0.0340/0.0950	0.0446/0.0898
<i>R</i> ₁ / <i>wR</i> ₂ (all data) ^a	0.0366/0.0975	0.0671/0.1000
GOF (on <i>F</i> ²) ^a	1.054	1.022
largest diff peak/hole (e.Å ⁻³)	0.925/-0.398	0.653/-0.692

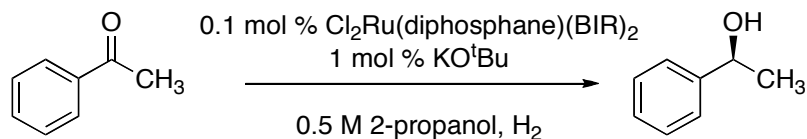
$${}^a R_1 = \frac{\sum | |F_o| - |F_c| |}{\sum |F_o|}; \quad wR_2 = \frac{(\sum [w(F_o^2 - F_c^2)^2])^{1/2}}{(\sum [w(F_o^2)])^{1/2}}; \quad \text{GOF} = \frac{(\sum [w(F_o^2 - F_c^2)^2])^{1/2}}{(n - p)^{1/2}}$$

The catalytic activity of these new complexes, synthesized from axially chiral, enantiomerically pure diphosphine ligands, was then tested in the hydrogenation of acetophenone under our standard conditions (1000:10:1 ketone/KO^tBu/Ru, 0.5 M in 2-propanol, 5 atm H₂, 20 °C) (Table 4-3). The methylbenzimidazole-modified catalyst (**4-37a**) gave the *S* enantiomer of the product alcohol in 27% *ee* (Table 4-3, entry 2). Increasing the size of the group on the benzimidazole from methyl to ethyl and eventually

phenyl and benzyl, resulted in only modest increases in the observed enantioselectivity, which is not surprising, as each of these structures exist in multiple conformations as demonstrated by their ^{31}P NMR spectra. As expected, however, a large increase in enantioselectivity was observed for the catalyst substituted with two equivalents of 1-(triphenylmethyl)benzimidazole (**4-37b**), which gave sec-phenethanol in 67% *ee* (Table 4-3, entry 3). Thus it appears that the presence of only one diastereomeric form in solution does lead to a more enantioselective catalyst. By decreasing the temperature of the reaction to 273 K, and increasing the pressure of hydrogen gas pressure to 20 atm, a slight increase to 71% *ee* was achieved (Table 4-3, entry 6). The use of the slightly bulkier (*R*)-XylBinap as the chiral diphosphine, gave marginal increases in enantioselectivity relative to the (*R*)-TolBinap catalysts.

Interestingly, the hydrogenation of acetophenone with **4-37b** does proceed under a nitrogen atmosphere (i.e. in the absence of hydrogen gas), however, at a significantly diminished rate. If the reaction is performed with 5 atm H_2 it reaches completion in 6 h, however under a nitrogen atmosphere, only 7% yield is achieved after 6 h and only 60 % after 72 h, demonstrating the extremely slow yet viable transfer hydrogenation pathway. The presence of base in the catalytic reaction is also essential; in its absence no conversion is observed. In studies of Noyori's catalyst the presence of base was deemed essential for activation of the Cl_2Ru pre-catalyst to the active $(\text{H})_2\text{Ru}$ catalyst, which may serve as some evidence that the mechanism of the two reactions is similar.

Table 4-3: Hydrogenation of acetophenone with [Cl₂Ru(diphosphine)] precatalysts bis-substituted with different benzimidazoles.^a



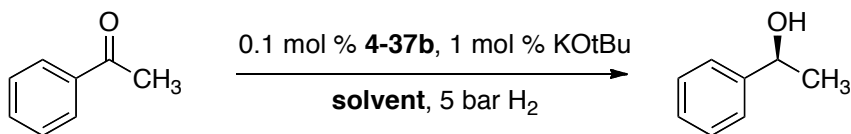
Entry	Catalyst	Amt of H ₂ (atm)	Temp (°C)	TOF (h ⁻¹) ^b	ee (%) ^c
1	[Cl ₂ Ru((<i>R</i>)-TolBinap)]	5	20	NR ^d	ND ^e
2	4-37a	5	20	320	27
3	4-37b	5	20	162	67
4	4-38a	5	20	293	34
5	4-38b	5	20	210	72
6	4-37b	20	0	67	71

^aReaction conditions: 1000:10:1 ketone/KO^tBu/Ru, 0.5 M in 2-propanol, H₂ gas. All catalytic runs were performed in duplicate and are reported as mean values (± 2%).

^bTurn-over frequencies determined at low conversion (t_R = 1.5 h) by ¹H NMR. ^c% ee was determined using super-critical fluid chromatography. ^dNo reaction was observed after 1.5 h. ^e% ee not determined.

Using catalyst **4-37b**, we then examined the effect of solvent on the reaction (Table 4-4). Neither CH₂Cl₂ nor THF gave any reaction, but aromatic solvents such as benzene and toluene were effective, giving comparable enantioselectivity. Interestingly, the use of *tert*-butanol as the solvent gave a much less reactive system than 2-propanol under the same conditions (entries 6 and 7, Table 4-4, the reaction was performed at 30 °C instead of 20 °C; mp(*tert*-butanol): 25 °C). Given the slow rate of background transfer hydrogenation operative in this system this is quite surprising, but could be attributable to the larger size of *tert*-butanol making approach into the coordination sphere of the metal to protonate and release a possible ruthenium-alkoxide intermediate more difficult. The hydrogenation activity observed in benzene and toluene, which are aprotic, may be a result of trace water in these solvents.

Table 4-4: Optimization of the solvent in hydrogenation of acetophenone by catalyst **4-37b**.^a



Entry	Solvent	TOF (h ⁻¹) ^b	ee (%)
1	2-propanol	162	67
2	THF	NR ^c	ND
3	CH ₂ Cl ₂	NR ^c	ND
4	benzene	40	70 ^d
5	toluene	80	58
6 ^e	<i>tert</i> -butanol	88	31
7 ^e	2-propanol	282	30

^aReaction conditions: 1000:10:1 ketone/KO^tBu/Ru, [substrate] = 0.5 M, 5 atm H₂, 20 °C. ^bTurnover frequencies determined at low conversion (t_R = 1.5 h) by ¹H NMR. ^c%ee was determined using super-critical fluid chromatography. ^dCatalyst **4-38b** used instead of **4-37b**. ^eT = 30 °C

Having chosen 2-propanol as our optimal solvent and encouraged by the moderate enantioselectivities achieved with this catalyst system, we next examined the effect of different chiral diphosphines on the catalyst precursor. In the recent literature, a number of atropisomeric chiral diphosphines have been reported which have shown exceptional results when employed as ligands in asymmetric hydrogenations.⁷¹ A number of these diphosphines were chosen (Figure 4-6), and, using a similar procedure for **4-37b**, the analogous ruthenium precatalysts were prepared (**4-39** – **4-43**) in moderate to good yields after recrystallization from THF/hexanes solutions (Scheme 4-17).

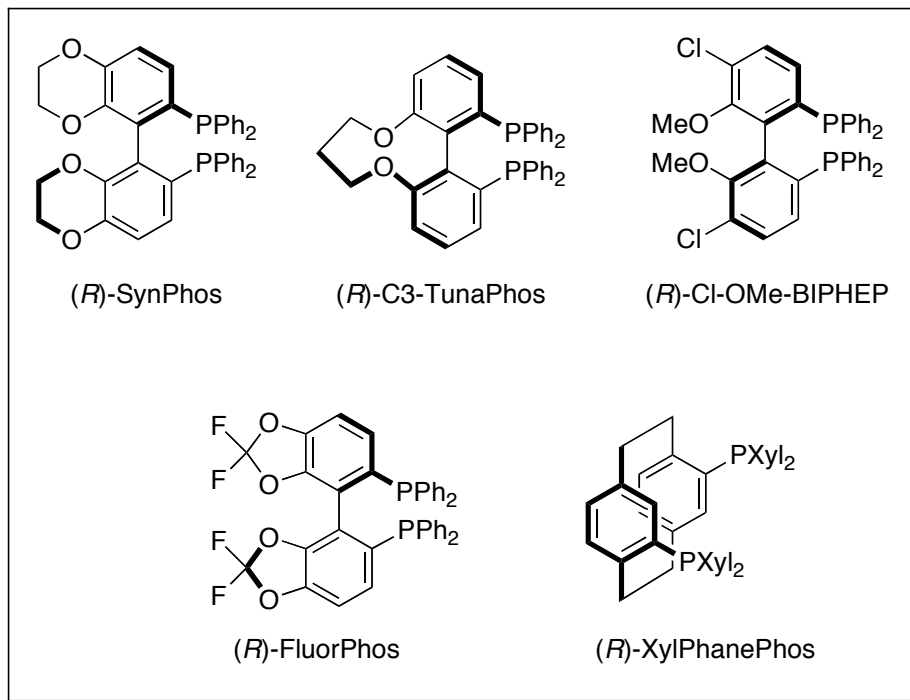
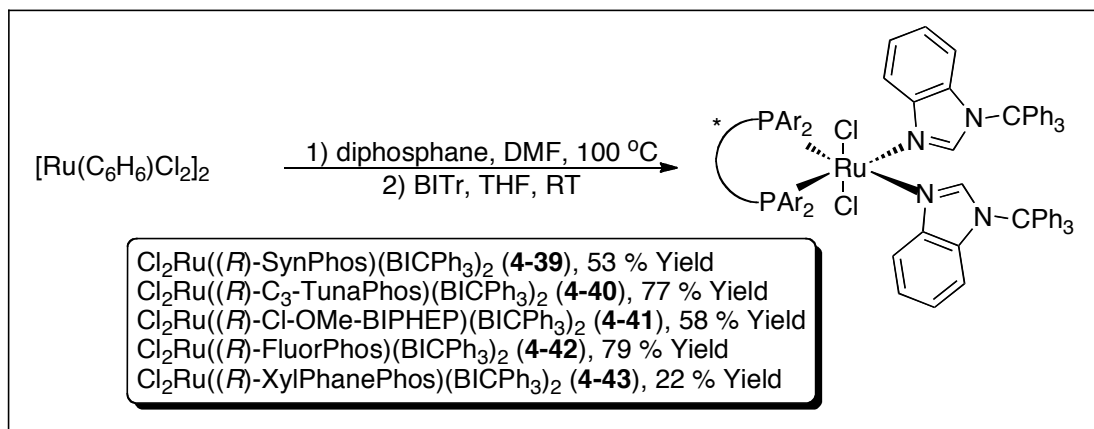


Figure 4-6: Chiral atropisomeric diphosphine ligands used in this study.⁷¹

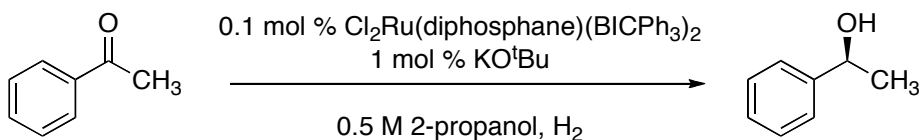


Scheme 4-17: Synthesis of BITr modified Ru(diphosphine) precatalysts.

While all of these new ruthenium species were able to efficiently hydrogenate acetophenone under our standard conditions, giving quantitative conversion in less than 6 h, none of them gave better enantioselectivity than the BINAP-based catalysts **4-37b** and

4-38b (Table 4-5). Interestingly catalyst **4-43**, prepared using (*R*)-XylPhanePhos, gives a nearly racemic product mixture, with a slight excess of the opposite enantiomer (Table 4-5, entry 7); this is consistent with previous reports in which (*R*)-PhanePhos matches with (*S,S*)-dpen (the opposite match to (*R*)-Binap) to give the *R* enantiomer.³⁵

Table 4-5: Turnover frequencies and enantioselectivities of 1-(triphenylmethyl)-benzimidazole-modified ruthenium-diphosphine precatalysts.^a



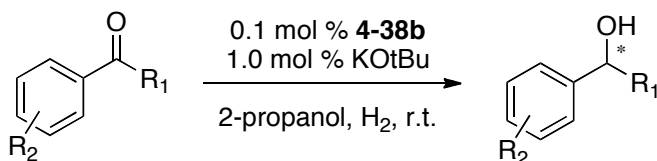
Entry	Diphosphine	TOF (h ⁻¹) ^b	ee (%) ^c
1	(<i>R</i>)-TolBinap (4-37b)	162	67
2	(<i>R</i>)-XylBinap (4-38b)	210	72
3	(<i>R</i>)-SynPhos (4-39)	302	57
4	(<i>R</i>)-C ₃ -TunaPhos (4-40)	337	59
5	(<i>R</i>)-Cl-OMe-BIPHEP (4-41)	261	4
6	(<i>R</i>)-FluorPhos (4-42)	388	65
7	(<i>R</i>)-PhanePhos (4-43)	306	-8

^aReaction conditions: 1000:10:1 ketone/KO^tBu/Ru, 0.5 M in 2-propanol, 5 atm H₂, 20 °C. ^bTurnover frequencies determined at low conversion (t_R = 1.5 h) by ¹H NMR. ^c% ee was determined using by super-critical fluid chromatography.

With 2-propanol as the solvent, and **4-38b** as our best catalyst, the hydrogenation of a number of other aromatic ketones was examined (Table 4-6). Under these conditions, benzophenone was readily reduced (Table 4-6, entry 1) negating the possibility of the catalyst hydrogenating an enolate intermediate. While aryl-methyl ketones with mild electron withdrawing groups *p*-bromo and *p*-fluoro, or electron-donating *p*-methoxy groups were all hydrogenated at faster rates than acetophenone, *p*-nitroacetophenone (Table 4-6, entry 2) was completely unreactive under our standard conditions. Of the compounds that were reactive, the highest enantioselectivity was

observed for the methylene dioxy substrate shown in entry 6, at 70% *ee*; all others gave enantioselectivities in the 50's.

Table 4-6: Hydrogenation of various aromatic ketones with **4-38b**.^a

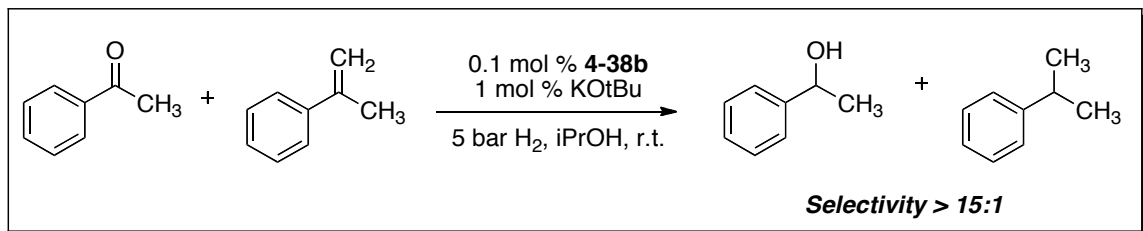


Entry	R ¹	R ²	TOF (h ⁻¹) ^b	<i>ee</i> (%) ^c
1	Ph	H	375	N/A
2	CH ₃	<i>p</i> -NO ₂	NR	ND
3	CH ₃	<i>p</i> -F	332	52
4	CH ₃	<i>p</i> -Br	286	55
5	CH ₃	<i>p</i> -OCH ₃	351	56
6 ^d	CH ₃	<i>m,p</i> -OCH ₂ O-	126	70

^aReaction conditions: 1000:10:1 ketone/KO^tBu/Ru, 0.5 M in 2-propanol, 5 atm H₂, 20 °C. ^bTurnover frequencies determined at low conversion (*t*_R = 1.5 h) by ¹H NMR. ^c%*ee* was determined using by super-critical fluid chromatography. ^dSolvent = 4:1 2-propanol/toluene.

Finally, we examined the chemoselectivity of catalyst **4-38b** under our optimized conditions for the hydrogenation of acetophenone *versus* the isoelectronic alkene α -methylstyrene (Scheme 4-18). At complete conversion of the ketone to its corresponding alcohol, only 6% yield of the corresponding styrene was detected by GC, indicating a greater than 15:1 selectivity for the carbonyl functionality under these conditions. While not nearly as selective as Noyori's diamine-modified catalyst, the observed preference for carbonyl hydrogenation is consistent with the catalyst acting similarly to those prepared with NH diamines. The decrease in selectivity relative to the Noyori catalyst may be related directly to the decreased rate of turnover of our catalyst relative to Noyori's making the alkene hydrogenation more competitive. Alternatively, dissociation of one of

the monodentate benzimidazole ligands to give an open coordination site capable of binding the alkene may also occur.



Scheme 4-18: Intermolecular competition experiment between acetophenone and α -methylstyrene.

4.3 Conclusions

A number of procedures were attempted to synthesize catalysts of the formula $[\text{Cl}_2\text{Ru}(\text{diphosphine})(\kappa\text{-C2-benzimidazole})_2]$ capable of enantio- and chemoselectively hydrogenating prochiral ketones. While these attempts were unsuccessful in forming complexes featuring NH-tautomers of the benzimidazole ligands, we were able to isolate new compounds of the formula $[\text{Cl}_2\text{Ru}(\text{diphosphine})(\kappa\text{-N3-benzimidazole})_2]$ with a variety of different chiral diphosphines and N1-substituted benzimidazoles. These complexes were characterized by ^{31}P and ^1H NMR, elemental analysis, and the connectivity verified via X-ray crystallography in the case of **4-38a**. For benzimidazoles with smaller substituents at N1 (Me, Et, etc.) the obtained complexes existed as mixtures of all three possible diastereomers. When N1 was substituted with the much larger triphenylmethyl substituent the resulting complexes existed as a single C_2 -symmetric diastereomer.

The isolated $[\text{Cl}_2\text{Ru}(\text{diphosphine})(\kappa\text{-N3-benzimidazole})_2]$ complexes proved to be efficient catalysts for the hydrogenation of simple aromatic ketones, yielding the corresponding secondary alcohols under 5 atm H_2 gas at room temperature. Employing chiral diphosphines yielded secondary alcohols with significant enantioselectivity, with the C_2 -symmetric complexes featuring 1-triphenylmethylbenzimidazole giving the product in up to 72% *ee*. The resulting catalysts were also chemoselective, displaying a preference of >15:1 for acetophenone over the isoelectronic alkene α -methylstyrene.

The enhanced reactivity of our catalysts relative to $[\text{Cl}_2\text{Ru}(\text{diphosphine})]$ catalysts is likely due to the polarization of the C2-H of the benzimidazole ligand upon coordination to ruthenium. A Lewis acid/base interaction of this protic C-H bond with the oxygen atom of the carbonyl substrate polarizes the C-O bond and places it in proximity of the Ru-H, thus promoting 1,2-insertion. Likely due to the coordinative saturation of the catalysts, the ability of alkene substrates to coordinate ruthenium and then undergo 1,2-insertion is compromised, explaining the selectivity for carbonyl substrates. Use of protic solvents yield optimal results, possibly due to their ability to liberate a ruthenium alkoxide intermediate via protonation. This unique example of bifunctional catalysis may have significant implications to future catalyst designs, and lends further credence to Bergens' recent mechanistic proposal for Noyori-type hydrogenation systems.

4.4 Experimental

General Considerations: $[\text{Cl}_2\text{Ru}(\text{C}_6\text{H}_6)]_2$, chiral diphosphines, methyl benzimidazole, ketone substrates and potassium *tert*-butoxide were purchased from commercial sources and used as received. Isopropanol was dried and purified by distillation from magnesium activated with iodine. Benzene, *d*₆-benzene, and *tert*-butanol were dried over CaH_2 and purified by distillation. All other solvents (THF, CH_2Cl_2 , hexanes, toluene) were purified using an MBraun SPS solvent system. All solvents and liquid reagents were purged of oxygen using a minimum of three freeze-pump-thaw cycles before being brought into the glovebox. ^1H , $^{13}\text{C}\{^1\text{H}\}$ and $^{31}\text{P}\{^1\text{H}\}$ NMR spectra were performed using Bruker Avance 400 and 500 MHz spectrometers. Elemental analysis was performed by Canadian Microanalytical Systems Ltd. X-ray data collection was performed on a Bruker SMART CCD 1000 X-ray diffractometer.

Synthesis of BITr Ligand:

1-triphenylmethylbenzimidazole: To a 100 mL flame dried round bottom flask was added benzimidazole (1.00 g, 8.46 mmol) and 20 mL of THF. Once dissolved, the mixture was cooled in an ice bath and sodium hydride (264 mg, 11.0 mmol) added in a single portion. After stirring for 30 minutes at 0 °C, trityl chloride (3.06 g, 11.0 mmol) and a catalytic amount of tetrabutylammonium iodide were added, the flask was fitted with a condenser and the reaction mixture was refluxed for 24 hours. The reaction mixture was then cooled to room temperature, quenched by the addition of water and extracted three times with 100 mL of CHCl_3 . The combined organic fractions were dried

over MgSO₄, the solvent evaporated and the residue purified by column chromatography (2:1 hexanes/EtOAc) to give 2.53 g of yellow solid (82 % yield). ¹H NMR (CDCl₃, 400 MHz): δ 7.82 (s, 1H, NCHN); 7.70 (d, 1H, *J* = 8.1 Hz, Ar-CH); 7.26-7.05 (m, 16H, Ar-CH); 6.81 (t, 1H, *J* = 8.1 Hz); 6.39 (d, 1H, *J* = 8.1 Hz) ppm. ¹³C NMR (CDCl₃, 100 MHz): δ 144.6, 144.2, 141.4, 134.8, 130.0, 128.2, 128.0, 122.3, 122.0, 120.3, 115.4, 75.4. HRMS (EI-TOF): calcd for [M]⁺ (C₂₆H₂₀N₂) *m/z* 360.1626; found 360.1620.

Synthesis of Catalysts [Cl₂Ru(diphosphine)(κ-N3-(1-R)-benzimidazole)₂].

General Procedure: In a nitrogen atmosphere glove box, [Ru(C₆H₆)Cl₂]₂ (0.050 mmol) and a chiral diphosphine (0.100 mmol) were added to a 50 mL Schlenk flask with a magnetic stirring bar and the solids dissolved in 5 mL of DMF. The reaction flask was then put on the Schlenk line and the solution degassed three times via freeze-pump-thaw cycles before being heated to 100 °C. After cooling to 35 °C, the volatiles were removed in vacuo overnight to give a brown, solid residue. The reaction flask was then brought back into the glove box, dissolved in 10 mL of THF, the benzimidazole added (0.220 mmol) and the reaction mixture stirred for 16 hours. The reaction mixture was then concentrated to about 1 mL on the glovebox vacuum pump and the concentrated mixture filtered through a plug of celite. This was then reduced to a minimal amount of THF, layered with hexanes, recrystallized at -20 °C and the solid collected by filtration.

[Cl₂Ru(*rac*-Binap)(κ-N3-(1-methyl)-benzimidazole)₂] (**4-35**): An orange solid, 46 % yield. Anal. Found (Calcd) for C₆₀H₄₈Cl₂N₄P₂Ru•H₂O: C, 67.11 (66.91); H, 5.09 (4.68); N, 5.14 (5.20). ³¹P NMR (C₆D₆, 161 MHz): δ 43.74 (d, *J* = 28 Hz), 43.03, 42.21 (br), 41.78 (d, *J* = 28 Hz). ¹H NMR (C₆D₆, 400 MHz): δ 9.45 (m, 2H, NCHN, 3 conformers);

8.83-8.17 (m, 12H, Ar-CH); 7.72-7.54 (m, 2H, Ar-CH_{Binap}, 3 conformers); 7.45-7.31 (m, 2H, Ar-CH_{BI}, 3 conformers); 7.01-6.39 (m, 24H, Ar-CH); 2.34, 2.30, 2.25 (6H, NCH₃, 3 conformers) ppm.

[Cl₂Ru((*R*)-TolBinap)(κ-*N*3-(1-methyl)-benzimidazole)₂] (**4-37a**): An orange solid, 56 % yield. Anal. Found (Calcd) for C₆₄H₅₆Cl₂N₄P₂Ru: C, 68.60 (68.94); H, 5.20 (5.06); N, 5.03 (5.02). ³¹P NMR (C₆D₆, 161 MHz): δ 41.40 (d, *J* = 35 Hz), 40.81, 40.20, 39.45 (d, *J* = 35 Hz). ¹H NMR (C₆D₆, 400 MHz): δ 9.48-9.27 (m, 2H, NCHN, 3 conformers); 8.87-8.10 (m, 12H, Ar-CH); 7.74-7.62 (m, 2H, Ar-CH_{Binap}, 3 conformers); 7.45-7.34 (m, 2H, Ar-CH_{BI}, 3 conformers); 7.08-6.30 (m, 20H, Ar-CH); 2.37, 2.32, 2.31 (6H, N-CH₃, 3 conformers); 1.77, 1.74, 1.71 (12 H, P-C₆H₄CH₃, 3 conformers).

[Cl₂Ru((*R*)-TolBinap)(κ-*N*3-(1-triphenylmethyl)-benzimidazole)₂] (**4-37b**): A yellow solid, 74 % yield. Anal. Found (Calcd) for C₁₀₀H₈₀Cl₂N₄P₂Ru: C, 76.96 (76.42); H, 5.13 (5.56); N, 3.56 (3.62). ³¹P NMR (C₆D₆, 161 MHz): δ 40.43 ppm. ¹H NMR (C₆D₆, 400 MHz): δ 9.03 (s, 2H, NCHN), 8.37 (m, 4H, Ar-CH_{P-Ar}), 8.15 (m, 2H, Ar-CH_{Binap}), 8.09 (d, 2H, *J* = 8.0 Hz, Ar-CH_{BI}), 8.01 (m, 4H, Ar-CH_{P-Ar}), 7.38 (d, 2H, *J* = 8.7 Hz, Ar-CH_{Binap}), 7.30 (d, 2H, *J* = 8.0 Hz, Ar-CH_{BI}), 7.01-6.87 (m, 30H, Ar-CH_{Tr}), 6.67 (d, 4H, *J* = 8.0 Hz, Ar-CH_{P-Ar}), 6.61 (t, 2H, *J* = 8.0, Ar-CH_{BI}), 6.48 (m, 6H, Ar-CH), 6.15 (d, 2H, *J* = 8.7 Hz), 1.93 (s, 6H, C₆H₄-CH₃), 1.83 (s, 6H, P-C₆H₄CH₃) ppm.

[Cl₂Ru((*R*)-XylBinap)(κ-*N*3-(1-methyl)-benzimidazole)₂] (**4-38a**): An orange solid, 23 % yield. ³¹P NMR (C₆D₆, 161 MHz): δ 42.79 ppm (d, *J* = 36 Hz), 41.69, 41.43, 40.79 (d, *J* = 36 Hz). ¹H NMR (C₆D₆, 400 MHz): δ 9.34 (m, 2H, NCHN, 3 conformers); 8.90-8.69 (m, 2H, Ar-CH_{Binap}, 3 conformers); 8.45-7.98 (m, 6H, Ar-CH); 7.70-7.58 (m, 2H, Ar-

CH_{Binap} , 3 conformers); 77.41-7.31 (m, 2H, Ar- CH_{BI} , 3 conformers); 7.06-6.20 (m, 16H, Ar- CH); 6.20, 5.96, 5.91 (4H, Ar- CH_{PAr} , 3 conformers); 2.32, 2.26, 2.21 (N- CH_3 , 3 conformers); 1.86, 1.72 (m, $\text{PC}_6\text{H}_3(\text{CH}_3)_2$, 3 conformers).

$[\text{Cl}_2\text{Ru}((R)\text{-XylBinap})(\kappa\text{-}N3\text{-}(1\text{-triphenylmethyl})\text{-benzimidazole})_2]$ (**4-38b**): A yellow solid, 28 % yield. Anal. Found (Calcd) for $\text{C}_{104}\text{H}_{88}\text{Cl}_2\text{N}_4\text{P}_2\text{Ru}\cdot 2\text{H}_2\text{O}$: C, 75.45 (75.08); H, 5.59 (5.57); 3.47 (3.37). ^{31}P NMR (C_6D_6 , 161 MHz): δ 38.86 ppm. ^1H NMR (C_6D_6 , 400 MHz): δ 8.93 (s, 2H, NCHN), 8.36 (d, 2H, $J = 8.4$ Hz, Ar- CH_{BI}), 8.31 (m, 2H, Ar- CH_{Binap}), 7.86 (br, 4H, Ar- $CH_{\text{P-Ar}}$), 7.37 (d, 2H, $J = 8.5$ Hz, Ar- CH_{Binap}), 7.31 (d, 2H, $J = 8.0$ Hz, Ar- CH_{Binap}), 7.03-6.87 (m, 30H, Ar- CH_{Tr}), 6.78-6.57 (m, 14H, Ar- CH), 6.41 (m, 4H, Ar- CH_{BI}), 5.92 (s, 2H, Ar- $CH_{\text{P-Ar}}$), 1.90 (s, 12H, $\text{PC}_6\text{H}_3(\text{CH}_3)_2$), 1.79 (s, 12H, $\text{PC}_6\text{H}_3(\text{CH}_3)_2$).

$[\text{Cl}_2\text{Ru}((R)\text{-SynPhos})(\kappa\text{-}N3\text{-}(1\text{-triphenylmethyl})\text{-benzimidazole})_2]$ (**4-39**): A yellow solid, 53 % yield. Anal. Found (Calcd) for $\text{C}_{92}\text{H}_{72}\text{Cl}_2\text{N}_4\text{O}_4\text{P}_2\text{Ru}\cdot \text{H}_2\text{O}$: C, 71.05 (71.31); H, 4.89 (4.81); N, 3.32 (3.62). ^{31}P NMR (C_6D_6 , 161 MHz): δ 38.25 ppm. ^1H NMR (C_6D_6 , 400 MHz): δ 9.09 (s, 2H, NCHN); 8.41 (m, 6H, Ar- $CH_{\text{Binap, PAr}}$); 8.21 (m, 4H, Ar- CH_{PAr}); 7.27 (m, 2H, Ar- CH_{biaryl}); 7.08-6.88 (m, 28H, Ar- CH); 6.73 (t, 4H, $J = 7.3$ Hz, Ar- CH_{PAr}); 6.64 (t, 2H, $J = 7.7$ Hz, Ar- CH_{BI}); 6.52 (d, 2H, $J = 8.4$ Hz, Ar- CH_{biaryl}); 6.46 (t, 2H, $J = 7.7$ Hz, Ar- CH_{BI}); 6.37 (d, 2H, $J = 8.4$ Hz, Ar- CH_{BI}); 3.48 (m, 8H, OCH_2) ppm.

$[\text{Cl}_2\text{Ru}((R)\text{-C3-TunaPhos})(\kappa\text{-}N3\text{-}(1\text{-triphenylmethyl})\text{-benzimidazole})_2]$ (**4-40**): A brown solid, 77 % yield. Anal. Found (Calcd) for $\text{C}_{91}\text{H}_{72}\text{Cl}_2\text{N}_4\text{O}_2\text{P}_2\text{Ru}$: C 73.52, (73.48); H, 4.88 (4.88); N, 3.77 (3.78). ^{31}P NMR (C_6D_6 , 161 MHz): δ 42.48 ppm. ^1H NMR (C_6D_6 , 400 MHz): δ 9.02 (s, 2H, NCHN); 8.44 (d, 2H, $J = 8.5$ Hz, Ar- CH_{BI}); 8.25-8.07 (m, 8H,

Ar-CH); 7.23 (m, 2H, Ar-CH_{biaryl}); 7.10-6.43 (m, 40H, aromatic H); 6.38 (d, 2H, $J = 8.5$ Hz, Ar-CH_{BI}); 3.80-3.57 (m, 4H, OCH₂); 1.31 (m, 2H, (OCH₂)₂CH₂) ppm.

[Cl₂Ru((*R*)-Cl-OMe-BIPHEP)(κ-*N*3-(1-triphenylmethyl)-benzimidazole)₂] (**4-41**): A yellow solid, 58 % yield. Anal. Found (Calcd) for C₉₀H₇₀Cl₄N₄O₂P₂Ru•H₂O: C, 68.92 (69.19); H, 4.83 (4.64); N, 3.49 (3.59). ³¹P NMR (C₆D₆, 161 MHz): δ 40.43 ppm. ¹H NMR (C₆D₆, 400 MHz): δ 9.00 (s, 2H, NCHN); 8.37 (d, 2H, $J = 8.3$ Hz, ArCH_{BI}); 8.14 (m, 8H); 7.28 (m, 2H, Ar-CH_{biaryl}); 7.01-6.72 (m, 44H); 6.67 (t, 2H, $J = 7.3$ Hz, ArCH_{BI}); 6.47 (t, 2H, $J = 8.3$ Hz, ArCH_{BI}); 6.42 (d, 2H, $J = 8.1$ Hz, ArCH_{BI}); 3.47 (s, 6H, OCH₃) ppm.

[Cl₂Ru((*R*)-FluorPhos)(κ-*N*3-(1-triphenylmethyl)-benzimidazole)₂] (**4-42**): A yellow solid, 79 % yield. Anal. Found (Calcd) for C₉₀H₆₄Cl₂F₄N₄O₄P₂Ru•2H₂O: C, 67.42 (67.08); H, 4.14 (4.25); N, 3.48 (3.48). ³¹P NMR (C₆D₆, 161 MHz): δ 41.96 ppm. ¹H NMR (C₆D₆, 400 MHz): δ 9.06 (s, 2H, NCHN); 8.31 (d, 2H, $J = 8.5$ Hz, Ar-CH_{BI}); 8.11 (m, 8H, Ar-CH_{P-Ar}); 7.09-6.65 (m, 46H, Ar-CH); 6.47 (t, 2H, $J = 8.1$ Hz, ArCH_{BI}); 6.40 (d, 2H, $J = 8.1$ ppm, ArCH_{BI}); 6.05 (d, 2H, $J = 8.5$ Hz, ArCH_{biaryl}) ppm.

[Cl₂Ru((*R*)-XylPhanePhos)(κ-*N*3-(1-triphenylmethyl)-benzimidazole)₂] (**4-43**): Anal. Found (Calcd) for C₁₀₀H₉₀Cl₂N₄P₂Ru•1H₂O: C, 75.46 (75.08); H, 6.21 (5.80); N, 3.64 (3.54). ³¹P NMR (C₆D₆, 161 MHz): δ 33.69 ppm. ¹H NMR (C₆D₆, 400 MHz): δ 10.02 (m, 2H, Ar-CH_{Phane}); 9.68 (s, 2H, NCHN); 9.48 (d, 2H, $J = 8.5$ Hz, Ar-CH_{BI}); 9.23 (m, 2H, Ar-CH_{Phane}); 8.17 (m, 2H, Ar-CH_{Phane}); 7.24 (m, 12H, Ar-CH_{Tr}); 7.06-6.49 (m, 32H, Ar-CH); 6.41 (d, 2H, $J = 8.5$ Hz, ArCH_{Phane}); 6.19 (d, 2H, $J = 8.5$ Hz, ArCH_{biaryl}); 3.18

(m, 2H); 2.76 (m, 2H); 2.34 (m, 2H); 1.98, 1.94, 1.83 (s, 24H, PC₆H₃(CH₃)₂); 1.75 (m, 2H) ppm.

Representative Hydrogenation Procedure. In the glove box, the glass liner of a steel autoclave was charged with acetophenone (5.0 mmol), potassium *tert*-butoxide (5.6 mg, 0.05 mmol), [Cl₂Ru(*R*)-TolBinap](κ-*N*3-(1-triphenylmethyl)-benzimidazole)₂] (**4-37b**) (7.9 mg, 0.005 mmol) and 1,4-dimethoxybenzene (69.1 mg, 0.5 mmol, internal standard). The solid mixture was then dissolved in 10 mL of 2-propanol and placed in the autoclave, which already contains 1 mL of solvent to prevent unwanted movement of the liner. The autoclave was removed from the glove box, the gauge block assembly attached and pressurized with 5 atm hydrogen gas. The reaction was then stirred at room temperature for six hours, after which time the pressure was released, and the crude reaction mixture passed through a plug of silica to remove the ruthenium catalyst. The crude mixture was then analyzed by chiral super-critical fluid chromatography to determine the enantiopurity and analysed by ¹H NMR in CDCl₃ to determine yield. All catalytic reactions were performed in duplicate to verify the reproducibility of both yields and enantiopurity.

4.5 References

- (1) Andersson, P. G.; Munslow, I. J. *Modern Reduction Methods*; Wiley: New York, 2008.
- (2) Akutagawa, S. In *Chirality in Industry: The Commercial Manufacture and Applications of Optically Active Compounds*; Collins, A. N., Sheldrake, G. N., Crosby, J., Eds.; Wiley: New York, 1997.
- (3) Ohkuma, T.; Noyori, R. In *Comprehensive Asymmetric Catalysis. Supplement*; Jacobsen, E. N., Pfaltz, A., Yamamoto, H., Eds.; Springer: New York, 2004.
- (4) Noyori, R. *Asymmetric Catalysis in Organic Synthesis*; Wiley: New York, 1994.
- (5) Noyori, R.; Ohkuma, T. *Angew. Chem. Int. Ed.* **2001**, *40*, 40-73.
- (6) Noyori, R. In *Asymmetric Catalysis in Organic Synthesis*; Wiley: Toronto, 1994, p 56-82.
- (7) Ohkuma, T.; Ooka, H.; Ikariya, T.; Noyori, R. *J. Am. Chem. Soc.* **1995**, *117*, 10417-10418.
- (8) Ohkuma, T.; Ikehira, H.; Ikariya, T.; Noyori, R. *Synlett* **1997**, *1997*, 467-468.
- (9) Haack, K.-J.; Hashiguchi, S.; Fujii, A.; Ikariya, T.; Noyori, R. *Angew. Chem. Int. Ed. Engl.* **1997**, *36*, 285-288.
- (10) Noyori, R.; Yamakawa, M.; Hashiguchi, S. *J. Org. Chem.* **2001**, *66*, 7931-7944.
- (11) Ohkuma, T.; Ooka, H.; Hashiguchi, S.; Ikariya, T.; Noyori, R. *J. Am. Chem. Soc.* **1995**, *117*, 2675-2676. Ohkuma, T.; Ooka, H.; Yamakawa, M.; Ikariya, T.; Noyori, R. *J. Org. Chem.* **1996**, *61*, 4872-4873. Doucet, H.; Ohkuma, T.; Murata, K.; Yokozawa, T.; Kozawa, M.; Katayama, E.; England, A. F.; Ikariya, T.; Noyori, R. *Angew. Chem. Int. Ed.* **1998**, *37*, 1703-1707.
- (12) Ohkuma, T.; Koizumi, M.; Doucet, H.; Pham, T.; Kozawa, M.; Murata, K.; Katayama, E.; Yokozawa, T.; Ikariya, T.; Noyori, R. *J. Am. Chem. Soc.* **1998**, *120*, 13529-13530.
- (13) Ohkuma, T.; Koizumi, M.; Ikehira, H.; Yokozawa, T.; Noyori, R. *Org. Lett.* **2000**, *2*, 659-662.
- (14) Ohkuma, T.; Koizumi, M.; Yoshida, M.; Noyori, R. *Org. Lett.* **2000**, *2*, 1749-1751.
- (15) Ohkuma, T.; Sandoval, C. A.; Srinivasan, R.; Lin, Q.; Wei, Y.; Muñiz, K.; Noyori, R. *J. Am. Chem. Soc.* **2005**, *127*, 8288-8289.

- (16) Ohkuma, T.; Ishii, D.; Takeno, H.; Noyori, R. *J. Am. Chem. Soc.* **2000**, *122*, 6510-6511.
- (17) Ohkuma, T.; Hattori, T.; Ooka, H.; Inoue, T.; Noyori, R. *Org. Lett.* **2004**, *6*, 2681-2683.
- (18) Sandoval, C. A.; Ohkuma, T.; Muniz, K.; Noyori, R. *J. Am. Chem. Soc.* **2003**, *125*, 13490-13503.
- (19) Hartmann, R.; Chen, P. *Angew. Chem. Int. Ed.* **2001**, *40*, 3581-3585. Abdur-Rashid, K.; Clapham, S. E.; Hadzovic, A.; Harvey, J. N.; Lough, A. J.; Morris, R. H. *J. Am. Chem. Soc.* **2002**, *124*, 15104-15118. Zimmer-De Iuliis, M.; Morris, R. H. *J. Am. Chem. Soc.* **2009**, *131*, 11263-11269.
- (20) Abdur-Rashid, K.; Faatz, M.; Lough, A. J.; Morris, R. H. *J. Am. Chem. Soc.* **2001**, *123*, 7473-7474.
- (21) Clapham, S. E.; Hadzovic, A.; Morris, R. H. *Coord. Chem. Rev.* **2004**, *248*, 2201-2237.
- (22) Sandoval, C. A.; Yamaguchi, Y.; Ohkuma, T.; Kato, K.; Noyori, R. *Magn. Reson. Chem.* **2006**, *44*, 66-75.
- (23) Alonso, D. A.; Brandt, P.; Nordin, S. J. M.; Andersson, P. G. *J. Am. Chem. Soc.* **1999**, *121*, 9580-9588. Yamakawa, M.; Ito, H.; Noyori, R. *J. Am. Chem. Soc.* **2000**, *122*, 1466-1478. Casey, C. P.; Johnson, J. B. *J. Org. Chem.* **2003**, *68*, 1998-2001.
- (24) Hamilton, R. J.; Leong, C. G.; Bigam, G.; Miskolzie, M.; Bergens, S. H. *J. Am. Chem. Soc.* **2005**, *127*, 4152-4153. Hamilton, R. J.; Bergens, S. H. *J. Am. Chem. Soc.* **2006**, *128*, 13700-13701. Hamilton, R. J.; Bergens, S. H. *J. Am. Chem. Soc.* **2008**, *130*, 11979-11987.
- (25) Kunz, D. *Angew. Chem. Int. Ed.* **2007**, *46*, 3405-3408.
- (26) Raczynska, E. D.; Kosinska, W.; Osmialowski, B.; Gawinecki, R. *Chem. Rev.* **2005**, *105*, 3561-3612.
- (27) Sundberg, R. J.; Bryan, R. F.; Taylor, I. F.; Taube, H. *J. Am. Chem. Soc.* **1974**, *96*, 381-392.
- (28) Sini, G.; Eisenstein, O.; Crabtree, R. H. *Inorg. Chem.* **2001**, *41*, 602-604.
- (29) Alvarez, E.; Conejero, S.; Paneque, M.; Petronilho, A.; Poveda, M. L.; Serrano, O.; Carmona, E. *J. Am. Chem. Soc.* **2006**, *128*, 13060-13061.
- (30) Conejero, S.; Lara, P.; Paneque, M.; Petronilho, A.; Poveda, M. L.; Serrano, O.; Vattier, F.; Álvarez, E.; Maya, C.; Salazar, V.; Carmona, E. *Angew. Chem. Int. Ed.* **2008**, *47*, 4380-4383.

- (31) Song, G. Y.; Li, Y. X.; Chen, S. S.; Li, X. W. *Chem. Commun.* **2008**, 3558-3560.
- (32) Song, G.; Su, Y.; Periana, R. A.; Crabtree, R. H.; Han, K.; Zhang, H.; Li, X. *Angew. Chem. Int. Ed.* **2009**, *49*, 912-917.
- (33) Hahn, F. E.; Langenhahn, V.; Meier, N.; Lügger, T.; Fehlhammer, W. P. *Chem.-Eur. J.* **2003**, *9*, 704-712.
- (34) Hahn, F. E.; Plumed, C. G.; Münder, M.; Lügger, T. *Chem.-Eur. J.* **2004**, *10*, 6285-6293.
- (35) Meier, N.; Hahn, F. E.; Pape, T.; Siering, C.; Waldvogel, S. R. *Eur. J. Inorg. Chem.* **2007**, *2007*, 1210-1214.
- (36) Ruiz, J.; Perandones, B. F. *J. Am. Chem. Soc.* **2007**, *129*, 9298-9299. Ruiz, J.; Berros, A.; Perandones, B. F.; Vivanco, M. *Dalton Trans.* **2009**, 6999-7007.
- (37) Ruiz, J.; Perandones, B. F. *Chem. Commun.* **2009**, 2741-2743.
- (38) Tan, K. L.; Bergman, R. G.; Ellman, J. A. *J. Am. Chem. Soc.* **2002**, *124*, 3202-3203.
- (39) Wiedemann, S. H.; Lewis, J. C.; Ellman, J. A.; Bergman, R. G. *J. Am. Chem. Soc.* **2006**, *128*, 2452-2462.
- (40) Gribble, M. W.; Ellman, J. A.; Bergman, R. G. *Organometallics* **2008**, *27*, 2152-2155.
- (41) Esteruelas, M. A.; Fernández-Alvarez, F. J.; Oñate, E. *J. Am. Chem. Soc.* **2006**, *128*, 13044-13045.
- (42) Esteruelas, M. A.; Fernández-Alvarez, F. J.; Oñate, E. *Organometallics* **2007**, *26*, 5239-5245.
- (43) Buil, M. L.; Esteruelas, M. A.; Garcés, K.; Oliván, M.; Oñate, E. *J. Am. Chem. Soc.* **2007**, *129*, 10998-10999.
- (44) Esteruelas, M. A.; Fernández-Alvarez, F. J.; Oñate, E. *Organometallics* **2008**, *27*, 6236-6244.
- (45) Esteruelas, M. A.; Fernández-Alvarez, F. J.; Oliván, M.; Oñate, E. *Organometallics* **2009**, *28*, 2276-2284.
- (46) Miranda-Soto, V.; Grotjahn, D. B.; DiPasquale, A. G.; Rheingold, A. L. *J. Am. Chem. Soc.* **2008**, *130*, 13200-13201.
- (47) Araki, K.; Kuwata, S.; Ikariya, T. *Organometallics* **2008**, *27*, 2176-2178.
- (48) Burling, S.; Mahon, M. F.; Powell, R. E.; Whittlesey, M. K.; Williams, J. M. J. *J. Am. Chem. Soc.* **2006**, *128*, 13702-13703.

- (49) Wang, X.; Chen, H.; Li, X. *Organometallics* **2007**, *26*, 4684-4687.
- (50) Brendler, E.; Hill, A. F.; Wagler, J. *Chem. Eur. J.* **2008**, *14*, 11300-11304.
- (51) Lewis, J. C.; Bergman, R. G.; Ellman, J. A. *Acc. Chem. Res.* **2008**, *41*, 1013-1025.
- (52) Lavorato, D.; Terlouw, J. K.; Dargel, T. K.; Koch, W.; McGibbon, G. A.; Schwarz, H. *J. Am. Chem. Soc.* **1996**, *118*, 11898-11904.
- (53) Huertos, M. A.; Pérez, J.; Riera, L.; Menéndez-Velázquez, A. *J. Am. Chem. Soc.* **2008**, *130*, 13530-13531.
- (54) Hahn, F. E.; Langenhahn, V.; Lügger, T.; Pape, T.; Van, D. L. *Angew. Chem. Int. Ed.* **2005**, *44*, 3759-3763.
- (55) Hahn, F. E.; Plumed, C. G.; M,nder, M.; L,gger, T. *Chem.-Eur. J.* **2004**, *10*, 6285-6293.
- (56) Tan, K. L.; Bergman, R. G.; Ellman, J. A. *J. Am. Chem. Soc.* **2001**, *123*, 2685-2686.
- (57) Tan, K. L.; Bergman, R. G.; Ellman, J. A. *J. Am. Chem. Soc.* **2002**, *124*, 13964-13965. Tan, K. L.; Park, S.; Ellman, J. A.; Bergman, R. G. *J. Org. Chem.* **2004**, *69*, 7329-7335.
- (58) Wiedemann, S. H.; Bergman, R. G.; Ellman, J. A. *Org. Lett.* **2004**, *6*, 1685-1687.
- (59) Wiedemann, S. H.; Ellman, J. A.; Bergman, R. G. *J. Org. Chem.* **2006**, *71*, 1969-1976.
- (60) Lewis, J. C.; Bergman, R. G.; Ellman, J. A. *J. Am. Chem. Soc.* **2007**, *129*, 5332-5333.
- (61) Lewis, J. C.; Wiedemann, S. H.; Bergman, R. G.; Ellman, J. A. *Org. Lett.* **2003**, *6*, 35-38.
- (62) Lewis, J. C.; Berman, A. M.; Bergman, R. G.; Ellman, J. A. *J. Am. Chem. Soc.* **2008**, *130*, 2493-2500.
- (63) Lewis, J. C.; Wiedemann, S. H.; Bergman, R. G.; Ellman, J. A. *Org. Lett.* **2004**, *6*, 35-38.
- (64) Alder, R. W.; Allen, P. R.; Williams, S. J. *J.C.S.-Chem. Comm.* **1995**, 1267-1268.
- (65) Bordwell, F. G. *Acc. Chem. Res.* **2002**, *21*, 456-463.
- (66) Crowhurst, L.; Mawdsley, P. R.; Perez-Arlandis, J. M.; Salter, P. A.; Welton, T. *Phys. Chem. Chem. Phys.* **2003**, *5*, 2790-2794.

- (67) Kamlet, M. J.; Abboud, J. L. M.; Abraham, M. H.; Taft, R. W. *J. Org. Chem.* **2002**, *48*, 2877-2887.
- (68) Chakraborti, A. K.; Roy, S. R. *J. Am. Chem. Soc.* **2009**, *131*, 6902-6903.
- (69) Akotsi, O. M.; Metera, K.; Reid, R. D.; McDonald, R.; Bergens, S. H. *Chirality* **2000**, *12*, 514-522. Leong, C. G.; Akotsi, O. M.; Ferguson, M. J.; Bergens, S. H. *Chem. Commun.* **2003**, 750-751.
- (70) Ohta, T.; Takaya, H.; Noyori, R. *Inorg. Chem.* **1988**, *27*, 566-569.
- (71) Duprat de Paule, S.; Jeulin, S.; Ratovelomanana-Vidal, V.; Genêt, J.-P.; Champion, N.; Dellis, P. *Tetrahedron Lett.* **2003**, *44*, 823-826. Zhang, Z.; Qian, H.; Longmire, J.; Zhang, X. *J. Org. Chem.* **2000**, *65*, 6223-6226. Maligres, P. E.; Krska, S. W.; Humphrey, G. R. *Org. Lett.* **2004**, *6*, 3147-3150. Jeulin, S.; Paule, S. D. d.; Ratovelomanana-Vidal, V.; Genêt, J.-P.; Champion, N.; Dellis, P. *Angew. Chem. Int. Ed.* **2004**, *43*, 320-325. Burk, M. J.; Hems, W.; Herzberg, D.; Malan, C.; Zanotti-Gerosa, A. *Org. Lett.* **2000**, *2*, 4173-4176.

Chapter 5: Conclusions and Future Work

In Chapter 2, the characterization of the dioxygen complexes [ClRh(IPr)₂(O₂)] (**2-4**) and [ClRh(IMes)₂(O₂)] (**2-5**) by X-ray diffraction, NMR spectroscopy and DFT calculations – as well as, IR, Raman, and XAS spectroscopy in the case of **2-4** – was described. The results were indicative of a strong O-O bond in the two complexes, relative to more commonly reported Rh^{III}-peroxo complexes. The best description of these compounds, based on all the characterization acquired is a rhodium(I) coordination complex of singlet oxygen. The unique bonding mode is predicted to result from the interaction of a filled Rh d orbital with one of the two degenerate O₂ π* orbitals. This results in splitting of the O₂ π* orbitals, favoring spin pairing in the O₂ HOMO, and the inability of Rh to donate electron density to the empty π* orbital.

The coordination chemistry of the [ClRh(NHC)₂] fragment with simple diatomic molecules was also reported and the resulting structures fully characterized by NMR and IR spectroscopy, as well as X-ray crystallography and elemental analysis. For example, the ability of this rhodium fragment to bind dinitrogen end-on yielding [ClRh(IPr)₂(N₂)] (**2-10**) was disclosed. While this complex is very stable in the solid state, dinitrogen is easily displaced in solution by O₂, CO and H₂. For these complexes of the formula [ClRh(IPr)₂(XY)], the relative binding affinity of the diatomic molecules was qualitatively determined, and appears to follow the order: CO > O₂ > H₂ > N₂.

Finally, the ability of the dioxygen complexes, **2-4** and **2-5**, to catalytically oxidize secondary alcohols under aerobic conditions was determined giving yields as high as 85% for the substrate 1-(4-methoxyphenyl)ethanol with a 5 mol% loading of catalyst **2-4**. By carrying out crossover studies, we were able to determine that

incomplete conversion of the alcohol substrate was apparently due to a resulting equilibrium between the alcohol and its ketone, and we therefore investigated the ability of **2-4** and Rh(N₂) complex **2-10** to reduce acetophenone. Under transfer hydrogenation conditions the resulting alcohol was isolated in up to 96% yield.

Future studies by our laboratory will focus on the systematic variation of the steric and electronic properties of the NHC ligands employed to generate a comparable series of dioxygen complexes of the formula [ClRh(NHC)₂(O₂)]. The recent synthesis of [Rh(NHC)₂(RCN)₂(O₂)]⁺X⁻ complexes in our laboratory, which are octahedral Rh^{III}-peroxo complexes, seems to indicate that addition of another ligand to the coordination sphere of rhodium increases its ability to reduce dioxygen. This insight into the oxidative addition of dioxygen by rhodium may be beneficial to the development of catalytic oxidative transformation with these rhodium complexes and their analogues.

In Chapter 3, the preparation and characterization of two new rhodium *N*-heterocyclic carbene complexes that possess unidentate carboxylato ligands as the anionic ligand were described. One of these complexes, [(AcO)Rh(IPr)(CO)₂] **3-11**, represents one of the most active NHC-modified rhodium catalysts reported to date for the hydroformylation of styrene derivatives. The hydroformylation of both aromatic and aliphatic alkenes with this compound were investigated. Both classes of substrate were transformed to their corresponding aldehydes in high yields, displaying high regioselectivities for the branched and linear aldehydes from the aromatic and aliphatic alkenes, respectively. Most importantly, the reactions of these substrates occur without concomitant isomerization of the alkene.

The inhibiting effect of the carboxylate ligand in complex **3-11** was also probed, and compared to those observed with the chloro-containing analogue **3-14**. It was shown that catalyst **3-11** was not only a more efficient catalyst than **3-14**, but that it also generated the active catalyst over five times faster.

Future work in this area could focus on a more detailed kinetic study of these two systems, with a focus on determining whether chloro- and acetato-containing precatalysts generate the same active catalyst *in situ*. By observing the effect of additives such as phosphines, triethylamine and imidazolium salts on the reaction rate for the two precatalysts, significant insights into their differences could be made. This may lead to the development of more effective Rh(NHC) precatalysts for the hydroformylation reaction.

In Chapter 4, the attempts to synthesize catalysts of the formula $[\text{Cl}_2\text{Ru}(\text{diphosphine})(\kappa\text{-C2-benzimidazole})_2]$ capable of enantio- and chemoselectively hydrogenating prochiral ketones were described. While these attempts to synthesize a bifunctional hydrogenation catalyst featuring a protic-NHC ligand were unsuccessful, we were able to isolate new compounds of the formula $[\text{Cl}_2\text{Ru}(\text{diphosphine})(\kappa\text{-N3-benzimidazole})_2]$ with a variety of different chiral diphosphines and N1-substituted benzimidazoles. The characterization of these complexes by ^{31}P and ^1H NMR spectroscopy, elemental analysis, and the connectivity verified via X-ray crystallography in the case of **4-38a** was also described. For benzimidazoles with smaller substituents at N1 (Me, Et, etc.) the obtained complexes existed as mixtures of all three possible diastereomers. When N1 was substituted with the much larger triphenylmethyl substituent the resulting complexes existed as a single C_2 -symmetric diastereomer.

The catalytic activity of isolated $[\text{Cl}_2\text{Ru}(\text{diphosphine})(\kappa\text{-N3-benzimidazole})_2]$ complexes for the hydrogenation of simple aromatic ketones, yielding the corresponding secondary alcohols was disclosed. These reactions proceeded under relatively mild conditions (room temperature and 5 atm H_2), and employing chiral diphosphines yielded secondary alcohols with significant enantioselectivity, with C_2 -symmetric complexes featuring 1-triphenylmethylbenzimidazole giving the product in up to 72% *ee*. The resulting catalysts were also chemoselective, displaying a preference of >15:1 for acetophenone over the isoelectronic alkene α -methylstyrene.

Although initial attempts to synthesize bifunctional Ru(protic-NHC) precatalysts was unsuccessful, future studies should focus on new synthetic strategies to achieve this novel design. For instance, use of a typical NHC featuring a removable protecting group at one nitrogen could initially generate $[\text{Cl}_2\text{Ru}(\text{diphosphine})(\text{NHC})_2]$. Removal of the protecting group at nitrogen could then furnish the desired $[\text{Cl}_2\text{Ru}(\text{diphosphine})(\kappa\text{-C2-benzimidazole})_2]$ complex. These complexes should fair better for enantio-discrimination during the catalytic hydrogenation, as the N-substituent of the benzimidazol-2-ylidene ligands would be in closer proximity to the ruthenium center.

Appendix A: Crystallographic Data

Table A-1: Atomic coordinates ($\times 10^4$) and equivalent isotropic displacement parameters ($\text{\AA}^2 \times 10^3$) for $[\text{ClRh}(\text{IPr})_2(\text{N}_2)]$ (**2-10**).

	x	y	z	U(eq)
Rh(1)	5000	0	920(1)	22(1)
N(1)	5436(1)	1467(1)	626(1)	27(1)
N(2)	3923(1)	1312(1)	1336(1)	27(1)
C(1)	4774(1)	983(1)	952(1)	23(1)
C(2)	5005(2)	2074(1)	802(2)	43(1)
C(3)	4051(1)	1976(1)	1236(2)	42(1)
C(4)	6490(1)	1403(1)	217(2)	27(1)
C(5)	7246(1)	1318(1)	1142(2)	31(1)
C(6)	8264(1)	1310(1)	736(2)	37(1)
C(7)	8512(1)	1382(1)	-508(2)	39(1)
C(8)	7752(2)	1469(1)	-1398(2)	36(1)
C(9)	6712(1)	1483(1)	-1059(2)	30(1)
C(10)	6982(2)	1277(1)	2526(2)	36(1)
C(11)	7578(2)	748(1)	3181(2)	62(1)
C(12)	7160(3)	1924(1)	3164(2)	88(1)
C(13)	5897(2)	1595(1)	-2053(2)	44(1)
C(14)	5767(2)	2329(1)	-2306(3)	73(1)
C(15)	6129(2)	1231(1)	-3269(2)	66(1)
C(16)	2932(1)	1055(1)	1687(2)	27(1)
C(17)	2265(1)	870(1)	722(2)	30(1)
C(18)	1267(1)	697(1)	1060(2)	38(1)
C(19)	954(1)	716(1)	2294(2)	41(1)
C(20)	1634(1)	901(1)	3231(2)	38(1)
C(21)	2644(1)	1067(1)	2950(2)	31(1)
C(22)	2576(1)	889(1)	-651(2)	34(1)
C(23)	2110(2)	1483(1)	-1296(2)	55(1)
C(24)	2294(2)	266(1)	-1334(2)	48(1)

C(25)	3364(1)	1266(1)	4006(2)	40(1)
C(26)	3301(2)	805(1)	5126(2)	55(1)
C(27)	3132(2)	1959(1)	4432(3)	72(1)
Cl(1A)	5000	0	3069(1)	31(1)
N(3A)	5000	0	-857(5)	25(1)
N(4A)	5000	0	-1890(5)	52(1)
Cl(1B)	5000	0	-1199(4)	29(1)
N(3B)	5000	0	2729(8)	25(1)
N(4B)	5000	0	3777(10)	52(1)

Table A-2: Atomic coordinates ($\times 10^4$) and equivalent isotropic displacement parameters ($\text{\AA}^2 \times 10^3$) for $[\text{ClRh}(\text{IPr})_2(\text{H})_2]/[\text{Cl}_2\text{Rh}(\text{IPr})_2]$ (**2-11/2-13**).

	x	y	z	U(eq)
Rh(1)	0	0	4078(1)	24(1)
N(1)	1066(2)	1315(1)	3695(3)	29(1)
N(2)	-466(2)	1468(1)	4369(3)	29(1)
C(1)	200(2)	981(1)	4048(3)	26(1)
C(2)	943(3)	1976(2)	3807(4)	45(1)
C(3)	-14(3)	2074(1)	4226(3)	43(1)
C(4)	2046(2)	1046(2)	3320(3)	30(1)
C(5)	2730(2)	870(2)	4266(3)	32(1)
C(6)	3726(2)	698(2)	3894(4)	40(1)
C(7)	4010(3)	704(2)	2645(4)	44(1)
C(8)	3307(3)	875(2)	1736(4)	45(1)
C(9)	2299(3)	1045(2)	2047(4)	38(1)
C(10)	1534(3)	1215(2)	1006(4)	54(1)
C(11A)	1800(10)	1948(7)	612(9)	63(2)
C(12A)	1636(8)	829(6)	-156(9)	63(2)
C(11B)	1798(10)	1765(7)	168(9)	63(2)
C(12B)	1346(8)	557(6)	187(9)	63(2)
C(13)	2440(3)	892(2)	5656(3)	38(1)

C(14)	2768(3)	278(2)	6336(4)	52(1)
C(15)	2878(4)	1503(2)	6266(5)	62(1)
C(16)	-1529(2)	1404(2)	4752(3)	29(1)
C(17)	-2269(2)	1318(2)	3813(3)	32(1)
C(18)	-3294(2)	1304(2)	4199(4)	39(1)
C(19)	-3554(3)	1374(2)	5445(4)	39(1)
C(20)	-2807(3)	1461(2)	6343(4)	36(1)
C(21)	-1765(2)	1481(2)	6022(3)	31(1)
C(22)	-1998(3)	1292(2)	2433(4)	39(1)
C(23)	-2606(4)	768(3)	1743(4)	73(2)
C(24A)	-1894(16)	1981(11)	1900(20)	67(4)
C(24B)	-2340(15)	1907(11)	1740(20)	67(4)
C(25)	-961(3)	1600(2)	7030(3)	43(1)
C(26)	-1184(4)	1218(2)	8236(4)	61(1)
C(27)	-872(4)	2318(2)	7336(5)	69(1)
C(28)	5000	0	-819(5)	101(3)
C(29)	5149(7)	605(2)	-1415(4)	122(3)
C(30)	5315(5)	1194(4)	-766(6)	141(4)
C(31)	5017(9)	1818(5)	-1072(9)	85(3)
Cl(1)	0	0	6300(1)	49(1)
Cl(2)	0	0	1891(3)	48(1)

Table A-3: Atomic coordinates ($\times 10^4$) and equivalent isotropic displacement parameters ($\text{\AA}^2 \times 10^3$) for $[\text{ClRh}(\text{IPr})_2(\text{CO})]$ (**2-12**).

	x	y	z	U(eq)
Rh(1)	0	0	942(1)	26(1)
Cl(1)	0	0	3112(2)	35(1)
Cl(1A)	0	0	-1205(4)	39(2)
N(1)	-436(1)	1467(1)	633(1)	31(1)
N(2)	1081(1)	1314(1)	1331(1)	30(1)
C(1)	228(1)	983(1)	964(2)	28(1)

C(2)	1(2)	2072(1)	794(2)	46(1)
C(3)	959(1)	1974(1)	1218(2)	45(1)
C(4)	-1491(1)	1403(1)	226(2)	31(1)
C(5)	-1713(1)	1479(1)	-1048(2)	34(1)
C(6)	-2751(1)	1465(1)	-1382(2)	40(1)
C(7)	-3509(1)	1382(1)	-496(2)	43(1)
C(8)	-3260(1)	1311(1)	750(2)	41(1)
C(9)	-2244(1)	1319(1)	1151(2)	34(1)
C(10)	-893(1)	1587(1)	-2044(2)	46(1)
C(11)	-1122(2)	1215(1)	-3249(2)	67(1)
C(12)	-772(2)	2311(1)	-2321(3)	77(1)
C(13)	-1980(2)	1280(1)	2541(2)	41(1)
C(14)	-2157(3)	1923(1)	3179(2)	97(1)
C(15)	-2573(2)	748(1)	3197(2)	66(1)
C(16)	2075(1)	1055(1)	1685(2)	31(1)
C(17)	2739(1)	872(1)	720(2)	34(1)
C(18)	3738(1)	698(1)	1065(2)	42(1)
C(19)	4045(1)	714(1)	2295(2)	45(1)
C(20)	3367(1)	900(1)	3230(2)	43(1)
C(21)	2358(1)	1066(1)	2944(2)	35(1)
C(22)	2432(1)	891(1)	-650(2)	38(1)
C(23)	2718(2)	270(1)	-1337(2)	53(1)
C(24)	2892(2)	1486(1)	-1293(2)	59(1)
C(25)	1636(1)	1267(1)	4003(2)	45(1)
C(26)	1860(2)	1961(1)	4421(3)	76(1)
C(27)	1704(2)	812(1)	5131(2)	59(1)
C(28)	0	0	-783(10)	37(3)
C(28A)	0	0	2678(11)	33(3)
O(1)	0	0	-1867(8)	57(1)
O(1A)	0	0	3766(12)	57(2)

Table A-4: Atomic coordinates ($\times 10^4$) and equivalent isotropic displacement parameters ($\text{\AA}^2 \times 10^3$) for *cis*-[(AcO)Rh(IPr)(CO)₂] (**3-11**).

	x	y	z	U(eq)
N(1)	2322(2)	1883(1)	5471(2)	32(1)
Rh(1)	4821(1)	2500	4461(1)	35(1)
O(1)	6334(3)	2500	6559(3)	96(1)
O(2)	8137(4)	2997(3)	6240(5)	78(1)
O(3)	7118(4)	2500	2966(4)	82(1)
O(4)	2471(4)	2500	1495(3)	72(1)
C(1)	3081(3)	2500	5254(3)	30(1)
C(2)	1094(2)	2118(1)	5814(2)	41(1)
C(3)	2780(2)	1090(1)	5485(2)	34(1)
C(4)	2102(2)	639(1)	4247(2)	40(1)
C(5)	2559(3)	-128(1)	4325(3)	50(1)
C(6)	3633(3)	-418(1)	5567(3)	52(1)
C(7)	4252(3)	35(1)	6777(3)	50(1)
C(8)	3844(2)	802(1)	6775(2)	41(1)
C(9)	879(3)	944(2)	2893(3)	54(1)
C(10)	-665(4)	672(3)	2867(5)	101(1)
C(11)	1147(5)	725(2)	1496(3)	89(1)
C(12)	4481(3)	1290(2)	8140(3)	60(1)
C(13)	3493(6)	1238(3)	9063(4)	94(1)
C(14)	6114(5)	1095(3)	9055(4)	91(1)
C(15)	7659(4)	2500	6950(5)	60(1)
C(16)	8716(6)	2500	8479(7)	126(3)
C(17)	6347(4)	2500	3614(4)	53(1)
C(18)	3390(4)	2500	2643(4)	46(1)

Table A-5: Atomic coordinates ($\times 10^4$) and equivalent isotropic displacement parameters ($\text{\AA}^2 \times 10^3$) for *cis*-[(AcO)Rh(IPr)₂(CO)] (**3-12**).

	x	y	z	U(eq)
Rh(1)	4941(1)	7649(1)	2080(1)	23(1)
C(1)	5166(2)	8620(1)	2083(1)	26(1)
C(2)	5890(2)	9590(1)	1891(1)	37(1)
C(3)	4996(2)	9685(1)	2205(1)	38(1)
C(4)	6901(2)	8696(1)	1475(1)	29(1)
C(5)	6933(2)	8786(1)	784(1)	36(1)
C(6)	7862(2)	8588(1)	481(2)	44(1)
C(7)	8704(2)	8324(1)	854(2)	48(1)
C(8)	8661(2)	8247(1)	1537(2)	41(1)
C(9)	7754(2)	8434(1)	1871(1)	32(1)
C(10)	6049(2)	9121(1)	358(1)	45(1)
C(11)	5615(4)	8739(2)	-243(2)	67(1)
C(12)	6468(3)	9758(2)	119(2)	70(1)
C(13)	7725(2)	8388(1)	2625(1)	38(1)
C(14)	8145(4)	8992(2)	2964(2)	71(1)
C(15)	8337(4)	7824(2)	2912(2)	64(1)
C(16)	3544(2)	9054(1)	2658(1)	29(1)
C(17)	3534(2)	9193(1)	3340(1)	35(1)
C(18)	2544(2)	9151(1)	3636(1)	41(1)
C(19)	1613(2)	8997(1)	3259(2)	43(1)
C(20)	1636(2)	8911(1)	2584(2)	45(1)
C(21)	2603(2)	8945(1)	2253(1)	38(1)
C(22)	4520(2)	9465(2)	3750(1)	51(1)
C(23)	4680(4)	9217(2)	4460(2)	72(1)
C(24)	4411(3)	10189(2)	3788(2)	60(1)
C(25)	2598(2)	8921(2)	1485(2)	55(1)
C(26)	2243(4)	8297(2)	1215(2)	89(1)
C(27)	1782(3)	9431(2)	1154(2)	82(1)
C(55)	5312(2)	7592(1)	1229(2)	44(1)
C(56)	4871(2)	7758(1)	3588(2)	45(1)

C(57)	4217(3)	7595(2)	4201(2)	70(1)
C(58)	4701(2)	6684(1)	2064(1)	25(1)
C(59)	4928(2)	5612(1)	2122(1)	32(1)
C(60)	3918(2)	5717(1)	1891(1)	33(1)
C(61)	6534(2)	6238(1)	2446(1)	33(1)
C(62)	7279(2)	6219(1)	1944(2)	42(1)
C(63)	8371(2)	6188(1)	2173(2)	60(1)
C(64)	8679(2)	6182(1)	2834(2)	63(1)
C(65)	7931(2)	6201(1)	3311(2)	56(1)
C(66)	6826(2)	6225(1)	3131(1)	41(1)
C(67)	6945(2)	6196(1)	1207(2)	52(1)
C(68)	7624(4)	6624(2)	778(2)	75(1)
C(69)	6993(4)	5519(2)	936(3)	78(1)
C(70)	6004(3)	6204(2)	3663(2)	55(1)
C(71)	6375(4)	6542(3)	4305(2)	81(1)
C(72)	5705(5)	5524(2)	3826(3)	90(2)
C(73)	2754(2)	6621(1)	1605(1)	32(1)
C(74)	2540(2)	6646(1)	911(1)	38(1)
C(75)	1486(2)	6809(1)	683(2)	49(1)
C(76)	721(2)	6941(1)	1131(2)	52(1)
C(77)	960(2)	6926(1)	1810(2)	46(1)
C(78)	1993(2)	6765(1)	2074(1)	34(1)
C(79)	3381(2)	6497(1)	411(1)	48(1)
C(80)	3209(4)	5837(2)	112(2)	70(1)
C(81)	3397(4)	6991(2)	-142(2)	72(1)
C(82)	2274(2)	6736(1)	2820(1)	39(1)
C(83)	2113(3)	6078(2)	3105(2)	57(1)
C(84)	1648(3)	7215(2)	3221(2)	57(1)
N(1)	5987(1)	8945(1)	1808(1)	28(1)
N(2)	4555(1)	9098(1)	2328(1)	27(1)
N(3)	5399(1)	6197(1)	2230(1)	26(1)
N(4)	3784(1)	6363(1)	1853(1)	26(1)
O(1)	5557(2)	7513(1)	689(1)	77(1)
O(2)	4404(2)	7636(1)	3042(1)	47(1)
O(3)	5754(2)	8016(1)	3679(1)	71(1)

Table A-6: Atomic coordinates ($\times 10^4$) and equivalent isotropic displacement parameters ($\text{\AA}^2 \times 10^3$) for $\text{HBI}t\text{Bu}^+[(\mu\text{-Cl}_3)\{\text{ClRu}(\text{Binap})\}_2]^-$ (**4-36**).

	x	y	z	U(eq)
Ru(1)	1347(1)	5179(1)	4315(1)	17(1)
Ru(2)	723(1)	5422(1)	5980(1)	17(1)
P(1)	1463(1)	6061(1)	6945(1)	21(1)
P(2)	-821(1)	5580(1)	6123(1)	18(1)
P(3)	2799(1)	5433(1)	4075(1)	19(1)
P(4)	390(1)	5288(1)	3008(1)	19(1)
Cl(1)	908(1)	4659(1)	6933(1)	24(1)
Cl(2)	2296(1)	5090(1)	5793(1)	21(1)
Cl(3)	806(1)	6035(1)	4867(1)	20(1)
Cl(4)	-12(1)	4768(1)	4780(1)	21(1)
Cl(5)	1738(1)	4226(1)	4070(1)	23(1)
N(1)	7637(3)	8357(2)	3170(2)	38(1)
N(2)	8484(3)	8759(2)	4311(2)	40(1)
C(1)	602(3)	6631(2)	7052(2)	22(1)
C(2)	647(3)	7141(2)	6651(2)	28(1)
C(3)	-18(3)	7577(2)	6626(2)	30(1)
C(4)	-752(3)	7533(2)	7023(2)	26(1)
C(5)	-1406(3)	7983(2)	7039(3)	38(1)
C(6)	-2118(3)	7934(2)	7411(3)	43(1)
C(7)	-2230(3)	7420(2)	7774(3)	37(1)
C(8)	-1624(3)	6971(2)	7770(2)	29(1)
C(9)	-830(3)	7014(2)	7409(2)	24(1)
C(10)	-155(3)	6549(2)	7412(2)	20(1)
C(11)	-373(2)	5996(2)	7724(2)	20(1)
C(12)	-312(3)	5951(2)	8562(2)	22(1)
C(13)	55(3)	6405(2)	9120(2)	28(1)
C(14)	16(3)	6373(2)	9889(2)	33(1)
C(15)	-386(3)	5891(2)	10158(2)	39(1)
C(16)	-717(3)	5442(2)	9651(2)	36(1)
C(17)	-683(3)	5461(2)	8839(2)	26(1)

C(18)	-1062(3)	5012(2)	8293(2)	28(1)
C(19)	-1089(3)	5052(2)	7505(2)	24(1)
C(20)	-764(2)	5548(2)	7204(2)	19(1)
C(21)	2145(3)	5792(2)	7965(2)	25(1)
C(22)	2139(3)	6072(2)	8671(2)	32(1)
C(23)	2810(3)	5914(2)	9411(2)	36(1)
C(24)	3501(3)	5478(2)	9467(2)	38(1)
C(25)	3486(3)	5194(2)	8761(2)	36(1)
C(26)	2814(3)	5353(2)	8017(2)	30(1)
C(27)	4253(3)	5320(3)	10269(3)	54(2)
C(28)	2520(3)	6509(2)	6859(2)	26(1)
C(29)	2941(3)	6902(2)	7473(3)	41(1)
C(30)	3714(4)	7253(2)	7458(3)	43(1)
C(31)	4121(3)	7236(2)	6822(3)	36(1)
C(32)	3704(3)	6850(2)	6214(3)	35(1)
C(33)	2929(3)	6489(2)	6235(2)	29(1)
C(34)	4983(3)	7611(2)	6807(4)	51(1)
C(35)	-1763(3)	5030(2)	5641(2)	23(1)
C(36)	-1509(3)	4454(2)	5759(2)	24(1)
C(37)	-2215(3)	4032(2)	5422(2)	27(1)
C(38)	-3194(3)	4174(2)	4946(2)	30(1)
C(39)	-3427(3)	4741(2)	4805(2)	32(1)
C(40)	-2742(3)	5164(2)	5138(2)	27(1)
C(41)	-3956(3)	3715(2)	4587(3)	39(1)
C(42)	-1581(3)	6223(2)	5781(2)	21(1)
C(43)	-1376(3)	6589(2)	5229(2)	25(1)
C(44)	-1982(3)	7065(2)	4962(2)	31(1)
C(45)	-2794(3)	7181(2)	5231(2)	31(1)
C(46)	-3017(3)	6800(2)	5758(2)	29(1)
C(47)	-2408(3)	6338(2)	6039(2)	24(1)
C(48)	-3409(4)	7717(2)	4963(3)	47(1)
C(49)	2956(2)	5078(2)	3176(2)	20(1)
C(50)	3602(3)	4605(2)	3273(2)	25(1)
C(51)	3645(3)	4293(2)	2617(2)	27(1)
C(52)	3073(3)	4443(2)	1835(2)	28(1)

C(53)	3086(4)	4109(2)	1155(3)	41(1)
C(54)	2518(4)	4260(2)	390(3)	43(1)
C(55)	1946(3)	4755(2)	263(2)	35(1)
C(56)	1926(3)	5094(2)	909(2)	29(1)
C(57)	2471(3)	4934(2)	1714(2)	24(1)
C(58)	2404(2)	5253(2)	2405(2)	22(1)
C(59)	1781(3)	5784(2)	2270(2)	21(1)
C(60)	2149(3)	6263(2)	1932(2)	23(1)
C(61)	3064(3)	6246(2)	1742(2)	29(1)
C(62)	3385(3)	6707(2)	1416(3)	36(1)
C(63)	2827(3)	7211(2)	1254(3)	38(1)
C(64)	1947(3)	7250(2)	1447(2)	31(1)
C(65)	1598(3)	6781(2)	1796(2)	24(1)
C(66)	702(3)	6816(2)	1997(2)	26(1)
C(67)	355(3)	6360(2)	2317(2)	25(1)
C(68)	872(2)	5833(2)	2457(2)	19(1)
C(69)	3130(3)	6170(2)	3917(2)	21(1)
C(70)	2525(3)	6617(2)	3984(2)	25(1)
C(71)	2772(3)	7171(2)	3832(2)	29(1)
C(72)	3641(3)	7290(2)	3632(2)	28(1)
C(73)	4257(3)	6836(2)	3590(3)	34(1)
C(74)	4009(3)	6280(2)	3723(2)	30(1)
C(75)	3888(3)	7880(2)	3426(3)	38(1)
C(76)	3903(2)	5204(2)	4921(2)	25(1)
C(77)	4581(3)	5593(2)	5396(2)	32(1)
C(78)	5327(3)	5423(2)	6096(3)	39(1)
C(79)	5455(3)	4870(2)	6329(3)	40(1)
C(80)	4784(3)	4472(2)	5858(3)	33(1)
C(81)	4012(3)	4636(2)	5175(2)	28(1)
C(82)	6288(4)	4678(3)	7072(4)	71(2)
C(83)	109(3)	4659(2)	2361(2)	22(1)
C(84)	188(3)	4646(2)	1581(2)	27(1)
C(85)	-81(3)	4165(2)	1103(3)	35(1)
C(86)	-491(4)	3697(2)	1359(3)	36(1)
C(87)	-634(3)	3727(2)	2120(3)	32(1)

C(88)	-323(3)	4190(2)	2613(2)	27(1)
C(89)	-713(5)	3153(2)	864(3)	58(1)
C(90)	-942(2)	5521(2)	2798(2)	22(1)
C(91)	-1610(3)	5483(2)	2019(2)	32(1)
C(92)	-2607(3)	5656(2)	1850(3)	40(1)
C(93)	-2971(3)	5862(2)	2449(3)	39(1)
C(94)	-2307(3)	5889(2)	3227(3)	37(1)
C(95)	-1303(3)	5723(2)	3403(2)	27(1)
C(96)	-4069(3)	6029(3)	2258(4)	62(2)
C(97)	8555(4)	8060(2)	3474(3)	36(1)
C(98)	8966(4)	7577(2)	3217(3)	46(1)
C(99)	9880(4)	7394(2)	3703(3)	52(1)
C(100)	10416(4)	7663(2)	4417(3)	48(1)
C(101)	10030(4)	8147(2)	4676(3)	42(1)
C(102)	9086(4)	8321(2)	4197(3)	34(1)
C(103)	7648(4)	8773(2)	3697(3)	40(1)
C(104)	6829(4)	8276(2)	2403(3)	50(1)
C(105)	7267(5)	8375(3)	1700(3)	66(2)
C(106)	6421(5)	7674(3)	2359(4)	71(2)
C(107)	5986(5)	8700(3)	2334(4)	68(2)
C(108)	5372(7)	5996(5)	8329(7)	78(4)
CI(6A)	6405(9)	6213(6)	8059(9)	80(4)
CI(7A)	6050(5)	5496(5)	9040(6)	136(5)
CI(6B)	6186(7)	6344(5)	7916(9)	36(2)
CI(7B)	5391(9)	6341(6)	9243(7)	143(7)
C(109)	7808(10)	7159(6)	-37(7)	82(5)
CI(8A)	6701(7)	7627(3)	-403(3)	72(1)
CI(8B)	7288(10)	7757(4)	-288(5)	72(1)
CI(9)	7879(3)	6885(2)	878(2)	72(1)
C(110)	3435(19)	8919(13)	-610(20)	180(30)
CI(10)	4174(17)	8329(17)	-368(10)	340(20)
CI(11)	3212(12)	9380(12)	66(13)	225(10)
C(111)	7402(4)	4311(3)	3112(4)	64(2)
CI(12)	7664(1)	3579(1)	3290(1)	70(1)
CI(13)	6129(1)	4438(1)	2632(1)	94(1)

C(112)	62(4)	8648(2)	2064(3)	55(1)
Cl(14)	1349(1)	8498(1)	2510(1)	77(1)
Cl(15)	-335(2)	8491(1)	1041(1)	96(1)

Table A-7: Atomic coordinates ($\times 10^4$) and equivalent isotropic displacement parameters ($\text{\AA}^2 \times 10^3$) for $[\text{Cl}_2\text{Ru}(\text{XylBinap})(\text{BIME})_2]$ (**4-38a**).

	x	y	z	U(eq)
Ru(1)	4702(1)	10000	0	43(1)
P(1)	6009(1)	10636(1)	-344(1)	36(1)
Cl(1)	4479(1)	9460(1)	-952(1)	57(1)
C(1)	7113(3)	10675(2)	212(2)	32(1)
C(2)	7926(3)	10259(2)	224(2)	32(1)
C(3)	8762(3)	10301(2)	681(2)	36(1)
C(4)	9630(3)	9905(2)	719(2)	41(1)
C(5)	10412(3)	9965(2)	1149(2)	51(1)
C(6)	10344(4)	10416(2)	1596(2)	54(1)
C(7)	9506(4)	10792(2)	1580(2)	48(1)
C(8)	8707(3)	10760(2)	1129(2)	35(1)
C(9)	7841(3)	11163(2)	1107(2)	37(1)
C(10)	7092(3)	11130(2)	662(2)	36(1)
C(11)	6807(3)	10567(2)	-1053(2)	37(1)
C(12)	7688(4)	10933(2)	-1133(2)	44(1)
C(13)	8299(4)	10924(2)	-1661(2)	46(1)
C(14)	8021(4)	10516(2)	-2117(2)	49(1)
C(15)	7161(4)	10137(2)	-2051(2)	45(1)
C(16)	6552(3)	10170(2)	-1518(2)	40(1)
C(17)	9237(4)	11329(2)	-1739(2)	62(1)
C(18)	6898(4)	9692(2)	-2538(2)	62(1)
C(19A)	5437(14)	11430(5)	-423(6)	43(5)
C(20A)	5570(12)	11731(5)	-969(6)	36(3)
C(21A)	5046(9)	12259(3)	-1065(4)	50(4)

C(22A)	4389(8)	12486(3)	-614(4)	53(4)
C(23A)	4256(10)	12185(4)	-68(4)	44(3)
C(24A)	4780(12)	11657(5)	27(5)	45(5)
C(25A)	5172(12)	12564(4)	-1648(5)	63(2)
C(26A)	3578(14)	12422(5)	472(5)	63(2)
C(19B)	5616(14)	11407(6)	-470(8)	32(4)
C(20B)	5888(13)	11725(6)	-997(7)	49(5)
C(21B)	5423(11)	12275(5)	-1107(6)	49(4)
C(22B)	4686(11)	12507(5)	-691(6)	51(4)
C(23B)	4415(12)	12189(5)	-165(6)	66(6)
C(24B)	4879(14)	11640(6)	-54(6)	46(6)
C(25B)	5763(14)	12636(5)	-1679(6)	63(2)
C(26B)	3538(16)	12454(6)	228(6)	63(2)
N(1A)	3382(4)	9438(2)	303(3)	43(1)
C(27A)	2621(5)	9259(2)	-69(4)	53(2)
N(2A)	1977(4)	8851(2)	182(3)	63(2)
C(28A)	2343(4)	8751(2)	765(3)	55(2)
C(29A)	2035(4)	8366(2)	1232(3)	79(3)
C(30A)	2592(6)	8360(3)	1787(3)	74(3)
C(31A)	3457(7)	8738(3)	1875(3)	69(4)
C(32A)	3766(5)	9123(3)	1407(3)	52(3)
C(33A)	3209(5)	9130(2)	853(2)	49(2)
C(34A)	1062(6)	8567(3)	-118(5)	77(3)
N(1B)	3622(16)	9470(9)	579(10)	43(1)
N(2B)	3159(13)	8835(7)	1327(9)	46(5)
C(27B)	3804(17)	9252(10)	1143(11)	31(6)
C(28B)	2427(12)	8752(7)	875(7)	55(3)
C(29B)	1574(11)	8370(7)	789(7)	55(3)
C(30B)	1006(11)	8380(6)	243(8)	55(3)
C(31B)	1290(12)	8772(7)	-219(8)	55(3)
C(32B)	2142(12)	9154(6)	-133(8)	55(3)
C(33B)	2711(11)	9144(7)	413(8)	55(3)
C(34B)	3180(30)	8513(17)	1810(15)	70(10)
O(1)	5374(15)	11967(18)	2044(17)	314(18)
C(35)	6333(12)	12067(7)	2278(6)	111(5)

C(38)	4451(14)	11918(9)	2350(8)	136(7)
C(37)	4904(14)	11905(12)	3025(8)	125(7)
C(36)	6136(11)	11937(8)	2951(7)	125(6)
